Metal behaviour in anaerobic sludge digesters supplemented with trace nutrients

Jimmy Roussel

A thesis submitted to
The University of Birmingham
for the degree of
DOCTOR OF PHILOSOPHY

Department of Civil Engineering
School of Engineering
The University of Birmingham
December 2012

ABSTRACT

Trace nutrients (metals) supplementation has been demonstrated to have a beneficial effect on the welfare of anaerobic digesters but there was a lack of information on the chemistry controlling their fate. The aim of this research was to determine the reactions governing the chemical behaviour of metals in anaerobically digested sludge and predict the fate of those metals when supplemented as MeEDTA.

After the assessment of a wide range of analytical techniques, a suite of suitable analytical techniques[1] were used to determine the metals behaviour in two case studies of metals supplementation: iron dosing and MeEDTA supplementation.

The behaviour of the metals was controlled by the solid phase throughout a primary reaction (sulphide precipitation) and secondary reactions (phosphate precipitation, adsorption and organic complexation). The competition between the strength of metal's binding and EDTA complexation controlled the fate of the supplemented metals in anaerobic digesters. Transfer of CoEDTA in the solid phase was found to be divided into two reactions, where the second has a slow kinetic depending on the availability of the counter-ion reacting with EDTA.

[1] BCR sequential extraction procedure; scanning electron microscopy coupled with energy dispersive spectroscopy, pH titration and geochemical equilibrium speciation model

A key conclusion was that the presence of weaker metal-bound compounds mixed with strong sulphide precipitates changed the understanding of metals speciation, especially concerning their potential availability and consequently their behaviour as trace nutrients.

ACKNOWLEDGEMENT

I am grateful to my supervisors, Dr. Cynthia Carliell-Marquet, Dr. Joanna Renshaw and Prof. Chris Buckley for all their guidance and support. Thanks Cynthia for giving me the opportunity to work on this project and helping me through all the difficulties that I encountered during this project. You always supported me and gave me the confidence that I needed to accomplish my investigations. Thanks Jo for all your help on the chemistry knowledge and your innovative point of view on this project. Finally thanks Chris for your fundamental input on the equilibrium model, for all the time you spent with me talking about research and for giving me the opportunity to visit South Africa.

Furthermore I would also like to acknowledge with much appreciation the help from Jayshree Bhuptani and Prof. Andrew Wheatley in the use of the ICP-AES at Loughborough University. I would like also to thank all the staff at the school of Civil Engineering of University of Birmingham, with a special mention to John Edgerton for his thoughtful advices in the lab. Thanks to Farryad Ishaq for all his help in this research and also the good times spent during the different conferences.

To my friends, Chibuzor Uchea and Dan “Chief” Brown, thank you so much for all the good times, memories and laughs we had during those years. There are so

many anecdotes that it will need another thesis volume to narrate them but thanks for sharing beers, cricket and English humour with me. I also express many thanks for helping me to develop my writing skills. I also thank Francesco Dorigatti for all the time spent together and for teaching me some Italian words while seating in front of your laptop. To Vinh Doan, thank you for being the first person to talk to me when I arrived in the office, all the dinners and those long conversations. I really had good times. Finally, to Jose Ramirez, Ursula Fernandez, Lasitha Kuruvita, Budi Gunawan and all the office F59B, thanks for the great time spent at the University and outside. You all contribute to make the work more fun!

To my old friends, Anael Aubey, Gautier Jue and Serge Perato, thanks for being here and make me feel close from home while I was away. Gautier, Anael and Amelie, thank you for offering shelter, food and beverage when I was back to France but mainly thank you for just being in my life. Congratulation to Serge for completing his thesis before me, an easy win.

Finally, the last but not the least, I would like to thank my family for all their support and love. Thanks to my grand-parents who believe in me and are always there for me. To my sister and her lovely husband, I would like to thank you for everything you have done for me in my life. You always gave me strength and courage to accomplish anything I wanted to. To my mum and dad, I would like to dedicate this thesis to you, thank you for your support, inspiration, encouragement, help and love. You are the most important persons in my life and I am glad to be your son.

TABLE OF CONTENTS

LIST OF FIGURES

LIST OF TABLES

LIST OF EQUATIONS

GLOSSARY

AD	Anaerobic Digestion
ADM1	Anaerobic digestion model 1
AES	Atomic emission spectometry
BCR	Bureau Communautaire de Reference
BOD	Biological oxygen demand
Ca	Calcium
CH_4	Methane
CPR	Chemical phosphorus removal
Co	Cobalt
Cu	Copper
CO_2	Carbon dioxide
COD	Chemical Oxygen Demand
°C	Degree(s) Celsius – unit of temperature
d.l.	detection limit
E^o	Reduction potential
EDS	Energy dispersive X-Ray spectroscopy
EEM	Excitation Emission matrice
EPS	Extracellular polymeric substances
FAAS	Flame atomic absorption spectroscopy
Fe	Iron
FSADSA	Full scale anaerobically digested sludge analysis
H_2	Dihydrogen
HCl	Hydrochloric acid
HNO_3	Nitric acid
HRT	Hydraulic retention time
ICP	Inductively coupled plasma
K	Kelvin- unit of temperature in equations
K	Potassium
K_{sp}	Solubility product constant

K_{sm}	Chelate stability constant
M / mol	Molar concentration
MeEDTA	Metal bound with EDTA
mg/l	Milligrams per litre
Mg	Magnesium
Mn	Manganese
N	Nitrogen
Na	Sodium
Ni	Nickel
NH_3	Ammonia
OLR	Organic loading rate
P	Phosphorus
%	Percentage
pC	log of element concentration (in mol/l)
pe	electron potential
pH	Hydrogen ion concentration (log_{10})
pK_{sp}	Log of solubility product constant
r^2	Regression coefficient
rpm	Revolutions per minute
SD	Standard deviation
SE	Sequential Extraction
SEM	Scanning electron microscopy
SMP	soluble microbial by-product
SOM	Soluble organic matter
SRT	Solids retention time
TMC	Trace metal combination
TS	Total solids
UASB	Upflow anaerobic sludge blanket
UK	United Kingdom
UPW	Ultra pure water
VS	Volatile solids
WWTP	Wastewater treatment plant.

XRD	X-Ray diffraction spectroscopy
XRF	X-Ray fluorescence spectroscopy
Zn	Zinc

MOLECULES AND PRECIPITATES

Aragonite	$CaCO_3$
Calcite	$CaCO_3$
Catechol	$C_6H_5O_2$
Citrate	$C_3H_5O(COO)_3^{3-}$
Delvauxite	$CaFe_4(PO_4)_2(OH)_8.4H_2O$
Dolomite	$CaMg(CO_3)_2$
EDTA	Ethylenediaminetetraacetic acid ($C_{10}H_{16}N_2O_8$)
Glycine	$C_2H_5NO_2$
Histidine	$C_6H_9N_3O_2$
NTA	Nitrilotriacetic acid ($C_6H_9NO_6$)
Rhodocrosite	$MnCO_3$
Phthalic acid	$C_8H_6O_4$
Pyrite	FeS_2
Salicylic acid	$C_7H_6O_3$
Sphalerite	ZnS
Vivianite	$Fe_3(PO_4)2.8H_2O$
Wurtzite	ZnS

CHAPTER 1. INTRODUCTION

1.1. Place of the anaerobic digestion process in the wastewater treatment plant

A wastewater treatment plant (WWTP) uses a series of processes to treat used water by removing organic matter (COD, BOD), nutrients (P and N) and other elements such as heavy metals, carbonate or sulphate compounds. Two different sludge wastes, requiring further anaerobic treatment, are produced at different stages of the treatment processes (figure 1.1). Primary sludge is extracted after the grit/screening and prior to any biological treatment. The main secondary treatment processes, e.g. activated sludge or trickling filters, generate waste biomass that is settled in secondary settlement tanks and it is called secondary sludge. Untreated sludge cannot be disposed of directly and a serie of different treatments are available to reduce the sludge volume and toxicity for the environment, such as thickening, anaerobic digestion, composting and dewatering.

Anaerobic digestion is an old process that has been integrated into the WWTP for its advantages and its simple working requirement in comparison with other sludge treatment processes. The main advantages of anaerobic digestion are the reduction of the sludge volume, pathogens and odour. Moreover, anaerobic digestion produces methane that can be used as renewable energy to reduce the

external energy consumption of the WWTP (Smith, 2006). However, anaerobic digesters (AD) do not work at their full potential and several research investigations have been conducted in the last forty years to improve the biogas production.

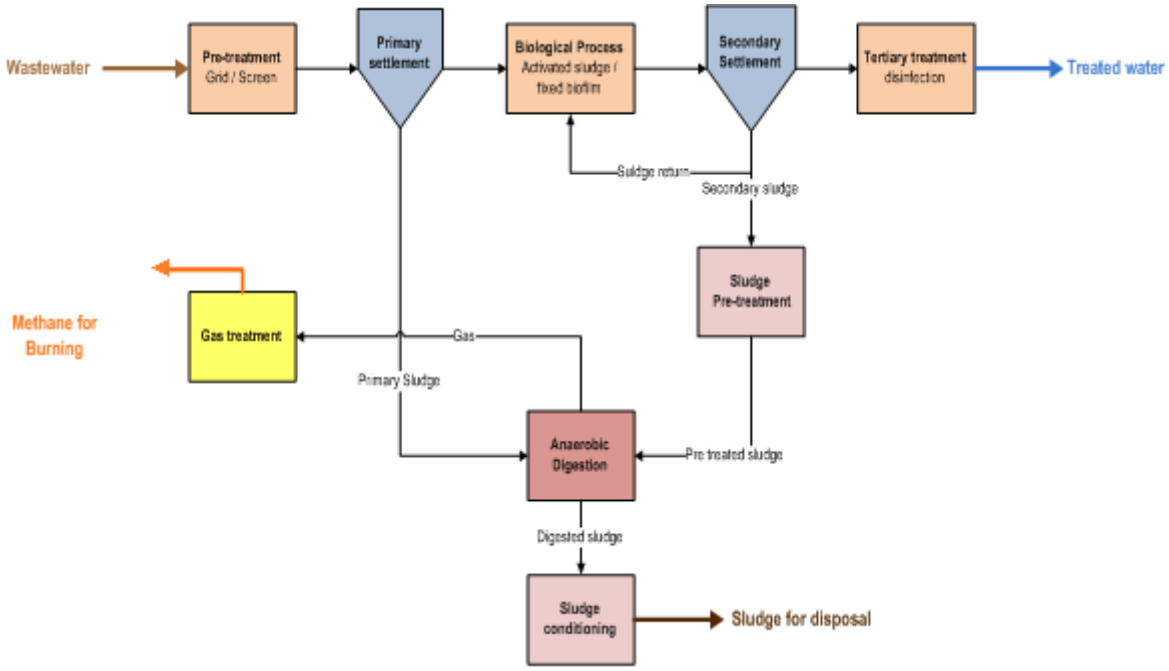

Figure 1.1. Example of a wastewater treatment plant flowchart

Bioenergy generation from biogas is driving the recent interest in improving the anaerobic digestion process, the objective being to increase the yield of methane in order to reduce WWTP energy consumption and carbon footprint and generate renewable energy to partially replace fossil fuel. The International Water Association is developing an anaerobic digestion model (ADM1) to understand all the biological, physical and chemical processes happening inside the digester in order to optimize its working condition (Batstone et al., 2002). From this model, a number of updates have been made on it by several researchers in order to improve the outputs and its range of application (Gali et al., 2009; Ramirez et al.,

2009 and Penumathsa et al., 2008). Biological and physic-chemical aspects of ADM1 (Batstone et al., 2002) are far more developed than the associated inorganic chemical aspects, which need to be explored further to understand the impact of metals on the digester and its methane production.

1.2. Introduction to the anaerobic digestion process

A sewage sludge anaerobic digester is a biological reactor designed to degrade organic matter and cellular by-products produced during the treatment of wastewater. Through a combination of different microbial processes, substrates are degraded under anaerobic conditions in adherence to an reasonably defined food chain plan (figure 1.2). Carbohydrates, lipids, fatty acids and other complex substrates are degraded to form a concentrated digested sludge and the gaseous by-products; methane (CH_4), carbon dioxide (CO_2) and dihydrogen (H_2) (Gerardi et al., 2003; Smith, 2006 and Ishaq, 2012) .

The first stage of this food chain is the hydrolysis of large complexes such as lipids and proteins to smaller compounds (sugar, amino acids; Zeikus, 1979). Then those compounds are degraded to acids and alcohols during the acidogenesis phase (Smith, 2006). The third phase (acetogenesis) is the transformation of acids and alcohols to acetate (Schink, 1992). Dihydrogen and dioxide carbon are by products of this phase. In the final stages of the degradation process, there is a co-dependence and/or competition between three main types of bacteria, which

can be grouped according to their substrate consumption/production: acetate forming, sulphate reducing and methane-forming bacteria. Acetate forming bacteria can only survive under very low concentrations of hydrogen (Batstone et al., 2002) so they are dependent on the two other types of bacteria reducing the hydrogen by converting it into methane, sulphide, or other compounds. Competition takes place between sulphate reducing bacteria and methane forming bacteria for the available hydrogen and acetate in the process (Ishaq, 2012). This competition and co-dependence creates a fragile equilibrium that can be readily affected by any exterior element, which ultimately could lead to failure of the digestion process (Gerardi, 2003).

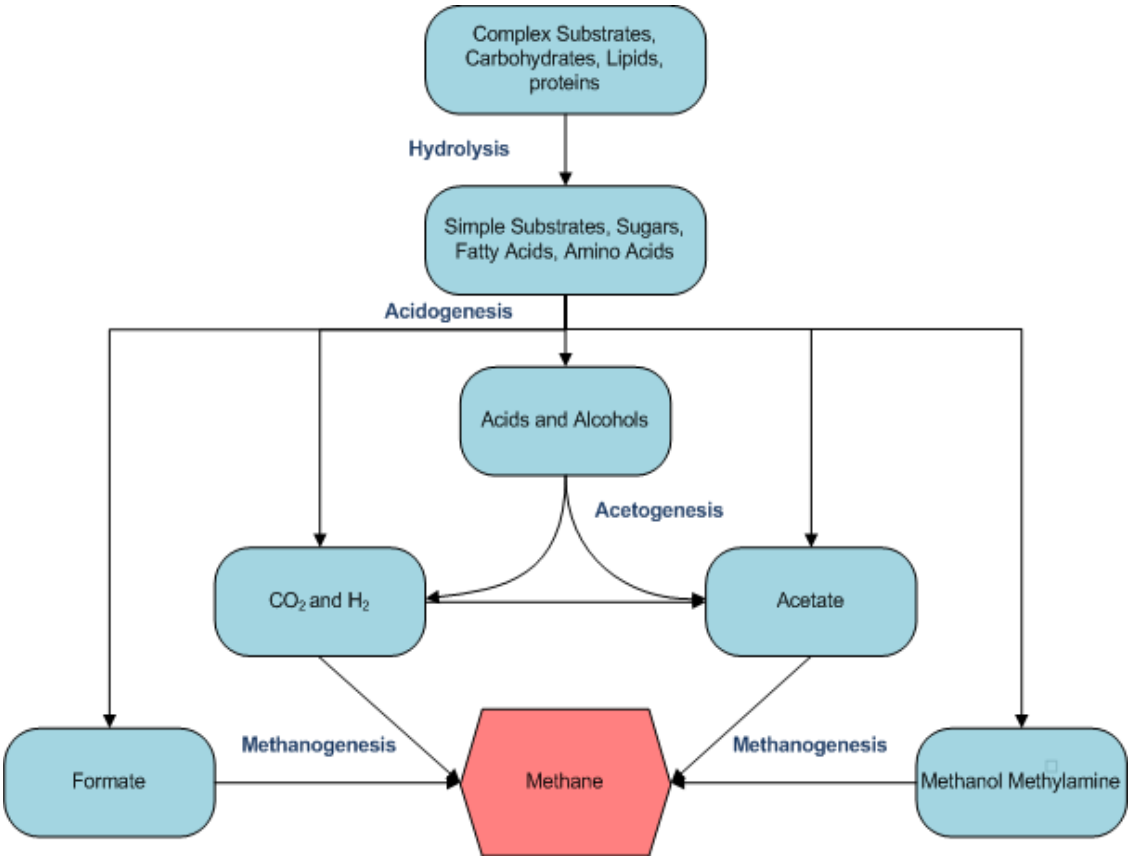

Figure 1.2. Anaerobic food chain scheme (adapted from Gerardi, 2003)

The sewage sludge being treated by anaerobic digesters is a complex mixture of compounds, each with their own potential reactive pathways. This mixture of compounds can be partitioned into several fractions: biological solids, organic compounds, inorganic compounds and metals. The biological solids are generally composed of coagulated non-degraded solids from primary settlement, dead organisms and flocs produced via the interactions of organic matter. Organic compounds come from a variety of different origins, principally; from degraded materials such as humic substance, volatile fatty acids, amino-acids or acetate, and organic matter produced by microorganisms. The last kind of compound present is inorganic compounds, which primarily come from wastewater by-products, carbonate, phosphate, sulphide, halogen and alkali and alkali-earth metals.

1.3. Research aims

As it will be discussed in chapter 2, metals interact with living organisms in the digestion processes, fulfilling a variety of essential cellular functions, however, these metal-microbe interactions must compete with interactions between metals and all the other compounds in the sludge. The limitation of bioavailable metals to organisms may be responsible for an inhibition/limitation of the anaerobic digestion process.

The first aim of this research was to investigate the chemical behaviour of six essential metals[2] for the micro-organisms in anaerobic digesters. To do so, two case studies of metals dosing in anaerobically digested sludge were used to determine the speciation of metals in the solid phase and characterize the reactions governing the different metals exchanges in the solid phase and between the liquid and solid phases.

The first case study focused on the behaviour of iron in anaerobic digesters with the analysis and comparison of iron dosed anaerobically digested sludge for the purpose of chemical phosphorus removal and non-iron dosed anaerobically digested sludge.

The second case study focused on the behaviour of cobalt (and the other 5 metals) in anaerobically digested sludge supplemented by metals bound with EDTA in the purpose of biogas production enhancement. This study on the behaviour of metals was conducted using experimental data from a suite of analytical techniques, predictions obtained with two geochemical equilibrium speciation models and theoretical data obtained from the literature (see figure 1.3).

The second aim of this research was to characterize the mechanism controlling the fate of supplemented metals in the anaerobic digesters. This study focused only on metals supplemented by a solution containing MeEDTA chelates. The mechanisms related to the fate of metals were investigated through an approach

[2] Six essential metals studied in this research were cobalt, copper, iron, manganese, nickel and zinc.

of disturbance of the metals equilibrium between the liquid phase and the solid phase. Cobalt, by its interest on the enhancement of the biogas production (Ishaq, 2012), was particularly studied to obtain information on its fate and the mechanisms that could be related with bioavailability. So two solutions, one containing a cocktail of different MeEDTA and another containing only CoEDTA, was used to study the effect of EDTA bindings on the supplementation of metals.

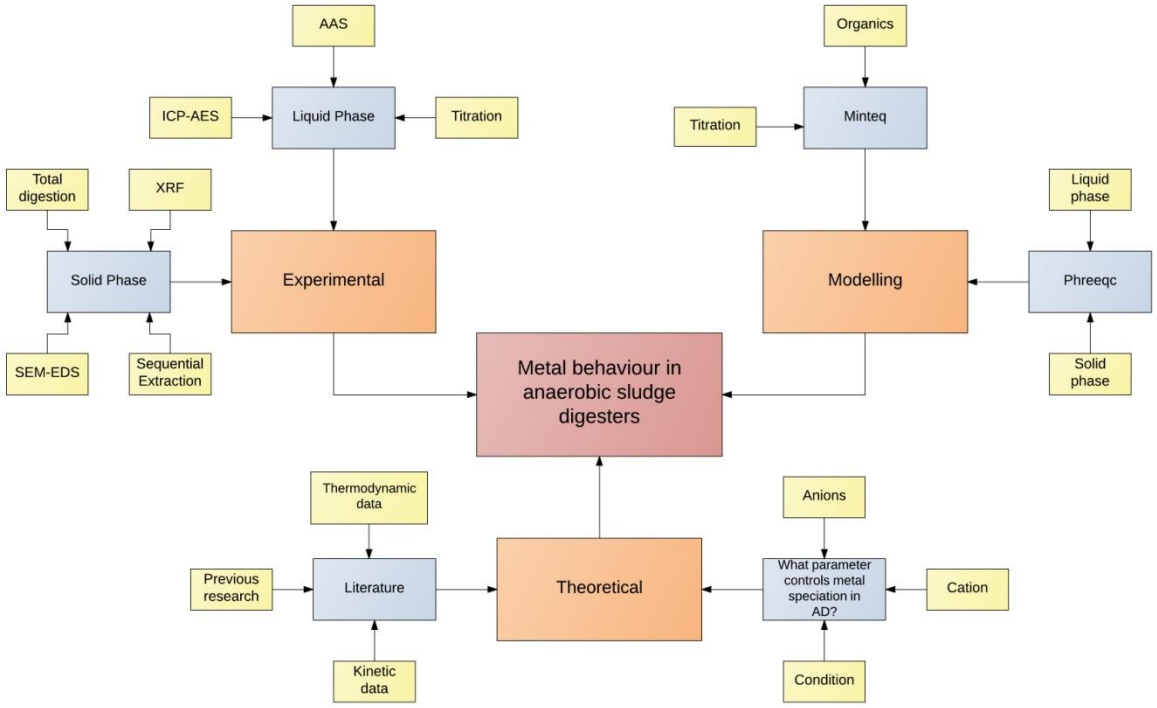

Figure 1.3. Diagram representing the study of metals behaviour using a combination of experimental and theoretical data coupled with model predictions.

CHAPTER 2. LITERATURE REVIEW

Within this chapter the importance of metals in anaerobic digesters, the interest of metals supplementation and an introduction to metals speciation are introduced (sections 2.1-2.3). Then the different chemical binding of metals in the inorganic and organic fraction, adsorption process and the liquid phase are critically reviewed (sections 2.4-2.8). Finally, a critical review on the different analytical techniques and geochemical equilibrium speciation models used in the study of metals speciation in environmental samples is presented in sections 2.9-2.11.

2.1. The importance of metals as nutrients in anaerobic digestion

Microorganisms need several elements to grow and develop such as ideal conditions (pH, temperature and redox potential), carbonaceous substrates, macronutrients (phosphorus and nitrogen) and micronutrients (metals and halogens). The balanced availability between the nutrients coupled with ideal growth condition is essential for a well working digester (Gustavsson, 2012), and any disruption of one of those factors can disturb the activity of a group of organisms. The decreasing activity of those organisms can lead ultimately to a reduction of the anaerobic digester performance, and so a reduction of the biogas production. In the anaerobic digestion process, the methanogenic group is considered to have one of the most fragile equilibriums and it is sensitive to

perturbation (Smith, 2006). Presence of oxygen or an increase of VFAs (dropping of pH) can create disequilibrium in the digester and a decreasing of the methane production (Smith, 2006).

Metals have a strong influence on methanogenic activities and inhibitory effects can occur in case of high concentration (toxicity) or low concentration. So a control of the metals availability is essential for the welfare of the digester. Most of the heavy metals are used by the microorganisms but not all can be defined as essential nutrients. From the literature, the main essential metals are iron, zinc, nickel, cobalt, copper and manganese; vanadium, molybdenum, selenium and tungsten can also be considered as essential but their low concentrations in the sludge in comparison with the six other metals reduce their interests in this study (Oleszkiewicz and Sharma, 1990; Fermoso et al., 2009).

Iron (Fe) is a particularly essential micronutrient as it is typically present in concentrations considerably higher than other metals, with a median concentration ten times higher than the second highest median concentration (Metcalf and Eddy, 2003). So iron speciation is likely to have an impact on the speciation of a wide range of other trace metals in the digester. Its role as a nutrient for AD bacteria is diverse, with it generally being used as co-enzyme, oxidation-reduction agent and terminal electron acceptor (table 2.1). Growth of methanogenesis bacteria requires the presence of iron and Hoban and Van Den Berg (1979) showed a strong link between iron availability and the acetate utilization rate. Consequently, iron plays a

major role in the biological and chemical systems and the study of its behaviour in anaerobically digested sludge is a key part of this research.

The five other main essential metals studied in this research, Cobalt (Co), Copper (Cu), Manganese (Mn), Nickel (Ni) and Zinc (Zn) play also an important biological role in the AD (table 2.1). Manganese acts as a co-factor and may be used in the different redox reactions occurring in anaerobically digested sludge (Fermoso et al., 2009). Cobalt plays a key role in the methanol degradation by methanogenic bacteria as a cofactor (vitamin B12), Nickel is used by methanogenic archea as coenzyme F430, while copper is also used as biological electron transport. Finally, zinc has been found to be an essential element in enzymes, such as methyl-coenzyme M (Fermoso et al., 2008c; Bartacek et al., 2008).

Table 2.1. Essential metals concentration and their biological roles in anaerobically digested sludge (adapted from Metcalf and Eddy, 2003).

Metal	Symbol	Range of concentration in AD (mg/kg DS*)	Biological role in AD
Cobalt	Co	11-2,490	protein cofactor, central component of the vitamin B12
Copper	Cu	84-17,000	coenzyme and biological electron transport
Iron	Fe	1,000-154,000	use for oxydoreduction and teminal electron acceptor and store as metal-protein
Manganese	Mn	32-9,870	enzyme cofactor
Nickel	Ni	2-5,300	Coenzyme (F430: use by methanogenic archea)
Zinc	Zn	101-49,000	found in enzyme, use as structural ions in transcription factor

*** Concentration in mg/kg of Dry Solid (DS)**

2.2. Interest of metals supplementation in anaerobic sludge treatment processes

Zandvoort et al. (2006) showed that the requirement of trace metals and their effects have a strong variation with metals species and that all metals could be toxic if their available concentrations are above the toxicity level. So before any metals supplementation, some questions have to be investigated to obtain the maximal effects, such as which metals are essential, how and when the metals supplementation should be occurring and when metals limitation starts (Zandvoort et al., 2006).

The necessity of metals supplementation implies that some of the essential metals are the limiting factor of the microorganisms' activities. This limitation can occur due to low concentrations of metals but can also be related to a kinetic limitation or metals bioavailability. Fermoso et al. (2008b and 2008c) showed that nickel and zinc limitation could lead to a failure of the upflow anaerobic sludge blanket (UASB) reactors. A clear reduction of the methanogenic activity was observed from methanol feed after 129 days due to metals limitation (Fermoso et al., 2008b). This activity's decreasing followed the decrease of the metals in the liquid phase (mainly Co and Ni) after 110 days and then an accumulation of methanol and acetate led to a pH dropping and a failure in the methanol removal. Addition of nickel helped the recovery of the UASB reactors with 99% of methanol removal. Fermoso et al. (2008c) showed similar results with a deprivation of zinc in UASB reactors. However, continuous zinc supplementation could not reduce the

acidification due to methanol/acetate accumulation and the failure was not recovered. Cobalt, with the lowest concentration in the sludge, was the first to be unavailable for microorganisms and its limitation was measured after only two days (Fermoso et al., 2008c).

This limitation and its effects can be reduced by supplementing essential metals into the process. However, metals supplementation is a complex process and several points need to be investigated to reach the maximum benefits from anaerobic digesters. Those points can be summarized by what, how and when. What form of the compound (binding molecules, oxidation, etc.) is the most appropriate and what is going to be its influence on the uptake of metals. How metals should be supplemented, continuously or by pulse. If metals are added by pulse, when is the most appropriate time to do it.

Effect of metals supplementation on anaerobic digesters is highly dependent on the metal species that are added. The choice of the compounds is determined by the balancing element. It needs to allow the metal to become available to the micro organisms and to have no toxic effect on the process. Kalis et al. (2006) and Fermoso et al. (2009) demonstrated that the metals bioavailability for microorganisms is highly dependent on the metals speciation and metals need to be present as free forms or bound with biological ligands to be available to microorganisms. So during the supplementation, metals need to be released in their free metal forms or biologically complexed at the suitable kinetic rate to avoid any precipitation or complexation prior to any uptake.

Generally two main forms of compounds are used for supplementation: inorganic and metal-organic compounds. The usual forms for inorganic compounds are metals bound with chloride ($MeCl_2$) or sulphate ($Me(SO4)_2$) (Smith et al., 2009; Fermoso et al., 2008c and Aquino and Stuckey, 2007). The choice of chloride as counter-ion is led by the high solubility of the compound formed with metals that allows the solubilisation of the metals when it is added to the digester. However, studies showed that metals were quickly precipitated, mainly with sulphide (Fermoso et al., 2008a). Increasing of chloride concentration in the liquid did not appear to have any inhibitory impact on the micro-organisms (Fermoso et al., 2008a).

The other main option is the supplementation of metals bound with organics such EDTA, citrate or NTA (Aquino and Stuckey, 2007 and Fermoso et al., 2010). The main advantage of using metal-organic compounds is that metals stays longer in solution as they are protected against sulphide precipitation (Fermoso et al., 2008a). However, Aquino and Stuckey (2007) stated that metals bound with organics are not completely available to the micro-organisms, even if they are kept in the liquid phase.

Several studies compared those two forms (inorganic and organic binding) as dosing strategy on UASB reactors to measure their advantages and disadvantages and observed their impacts on the biomass activity. Fermoso et al. (2008a) tested two forms of cobalt supplementation ($CoCl_2$ and CoEDTA) in an

UASB reactor. Results showed that cobalt bound with EDTA stayed in solution and cobalt added with chloride precipitated quickly. This result was confirmed by Bartacek et al. (2008), who found that 90% of cobalt stayed in solution when it was added as CoEDTA and only 30% (maximum) of cobalt stayed in solution when it was added as $CoCl_2$.

For UASB reactors, it is important that cobalt is retained in the reactor and not washed through rapidly with the hydraulic load, to avoid the loss of the supplemented cobalt. EDTA by its binding strength kept the metal into solution and it was washed out quickly due to the low hydraulic retention time of the UASB reactor. Conversely, chloride allowed cobalt to be precipitated or adsorbed and so increased its retention time due to a higher sludge retention time. Fermoso et al. (2010) found that a higher retention of metals minimised the amount of metals required to be supplemented and maximised the organic removal efficiency, and so inorganic supplementation or/and use of weaker organic binding compounds (citrate) are more appropriate for UASB reactors.

However, in the case of a completely mixed sludge anaerobic digester, the hydraulic retention time and solids retention time are the same so the risk of metals washing out faster than the biomass is reduced. The potential of EDTA for keeping the metal in solution is hence more interesting with respect to increasing trace metals availability and so a study needs to be undertaken to evaluate this potential. Finally, EDTA has been found to have negative side effects on the granular sludge by extracting metals from metal active sites of enzymes involved

in methylotrophic methanogenesis (Fermoso et al., 2008a). So an evaluation of the potential toxicity of EDTA on anaerobically digested sludge should also be considered prior any validation of the supplementation of metals bound with EDTA.

Most of the studies on the fate of supplemented metals and their beneficial effects on the biomass activity have been done on UASB reactors (Fermoso et al., 2008b and 2008c; Bartacek et al., 2008; Osuna et al., 2004 and Zandvoort et al., 2006). Similar studies need to be undertaken on completely mixed sludge anaerobic digesters, with a study of the chemical reaction that occurred or might occur in anaerobically digested sludge in order to understand metals bioavailability. This includes a full understanding of the metals speciation in anaerobically digested sludge and the major chemical reactions governing the metals behaviour.

2.3. Presentation of the metals speciation in anaerobically digested sludge

The metals bioavailability is not only limited to the metals present in the liquid phase but it needs to consider the potential of a metals reserve moving from the solid phase (SP) to the liquid phase (LP) (Jansen et al., 2007). This reserve would be used to dissolve metals to support microorganism needs. So during the evaluation of the metals availability in an anaerobic digester, it is essential to take into account the metals present not only in the liquid phase but also in the solid

phase. Availability of metals is not only dependent on their concentrations in the different phases but mainly on their speciation (Hassler et al., 2004). In the liquid phase, all the metals are not necessarily available for micro-organisms (Fermoso et al., 2009); in the solid phase, metals can be ad-(ab)-sorbed or bound inorganically or organically. The binding strength of those compounds establishes the reserve of available metals.

The metal speciation refers to the distribution of this metal amongst its chemical forms or species (Bourg, 1995) and it is dependent on the conditions (e.g. temperature, redox potential and pH) and composition (e.g. cation competitions, anions concentration and organics) of the anaerobic digester.

Metals speciation can be divided using two different systems that are inter-combined. The first is a division solid/liquid phase and the second is a division related to metals binding (inorganic, organic and sorption). Metals are divided in three main groups: inorganic (precipitated in SP and molecule/complex ion in LP), organic (humic substance in SP and chelate ion in LP) and sorption (biomass and sludge floc in the SP). Finally metal can also be present as free ion in the liquid phase (see figure 2.1).

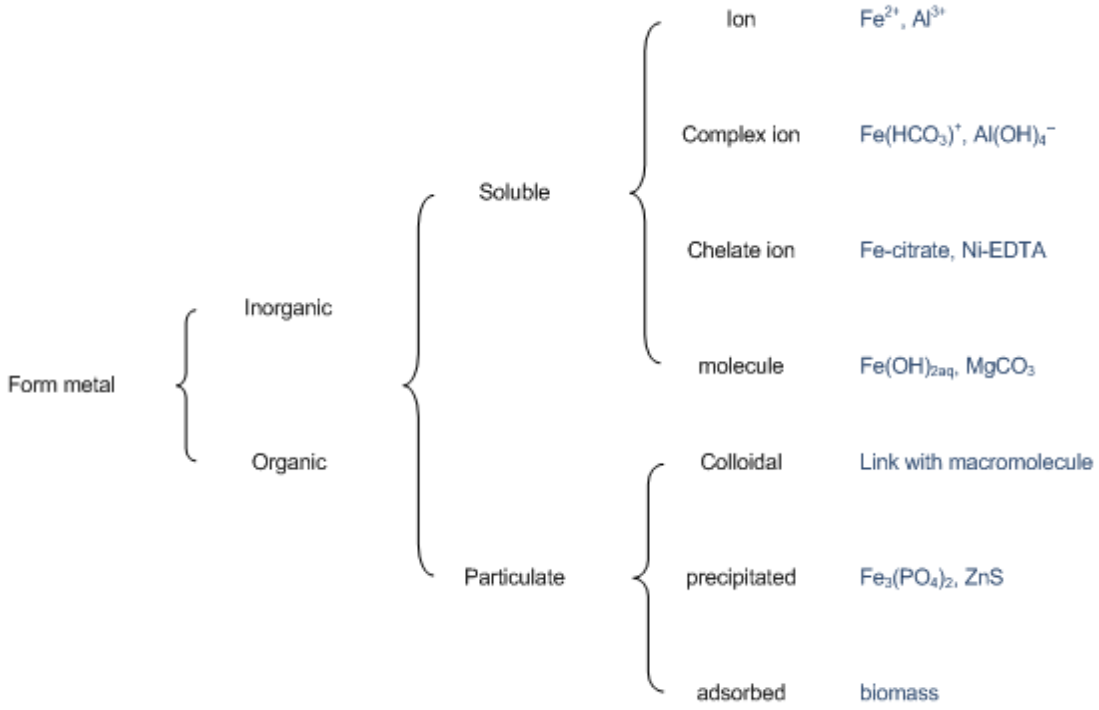

Figure 2.1. Metal species present in anaerobically digested sludge illustrated with some examples (adapted from Sigel, 1984).

To achieve a chemical equilibrium, metals are exchanged between the different phases and species. Those exchanges obey to the thermodynamic and kinetic constants, e.g. solubility product, acidity constant and kinetic reaction order. All those constants control the metals speciation and by calculation, the chemical species should be predicted as a function of the AD condition and composition.

2.4. Chemical forms of metals present in the inorganic fraction of the solid phase under anaerobic condition

It has been widely accepted that the three main inorganic anionic systems present in anaerobic digesters are carbonate, phosphate and sulphide systems (Callander

and Barford, 1983a; Fermoso et al., 2009; Van der Veen et al., 2007; Carliell-Marquet et al., 2010; Mosey et al., 1971). The main species present in each system is controlled by acid-base and gas-liquid equilibrium reaction (equation 2.1). Callander and Barford (1983a) calculated the proportion of each species present in a typical digester condition (pH 7.3) and found that the dominant species for each system are HCO_3^-, $H_2PO_4^-/HPO_4^{2-}$ and HS^-. However, using solubility product constant, it has been achieved that metals mainly precipitate with the most anionic forms (CO_3^{2-}, S^{2-} and PO_4^{3-}) to form $MeCO_3$, MeS and $Me_3(PO4)_2$ precipitates. The low proportion of those species (less than 0.1% of their total soluble concentrations) might have an impact on the metal speciation by becoming a kinetic limiting factor.

$$CO_{2\,(l)} + H_2O \longleftrightarrow HCO_3^- + H^+ \longleftrightarrow CO_3^{2-} + 2H^+$$

pKa : 6.4 pKa : 10.3

$$H_2S_{\,(l)} \longleftrightarrow HS^- + H^+ \longleftrightarrow S^{2-} + 2H^+$$

pKa : 7.0 pKa : 12.9

$$H_3PO_4 \longleftrightarrow H_2PO_4^- + H^+ \longleftrightarrow HPO_4^{2-} + 2H^+ \longleftrightarrow PO_4^{3-} + 3H^+$$

pKa : 2.0 pKa : 7.3 pKa : 12.3

Equation 2.1 Acid-base equilibrium reactions for carbonate, phosphate and sulphide (pKa given at 25°C, adapted from Callander and Barford, 1983a)

Each metal has a specific affinity with each anionic system and the order of precipitation is dependent on the different solubility products values (Ksp). From the literature and Ksp (table 2.2; Callander and Barford, 1983a; Mosey et al.,

1971; Fermoso et al., 2009), sulphide appears to be the controlling species for the precipitation of metals by forming the most stable precipitates under anaerobic conditions. Phosphate precipitates have also high solubility product values for metals but their impact in the inorganic fraction, as controlling species, was not demonstrated except in the case of high phosphate concentration or sulphide limitation (Miot al., 2009 and Carliell-Marquet et al., 2010). Metal-hydroxide and metal-carbonate have low solubility product values in comparison with metal-phosphate and metal-sulphide and so the formation of those precipitates should not occur in anaerobic digesters. However, concerning carbonate precipitates, Callander and Barford (1983a&b) calculated that carbonate should precipitate with manganese and could precipitate with other metals as the second or third precipitate in the case of sulphide limitation.

Sulphide precipitates are thermodynamically the most abundant product in the inorganic fraction under anaerobic condition (Morse and Luther, 1999; Fermoso et al., 2009), and any heavy metals (except chromium) precipitate with sulphide to form insoluble salts (Mosey et al., 1971). Callander and Barford (1983b) calculated that, using solubility products constants (table 2.2), all the metals should be principally precipitated as metal sulphide. Copper has the highest solubility product with sulphide and shall be the first metal to bind with it. Then cobalt, nickel and zinc have a different order depending on the reference, but their solubility products values are close. Finally, iron and manganese are the metals with the lowest solubility product constants.

Table 2.2. Metal precipitate solubility values for the six metals under study

Precipitate	pK_{sp}	Reference
$CoCO_3$	10	HydroGeologic and Allison Geoscience Consultants (1999)
		Callander and Barford (1983)
$Co_3(PO_4)_2$	34.7	HydroGeologic and Allison Geoscience Consultants (1999)
		Callander and Barford (1983)
CoS	25.5	Högfeldt (1982) and Chemical Rubber Company (1972)
	20.3	Callander and Barford (1983)
$CuCO_3$	11.5	HydroGeologic and Allison Geoscience Consultants (1999)
	34	Callander and Barford (1983)
$Cu_3(PO_4)_2$	37	Callander and Barford (1983)
	35.1	HydroGeologic and Allison Geoscience Consultants (1999)
CuS	44.1	Högfeldt (1982) and Chemical Rubber Company (1972)
	37.4	Callander and Barford (1983)
	40.9	Jong and Parry (2009)
$FeCO_3$	10.7	Callander and Barford (1983)
	10.2	HydroGeologic and Allison Geoscience Consultants (1999)
Vivianite $(Fe_3(PO_4)_2.8H_2O)$	35.8	Al-Borno and Tomsen (1994)
	36	HydroGeologic and Allison Geoscience Consultants (1999)
FeS	18.4	Högfeldt (1982) and Chemical Rubber Company (1972)
	22.4	Jong and Parry (2009)
	18	Oleskiewicz and Sharma (1990)
	18	Callander and Barford (1983)
Pyrite - FeS_2	18.5	HydroGeologic and Allison Geoscience Consultants (1999)
$MnCO_3$	10.1	Callander and Barford (1983)
	7.5	HydroGeologic and Allison Geoscience Consultants (1999)
$Mn_3(PO_4)_2$	23.3	HydroGeologic and Allison Geoscience Consultants (1999)
MnS	14.8	Högfeldt (1982) and Chemical Rubber Company (1972)
	15.2	Callander and Barford (1983)
$NiCO_3$	6.9	Callander and Barford (1983)
		HydroGeologic and Allison Geoscience Consultants (1999)
$Ni_3(PO_4)_2$	31.3	HydroGeologic and Allison Geoscience Consultants (1999)
NiS	23.8	Högfeldt (1982) and Chemical Rubber Company (1972)
	27	Oleskiewicz and Sharma (1990)
	28	Jong and Parry (2009)
	20.7	Callander and Barford (1983)
$ZnCO_3$	10.2	Callander and Barford (1983)
	10.3	HydroGeologic and Allison Geoscience Consultants (1999)
$Zn_3(PO_4)_2$	32	Callander and Barford (1983)
	35.4	HydroGeologic and Allison Geoscience Consultants (1999)
ZnS	22.9	Högfeldt (1982) and Chemical Rubber Company (1972)
	28.4	Jong and Parry (2009)
	23	Callander and Barford (1983)

X-ray spectroscopy analysis on the cross section of UASB reactor granule confirmed the formation of nickel, copper and iron sulphide precipitates under anaerobic condition (Liu and Fang, 1998). Using sulphate reducing bacteria to produce sulphide, Kaksonen et al. (2003) showed that 99.8% of the iron and zinc were precipitated as MeS and X-ray diffraction spectroscopy analysis revealed that FeS, FeS_2 and ZnS were the predominant compounds. Acid volatile sulphide analysis has also been used to prove that cobalt and nickel were present as CoS and NiS in anaerobic digesters (Van der Veen et al., 2007).

By its high concentration, precipitation of sulphide with iron has been more studied than with any other metals. The two main precipitates that have been observed are pyrite (FeS_2) and an amorphous iron sulphide compound, FeS (Kaksonen et al., 2003 and Van der Veen et al., 2007). Under anaerobic digester condition, the pourbaix diagram showed that pyrite is supposed to be the most stable inorganic precipitate and so should be the main compound found in anaerobic digesters (Pourbaix, 1963 and Nielsen et al., 2005, Morse and Luther, 1999). However pyritization is a slow process with an oxido-reduction potential below -200mV, so meta-stable amorphous FeS compound is likely to precipitate as a precursor prior to the transformation to pyrite (Nielsen et al., 2005). Other iron-sulphide compounds have also been detected in anaerobic digesters such as greigite (Fe_3S_4), mackinawite (moncrystalline FeS) and pyrrhotite ($Fe_{1-x}S$) (Jong and Parry, 2004, Gustavsson, 2012 and Dewil et al., 2009), The presence of these compounds, depending on their binding strengths and concentrations, might also have an impact on the iron behaviour in anaerobically digested sludge.

Kaksonen et al. (2003) demonstrated that most of the metals were present in the solid phase (less than 0.2% of the total iron and zinc are present in the liquid phase) and Van der veen et al. (2007) found that sulphide could remove over 99% of heavy metal from acid mining sludge. One of the main research on the control of solubility was done by Mosey et al. (1971) and Mosey and Hughes (1975). They used the sulphide solubility to measure the potential toxicity of heavy metal in anaerobic digesters. They calculated the limit for metal toxicity was obtained for a sulphide concentration measured at pS = 17.2. Several approximations have been made to obtain this limit, e.g. only two inorganic systems have been used (carbonate and sulfide system) and free metal ions were responsible for the inhibition. This research indicated the importance of sulphide in the control of metals availability in anaerobic digesters. However, it was only a first step on the understanding of metals behaviour. Other factors, which have not been taken into account by Mosey et al. (1971), can have an effect on the metals speciation such as phosphate bulking (Zhang et al., 2009) and sorption effect (Hayes and Theis, 1978).

Phosphate anion can be considered apart from the carbonate and sulphide system as the reactive species (PO_4^{3-}) has an oxidation number of –III (carbonate and sulphide have an oxidation number of -II). So the reaction of bivalent metals (with oxidation number of + II) with phosphate should not follow a 1:1 ratio but a 3:2 ratio or similar, i.e. $Me_3(PO_4)_2$. With the secondary sludge, the concentrations of phosphate can be increased if iron salts have been added to remove phosphate from the wastewater. During this process (e.g. activated sludge process), iron is in

its oxidized form (iron (III)) due to the aerobic condition. Iron (III) is highly reactive with phosphate (K_{sp}: -26, Högfeldt, 1982) and precipitate as ferric phosphate ($FePO_4$). Ferric-phosphate precipitates are dissolved under anaerobic conditions to reduce the iron (III) to iron (II) while entering into the anaerobic digester.

Iron (II) should react differently from its oxidized form and the formation of ferrous sulphide is expected (Callander and Barford, 1983b; Zhang et al., 2010; Nielsen and Keiding, 1998). However, Miot et al. (2009) found that iron might react again with the phosphate also released to form ferrous phosphate compounds under anaerobic condition at high phosphate concentration. The formation of those precipitates is against the thermodynamic evolution but can be explained from an availability/kinetic point of view. Zhang et al. (2009) and Miot et al. (2009) showed that the phosphate creates a bulk around the iron (II) which limits the sulphide's availability for precipitation of iron and favours the formation of ferrous phosphate such as vivianite ($Fe_3(PO_4)_2.8H_2O$) with a high solubility product (35.8, Al-borno and Tomson, 1994). The formation of this compound has been reported by Ofverstrom et al. (2011) in an anaerobic digester when iron has been directly added as iron salts. The competition of iron precipitation by sulphide and phosphate needs to be investigated as iron is the most abundant metal in the AD and its speciation is likely to affect the other metal precipitates.

The balance between iron-phosphate/sulphide can be changed by the presence of iron dosing in the wastewater treatment scheme (chemical phosphorus removal process). Carliell-Marquet et al. (2010) observed a 10 fold increase of iron

concentration in iron dosed sewage treatment work (STW) sludge in comparison with non-iron dosed STW sludge (respectively average are 107g Fe/kg TS and 13 g Fe/kg TS). Their study on the inorganic profile showed that iron was introduced into the digester as Fe(III)-hydroxy-phosphate and confirmed its dissolution for the reduction of iron. Then most of the iron was re-precipitated as ferrous phosphate and only a small fraction was precipitated as ferrous sulphide. Carliell-Marquet et al. (2010) also observed a change in the speciation of some metals (copper and zinc particularly) due to the presence of iron dosed sludge. A co-precipitation with ferrous phosphate precipitates has been given to explain the change in copper and zinc speciation, rather than sulphide limitation, as the concentration of iron sulphide precipitate did not increase proportionally to the increasing iron concentration in the sludge.

The last species that need to be taken into account in the inorganic fraction are the potential of metal co-precipitation and metal inclusion. Morse and Luther (1999) used the crystal field theory to understand the mechanism of metal incorporation in ferrous sulphide precipitates. Metal incorporation and precipitation is a kinetic competition in the exchange of the ligand (water) bounds with the metals. Depending on the orbital configuration and ligand field stabilization energy of the metal, they obtained an order of metal contents in pyrite and FeS precipitates (Cd<Pb<Zn<Mn<Ni<Co). Van der Veen et al. (2007) showed that Co and Ni enrichment in the inorganic fraction could be caused not only by precipitation but also with adsorption on metal sulphide. Van Hullesbusch et al. (2006) observed the chemisorptions of Ni and Co with FeS and confirmed the potential of these two

metals to form co-precipitate. The other elements (Mn, Zn, Cu, Pb) should not be incorporated into FeS/FeS_2 as they were reacting quicker with sulphide than iron. In opposition CoS and NiS had a slower kinetic and so were available to be included into FeS/FeS_2 (Morse and Luther, 1999).

Metals behaviour in the inorganic fraction has only been studied by small fraction using theoretical and experimental values. However, the complexity of the entire inorganic fraction has not been completely understood due to the high number of reactions occurring. Moreover, some other factors, such as organics complexation and sorptions, kinetics and sulphide limitation will have an impact on the metals availability in the inorganic fraction.

2.5. Complexation of metals with natural organic matter in sewage sludge

Anaerobic digestion is a process rich in organic contents and Fletcher and Beckett (1987) measured a concentration of soluble organic matter (SOM) in an anaerobic digester of around 1 $g.dm^{-3}$. The organic matter is composed of biomass, humic substance and other organics from the biodegradation, such as volatile fatty acids, alcohol and acetate. Their formation is believed to be one of the major chemical reactions in anaerobic digestion (Gould and Genetelli, 1978) and so organic substrates as chelating agent might influence the metal speciation (Fermoso et al., 2009). Organics, with some of their functional groups, react with metals to form

metal-organic chelates. So the complexation of metals by humic substances and organics can be reduced to the interaction between the organics functional groups and metals. Those interactions are dependent on the metal capacity to form metal-organic chelate, the potential of functional group to form stable metal binding site and the competition with other cations such as protons. The different functional groups interacting with metals are carboxyl, amino, phenolic and sulphur containing groups (Fletcher and Beckett, 1987; Gamble et al., 1970; Plaza et al., 2006; Saar and Weber, 1982).

As for the inorganic fraction, thermodynamic values can be used to predict the affinity of each metal with the different organics present in anaerobically digested sludge. The understanding of the coordination chemistry of metals with organics is essential to identify and quantify the metal complexation and its impact on the metal speciation. Metal interactions with organics have been described using two theories, the electrostatic crystal field theory and the molecular orbital theory (Basolo and Johnson, 1964).

Most of the studied metals form octahedral complexes except copper that forms tetragonally distorted octahedral complexes (metals are bound with six ligands). An order of stability of the metal-organic chelates has been calculated using the crystal field theory and classified the metals in function of their affinities to bind with organics, $Mn^{2+} < Fe^{2+} < Co^{2+} < Ni^{2+} < Cu^{2+} > Zn^{2+}$ (Basolo and Johnson, 1964). Irving and Williams (1948) confirmed experimentally this order using different ligands and found that zinc is included between cobalt and iron, $Cu^{2+} > Ni^{2+} > Co^{2+} >$

Zn^{2+}> Ni^{2+}> Fe^{2+}> Mn^{2+}. The values of chelate stability constant (K_{sm}) for some organics from the literature are shown in tables 2.3 and 2.4.

Copper forms the strongest complexes with organics in comparison with other metals studied in this research (Co, Ni, Zn, Fe and Mn) and it has been corroborated by the literature (Gould and Genetelli, 1978; Gould and Genetelli, 1984; Ryan et al., 1983; Fletcher and Beckett, 1987; and Plaza et al., 2006). By opposition, iron and manganese also have respectively the lowest stability constant and so they should be the least able to form metal-organic chelates of the six metals studied.

The complexation order between cobalt, nickel and zinc may vary depending on the organics. For most of the organics present in the tables (EDTA, NTA, histidine) the order follows the stability order described by Irving and Williams (1948) with Ni> Co> Zn. However, for glycine, the stability constant (table 3) of zinc is higher than with cobalt and so the order changes to Ni> Zn> Co. For catechol, nickel has the lowest stability constant value and so the new order is Zn> Co> Ni. This difference may be explained by a difference in the functional groups, size and conformation of the molecules. Glycine and catechol have the lowest molecular mass of all the described organics.

Table 2.3. Chelate stability constant for the six metals under study with natural organics

Complex	pK_{sm}	Reference
Citric acid		
Co-Citrate	4.1	Högfeldt (1982)
	5	Callander and Barford (1983)
Cu-Citrate	6	Högfeldt (1982)
	5.9	Callander and Barford (1983)
Fe-Citrate	4.4	Callander and Barford (1983)
Mn-Citrate	3.6	Högfeldt (1982)
	3.7	Callander and Barford (1983)
Ni-Citrate	4.3	Högfeldt (1982)
Zn-Citrate	5	Callander and Barford (1983)
Glycine		
Co-Glycine	8.6	Högfeldt (1982)
	8.9	Callander and Barford (1983)
Cu-Glycine	14.7	Högfeldt (1982)
	15.2	Callander and Barford (1983)
Fe-Glycine	7.7	Högfeldt (1982)
	7.8	Callander and Barford (1983)
Mn-Glycine	4.8	Högfeldt (1982)
	4.7	Callander and Barford (1983)
Ni-Glycine	10.6	Högfeldt (1982)
Zn-Glycine	9.2	Högfeldt (1982)
	9.5	Callander and Barford (1983)
Histidine		
Co-Histidine	13.5	Högfeldt (1982)
	13.9	Callander and Barford (1983)
Cu-Histidine	18.9	Högfeldt (1982)
	18.3	Callander and Barford (1983)
Fe-Histidine	10.4	Högfeldt (1982)
	9.3	Callander and Barford (1983)
Mn-Histidine	6.6	Högfeldt (1982)
	7.7	Callander and Barford (1983)
Ni-Histidine	15.4	Högfeldt (1982)
Zn-Histidine	12.7	Högfeldt (1982)
	12.9	Callander and Barford (1983)

The main functional groups used to bind metals are carboxylic and phenolic groups and also sometimes amino groups (present in EDTA, Glycine, histidine and

NTA). The ability of humic substance to bind with metals is due to the presence of adjacent functional groups that forms a strong chelating ring (Saar and Weber, 1982). However, it is complicated to study directly complexation of metals by humic substances due to the large size of the molecule and the multitude of binding sites. So smaller organics, holding similar functional group as the humic substances under study, have been used to understand the metal-organic binding, e.g. catechol (Stiff, 1971; figure 2.2), salicylic acid (Ryan et al., 1983; Gamble et al., 1970 and Plaza et al., 2006; figure 2.4) or phthalic acid (Gamble et al., 1970 and Plaza et al., 2006; figure 2.5).

Artola et al. (1997) chose glycine to reproduce the amino-acid binding group of proteins present in the sludge that have been expected to be one of the binding sites for copper. The copper-glycine system showed similarity in the equilibrium with copper-sludge system that proved the interest of using basic compounds as models for understanding metal-humic acid complexation. Artola et al. (1997) also found that the ratio glycine:copper was 2:1 and so suggested that 2 molecules of glycine were binding with one atom of copper (figure 2.3, Fernandes et al., 1997). On the other hand, Plaza et al. (2006) also found a ratio 2:1 between humic acid and copper complexation, confirming that the interest of using smaller organic in the study of metal complexation by humic substances. However, the use of those organics is not adapted to the study of multiple binding sites as the glycine molecule possesses only one binding site.

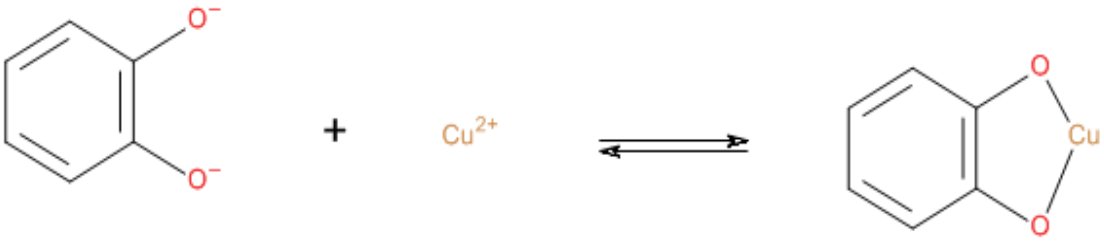

Figure 2.2 Reaction of complexation between catechol and copper ion

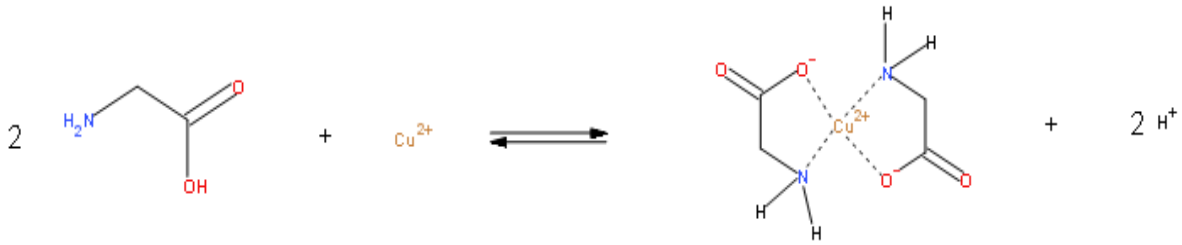

Figure 2.3. Reaction of complexation between copper ion and two glycine molecules (adapted from Fernandes et al., 1996)

The large number of functional groups offers a multiplication of binding sites for only one organic molecule. Some of the binding sites present in soluble organic matter are only available for copper and lead while other sites are available for all the metals (Fletcher and Beckett, 1987; Jensen et al., 1999, Irving and Williams, 1948). Fulvic acid possesses three functional groups, one phenolic group and two carboxylic groups (at the ortho and meta position to the phenolic group), that are able to form two different binding sites (Gamble et al., 1970). The two reactions with metals are displayed in figures 2.4 and 2.5 using salicylic acid and phthalic acid as model compounds for each reaction. The largest binding (over 50% of copper complexation) occurred when both carboxylic and phenolic groups were bound with the metal.

Plaza et al. (2006) also noticed that the binding capacities of humic acids were strongly depend of the pH due to the importance of their acidic functional groups (see below). Gamble et al. (1970) demonstrated that the carboxylic group in ortho position to the phenolic group was completely ionized for a pH over 5 (in comparison, the meta carboxylic groups had only 43% of the group ionized). At the usual pH of anaerobically digested sludge (7-8), the complete ionization of this carboxylic group favoured its reaction with metals.

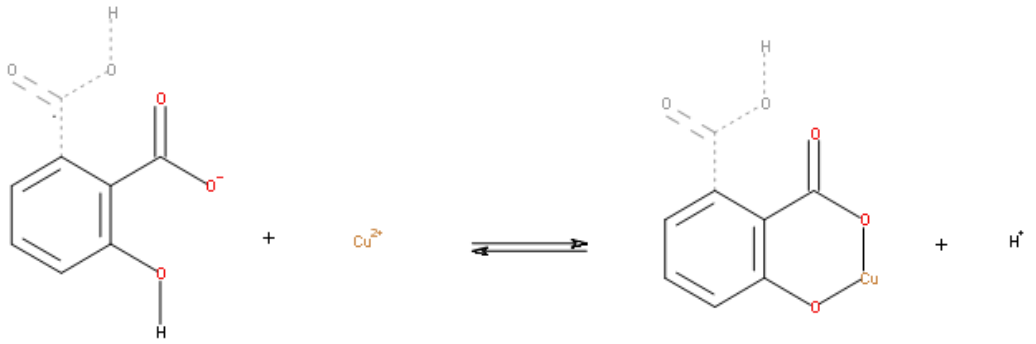

Figure 2.4. Reaction of complexation between Cu^{2+} and salicylic acid to reproduce the reaction between copper and one binding site of fulvic acid.

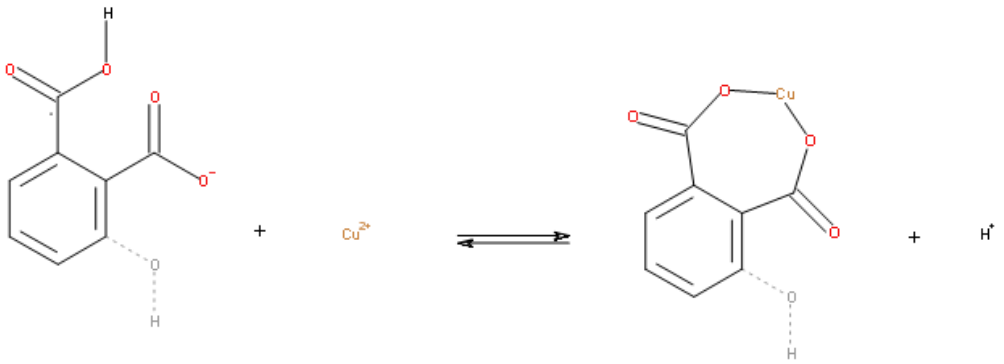

Figure 2.5. Reaction of complexation between Cu^{2+} and phthalic acid to reproduce the reaction between copper and one binding site of fulvic acid.

The distinction between different binding sites has also been approached by Hering and Morel (1990) from a kinetic point of view. They showed that humic acid had also two sites for copper binding with two different reaction pathways, one had a slow kinetic while the other reaction was fast. Unfortunately Hering and Morel (1990) did not specify any sites but a correlation can be made with the work from Gamble et al. (1970) and Plaza et al. (2006). The reaction between phenolic and carboxylic groups was dominant by the kinetic, which is influenced by steric effects and electrostatic factors.

Previous paragraphs showed that metals are bound with humic substance through some of their functional group such as carboxylic, phenolic or amino groups. The binding between those groups and the metal occurs following an acid-base reaction where the proton can be considered as competitive ion. The metal complexation is consequently highly dependent of the pH (Fletcher and Beckett, 1987). The acid-base property of each functional group described in figure 2.6 determined their capacities to bind with metals. An increase of pH increases the chelation of weak acid ligands with metals by reducing the competition between protons and metals due to a limitation of the proton availability (Ryan et al., 1983). Fletcher and Beckett (1987) also showed that a variation of pH did not change the specific site affinity with the metal ion but only affected the proton affinity. Cheng et al. (1975) noticed that metal complexation by fulvic acid had a pH dependence with a decrease of the pH inducing an increase of metal solubilisation. However, this dependence was not equal for the different metals. Complexation of zinc and nickel with humic substance were very pH sensitive and the complexation

occurred only around a neutral pH. Copper complexation only varied for acidic solution and the degree of binding did not evolve for a pH over 7. Fletcher and Beckett (1987) obtained similar phenomena with most of the copper bound with soluble organic matter for a pH over 6 and the maximum binding was obtained at pH 6.5.

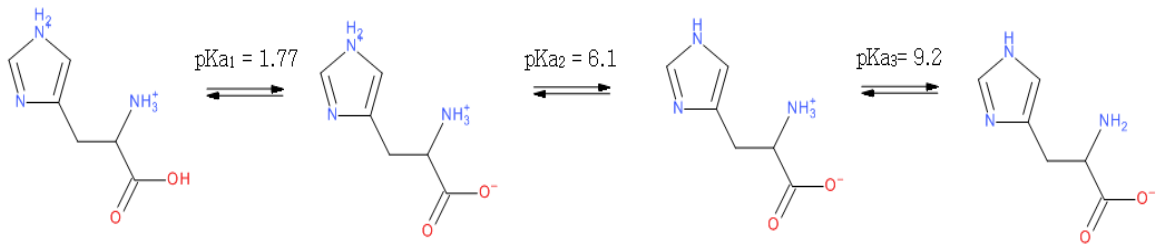

Figure 2.6. Acid and conjugate base forms of histidine (pKa given at 25°C)

Natural organic matter plays a role in the metal speciation in anaerobically digested sludge. The multiple binding sites present and their different affinities with metals allow a wide of range of degree of complexation. The presence of small organics can reduce the percentage of metals in their free form by sequestrating the metals into metal-organics complexes while keeping them in the liquid phase (Saar and Weber, 1982). Humic acids and other organic matters also react with metals and keep them in the solid phase. The degree of complexation of metals by humic substances is highly dependent of the sludge pH as protons are the main competitive ion to the organics' functional group. Under anaerobic digester conditions, the neutral-basic pH favours the metal complexation over proton competition, confirming the role of organics chelation on the speciation of metals.

The pH titration methods (section 4.3.4) used this influence of pH on the metal complexation to determine quantitatively the impact of organics in the study of metals speciation in the solid phase of anaerobically digested sludge.

2.6. Impact of EDTA on metals speciation in anaerobically digested sludge

Humic substances have the ability to bind metals (particularly copper) under AD conditions; nonetheless they form weaker complexes than metal-sulphide precipitates (Fermoso et al., 2009). However, presence of synthetic organics such as EDTA or NTA can form stronger complexes with metals and influence metals precipitation (Fermoso et al., 2009, table 2.4). Oleszkiewicz and Sharma (1990) and Aquino and Stuckey (2007) showed that EDTA was the organic compound offering the strongest binding to metal in comparison with NTA or citrate. This strong binding capacity of EDTA is related to the presence of six available sites that bound with the metal to sequester it and avoid any direct attack from other ligands (figure 2.7). Two liaisons are made with the two amino groups and the four others by the carboxylic groups. So MeEDTA chelate forms a stable octahedral system following the crystal field theory. In comparison, NTA can only form 4 liaisons with metals and so the complex required two more ligands (principally water) to complete the octahedral system and so its stability is reduced (figure 2.8).

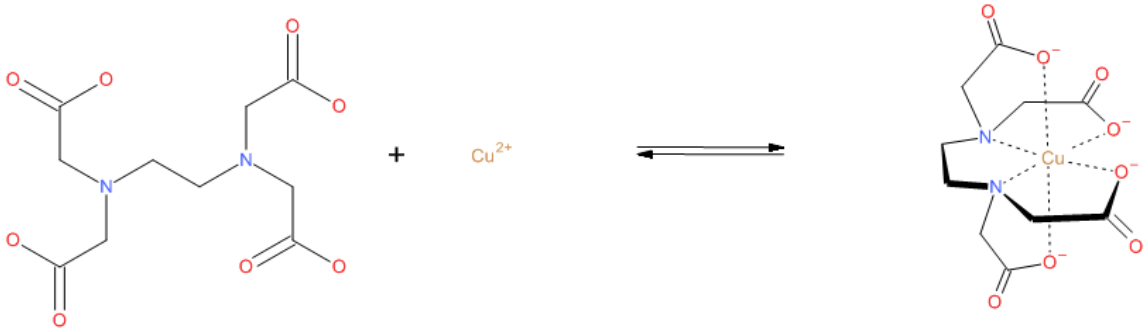

Figure 2.7. Complexation reaction between copper ion and EDTA

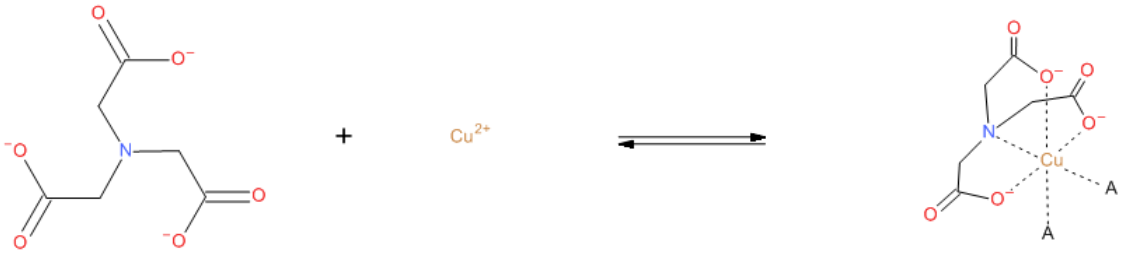

Figure 2.8. Complexation reaction between copper ion and NTA

The presence of EDTA in anaerobically digested sludge increases the concentration of metals in the liquid phase by forming strong metal-organic chelates (Fermoso et al., 2009 and Bartacek et al., 2008). Metals adsorbed onto sludge may be removed by EDTA that acts as a washing agent (Osuna et al., 2004) and reduces the extracellular polymeric substances (EPS) binding capacity (Alibhai et al., 1985). EDTA may also bind and extract metals precipitated as carbonates or phosphates (Smith, 2006) and Stover et al. (1976) used EDTA as extracting agent in their sequential extraction procedure. The metal toxicity is also not affected by the increase of metals concentrations in the liquid phase as metals bound with EDTA are protected from any extracellular polymers and cell wall's site binding as the EDTA forms stronger chelate (Hayes and Theis, 1978). Fermoso et

al. (2008b) calculated that the concentration of free nickel was reduced from 2.10^{-3} µM to 10^{-7} µM in presence of EDTA and Bartacek et al. (2010) found that between 89% to 98% of nickel in solution was as (NiEDTA). Moreover the reduction of free metal form in solution reduced the potential toxicity of some metals by its complexation (Bartacek et al., 2008).

Table 2.4. Chelate stability constant for the six metals under study with EDTA and NTA

Complex	pK_{sm}	Reference
Ethylenediaminetetraacetic acid (EDTA)		
CoEDTA	16.3	Högfeldt (1982)
	16.2	Callander and Barford (1983)
CuEDTA	18.9	Högfeldt (1982)
	18.3	Callander and Barford (1983)
FeEDTA	14.2	Högfeldt (1982)
	14.3	Callander and Barford (1983)
MnEDTA	14.1	Högfeldt (1982)
	13.6	Callander and Barford (1983)
NiEDTA	18.7	Högfeldt (1982)
ZnEDTA	16.2	Högfeldt (1982)
	16.3	Callander and Barford (1983)
Nitrilotriacetic acid (NTA)		
CoNTA	10.6	Callander and Barford (1983)
CuNTA	13.3	Högfeldt (1982)
	12.8	Callander and Barford (1983)
FeNTA	1.2	Högfeldt (1982)
	8.8	Callander and Barford (1983)
MnNTA	7.4	Callander and Barford (1983)
NiNTA	11.3	Högfeldt (1982)
	11.3	Callander and Barford (1983)
ZnNTA	10.5	Högfeldt (1982)
	10.5	Callander and Barford (1983)

Metals with humic substances form generally weaker chelates than some metal precipitates (sulphide) and may have an impact only for copper speciation due to its high capacity to form metal-organic compounds. Buzier et al. (2006) found that between 84% and 94% of the copper was present in municipal wastewater as metal-organic complexes. Its impact is less for nickel, cobalt and zinc and unlikely for manganese and iron; those have the smallest stability constant with organics. However presence of strong chelating agents such as EDTA or NTA may compete with metal precipitation and increase the concentration of metal into the soluble fraction without increasing their availability for microorganism. For insoluble and large organic molecules the complexation of metal can be associated with sorption process that is described below.

2.7. Sorption of metals in the solid phase under anaerobic condition

The sorption of metals by the biomass and other solids (e.g. dead cells or inorganic precipitate) represents another part of the metals speciation in the solid phase (Figure 2.1). Artola et al. (1997) found that some amino acids and others groups present on the cell surface were used as binding sites for metals and could be assimilated to the complexation of metals by organics. The main mechanism of the binding is carried by ion-exchange process between proton and metals. In addition to chemisorptions on minerals, cobalt was found to be adsorbed onto EPS produced during the microbial activity (Van Hullebusch et al., 2006). The biomass sorption is also dependent on the pH that affects the binding sites competition

(Osuna et al., 2004; Artola et al., 1997, Alibhai et al., 1985, Fristoe and Nelson, 1983).

Sorption processes in anaerobic digestion can also occur on mineral supports; principally sulphide precipitates (Jong and Parry, 2004). Van Hullebusch et al. (2006) found that cobalt had a high affinity with iron sulphide precipitates in anaerobic granular sludge and agreed with Watson et al. (1995) that found an adsorption of cobalt and nickel onto FeS. The adsorption of metal onto mineral is difficult to distinguish with co-precipitation that has been developed earlier in this chapter. Co-precipitation is the inclusion of metals into the solid and adsorption is only a reaction occurring on the surface of the solid.

Adsorption processes and equilibriums are generally calculated using isotherms. The two main isotherm used are Langmuir isotherm (Jong and Parry, 2004; Van Hullebusch et al., 2006) and Freundlich isotherm (Van Hullebusch et al., 2006). The difference between the two isotherms is the potential of obtaining a saturation of the adsorptive surface (Langmuir isotherm). Van Hullebusch et al. (2006) also used an intermediate isotherm, Redlich-Paterson, which can be reduced to the Langmuir isotherm when β is equal to 1.

Those isotherms have been applied to the equilibrium between soluble and solid fraction and Langmuir isotherm presented the best fit for metal adsorption (Jong and Parry, 2004 and Van Hullebusch et al., 2006). However, Van Hullebusch et al. (2006) noticed that concerning the cobalt accumulation in the carbonate and

exchangeable fraction, a Freundlich-type isotherm was followed. Gould and Genetelli (1978) also found that for the adsorption, as chemisorption, Freundlich isotherm was superior to the Langmuir isotherm.

2.8. Metals speciation in the liquid phase under anaerobic condition

Concentration of metals present in the liquid phase is lower than in the solid phase. The percentage of metals in the liquid phase represents only between 0.5% and 4% of their total concentrations (Oleszkiewicz and Sharma, 1990). This fraction contains free metal ions, metal-organic compounds and inorganic molecules. Inorganic molecules and/or ions are intrinsically linked with the precipitates present in the solid phase and consequently the main compounds are for example, MeS and $MeCO_3$ (Jansen et al., 2007; Fermoso et al., 2009) or $Fe(HS)^+$ and $Fe(HCO_3)^+$ (Callander and Barford, 1983b). Soluble metal sulphides (and carbonate) are strongly bound and their reactivity is consequently reduced (Fermoso et al., 2009). Metals, which are bound with hydroxide or halogen are more reactive due to a weaker binding (Fermoso et al., 2009).

Soluble organic compounds complexing with metals have two origins. The first group is produced by microorganisms and have a tendency to be mainly bound with Zn, Ni and Cu (Fermoso et al., 2009). The second group of organics, such as EDTA or NTA, comes from wastewater entering into the anaerobic digester in the same time as the sludge. The attraction between metals and these compounds

allows the metals to stay in the liquid phase; but metal in those forms are not necessarily available (Osuna et al., 2004; Fermoso et al., 2008a, Zhang et al., 2003). Fermoso et al. (2008a) investigated the difference between a cobalt supplementation with $CoCl_2$ versus $CoEDTA^{2-}$ and found that presence of EDTA prevented metal precipitation or sorption. However, they failed to prove that EDTA increased the bioavailability. Finally, in the liquid phase (figure 2.1), only a small fraction remains bioavailable to microorganisms (free metal ions or specific biological organic chelates).

Metals speciation in anaerobic digesters has only been partially understood and research on all the mechanisms, including the factors controlling metals behaviour and bioavailability, need to be undertaken in order to optimize digester performance. This lack of information on metals speciation is mainly due to the complexity of the anaerobic digester, which limits the use of the different analytical techniques in the study of metals and their speciation.

2.9. Study of metals speciation in natural biological systems

Study of metals behaviour in natural biological systems has been generally done to control their toxicity in the media. The different environments are soils, sludge amended soil, dust and sewage sludge. The use of sewage sludge as fertilizer is dependant on the heavy metal content and limits have been established to avoid any contamination and potential bioaccumulation (Fuentes et al., 2008 and

Carlson and Morrison, 1992). However, the use of metals total concentrations to assess their potential toxicity is not satisfactory (Adamo et al., 1996 and Pueyo et al., 2008) and so different analytical techniques have been developed to evaluate metals behaviour, lability and mobility.

The importance of metals speciation over metals concentration is not only limited to soil but also for aquatic organisms (Hassler et al., 2004), dust (Barnejee et al., 2002) and sewage sludge (Mingot et al., 1995 and Scancar et al., 2000). Single extraction and sequential extraction procedures have been developed to evaluate metals mobility and/or bioavailability in sludge, soil or sediment (Chao et al., 2006). Other techniques have also been used to characterize metals speciation in the solid phase such as X-ray diffraction spectroscopy (XRD), scanning electron microscopy coupled with energy-dispersive X-ray spectroscopy (SEM-EDS) or X-ray absorption spectroscopy (XAS) (Bertrand et al., 2003; Hassler et al., 2004 and Gonzalez Gil et al., 2001) and in the liquid phase such as donnan membrane technique (DMT) or anodic stripping voltammetry (ASV) (Kalis et al., 2006 and Fitch and Hemke, 1989).

The importance of those techniques in the aim of establishing the metals speciation in anaerobic digestion can be subjected to some approximation due to the different condition of the matrices. So the results found cannot be directly used or compared with metals chemical forms in anaerobically digested sludge as the difference of condition, such as temperature, redox potential and pH, has a strong impact on the metals behaviour. The change in the redox potential between

anaerobically digested sludge and soil alters the oxidation numbers of metals and other ions, mainly iron and sulphur. Andres et al. (2008) found that redox potential in soil varies between 50 mV to -125 mV, and anaerobic condition starts for a redox potential below -250 mV. At soil redox potential and neutral pH (6.5-8), sulphur is present as S (VI) and iron as Fe (II) but also Fe (III) (for high redox) (Takeno, 2005). Under anaerobic condition sulphur is present as S (-II) and iron exclusively as Fe (II). This difference has an impact on metals speciation, favouring MeOH, $MeCO_3$ and $MeSO_4$ precipitation for high redox potential rather than MeS for low redox potential. So the extraction procedures have been developed in function of those precipitates and they may not be completely adapted to be used for anaerobically digested sludge.

However, similarities between the different environmental media such as soil, sediment or sludge allow the transfer of analytical techniques from one medium to another. All the media are organically-rich and their compositions contain similar cations (Ca, Mg, Na and K), anions (P, S, N) and metals (Fe, Cu, Mn, Ni and Zn). Moreover the reaction occurring between the different elements are also similar and represent mainly sorption, complexation and precipitation reactions. The different techniques developed in the study of metals speciation are able to detect a wide range of metal forms as the conditions that influence the reaction products vary widely in soil and sludge samples. The anaerobic condition present in the digested sludge is included in this range and so the information gathered on this difference can be used in our research.

2.10. Methods used in the characterization of metals speciation in natural biological systems

The analysis of the metals species in natural biological systems has to be done quantitatively and qualitatively. However, it is complicated to achieve both using only one analytical technique and so a combination of techniques is used to obtain the maximum of information. The identification of the different metal forms present in the environmental samples can be made by measuring the strength of the metal bonding (e.g. sequential extraction procedure), the molecular composition of the compound (e.g. X-ray fluorescence spectroscopy, energy dispersive X-ray spectroscopy) or its size (filtration) and finally by measuring the valence state of the metal (e.g. X-ray absorption spectroscopy).

Sequential extraction procedure is a chemical method used to separate and quantify different fractions of the metals speciation. The principle behind the process is based on releasing different metal fractions using chemical reagents. Dodd et al. (2000) expressed that metals are extracted in function of their reactivity rather than their individual characterizations. The first applications of sequential extractions were developed by Stover et al. (1976) and Tessier et al. (1979) in the 1970's. These methods have since been applied and improved on a range of different materials including; anaerobic granular sludge (Van Hullebusch et al., 2005), sewage sludge (Perez-Cid et al., 1996) and contaminated soil (Pueyo et al., 2008). The Bureau Communautaire de Reference (BCR) has provided a three steps sequential extraction procedure, suitable for soil and sediments to

harmonize the results between the different studies (Davidson et al., 1994; Rauret et al., 2000). This methodology has been certified by a series of inter-laboratory analysis using certified analytical grade test material (Rauret et al., 2000) and validated using certified reference materials (Pueyo et al., 2008). The BCR sequential extraction procedure has also been modified and successfully tested on sewage sludge (Van Hullebusch et al., 2005; Perez-Cid et al., 1996 and Van der Veen et al., 2007). The low number of fractions, in comparison with other procedures, increases the reliability (by a reduction of loss materials) and allows for its use in large scale application. However, the main disadvantage is a lack of characterization of the metal binding by a simultaneous extraction of several precipitates, i.e. metal carbonate are dissolved during the first stage with other weakly bound compounds such as adsorbed metals.

Each of the extraction steps suffers from the difficulty of finding a single reagent suitable to dissolve qualitatively the desired substance, without attacking the other substance present in the substrate (Tessier et al., 1979). Therefore, sequential extraction procedure proceeds by extracting products form by form, beginning with readily extractable (mobile) substances moving to the more resistant, difficult to remove fraction (residual and stable compounds). The common order of applied reagents is classified as unbuffered salts, weak acids, reducing agent, oxidising agent and strong acid (Van Hullebusch et al., 2005 and Fuentes et al., 2008).

Unfortunately, sequential extraction procedures have some underlying problems that lead to inaccuracies in the results. The main issue is due to a potential

remobilization and re-adsorption of metals through alternative binding and consequently there is a distortion in the partitioning results. Sulphide precipitates, for example, are not completely dissolved using the oxidising agent and are therefore extracted during the last fractions (Adamo et al., 1996; van der Veen et al., 2007 and Gustavsson, 2012). Tessier et al. (1979) also observed a change in the overall material composition after treatment with each successive reagent. The second issue is the heterogeneity of the material that occurs as well with single extraction procedure (Tessier et al., 1979). Homogenisation by powdering or shaking aids in reducing this negative effect.

The use of sequential extraction procedure is far from being a complete technique in the study of metals speciation, and information is still missing with regards to metals binding and localization. The use of complementary techniques is therefore applied in partnership with sequential extraction procedure to characterize the metals bindings in each fraction. Dodd et al. (2000) applied a SEM-EDS analysis on each fraction of two sequential extraction procedures and demonstrated the presence of several compounds such as sulphide precipitates or calcite. Another example of the interest of combining several analytical procedures is to distinguish the chemical forms of metals extracted in the oxidisable fraction (bound with organic matter or sulphide). The use of SEM-EDS and XRD demonstrated that nickel extracted in this fraction was mainly linked with sulphide while copper was more bound with organic matter (Adamo et al., 1996).

X-Ray technology is the main analytical technique used to determine the metal chemical forms in the solid phase and the microbial-ecological structure (Osuna et al, 2004). SEM-EDS was used to determine the cluster morphology of anaerobic granular sludge and the spatial distribution of metal into the granules (Gonzalez-Gil et al., 2001). This analytical technique can also be applied to verify the presence of minerals and/or solids in environmental samples (Lobinski et al., 2006 and Dodd et al., 2000). The mineralogy of precipitates can be qualitatively determined by XRD only if it has precipitated as crystalline forms. Adamo et al. (1996) proved the inclusion of metals into metal sulphide and found some solids such as $(Fe,Ni)_9S_8$, $FeCuS_2$ and FeS_2.

Information about metals local structure in molecular complexes, oxidation states, fingerprint speciation of metal site and structure can be analysed by X-ray absorption spectroscopy (Lobinski et al., 2006). Concentrations of metals in the cell can be measured by Particle-induced X-ray emission (PIXE). PIXE is easy to manipulate, a non destructive method and allows for multi-elementary analysis. However, there is no metal location into the cells and their chemical forms stay unknown (Bertrand et al., 2003). X-ray fluorescence spectroscopy (XRF) or Synchrotron XRF measures the distribution of trace elements into cells, e.g. Cu has been found in mitochondria and Golgi apparatus (Lobinski et al., 2006).

Study of metals speciation in the liquid phase is typically done by chromatography or voltametry. Organic ligands and metal-organics concentrations might be measured by high-pressure liquid chromatography (HPLC) and the wide range of

columns offers a large number of compounds detection (Robards et al., 1991). Free metal ions are generally separated using the Donnan Membrane Technique, which has been demonstrated to be an easy and reliable method to measure only free metals (Kalis et al., 2006; Bartacek et al., 2008; Temminghoff et al., 2000). Gonzalez-Gil et al. (2003) used an adsorptive stripping voltametry to measure the metal bioavailability (regrouping free metal ion and other weakly bound metal-organic complexes).

Most of those techniques have been applied on diverse natural biological samples and unfortunately some of them cannot be applied in the study of metal speciation in anaerobically digested sludge due to the specific structure of the sludge and/or the chemical form of metals. XRD technique detects only crystalline forms and in anaerobic digesters, metals are mainly precipitated as amorphous precipitates. So the interest and limitation of each technique used in this research needs to be assessed to develop a suite of analytical techniques to obtain clear information on the metals behaviour in anaerobic digesters.

2.11. Use of geochemical equilibrium speciation models in the study of metals speciation

Visual Minteq and Phreeqc are two geochemical equilibrium speciation models that are used to simulate equilibrium state in aqueous solution. The thermodynamic database, which is shared by both programs, is used to predict

complexation, dissolved species, solubility, precipitation, multiple solid phases and adsorption. These programs have been used to predict the metals speciation in different environmental cases, such as the effects of metals leaching on different soils (Andres et al., 2008 and Jensen et al., 1999). These models can also be applied to simulate speciation models in different wastewater treatment systems (Zhang et al., 2008).

Models can be run in Visual Minteq and/or Phreeqc under the anaerobic conditions to investigate the behaviour of metals in anaerobically digested sludge. In order to apply those models, the environmental condition such as atmospheric composition, temperature, pH or redox condition must be set up to recreate the sludge condition. The main components of an anaerobic digester such as carbonate, phosphate, cations and all metals have to be added in the model at appropriate concentrations. Dissolved organic carbon (DOC) and adsorption reactions are generally included using pre-defined values in the model due to the complexity and difficulty in characterizing these parameters in anaerobic digesters.

The amounts of precipitates, complexed and adsorbed metals are estimated using thermodynamic constants and equations. Previous studies have reported that the predictions of precipitation during the process are closed for the experimental results. Celen et al. (2007) used Visual Minteq to predict the production of struvite ($(NH_4)MgPO_4 \cdot 6H_2O$) and monetite ($CaHPO_4$), whilst in the experiment struvite, monetite and brushite ($CaHPO_4 \cdot 2H_2O$) were found. The third solid, brushite, was not predicted by Visual Minteq but was thought to be already present in the raw

wastewater. Zhang et al. (2008), found good agreement between Minteq's solid prediction and experimental results, but pointed out that there are some unresolved issues regarding re-precipitation with Visual Minteq. Complexation of metals with organic compounds is predicted by Visual Minteq in the same way as precipitation using K_{sm} values. However, Serkiz et al. (1996) found several errors in the Visual Minteq calculation for some organic compounds.

A submodel, ligand model, has been developed for the metals chelation using a Gaussian affinity distribution. Only one site is characterized as "carboxylic" and no electrostatic interaction is taken into account. This model is not totally satisfactory and it is improved by adding a second type of binding (Christensen et al., 1999). Another model, NICA-Donnan, has been used by Unsworth et al. (2006) to describe binding between metals and humic substances. This model uses bimodal, continuous distribution of affinities for protons and metal ions. Unsworth et al. (2006) pointed out that this model predicted the distribution of predominant species but under-estimated free metal ion. One of the main examples of the use of Minteq on anaerobic digester is the comparison between experimental and predicted values done by Aquino and Stuckey (2007). They used the model to predict the impact of the addition of NTA and EDTA in anaerobic digester by measuring methane production and dissolved metals. Unfortunately, they only used Minteq as a suggestion and they did not really compare the Minteq prediction with the real metals speciation found during their experiments.

The use of chemical equilibrium models has been proven useful in the study of metals speciation in environmental samples. However, models cannot be sufficient on their own and are more useful as complementary data from experimental results. The models establish their simulation following only thermodynamic constants and they do not take into account the kinetic impact on the metals speciation. The other disadvantages are the lack of clear information on the different reactions (mainly sorption model and organic reactions) and the underestimation of secondary reactions that can occur under anaerobic condition.

2.12. Review of previous research and knowledge gaps

The growing interest surrounding anaerobic digestion has developed a requirement for an increased understanding on the reactions occurring in the digesters from a biological, physical and chemical point of view. The work undertaken by the International Water Association (IWA) throughout its anaerobic digestion model 1 (ADM1) showed the biological and physic-chemical relations, interactions and reactions present in an anaerobic digester (Batstone et al., 2002). However, the model lacks a clear understanding with regards to solid precipitation and metals speciation, neither of which has been explored in sufficient detail. Some metals have been found to play an important biological role in the anaerobic digester and a metal deficiency has a direct impact on the biogas production (Ishaq, 2012; Fermoso et al., 2008b&c; Fermoso et al., 2009; Lin et al., 1998).

The availability of metals is not only dependent on its concentration in the sludge but on their speciation (Adamo et al., 1996; Hassler et al., 2004 Oleszkiewicz and Sharma, 1990 and Hayes and Theis, 1978). So it is essential to understand the behaviour of metals in order to control the increase of the metals bioavailability, if required.

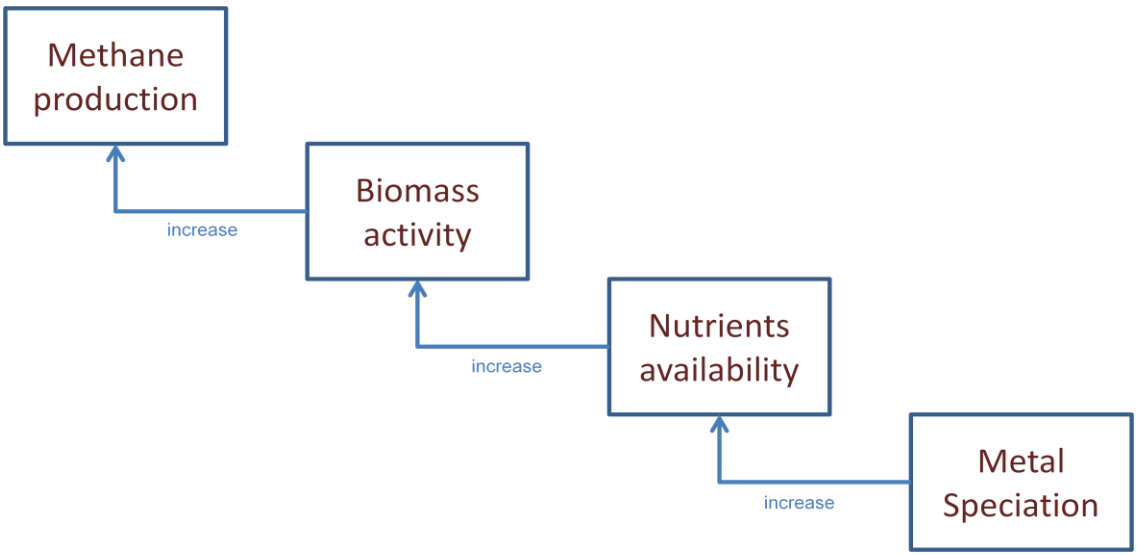

Figure 2.9. Enhancement of the biogas production from the study of metals speciation

Metals supplementation has been used to fulfil the metals requirement needed to obtain a good biomass yield (figure 2.9). Several research investigations have been undertaken to study the benefits of metals supplementation on the biogas production. They observed that beneficial effects were dependent on the added metals chemical forms and their behaviour in anaerobically digested sludge (Fermoso et al., 2008a and Zandvoort et al., 2006). So the enhancement of biogas production by metals supplementation requires a full understanding of the metals speciation and behaviour in anaerobic digesters.

The interest on metals speciation in anaerobic digesters originated from the work done by Callander and Barford (1983a&b), who used thermodynamic constants to measure metal precipitations with inorganic compounds (PO_4^{3-}, CO_3^{2-} and S^{2-}) and metal complexation with organics. Subsequent research by different groups have explored in more details different metals in sludge but most have tended to look at specific parts of the speciation (Francis and Dodge, 1990; Van Hullebusch et al., 2006), metals (Gonzalez-Gil et al., 2003; Fletcher and Beckett, 1987) or materials (Chao et al., 2006), rather than taking a global, holistic view. The majority of research reports on the mobility and availability of heavy metals in sludge and contaminated soil for the purpose of the sludge disposal (Andres and Francisco, 2008; Lake et al, 1989; Pueyo et al., 2008 or Scancar et al., 2000). Other papers have focussed on the relationship between metal and bacteria, uptake and toxicity (Aquino and Stuckey, 2007; Bartacek et al., 2008; Fermoso et al., 2008 and Zhang et al., 2003).

The lack of global information on the metals speciation is mainly due to the complexity of metals analysis in anaerobically digested sludge. One of the main methods used in the study of metals speciation in environmental samples is sequential extraction procedures (Fuentes et al., 2008; Van Hullebusch et al., 2005; Solis et al., 2002; Perez-Cid et al., 1996 and Chao et al., 2006). However, those procedures are not powerful enough to obtain a clear understanding of metals behaviour in anaerobic digesters and several issues have been pointed out on the fraction definition and/or the extraction of some chemical forms (Perez Cid

et al., 1999; Pueyo et al., 2008 van der Veen et al., 2007 and Gustavsson, 2012). Complementary techniques, such as SEM-EDS or XRD, have been used to identify qualitatively or quantitatively some specific metal chemical forms or precipitates in the sludge (Fermoso et al., 2009; Osuna et al., 2004; Gonzalez-Gil et al., 2001 and Dodd et al., 2000).

So an assessment of those analytical techniques to study the metals speciation and the development of a method combining several analytical techniques is necessary prior to any research on the chemical behaviour of metals in anaerobically digested sludge. Moreover, geochemical equilibrium speciation models need also to be combined with experimental values in order to develop a suite of techniques able to determine precisely the metals behaviour in anaerobically digested and predict the fate of supplemented metals in anaerobic digesters.

CHAPTER 3. AIMS AND OBJECTIVES

Within this chapter, the aims, hypotheses and objectives of this research are presented. The accomplishment of some objectives was done across several chapters of this thesis. The chapters concerning each objective have been noted in brackets.

3.1. Research aims

The first aim of this research was the determination of the behaviour of the six main essential metals (Co, Cu, Fe, Mn, Ni and Zn) in the solid phase of anaerobically digested sludge by the characterization of the metals speciation and the chemical reactions governing it.

The second aim of this research was the characterization of the mechanisms controlling the fate of supplemented metals in the case of supplementation using metals bound with EDTA solution.

3.2. Research hypotheses

The metal speciation can be represented as a basic model where metals species are divided in two phases : solid and liquid phase (filtration limit at Ø = 0.45µm).

There is an equilibrium relationship between these two phases depending on the AD condition (temperature, potential redox, HRT and SRT) and composition (elements concentration).

The solid phase is considered to be the central and controlling phase for the metals speciation.

Finally, addition of metals in anaerobically digested sludge disturbs the equilibrium between solid and liquid phase and influences the metals speciation.

"If a chemical system at equilibrium experiences a change in concentration, temperature, volume, or partial pressure, then the equilibrium shifts to counteract the imposed change and a new equilibrium is established". LeChatelier (1885)

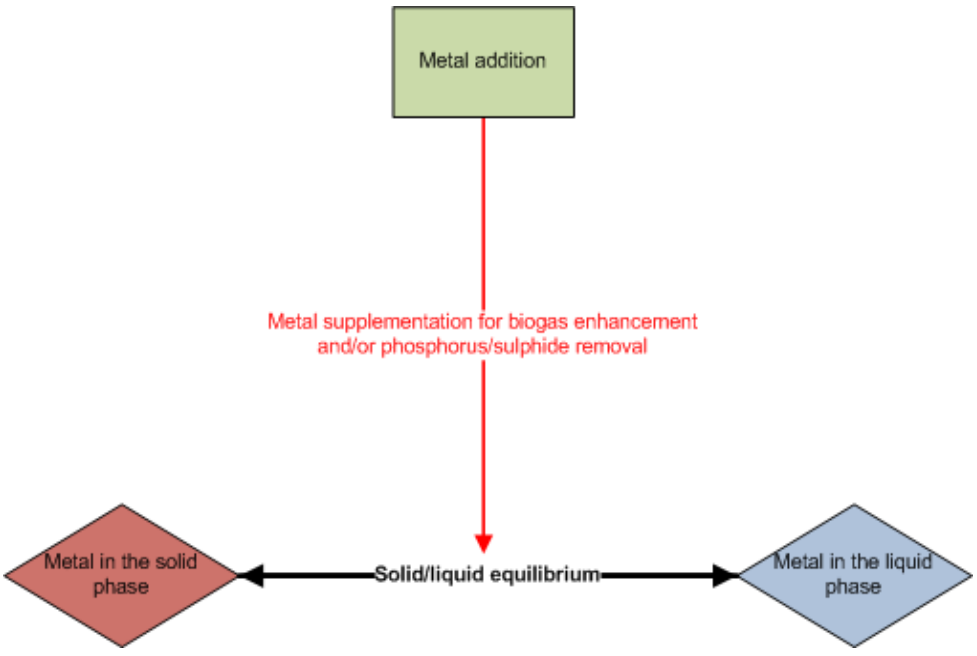

Figure 3.1. Illustration of the research hypotheses

3.3. Research objectives

To successfully respond to the aims, the research objectives (figure 3.2) were:

- Investigate different analytical techniques used in the study of metals speciation in environmental samples and assess their use, interest and limitation in order to develop a suite of techniques to characterize the metals behaviour in anaerobically digested sludge. (*Chapter 5*)

- Characterize the metals speciation in the solid phase of anaerobically digested sludge using two case studies of metals supplementation; iron dosing for chemical phosphorus removal (CPR) and MeEDTA supplementation for the enhancement of the biogas production *(Cu and Ni in chapter 5; Fe in chapter 6; Mn, Zn and Co in respectively sections 7.3, 7.4 and 7.5)*

- Investigate the effect of metals addition on the metals speciation in the solid phase in the two case studies mentioned above to characterize the reaction controlling the metals speciation *(Fe, chapter 6; Mn section 7.3 and Co section 7.5)*

- Investigate the impact of metals supplementation on the solid/liquid phases equilibrium in anaerobically digested sludge to evaluate the effect of EDTA on the fate of supplemented metals *(sections 7.2 and 7.6)*

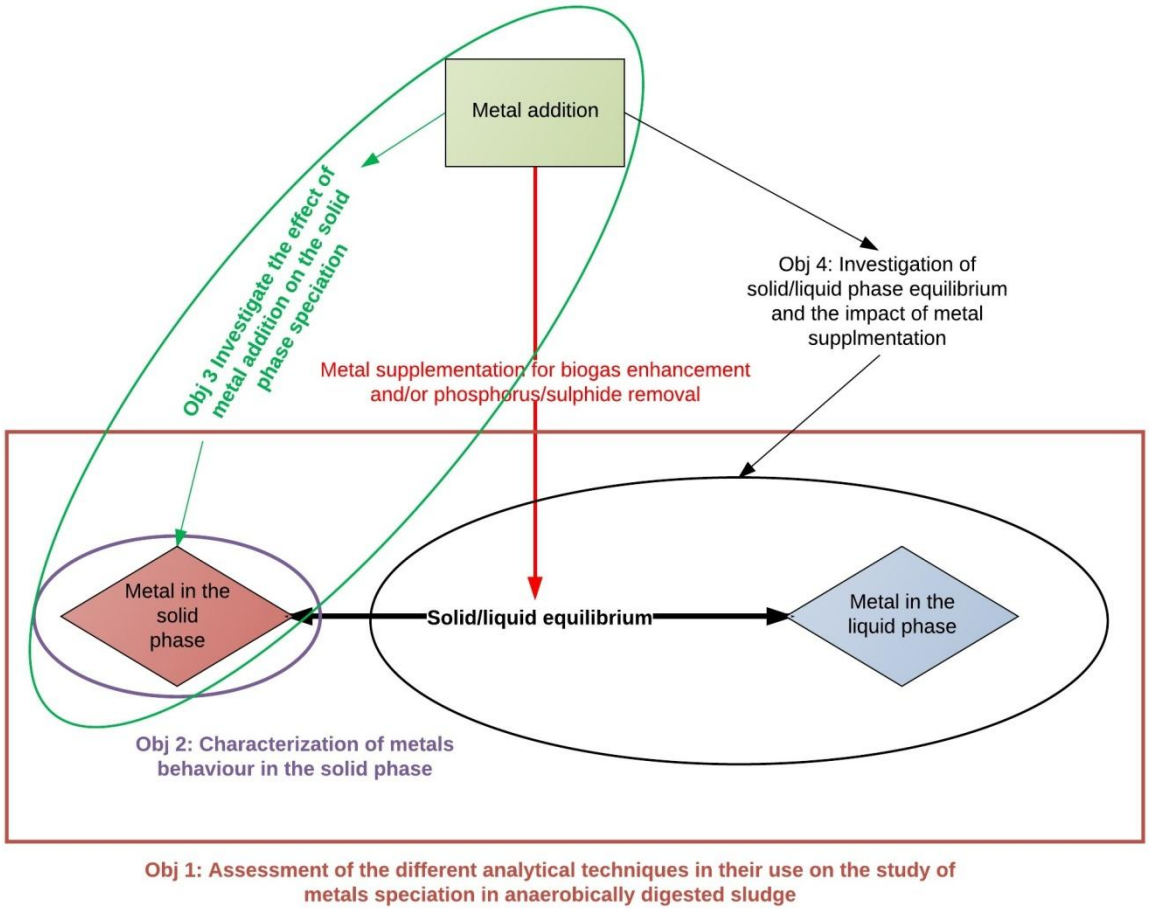

Figure 3.2. Illustration of the research objectives

CHAPTER 4. MATERIALS AND METHODS

Within this chapter, the main materials and methods used throughout this research are detailed in five sections.

- The first section, experimental set-up, presents the two main experiments used in the two case studies.
- The second section, general sludge analysis, details the different analytical techniques used to characterize the different type of anaerobically digested sludge.
- The third section, metals extraction techniques, presents the different techniques used to extract metals from the solid phase.
- The fourth section, elemental analysis, details the different techniques used in the analysis of metals, cations, anions, organics and precipitates.
- The last section, geochemical equilibrium speciation models, presents the two models used to simulate the metals speciation in the solid and liquid phases.

4.1. Experimental set-up

4.1.1. Full scale anaerobically digested sludge analysis experiment

Full scale anaerobically digested sludge analysis (FSADSA) experiment was developed to obtain an overview of the metals speciation in different anaerobic digesters. Seven West Midlands wastewater treatment plants (WWTP) were

chosen for this experiment. Sludge was collected twice over a period of a month. Four types of sludge were collected each week (2 on Monday and 2 on Tuesday) during 3 weeks and only two types of sludge (Tuesday) the last week. The main criterion was the presence or not of iron dosing during the wastewater process or the import of iron dosed sludge from other WWTPs (mix). The details of the WWTP anaerobic digesters are described below in table 4.1.

Table 4.1. Information on the seven anaerobic digesters and WWTPs used during FSADSA experiment

Sludge	Population equivalent (p.e.)	Number of digesters per site	Digester capacity (m^3)	Average Site feed /24hrs (m^3)	Iron-dosing	Collection Date
F	427,000	8	18,000	880	yes	16/03/2010 & 23/03/2010
G	258,000	3	9,000	690	no	08/03/2010 & 15/03/2010
H	131,000	2	6,000	250	mix	08/03/2010 & 15/03/2010
K	106,000	3	7,000	525	no	01/03/2010 & 09/03/2010
M	1,638,000	16	83,000	3,600	mix	02/03/2010 & 23/03/2010
R	82,000	4	11,000	500	yes	01/03/2010 & 09/03/2010
S	190,000	2	11,00	820	mix	02/03/2010 & 16/03/2010

Sludges were collected directly from the anaerobic digester and kept sealed in a hermetic container during transport. Arriving in the laboratory, pH and redox potential were the first measurements done on the sludge and the values are shown in table 4.2 (with alkalinity, VS and TS measurement). Then the liquid and solid phases were separated by centrifugation (6000 rpm for 10 min). Solid phase

was kept in polyethylene bottle and stored at 4°C. The liquid phase was filtered at 0.45 µm and stored in polyethylene bottle at 4°C (section 4.2).

Table 4.2. Sludge conditions measured at the sludge arrival (FSADSA experiment)

Sludge	pH	ORP (mV)	TS (g/l)	VS (g/l)	Total Alkalinity ($mgCaCO_3/l$)
F	7.25	-350	25	18	5,300
G	7.25	-330	22	15	4,800
H	7.15	-280	23	15	4,200
K	7.4	-345	18	13	3,500
M	7.2	-290	23	16	5,200
R	7.3	-260	20	14	3,900
S	7.1	-330	21	15	5,600

On the arrival day, several analyses on the sludge were undertaken such as dry solid/volatile solid, alkalinity (table 4.2) and first stage of the BCR sequential extraction (section 4.2). Total acid digestion extraction was done at the same time as the last stage of the BCR sequential extraction (3 days after collection).

4.1.2. Metals supplementation experiment

The metals supplementation experiment was based on laboratory scale anaerobic digester simulation. Destructive serum bottles were used as digesters to observe any change in the metals speciation during the digestion.

Anaerobically digested sludge was collected from a full scale WWTP anaerobic digester and inoculated into the serum bottle with feed (acetate) and metals solution. Same condition between the bottles were insured by the inoculation of the same concentration of volatile solid (VS) and feed. The composition of each bottle was 0.5 g of VS and 60 mmol of acetate buffer (99.75% sodium acetate and 0.25% glacial acid acetic). The 100 ml of the inoculums and feed was inoculated in the 120 ml serum bottle leaving 20 ml headspace for the gas production (figure 4.1).

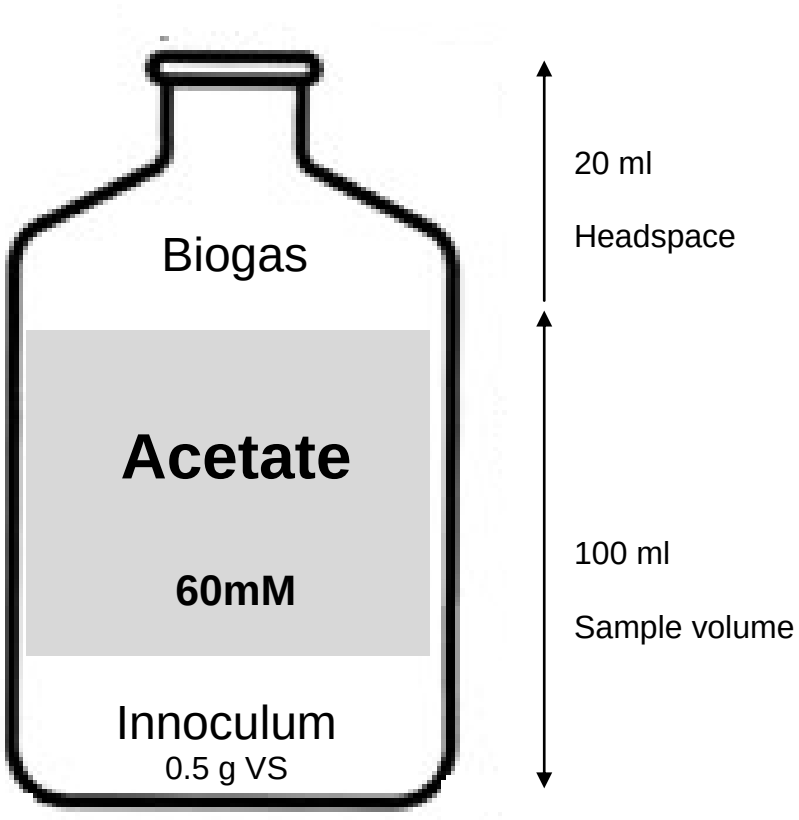

Figure 4.1. Illustration of metals supplementation experiment (Ishaq, 2012)

Two solutions containing metals from OMEX© were used to measure their impact on the metals speciation and the gas produced by aceto-methanogenesis. The

first solution, TMC, was a mix of different essential metals with specific concentrations. The main elements present in the solution and analysed in this research were iron (6.72 ppm), cobalt (2.24 ppm), manganese (2.24 ppm), nickel (2.24 ppm), zinc (0.224 ppm), copper (0.0224 ppm). Other trace elements were also contained in the solution but they were not taken into account in the analyses. All those elements were bound with EDTA with a molar ratio of 1:1. The second solution (CoA), provided by OMEX©, contained only cobalt bound with EDTA at the standard concentration of 2.24 ppm. A solution (CoAx2) with a concentration of cobalt of 4.48 ppm was also used. A blank solution (feed without any metal addition) was used as reference and control.

Experiments were conducted during a period over approximately 12-14 days. The mixing was limited to hand shaking (3 times per day). Serum bottles were destructed over this period to analyze metals concentrations and speciation in the liquid and solid phases. Gas production was measured regularly in the serum bottles to release the gas pressure and confirm the microorganism activity. Gas measurement was also used to certify the uniformity between the different serum bottles (see appendix A).

Two sludges (F and K) have been used during this experiment (chapter 7). The details of the two anaerobic digesters were the same as for the FSADSA experiment and are described in table 4.1. Two sets of each sludge have been used; sludge F and K (called F1 and K1 in section 7.6) for all sections of the

chapter 7 and sludge F2 and K2 for the section 7.6 only. The conditions of the two types of sludge are shown in table 4.3.

Table 4.3. Sludge conditions measured at the sludge arrival (metals supplementation experiment)

Sludge	pH	ORP (mV)	TS (g/l)	VS (g/l)	Total Alkalinity ($mgCaCO_3/l$)
F/F1	7.2	-350	24	18	5,200
F2	7.2	-355	23	17	5,250
K/K1	7.45	-340	20	14	3,600
K2	7.4	-345	19	14	3,650

4.2. General sludge analysis

4.2.1. Solid and liquid separation

Solid and liquid phases were obtained from the sludge by centrifugation. The separation was achieved using a centrifuge set at 6,000 rpm for 10 minutes. The liquid, after a filtration at 0.45 µm, and solid were stored in two different polypropylene bottles at 4°C prior to future analyses.

4.2.2. Total and volatile solids

The total solid, volatile solid and dry solid contents were measured in triplicate. The procedure is described in the Standard Method (2540 G, APHA-AWWA-WEF,

1998). All the tins were washed, dried, heated at 500°C and cooled at ambient temperature in the desiccators prior their uses. Tins were first weighted (W_t) and then sample (25 ml (V_s) of sludge or 1-3 g of solid) was added. Then tin and sample were weighted (W_{hs}). Samples were placed in an oven at 105°C for a minimum of two hours and then they were cooled off at ambient temperature in the desiccators prior to be weighted (W_{ds}). Samples were placed again in a furnace at 500°C for a minimum of 1 hour. Then they were cooled off and weighted (W_{vs}).

The total solid was measured by:

$$TS\ (g/l) = (W_{ds}-W_t)/V_s$$

The volatile solid was measured by:

$$VS\ (g/l) = (W_{vs}- W_{ds})/ V_s$$

The dry solid percentage was measured by:

$$\%DS = ((W_{ds} - W_t)/(W_{hs} – W_t)) \times 100$$

4.2.3. Alkalinity

The method used to measured alkalinity is described in Standard Methods (2320 B, APHA-AWWA-WEF, 1998). A 10 ml of sample was added in a beaker and mixed during the titration. Normalized sulphuric acid at 0.1 N was used as reagent and a calibrated pH meter to indicate the pH end point (4.5).

Alkalinity was measured using the volume of reagent (V_a) needed to obtain the pH 4.5 in function of the volume of sample (V_s). The total alkalinity was measured by:

$$TA\ (mg\ CaCO_3/l) = V_a \times 0.1 \times 5000 / V_s$$

4.2.4. Dissolved and total organic carbon

DOC was measured in the liquid phase after 0.45 µm filtration while TOC was measured on the acid digested solution or BCR sequential extraction fractions. The apparatus used was a Shimadzu TOC-V CSH with an auto-sampler TOC ASI V. With this apparatus, the TOC was measured as NPOC (non-purgeable organic carbon). For NPOC measurement, the sample inorganic carbon was purged by the acidification of sample in a carbon free gas.

4.3. Metals extraction methods

4.3.1. Acid washing

All glassware and plasticware employed during any metals extraction and/or analysis was cleaned following the protocol described below to eradicate any contamination.

- Washed in hot water using phosphate-free soap.
- Rinsed thoroughly with tap and ultra pure water (UPW).

- Soaked overnight in analar-grad HCl at 10%.
- Rinsed thoroughly with UPW and soak in UPW overnight.
- Dried in hot and ventilated cabinet.

4.3.2. Total acid digestion

The total acid digestion method used an aqua regia solution to dissolve all the metal compounds present in the sludge. The method is described in Standard Methods (3030F, APHA-AWWA-WEF, 1998) and modified by Smith (2006). Health and safety considerations precluded the use of hydrofluoric acid (HF) in the laboratory hence it was not included in the total acid digestion solution. The protocol is described below:

- 0.5-0.8 g of centrifuge sludge pellet was added in a 250 ml beaker with 30 ml of UPW.
- 6 ml of analar-grad HCl and 2 ml of analar-grad HNO_3 was added in the beaker.
- Solution was heated using a hotplate and boiled until approximately 10 ml remains.
- Beaker was removed and allowed to cool to the ambient temperature.
- 30 ml UPW, 6 ml of analar-grad HCl and 2 ml of analar-grad HNO_3 was added again in the solution.
- Solution was heated and boiled until approximately 10 ml remains and the solution was cooled.

- Solution was filtered through Whatman 540 filter into a 50 ml volumetric flask
- UPW was added to flasks to bring the volume to 50 ml.

4.3.3. BCR sequential extraction procedure

Sequential extraction method used in this research followed the modified BCR procedure described by Chao et al. (2006). Sequential extraction proceeds by extracting products form by form, beginning with readily extractable substances moving to more resistant substances (stable compounds). The order of applied reagents in the BCR sequential extraction is classified as weak acids, reducing agent, oxidising agent and strong acid (Van Hullebusch et al, 2005). The interpretation of each BCR sequential extraction fraction and the reagent used is described in table 4.4

Table 4.4. Interpretation of each fraction of the BCR sequential extraction (Fuentes et al., 2008)

Fraction	Reagent	Extracted metals
Exchangeable	Acetic acid	Metal-phosphate precipitates
		Metal-carbonate precipitates
		Weakly bound metal compounds
		Adsorbed metals
Reducible	Hydroxylamine-hydrochloride	Metals incorporated within Fe and Mn oxides
		Metal-oxide precipitates
Oxidisable	Hydrogen peroxide	Metal-organic complexes
		Metal-sulphide precipitates
Residual	Aqua regia	Strongly bound metal compounds

The extractions were carried out over a period of 4 days. All extractions were performed in triplicate on the sludge. All the reagents were analytical grade. The protocol is described below:

- 0.5-0.8 g of samples (solid phase after centrifugation) were weighted in the centrifuge tube.
- 1st step (exchangeable fraction): 20 ml of 0.11M acetic acid was added in the tube and shaken at 18°C over a period of at least 16h.
- The extract was separated from the residue by centrifugation (6,000 rpm, 10 minutes), filtered (Whatman 540) in 50 ml volumetric flask completed with UPW and stored at 4°C.
- 10 ml of UPW was added in the tube and shaken for 10 min for washing. The rinse solution was removed by centrifugation (6,000 rpm, 10 minutes).
- 2nd Step (reducible fraction): 20 ml of 0.1M hydroxylamine hydrochloride after acidification at pH 2 with HNO_3 was added in the tube and shaken at 18°C over a period of at least 16h.
- The extract was separated from the residue by centrifugation (6,000 rpm, 10 minutes), filtered (Whatman 540) in 50 ml volumetric flask completed with UPW and stored at 4°C.
- 10 ml of UPW was added in the tube and shaken for 10 min for washing. The rinse solution was removed by centrifugation (6,000 rpm, 10 minutes).
- 3rd step (oxidisable fraction): 20 ml of hydrogen peroxide 30% acidified at pH 2 with HNO_3 was added in the tube, hand mixed and then transferred into a 250 ml beaker. Solution was shaken at 18°C for at least 16h.
- After an hour of shaking, 15 ml of 1.7 M ammonium acetate after acidification at pH 2 with HNO_3 was added into the beaker.

- The extract was separated from the residue by centrifugation (6,000 rpm, 10 minutes), filtered (Whatman 540) in 50 ml volumetric flask completed with UPW and stored at 4°C.
- 10 ml of UPW was added in the tube and shaken for 10 min for washing. The rinse solution was removed by centrifugation (6,000 rpm, 10 minutes).
- 4^{th} step (residual fraction): the residue was extracted as the total digestion described above.

4.3.4. pH titration

Titration was performed on the whole sludge (liquid and solid phase) to draw a pC-pH diagram for each metal. Titration was carried out in an anaerobic cabinet (under argon atmosphere) to avoid any alteration in the metals speciation. Eight different pH values were chosen to obtain 8 points on the pC-pH diagram: 2, 4, 6, 7, 8, 9, 10 and 12. The pH was adjusted with analar-grad HCl for the acid pH and NaOH for the basic pH. The procedure is described below:

- 100 ml of well-mixed sludge was added in a 250 ml beaker.
- Acid or Base solution was added to obtain the wanted pH (measured using a calibrated pH meter).
- Solution was mixed during 1h and the pH checked to avoid any change.
- Solution was centrifuged and filtered (Whatman 540).

4.4. Elemental analysis

4.4.1. Flame atomic absorption spectroscopy

Flame atomic absorption spectroscopy (FAAS) was used to measure the concentration of iron, calcium, magnesium, sodium and potassium in all the solutions obtained during the different metal extraction methods. For solution with high metals concentrations, FAAS was also used to measure the concentrations for cobalt, copper, manganese, nickel, phosphorus and zinc.

The apparatus was a Perkin Elmer AAS 800 and the flame condition followed the recommended condition by the Perkin Elmer©. The absorption wavelengths were 422.7 nm (Ca), 240.7 nm (Co), 324.7 nm (Cu), 248.3 nm (Fe), 766.5 nm (K), 285.2 nm (Mg), 279.5 nm (Mn), 589.0 nm (Na), 232.0 nm (Ni), 213.6 nm (P), 213.9 nm (Zn).

Calibration curves were calculated before any sample analysis and standard solutions were freshly made and diluted from a 1,000 ppm standard solution provided by Fisher©. Calibration curves were only accepted with a correlation coefficient of 0.999 and standard solutions were used as control (10% error) for every 10 samples measured.

4.4.2. Inductive coupled plasma-atomic emission spectroscopy

Inductive coupled plasma - atomic emission spectroscopy (ICP-AES) was used to measure the concentration of iron (low concentration), cobalt, copper, nickel, manganese, zinc, phosphorus and sulphur in all the solution obtained during the different metal extraction methods.

The apparatus was an AtomScan 16 provided by Thermo Jarrel Ash. The emission wavelengths were 228.6 nm (Co), 324.7 nm (Cu), 259.9 nm (Fe), 257.6 nm (Mn), 231.6 nm (Ni), 180.7 nm (S), 213.9 nm (Zn).

Calibration curves were calculated before any sample analysis and standard were freshly made and diluted from a 1,000 ppm standard solution provided by Fisher©. Calibration curves were only accepted with a correlation coefficient of 0.999 and standard solutions were used as control (10% error) every 10 samples measured.

4.4.3. X-Ray fluorescence and X-Ray diffraction spectroscopy

X-ray fluorescence spectroscopy (XRF) requires dry compounds for analysis and so a fraction of the solid phase was dried at 105°C before being ground. The powdered compound was mixed with a silicate gel and pressed as a pellet. The pellet was directly analysed with the S8 Tiger wavelength dispersive X-Ray fluorescence spectrometer provided by Bruker©.

Analytical results were given as weight percentage of each element (molecular weight over 16) present in the sample. The weights of elements with a lower molecular weight (from hydrogen to oxygen included) were not measured by the spectrometer but were included in the total sample weight. Compton count is an internal control that was used to assess the accuracy of the analysis. For synthesised chemical compounds, the Compton count was measured around 95-100%, but for biological compounds, the Compton count decreased around 50% due to the high concentration of oxygen, carbon and hydrogen molecules.

Concerning the X-Ray diffraction spectroscopy, the powdered samples was directly applied on the support and inserted into the Bruker© Smart 6000 CCD diffractometer. The results are shown appendix B.

4.4.4. Scanning electron microscopy coupled with energy dispersive X-ray spectroscopy

Scanning electron microscopy coupled with energy dispersive X-ray spectroscopy (SEM-EDS) requires dry compounds for analysis and so a fraction of the solid phase was dried at 105°C before being ground. The powdered compound was applied on an analytical disc and fixed with a carbon spray (carbon coated).

The microscope, XL-30 (with LaB6 filament) provided by Philips©, was fitted with a HKL EBSD system with NordlysS camera to obtain electron backscattering

pictures to observe elements with high atomic number in the samples. As high-energy electrons are more strongly reflected out of the samples by elastic scattering interactions with high atomic number element than with low atomic number, the high atomic number elements appear brighter in the picture and can easily be detected.

The microscope was also fitted with INCA EDS system provided by oxford instrument to do microanalysis on the sample using X-ray spectroscopy. The X-Rays emitted from the element initially excited were measured by an energy dispersive spectrometer. The spectrum of energy analyzed during the analysis was 0-9.5 keV.

4.4.5. Fluorescence spectroscopy

Fluorescence spectroscopy used the chemical property of some organics to absorb specific UV lights and re-emitted the energy gained as UV/visible light. Electrons from one atom or molecule were excited from their ground state to the first or second excitation level at a UV wavelength. During the relaxation time, electrons return to their ground state releasing the energy at another wavelength. Each compound possesses a single couple excitation and emission wavelength. Excitation Emission Matrix (EEM) is a technique used in fluorescence

spectroscopy to scan a range of excitation and emission wavelengths. This scan can be plotted in a 3-D graph showing the peak intensity for each Ex/Em couple.

Supernatant and BCR sequential extraction fractions were analysed using a Varian Cary Elipse fluorescence spectrophotometer provided by Agilent©. The excitation wavelengths range was from 200 nm to 400 nm and the emission wavelengths range was from 275 nm to 500 nm. Excitation step was 5nm and emission step was 2 nm. Results were collected into tables and 3D graphs were plotted.

4.5. Geochemical equilibrium speciation model simulation

Phreeqc (version 2) and Minteq (Visual Minteq version) are computer programs written in the C programming language that were designed to perform a wide range of chemical calculations. Both models have been designed for geochemical simulation but in this research, they were programmed to simulate metals reactions in anaerobically digested sludge. Some materials related to the model simulation have been included in the appendices to assist its understanding (appendix E: input values for all the simulations; appendix F: predictions of metals speciation using Phreeqc; appendix G: example of Phreeqc simulation using the sludge K; and appendix H: illustration of the Visual Minteq software).

In chapters 5 and 6, the simulations of the seven anaerobically digested sludges were performed using Phreeqc with the database minteq.v4 (already developed by USGS). Experimental values (elements concentrations and sludges conditions) were used as input values. Each element was added in the liquid phase in its atomic form. The model would determine its speciation in function of the conditions and different exchanges/reactions allowed in the simulation (appendix G).

The parameters described in the model, which represented the anaerobic digester conditions were limited to temperature, electric potential (pe) and pH. The input pH was between 8-8.2 to allow a potential charge balance during the simulation and produced an output pH value agreeing with the measured pH of each sludge (7.1-7.4). The input potential electric (pe) was -6.7 to insure anaerobic condition and avoid any oxidation during the simulation. The input values and the predicted speciation of each metal are shown respectively in the appendix E and F. An example of the sludge K simulation is displayed in the appendix G.

The model was limited to simulate inorganic reactions with no organic complexation or biomass adsorption. The only exchange between phases allowed in this simulation was solid-liquid and no consideration of the gas composition or potential H_2S exchange was considered. The exchange between solid-liquid phases was controlled by the saturation index of each precipitate.

Visual Minteq with the database vminteq30 was used to simulate the variation of iron, phosphorus and sulphur concentrations in each sludge in chapter 6. The

choice of Visual Minteq model was due to its ease of use for the simulation of the variation of one parameter, such as iron concentration or pH. The similarities of results for each sludge from the two models (using identical inputs values) were used to confirm the veracity of the simulation from the two models.

In chapter 7, Visual Minteq model was used to simulate pH titration experiments for each metal concerned using the same database (vminteq30). The sludges F and K were first simulated using experimental input values (as in chapter 6). Due to the importance of the biomass on the behaviour of some metals, soluble organic matter was added into the model using a pre-defined model (NICA-Donnan model; Unsworth et al. (2006)) to simulate the binding between metals and organics. Subsequently two titrations (one acid and one basic) were simulated using the titration option in the multiple-problem menu (see figure H.2). The volumes and concentrations of the titrants (HCl and NaOH) and sludges used during the simulations were identical to the experiments. In order to obtain a pC-pH curve similar to the experimental curve, some precipitates of the studied metal were not allowed to be formed to favour the formation of secondary compounds. These limitations have been noted in the different results sections.

Finally, Visual Minteq model was also used in section 7.6 to simulate the thermodynamic equilibrium of the sludge after addition of CoEDTA. The sludges F and K were first simulated using experimental input values and then CoEDTA solution was added using a single titration simulation.

CHAPTER 5. ASSESSMENT OF ANALYTICAL TECHNIQUES FOR METALS SPECIATION ANALYSIS

5.1. Introduction

A review of the different analytical techniques used on the metals speciation investigation in environmental samples has been done in chapter 2 (sections 2.9-2.10) and showed that their full potential was not clearly defined in their use on anaerobically digested sludge. In this chapter, an assessment of each analytical technique was achieved to determine their strengths and weaknesses to complete this research on metals behaviour in anaerobically digested sludge.

The range of assessed analytical techniques focusing on metals speciation included BCR sequential extraction (SE), scanning electron microscopy coupled with energy dispersive x-ray spectroscopy (SEM-EDS), pH titration and model simulation. One of the main limitations observed using sequential extraction procedures was the multiple compounds extraction in each fraction. So SEM-EDS analysis was used to obtain qualitative information on the inorganic fraction and to confirm or not the results suggested from the BCR sequential extraction procedure.

The pH titration was a potential complementary technique to characterize the speciation of metals extracted in the BCR exchangeable and reducible fractions.

The potential of fluorescence spectroscopy coupled with sequential extraction procedure was also explored to understand the relation between organics and metals and their extractions during the BCR sequential extraction procedure. Prior to any work on the metals speciation, the potential of using X-Ray fluorescence spectroscopy to measure the total concentrations of metals in the solid phase was assessed to replace the total acid digestion method defined as standard method (3030F, APHA-AWWA-WEF, 1998).

The aim of this chapter was to develop a suite of techniques able to determine the metals speciation in anaerobically digested sludge. Using copper and nickel as test metals, each analytical technique (BCR SE, SEM-EDS, fluorescence spectroscopy, pH titration and model simulation) was assessed to establish their potential and limits for investigating metals speciation in anaerobically digested sludge. The assessment has been done using several digested sludge obtained from full scale WWTP and the complete description of the FSADSA experiment is described in chapter 4 (4.1.1, 4.2, 4.3, 4.4 and 4.5).

5.2. Comparison of two analytical methods to measure total metals concentration in the solid phase of anaerobically digested sludge

The concentration of some elements in a solid phase can be measured using direct analytical methods or by dissolving the solid phase and analysing the extracting solution. Two methods, one of each, have been assessed to determine

the total quantities of five of the six essential metals (copper, iron, manganese, nickel and zinc) studied in this research (section 2.1). Cobalt was not used in the assessment due to a total concentration in some sludge below the detection limits for XRF analysis.

X-ray fluorescence spectroscopy was used to obtain a direct measurement of metals concentration in the solid phase. The total acid digestion method was used to dissolve the digested sludge and each element was measured in the extracted solution by FAAS and ICP-AES (see sections 4.4.1 and 4.4.2). Both methods have been described in sections 4.4.3 and 4.3.2. .

Total acid digestion method is mainly used in the literature (see section 2.10) to determine metal concentration in sewage sludge and soil as it has been defined as standard method (3030 F, ALPHA AWWA WEF, 1998). However, this method requires a long sample preparation prior to the elemental analysis and so the risk of contamination or manipulation errors is increased. The use of the XRF method can reduce those by reducing the sample preparation as no extraction is needed.
The aim of this comparison was to obtain information on the benefit of using the XRF method in the study of metals speciation in anaerobically digested sludge and its potential to replace the total acid digestion method.

The ideal comparison would have been the use of certified material, but in the case of anaerobically digested sludge, the analysis of wide range of sludge have been chosen as there was no available certified anaerobically digested sludge

material. However, the total acid digestion method has already been validated as a standard method to measure the total metal concentration in sludge and its results were used as reference in this study.

5.2.1. Results

Concentrations of five metals (Cu, Fe, Mn, Ni and Zn) measured using the total acid digestion method, are displayed in table 5.1. Iron concentration was the highest of the heavy metals in all the sludge samples and varied between 13 g/kg Dry Solid (DS) for the sludge K and G and 33 g/kg DS for the sludge F. Then concentrations of nickel and zinc were included respectively between 1.1-1.4 g/kg DS and 0.58-1.6 g/kg DS. The two lowest metals concentrations concerned copper and manganese with a respective range of 0.20-0.62 g/kg DS and 0.22 and 0.72 g/kg DS.

Concentrations of five metals (Cu, Fe, Mn, Ni and Zn) measured using XRF are displayed in table 5.2. Iron concentration was also the highest of the heavy metals in all the sludge and varied between 48 g/kg DS for the sludge K and 177 g/kg DS for the sludge F. Zinc had a concentration varying between 2.0 and 5.0 g/kg DS. Copper concentration was comprised between 0.95 g/kg DS and 2.1 g/kg DS. The two lowest metal concentrations concerned nickel and manganese with a respective range of 0.20-0.95 g/kg DS and 0.65-1.9 g/kg DS.

Table 5.1. Concentrations of metals in the solid phase of anaerobically digested sludge using the total acid digestion method (g/kg DS)

Element	Sludge						
	F	K	G	H	M	R	S
Cu	0.20 ± 0.02	0.51 ± 0.06	0.30 ± 0.02	0.62 ± 0.14	0.35 ± 0.02	0.40 ± 0.04	0.27 ± 0.06
Fe	33 ± 1	13 ± 1	13 ± 1	23 ± 1	21 ± 3	27 ± 2	26 ± 1
Mn	0.35 ± 0.03	0.35 ± 0.04	0.35 ± 0.01	0.22 ± 0.04	0.72 ± 0.02	0.30 ± 0.01	0.24 ± 0.01
Ni	1.4 ± 0.2	1.1 ± 0.4	1.2 ± 0.2	1.3 ± 0.2	1.2 ± 0.4	1.3 ± 0.4	1.1 ± 0.3
Zn	0.86 ± 0.08	0.73 ± 0.06	0.58 ± 0.03	0.66 ± 0.06	1.6 ± 0.1	0.82 ± 0.02	0.89 ± 0.07

The concentrations are expressed as mean ± standard deviation (n=6).

Table 5.2. Concentrations of metals in the solid phase of anaerobically digested sludge using XRF analysis (g/kg DS)

Element	Sludge						
	F	K	G	H	M	R	S
Cu	0.95	2.1	1.1	1.9	1.4	1.1	1.2
Fe	177	48	54	97	93	145	101
Mn	1.0	1.0	0.80	0.65	1.9	1.0	0.60
Ni	0.60	0.95	0.45	0.20	0.45	0.60	0.80
Zn	2.9	1.9	2.1	2.0	5.0	1.9	2.9

No standard deviation was calculated due to limited data point (n=2).

All metals under study, except nickel, had a higher value measured using the XRF method than using the total acid digestion method. However, the variation of each metal concentration across the sludge presented some similarities between the two methods (figures 5.1-5.3). In figure 5.1, Iron exhibited a linear relation between the concentrations measured using XRF and total acid digestion. The linear regression using the plotted point gave a slope of around 6.

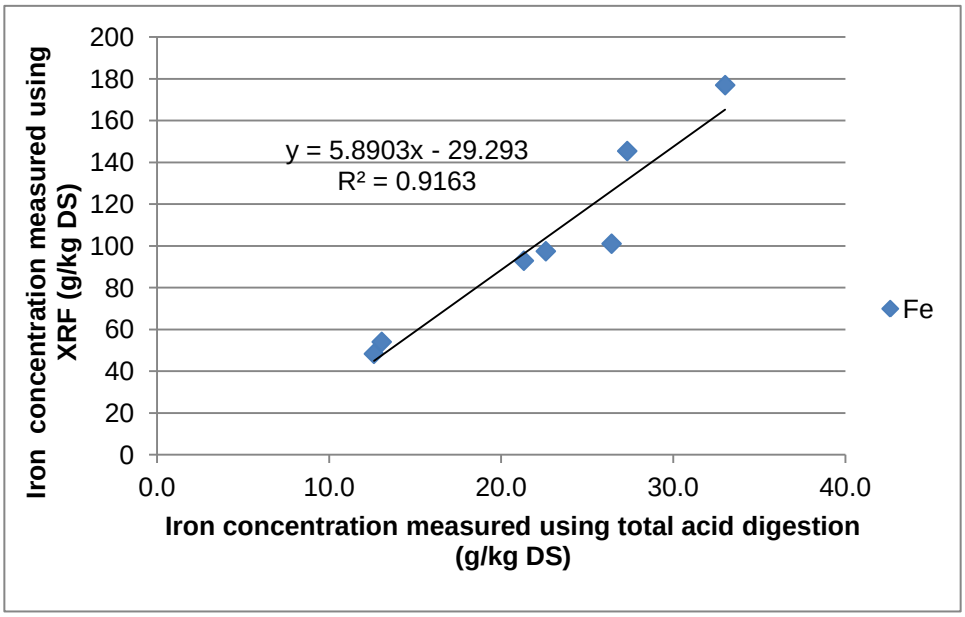

Figure 5.1. Concentrations of iron measured in anaerobically digested sludge using XRF in function of their concentrations measured using total acid digestion

In figure 5.2, copper and manganese exhibited both a similar linear relation with a slope of 2.6 between the concentrations measured using the two methods. Finally in figure 5.3, only zinc exhibited this similar linear relation with a slope of 3, but no linear relation was observed for the two sets of nickel concentrations.

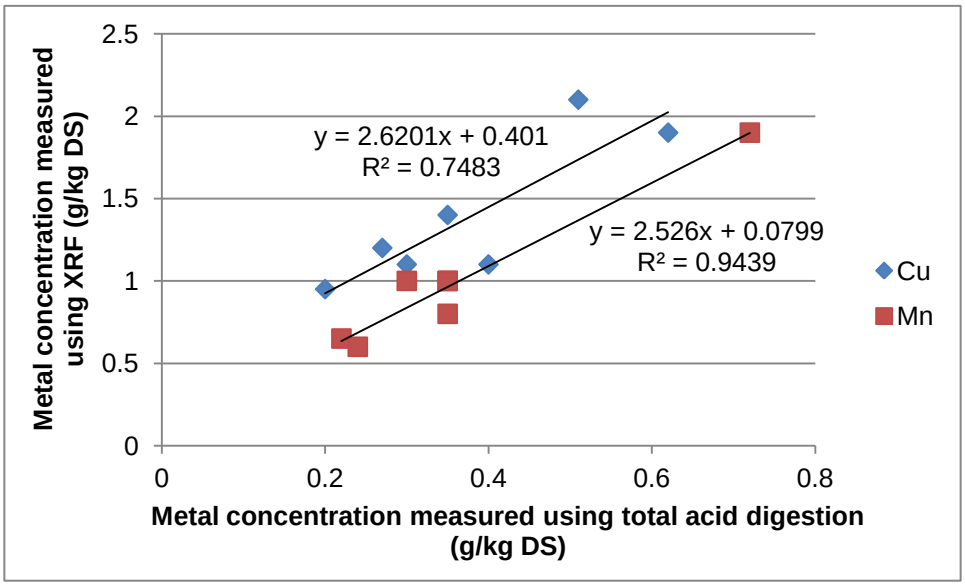

Figure 5.2. Concentrations of copper and manganese measured in anaerobically digested sludge using XRF in function of their concentrations measured using total acid digestion

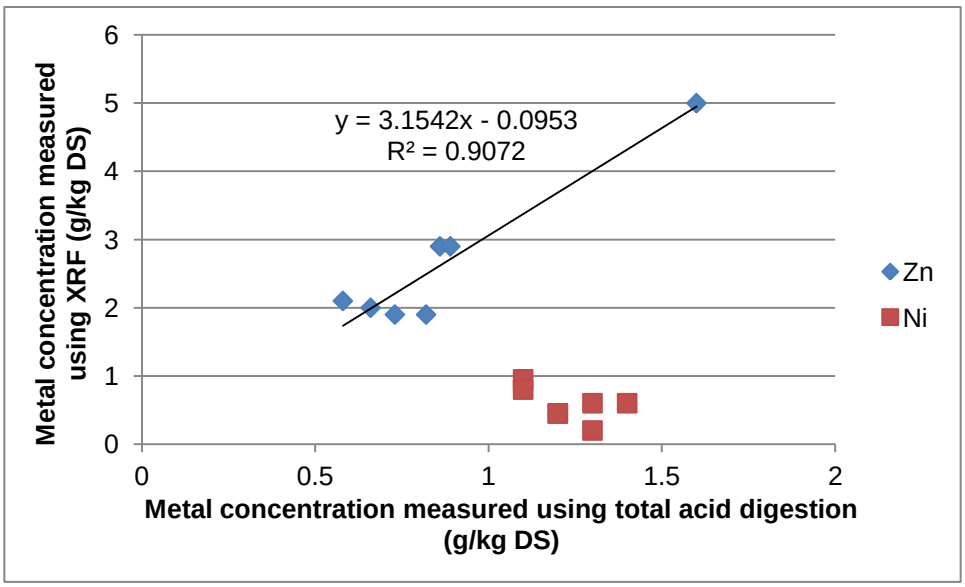

Figure 5.3. Concentrations of zinc and nickel measured in anaerobically digested sludge using XRF in function of their concentrations measured using total acid digestion.

5.2.2. Discussion

The concentrations measured using both analytical techniques were included in the wide range of metals concentration described in Metcalf and Eddy (2003) except for the highest iron concentration measured using XRF (177 g/kg DS, XRF and 154 g/kg DS, Metcalf and Eddy, 2003). Moreover, the presence of those high iron concentrations in this study were in contradiction with Carliell-Marquet et al. (2010) who found a maximum iron concentration of 119 g/kg DS in the study of the inorganic profiles of chemical phosphorus removal sludge. They found, on average, an iron concentration of 11 g/kg DS for undosed sludge and 92 g/kg DS for iron dosed sludge using total acid digestion.

In this study, sludge K and G were both undosed sludge (see section 4.1.1) and their concentrations measured using total acid digestion method (13 g/kg DS) were similar to the average described by Carliell-Marquet et al. (2010) and in opposition the values obtained using XRF were around 4 times higher (48 and 54 g/kg DS). For iron dosed sludge, the highest value found in this study was 33 g/kg DS (total acid digestion) and 177 g/kg DS (XRF). The comparison of iron concentrations measured in this study with the literature review suggested that XRF method over calculated the amount of iron present in the sludge. Concerning the total acid digestion, the values obtained were comparable to the values reported from previous studies.

Concentrations of zinc, copper and manganese measured by total acid digestion method were also included in the range of values found in previous studies on anaerobically digested sludge, Cu 0.2-0.7 g/kg DS, Mn 0.1-1.2 g/kg DS and Zn 0.7-1.7 g/kg DS (Alvarez et al., 2002; Carliell-Marquet et al., 2010; Fuentes et al., 2008; Scancar et al., 2000). However, results obtained by XRF were higher than those ranges of values. Concerning nickel, its concentrations obtained using XRF were closer to the values found in the literature (0.02-0.9 g/kg DS, Alvarez et al., 2002; Carliell-Marquet et al., 2010; Fuentes et al., 2008; Scancar et al., 2000) than its concentrations measured using the total acid digestion method.

Results from XRF and total acid digestion methods did not agree on the concentrations of elements in the solid phase of anaerobically digested sludge but both methods agreed on their variation across the seven types of sludge. So the differences between the values were not due to any random contaminations but they could be related with a systematic over-evaluation of metals concentrations by XRF due to analytical uncertainties developed below (a factor 6 for iron, 2.6 for copper and manganese and 3 for zinc). Nickel demonstrated a specific behaviour in comparison with other metals as there was no relation between the concentrations measured by XRF and total acid digestion. This was the consequence of the high values of nickel concentration measured by the total acid digestion method in comparison with the values obtained by XRF or from the literature. Finally, the potential of an under-evaluation of metals concentration by the total acid digestion method could also be responsible of an increase of the gap between the values measured by those two methods.

The total acid digestion extracting solution used in this study did not include any hydrofluoric acid (HF, see section 4.3.2) so silicate compounds might not be totally dissolved into the extracting solution (Kojima et al., 1992). So the absence of HF in the extracting solution might reduce the dissolution of the metals under study due to the possibility of metals incorporation into silicate compounds or the presence of co-precipitated. Finally the risk of loss of materials during the extraction might also be responsible for the attenuation of the metals concentrations measured using this method.

In another hand, the accuracy of the XRF method was clearly influenced by the dried sludge constitution (see 4.3.3). Sludge structure was not an ideal material for the use of XRF, as it was generally used to check the impurities in pure compounds or the composition of chemically produced compounds. The thickness of dried sludge and the high proportion of elements below the fluorine such as organic matter may reduce the X-ray energy and alter the metals detection. The Compton count used to assess the accuracy of the analysis was around 20-30%, which was low to certify the accuracy of results (generally 95%) Furthermore the concentration of an element was calculated from the percentage of each element in the sludge and, a high concentration of organics in the sample disturbed the metals percentages and consequently their calculated concentrations.

The second inconvenience with the use of XRF for the elemental analysis of anaerobically digested sludge was the non homogeneity of the sample (see section 4.4.3). The surface analysis required that the sample was similar in any

point of the pellet and the use of dry sludge could not guarantee the complete homogeneity of the sample although the powdering and mixing reduced the heterogeneity concern at its minimum.

Following this study, the use of XRF method was discarded to measure the concentrations of metals in anaerobically digested sludge. The specificity of the sample composition was thought to disturb the calculation of the element concentrations and the values were systematically over evaluated.

5.3. Assessment of the use of the BCR sequential extraction procedure in the study of metals speciation in anaerobically digested sludge

Sequential extraction procedures have been used in previous studies to estimate the speciation and mobility of metals in soil and sludge samples (see section 2.9). However, those results were only indicating the strength of metal bindings and there was a lack of information on the exact composition of the metal compound. The aim of this section was to determine the interest of using the BCR sequential extraction procedure in the study of metals speciation and to find out potential limitations.

Nickel and copper were chosen as test elements for this section as the other metals speciation has been developed in the following chapters. Furthermore,

results from nickel and copper BCR sequential extraction were suitable in showing the limitations of this technique.

5.3.1. Results

Nickel concentrations in each BCR sequential extraction fraction are shown in table 5.3 and the nickel fractionation profile in anaerobically digested sludge is detailed in figure 5.4.

Table 5.3. Concentrations of nickel in each BCR SE fraction for the 7 anaerobically digested sludge.

Concentrations of nickel in each BCR sequential extraction fraction									
Sludge	Σ fractions	Exchangeable		Reducible		Oxidisable		Residual	
	mg/kg DS	%	mg/kg DS	%	mg/kg DS	%	mg/kg DS	%	mg/kg DS
F	1245 ± 143	31	382 ± 131	24	299 ± 100	20	244 ± 105	26	320 ± 49
K	1225 ± 83	17	204 ± 33	12	148 ± 92	21	251 ± 120	51	622 ± 41
G	1178 ± 219	38	445 ± 43	9	109 ± 40	22	256 ± 104	31	369 ± 80
H	1363 ± 301	14	191 ± 79	9	118 ± 80	67	920 ± 173	10	133 ± 36
M	679 ± 205	25	168 ± 68	28	188 ± 116	18	125 ± 31	29	199 ± 58
R	1110 ± 124	15	163 ± 65	13	149 ± 40	8	90 ± 47	64	709 ± 158
S	929 ± 166	29	268 ± 34	28	261 ± 163	21	194 ± 47	22	207 ± 102

The concentrations are expressed as mean ± standard deviation (n=6) and percent of total

Concentrations of nickel in the solid phase calculated by the sum of the BCR sequential extraction fractions were mostly in the same range as the concentrations measured with the total acid digestion method (see section 4.3.2 and 5.2). The percentage of recovery from the sum of the BCR SE fractions in function of the total acid digestion was included between 80-110% except for the

sludge M with a recovery of only 50%. Nickel total concentrations in the different sludge varied from 930 to 1360 mg/kg DS except for the low concentration measured in the sludge M (680 mg/kg DS).

The BCR sequential extraction profile was different across the sludge and no clear dominant fraction was detected. Residual and oxidisable fractions had the highest range of nickel concentrations with respectively 10-64% and 8-67% of the total nickel in the solid phase. Exchangeable and reducible fractions had the smallest range with respectively 14-38% and 9-28% of the total nickel in the solid phase.

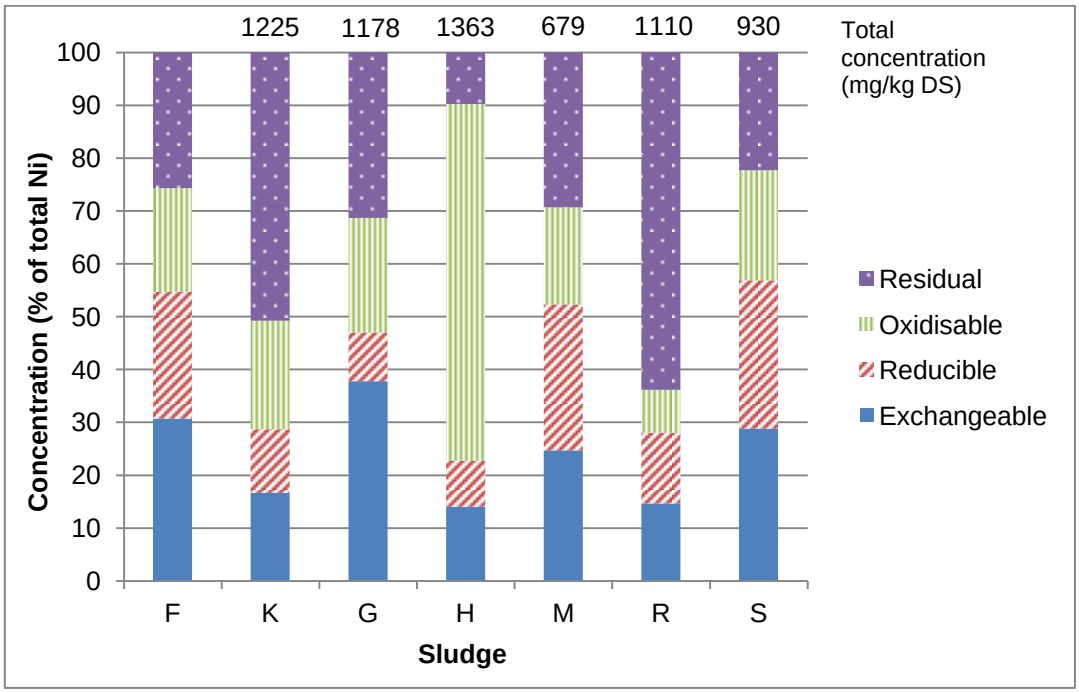

Figure 5.4. Nickel fractionation profiles in the 7 anaerobically digested sludge

Copper concentrations in the different BCR sequential extraction fractions are shown in table 5.4 and their fractionation profiles are detailed in figure 5.5.

Table 5.4. Concentrations of copper in each BCR SE fraction for the 7 anaerobically digested sludge.

Concentrations of copper in each BCR sequential extraction fraction									
Sludge	Σ fractions	Exchangeable		Reducible		Oxidisable		Residual	
	mg/kg DS	%	mg/kg DS	%	mg/kg DS	%	mg/kg DS	%	mg/kg DS
F	193 ± 12	1	2 ± 1	42	81 ± 3	55	106 ± 8	2	4 ± 2
K	504 ± 6	1	2 ± 1	28	143 ± 36	68	342 ± 23	3	17 ± 7
G	267 ± 30	1	1 ± 1	10	26 ± 8	81	217 ± 14	8	23 ± 14
H	440 ± 81	0	< d.l.	25	111 ± 42	72	317 ± 50	3	12 ± 8
M	346 ± 40	0	< d.l.	14	48 ± 23	82	284 ± 50	4	13 ± 6
R	403 ± 33	0	< d.l.	14	57 ± 10	80	324 ± 19	6	22 ± 6
S	307 ± 10	0	< d.l.	37	115 ± 9	60	184 ± 12	3	8 ± 6

The concentrations are expressed as mean ± standard deviation (n=6) and percent of total
<d.l. : below detection limit

Concentrations of copper in the solid phase calculated by the sum of the BCR SE fractions were close to the concentrations measured with the total acid digestion method. Copper total concentration in the different sludge varied from 200 to 500 mg/kg DS. The percentage of recovery from the sum of the BCR SE fractions in function of the total acid digestion was included between 97-100% except for the sludge G and H with a percentage of recovery below 90%.

Concerning the BCR sequential extraction profile, the oxidisable fraction was the main fraction with 55-82% of the total copper. The remaining copper was extracted in the reducible fraction (10-42 %). The two last fractions (residual and exchangeable fractions) extracted respectively less than 10 % and 2% of the total copper (see figure 5.5).

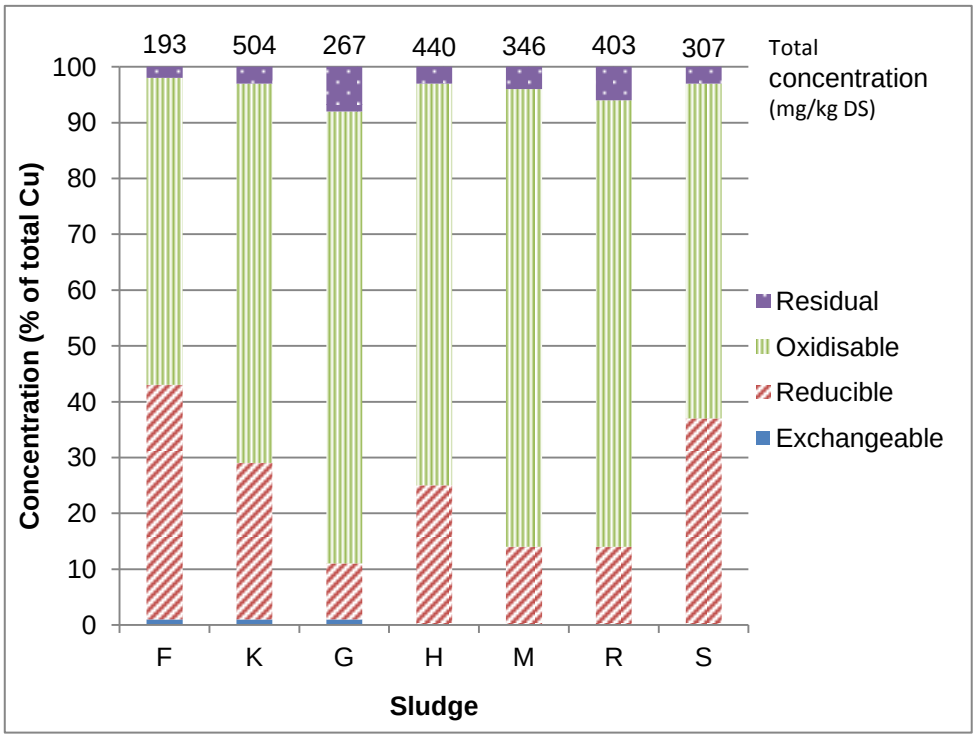

Figure 5.5. Copper fractionation profiles in the 7 anaerobically digested sludge

5.3.2. Discussion

Nickel was extracted in all the BCR sequential extraction fractions across the sludge and there was no dominant fraction. Alvarez et al. (2002), Fuentes et al. (2008) and Solis et al. (2002) found that nickel was also extracted in the four BCR SE fractions and Lake et al. (1985) observed the absence of a dominant fraction. Moreover, Fuentes et al. (2008) and Solis et al. (2002) also observed a large difference in the nickel partitioning between different sludge (primary, secondary and digested sludge) but no comparison has been done on several anaerobically digested sludges. A difference in the nickel extraction profiles across five sewage sludges has been noticed by Chao et al. (2006).

This absence of a specific partitioning for nickel can be related to the potential of multiple bindings and their dependences on the sludge condition and other metals speciation. The precipitation of nickel with sulphide has been predicted to be the main binding (Callander and Barford, 1983b) but the results above exhibited the presence of other bindings. Nickel sulphide precipitates have also been detected in several digested sludges by Fermoso et al. (2008b), Liu and Fang (1998) and Jong and Parry (2004). Adamo et al. (1996) showed that the nickel extracted in the BCR exchangeable fraction was likely to be bound with carbonate. Finally, nickel has also been detected included with iron precipitates and siliceous compounds (Adamo et al., 1996) and the presence of co-precipitate was likely to be one of the cause of disparities in nickel fractionation profiles.

Copper was mainly extracted in the BCR oxidisable fraction for the seven type of anaerobically digested sludge and the remaining was extracted in the BCR reducible fraction. From the definition of the BCR SE fractions, metal-organics are extracted in the oxidisable fraction in the same time as sulphide compound. Unfortunately, literature and thermodynamic data showed that copper binds easily with organics and sulphide (see sections 2.4 and 2.5) and sequential extraction cannot measure the proportion of copper bound with each of them. Callander and Barford (1983b) and Lake et al. (1985) found that copper was mainly bound with sulphide and the presence of copper sulphide in anaerobic digester was observed by Liu and Fang (1998). Moreover, Jong and Parry (2004) demonstrated that the copper extracted in the BCR oxidisable fraction was more from sulphide binding than from organic binding. However, the potential of copper to bind with organics

and humic substance have been demonstrated by Gamble et al. (1970), Saar and Weber (1982) and Plaza et al. (2006).

The example of the use of sequential extraction in the study of the nickel speciation in anaerobically digested sludge was not enough to obtain clear information on the nickel bindings and its different chemical species. In the oxidisable fraction, there is a potential of extracting two kinds of copper compounds (inorganic and organic binding) and the sequential extraction procedure cannot distinguish between both. This incapacity of distinguishing the different compounds extracted in the same fraction was also noticed in different studies, which used sequential extraction procedures to describe metal speciation (Adamo et al., 1996 and Banerjee, 2002). Finally, the possibility of an early or late release of a compound in another sequential extraction fraction can also disturb the quantitative and qualitative lecture of the results (Dodd et al., 2000). The presence of copper in the reducible fraction could not be explained by the extraction of a specific copper compound (e.g. CuO) and so it might be related with an early release of copper bound with sulphide or organics.

BCR sequential extraction procedure is an interesting quantitative and semi qualitative analytical technique in the study of metal speciation in anaerobically digested sludge, but complementary techniques needed to be applied with it to obtain clear information on the compounds extracted in each fraction. Qualitative analytical techniques such as SEM-EDS gave information on the inorganic fraction

of the sludge and fluorescence spectroscopy was helpful to characterize the different fractions containing organics.

5.4. Assessment of the use of the SEM-EDS in the study of metals speciation in anaerobically digested sludge

Several X-Ray spectroscopy techniques might be used to determine the chemical forms of metal in environmental samples. Those qualitative analytical techniques offer direct information on the metals speciation and can be easily emphasized the sequential extraction procedure results. However, those techniques are not necessarily adapted to the analysis of anaerobically digested sludge samples particularly due to the absence of crystalline precipitates and the presence of organics.

SEM-EDS analysis presents some interests in the study of metals speciation in anaerobically digested sludge by its spatial and qualitative analysis, the large range of elements detection and its simple sample preparation and analysis. Through the examples of calcium, silver and nickel compounds, the aim of this chapter was to demonstrate the interest of using this technique coupled with the BCR SE procedure but also its limits for the detection of some metal compounds.

5.4.1. Results

From the SEM-EDS analysis, four compounds have been detected in the different sludge and illustrated in figure 5.6 and table 5.5.

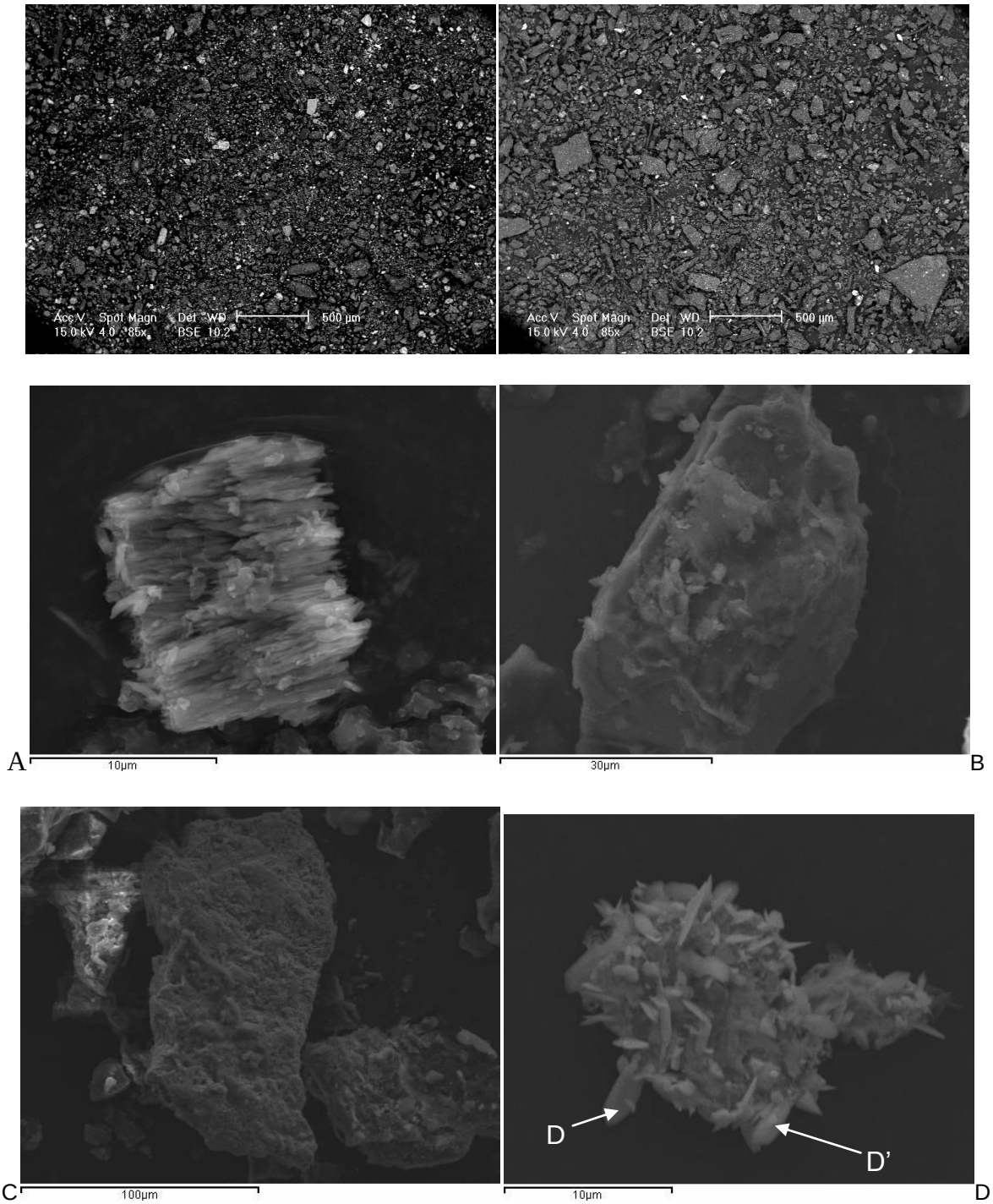

Figure 5.6. Sludge BSE pictures (top), SEM pictures of four different compounds (A-D).

Table 5.5. Elemental analysis for compounds A to D by EDS

Sample	Element concentration (as atomic percent)										
	Al	Ag	Ca	Fe	Mg	Na	Ni	O	P	S	Si
A	<1	-	23	-	-	1	-	75	<1	-	<1
B	1	-	11	2	12	2	-	70	-	2	-
C	1	-	2	-	1	3	25	62	3	-	3
D	1	35	-	-	-	1	-	46	-	17	-
D'	-	61	-	-	-	-	-	-	-	39	-

The compound A was composed of two main elements, calcium (23% of the total elements) and oxygen (75%). Sodium, phosphorus, aluminium and silicon were also detected in the compound as traces. As the carbon percentage was not taken into account due to the carbon coding of the sample, there was no information on the carbon contents of each sample (see chapter 4.4.4). The absence of phosphorus and sulphur in the compound A and a ratio between the percentage of oxygen and calcium around 3 induced that the compound A could be identified as calcium carbonate ($CaCO_3$). The specific crystal structure of the compound observed on the microscope picture (figure 5.6.a) presented similarities with the structure of the aragonite ($CaCO_3$), confirming the identification of the compound A as a crystal calcium carbonate precipitate (see appendix C.1).

The compound B had a similar atomic composition as the compound A with half of the calcium replaced by magnesium. The composition of compound B was still dominated by oxygen (70%) and then magnesium and calcium were present at the same percentage (respectively 12 and 11%). Sulphur, iron, sodium and aluminium were also present as trace in this compound. The ratios O/Ca and O/Mg were

around 6 and so the compound B could be identified as $CaMg(CO_3)_2$, denominated as dolomite. The crystal structure analysis of the compound B corroborated its identification as dolomite (see appendix C.2).

The compound C was mostly composed with two elements, nickel (25%) and oxygen (62%). The absence of high proportion of phosphorus and sulphur suggested that nickel was also bound with carbonate. So the compound could be assimilated as $NiCO_3$, but the basic nickel carbonate, following IUPAC recommendation, was generally present as $Ni_4CO_3(OH)_6(H_2O)_4$. However the ratio O/Ni (2.5) was lower than expected from the formula (3.25). This difference could be explained by a dehydration of the compound during the sample preparation.

The last compound was shown in table 5.5 and figure 5.6 as D and D'. The two atomic compositions have been obtained in different point of the compound. The difference in the composition between D and D' was the presence of oxygen (46%) in the compound D. The two main elements of D and D' were silver (35% D and 61% D') and sulphur (17% D and 39% D'). The ratio between silver and sulphur was around 2 for both measurements and suggested that it could be identified as Ag_2S. The presence of oxygen in the measurement D could be explained by an oxidation of the silver sulphide during the sample preparation. It could also be noticed that sulphide silver grown on the other compound containing a high percentage of aluminium (results not shown).

5.4.2. Discussion

SEM-EDS analysis is a powerful analytical technique in the determination of the molecular composition of compounds present in anaerobically digested sludge. Gonzalez-Gil et al. (2001) used the SEM analysis with a backscattering electron (BSE) imaging in the UASB reactor for the localisation of metals into granular sludge. The BSE system, that highlights the presence of high atomic number elements (see section 4.4.4), was used to detect the presence of metal precipitates in the dried sludge sample (figure 5.6, top pictures) or the sorption of metal on biomass or other precipitates (see section 6.2.2).

Dodd et al. (2000) and Adamo et al. (1996) used SEM-EDS to detect and characterize minerals present in anaerobic canal bed mud and contaminated soil. The different examples of compounds in this study showed the broad range of the precipitates present in anaerobically digested sludge. The three main inorganic anionic systems (carbonate, phosphate and sulphide, section 2.4) have been detected by the SEM-EDS, carbonate with calcium, magnesium and nickel (figure 5.6); phosphate with iron (section 6.2.2, figures 6.11-6.12) and sulphide with silver (figure 5.6) and iron (section 6.2.2, figure 6.13).

EDS analysis gave the atomic percent of each element present on the surface of the compound (only for elements with an atomic number higher than 12). So the molecular composition of each compound could be deduced from the ratio between the main elements detected. In each compound shown in figure 5.6, the

presence of trace elements has also been detected and they are mainly the major elements present in the sludge, e.g. aluminium, silicon, sodium, iron, magnesium, calcium, phosphate and sulphur. Aluminium and sodium were present at approximately 1% in each of the four compounds (table 5.5). The presence of those trace elements, resulting from a co-precipitation or sorption, can complicate the identification of the compounds by disturbing the different ratios between elements.

Those ratios could also be modified during the sample preparation. The open-air drying stage could lead to surface oxidation of the compound and the grounding stage could also alter the surface composition. Those alterations were confirmed by the difference in the silver and sulphur percentage between the compounds D and D' and the presence of some trace elements in the different compounds. Finally the carbon coding of the samples prior to their analysis avoided any information on the carbon content of each compound and so complicated the identification of metals bound with organics and carbonate.

SEM-EDS analysis is only a qualitative analytical technique and cannot measure the concentration of each compound in anaerobically digested sludge. All the precipitates detected during this analysis could not be considered as a compound usually present in anaerobic digesters. So the main use of SEM-EDS was the confirmation of the presence of a compound measured or suggested using other quantitative techniques such sequential extraction procedures. The use of SEM-EDS on the solid phase after the application of each extracting solution from the

sequential extraction procedure was already done by Dodd et al. (2000) on anaerobic canal mud. They found that calcite or vivianite were not completely dissolved during the first extraction. However, the results of the combination of those two techniques contained a large part of uncertainty due to the non quantitative aspect of the SEM-EDS results: did the non detection of a specific compound after the use of an extracting solution mean that all of them have been extracted? The same thoughts could be applied for the opposite case, when a precipitate was detected after the use of an extracting solution, did it mean this solution do not extract any of this precipitate?

In conclusion, SEM-EDS analysis is an interesting qualitative analytical technique but its results need to be treated with care. The absence of quantitative results and the different difficulties of analysis mentioned above can easily lead to a misinterpretation of those results. However, its use can confirm the presence of compounds predicted or induced by other analytical techniques.

5.5. Assessment of the use of the fluorescence spectroscopy in the study of metals speciation in anaerobically digested sludge

Organics in anaerobically digested sludge can be divided in two categories: biomass related organics (such as soluble microbial products (SMP) and EPS) and humic substances (such as fulvic and humic acid-like). These two kinds of organics are extracted in two different fractions of the BCR sequential extraction

following the description of the procedure (Fuentes et al., 2008). All metals sorbed and chelated with biomass related organics are extracted in the exchangeable fraction as their bindings are usually weak (Smith, 2006 and Van Hullebusch et al., 2005). Metals bound with humic substance are extracted in the BCR oxidisable fraction as their bindings are stronger and so, an oxidising agent is necessary to breakdown the organics and to release the metals (Smith, 2006 and Van Hullebusch et al., 2005).

Fluorescence spectroscopy analysis (section 4.4.5) was used in this research for the determination of the release of metal-organics in the different fractions of the BCR sequential extraction procedure. Several studies used the quenching on the signal intensities by the binding of organics with metals to measure the degree of complexation in function of the metal concentrations (Ryan and Weber, 1982; Da Silva et al., 1998 and Plaza et al., 2006). However, in this research a lack of reference on the intensity of organics without metals and the presence of other sources of quenching (i.e. acidity) prevented from using this technique to evaluate the metal-organics complex system in anaerobically digested sludge.

The aim of this section was the characterization of the different fluorescence spectroscopy peak intensities in the fractions of the BCR sequential extraction in order to get information on the extraction of organics in the fractions and consequently on the extraction of metal-organics chelates.

Fluorescence spectroscopy uses the specific combination of the excitation and emission wavelengths to detect each organics. However, this technique would increase the analyzing time if multiple detections are needed. To remedy this problem, the 'Excitation Emission Matrix' (EEM) has been developed (section 4.4.5). EEM is a recent technique used in fluorescence spectroscopy to scan a range of excitation and emission wavelengths. This scan can be plotted in a 3-D graph showing the intensity for each Ex/Em couple.

5.5.1. Results

Excitation-Emission Matrix (EEM) fluorescence spectroscopy was applied on each BCR extracted solution; the 3D-graphs are displayed on the figure 5.7 and fluorescence peak intensity in table 5.6 and figure 5.8. Figure 5.7 shows that organics were not equally extracted in the different extracting solutions. The three peaks representing organics from biomass were mainly present in the BCR exchangeable fraction. Peaks from humic substances were present in the four fractions but the peak location varied in the different solutions.

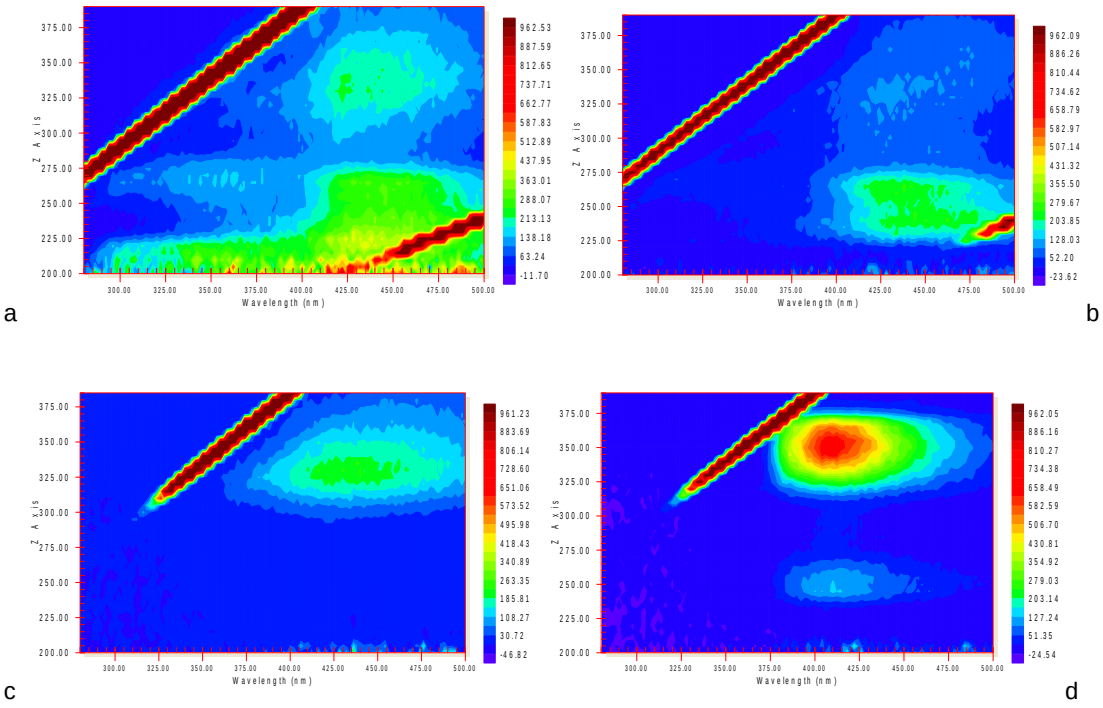

Figure 5.7.EEM scans from the 4 BCR SE fractions applied on anaerobically digested sludge a) Exchangeable, b) Reducible, c) Oxidisable, d) Residual

Y axis represents excitation wavelength and x axis represents emission wavelength.

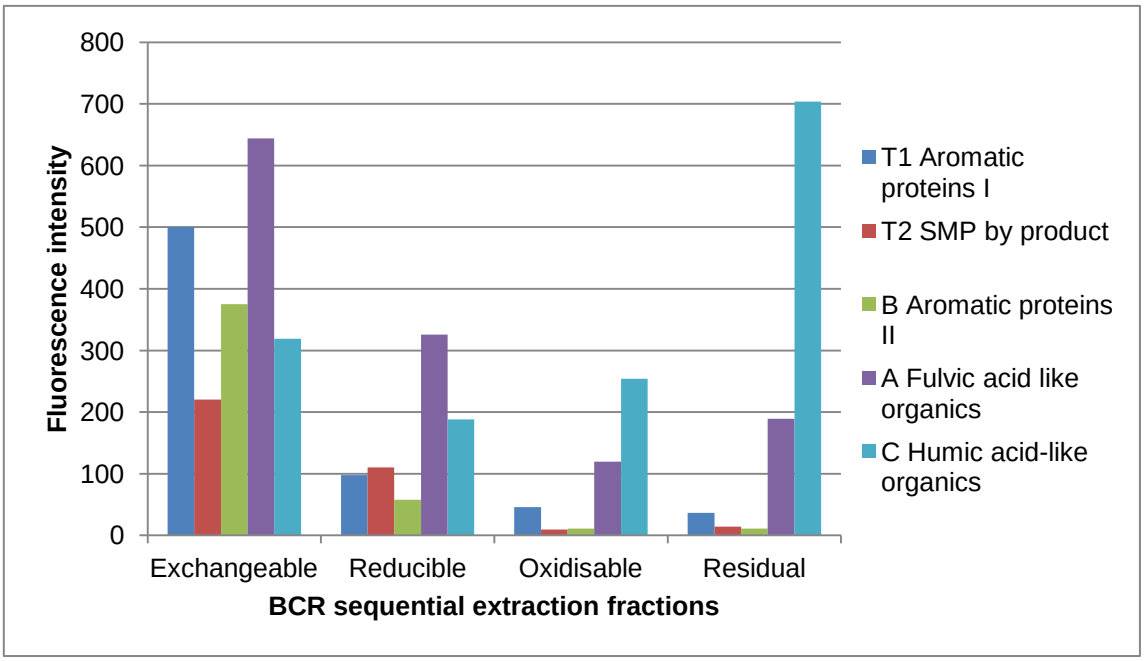

Figure 5.8. Intensities of each organic group peaks in the four BCR SE fractions applied on anaerobically digested sludge

The exchangeable fraction contained the five peaks for each group of organics (figure 5.8). Low excitation wavelength peaks had a higher intensity than the SMP-like and HA-like peaks (high excitation wavelength). In the reducible fraction, only two peaks (HA and FA) were obviously present. Fulvic acid peak intensity was higher than humic acid peak intensity. In the third fraction, oxidisable, the two humic substance peaks were still present but the intensity had been inverted with humic acid peak intensity higher than the fulvic acid peak intensity. The residual fraction was similar to the previous one with an increasing of the signal for the humic acid peak (figure 5.8).

Results displayed in table 5.6 and figure 5.8 confirmed that the biomass related peaks (SMP, Aromatic protein I &II) were mainly extracted in the first fraction (exchangeable) with peak intensity over 200. In the reducible fraction some those peaks had intensities between 50 and 100 and in the two last fractions the intensity decreased under the 50. Fulvic acid peak had a maximum in the first fraction with peak intensity around 600 and then decreased with the fraction and finish in the last fraction with a peak intensity under 200. Humic acid peak followed an opposite direction and the signal increased with the strength of the fraction (reducible with a peak intensity of 200 to residual fraction with 700), at the exception of the first fraction where the peak intensity was around 300.

Table 5.6. Intensities of each organic group peaks in the four BCR SE fractions applied on anaerobically digested sludge

Sludge	BCR SE fractions	T1 simple aromatic proteins	T2 SMP by-product	B simple aromatic proteins	A Fulvic acid-like organics	C Humic acid-like organics
F	1	492 ± 46	233 ± 12	459 ± 43	713 ± 147	355 ± 37
	2	123 ± 90	122 ± 62	52 ± 15	253 ± 40	160 ± 14
	3	39 ± 20	10 ± 7	11 ± 6	94 ± 53	191 ± 66
	4	38 ± 19	14 ± 2	14 ± 5	169 ± 35	607 ± 145
K	1	488 ± 60	220 ± 6	332 ± 54	597 ± 64	308 ± 15
	2	56 ± 7	84± 19	57 ± 12	366 ± 7	168 ± 33
	3	61 ± 33	9 ± 3	17 ± 11	156 ± 53	312 ± 27
	4	31 ± 17	14 ± 8	12 ± 7	189 ± 88	702 ± 243
G	1	472 ± 50	228 ± 20	305 ± 46	483 ± 22	244 ± 16
	2	97 ± 21	103 ± 4	66 ± 16	276 ± 20	150 ± 11
	3	38 ± 13	9 ± 3	7 ± 3	117 ± 6	236 ± 43
	4	28 ± 9	12 ± 1	10 ± 4	185 ± 46	685 ± 166
H	1	495 ± 75	235 ± 39	337 ± 51	521 ± 64	288 ± 37
	2	90 ± 16	110 ± 19	64 ± 16	394 ± 33	229 ± 36
	3	45 ± 11	7 ± 1	12 ± 3	122 ± 21	261 ± 64
	4	31 ± 13	14 ± 5	11 ± 4	184 ± 85	647 ± 246
M	1	552 ± 142	205 ± 40	456 ± 147	831 ± 226	395 ± 75
	2	127 ± 43	130 ± 19	58 ± 10	370 ± 55	217 ± 32
	3	56 ± 28	13 ± 7	12 ± 4	131 ± 43	240 ± 116
	4	45 ± 18	13 ± 2	8 ± 4	178 ± 43	647 ± 207
R	1	455 ± 79	179 ± 24	309 ± 60	669 ± 171	314 ± 31
	2	84 ± 19	92 ± 13	56 ± 23	287 ± 93	199 ± 26
	3	29 ± 12	6 ± 1	9 ± 2	94 ± 41	315 ± 34
	4	40 ± 12	17 ± 3	11 ± 5	240 ± 28	963 ± 146
S	1	448 ± 61	210 ± 24	278 ± 30	545 ± 79	300 ± 39
	2	64 ± 6	76 ± 14	60 ± 18	282 ± 81	179 ± 31
	3	36 ± 16	9 ± 1	8 ± 5	115 ± 34	301 ± 38
	4	33 ± 19	15 ± 8	10 ± 6	217 ± 172	887 ± 263

Intensities are expressed as mean ± standard deviation (n=6).
SE fractions: 1 exchangeable, 2 reducible, 3 exchangeable and 4 residual

Table 5.7 shows the position (Ex/Em) of the different organics peaks in each fraction. In the exchangeable fraction, the five peak positions were detected at 220/304 for simple aromatic protein I, at 277/355 for soluble microbial product, at 220/355 for aromatic protein II, at 224/421 for fulvic acid-like and at 344/424 for humic acid-like. For the three other fractions only FA and HA peaks have been shown as the intensity of biomass related peaks were too low to be taken into account. FA peak was moving at different positions within the fractions. In the reducible fraction the maximum was at 262/427, 220/427 in the oxidisable fraction and 256/410 in the residual fraction. Concerning the HA peaks, reducible and oxidisable fractions had similar peaks that exchangeable fraction with respectively 339/428 and 345/430. However, the HA peak in the residual fraction was detected at 360/409.

Table 5.7. Average of excitation and emission wavelengths for each organic group peaks in the different fractions of the BCR SE applied on anaerobically digested sludge

BCR SE Fractions	T1 simple aromatic proteins		B simple aromatic proteins		T2 SMP by-product		A Fulvic acid-like organics		C Humic acid-like organics	
	Ex	Em	Ex	Em	Ex	Em	Ex	Em	Ex	Em
Exchangeable	220 ± 1	304 ± 3	220 ± 1	355 ± 6	277 ± 3	354 ± 5	224 ± 8	421 ± 7	344 ± 6	423 ± 6
Reducible	-	-	-	-	-	-	262 ± 9	427 ± 2	339 ± 9	428 ± 5
Oxidisable	-	-	-	-	-	-	220 ± 1	414 ± 6	345 ± 4	429 ± 6
Residual	-	-	-	-	-	-	256 ± 3	410 ± 4	361 ± 2	409 ± 3

Intensities are expressed as mean ± standard deviation (n=36).

5.5.2. Discussion

The combination of fluorescence spectroscopy coupled with BCR sequential extraction procedures gave information on the extraction of organics in the different sequential extraction fractions, and so consequently indication on the extraction of metal-organic compounds. Small organics and SMP were extracted mostly in the first fraction (exchangeable), with a remaining in the second fraction (reducible). The EEM fluorescence spectroscopy confirmed that metal extracted in the exchangeable fraction might be associated with the biomass, extracellular polymeric substances (EPS) and other by product compounds by absorption, assimilation or complexation. Following the EEM fluorescence spectroscopy, humic substances were extracted in the three last fractions of the BCR sequential extraction. Fulvic acids were dominating in the reducible fraction and humic acids in the oxidisable and residual fractions.

Sheng and Yu (2006) found that extracellular polymeric substance can be detected using EEM fluorescence and determined the three peaks related to it. The three peaks have been defined at Ex/Em of 225/340-350, 280-285/340-350 and 330-340/420-430. Those three peaks were also detected in the BCR exchangeable fraction, even if a slightly shift has been observed concerning the emission wavelength of some peaks. Sheng and Yu (2006) and Reynolds (2002) showed that the emission wavelength can be affected by the pH and the metal concentrations, and this quenching can explain the gap between Sheng et al.'s values and the values observed in the exchangeable fraction.

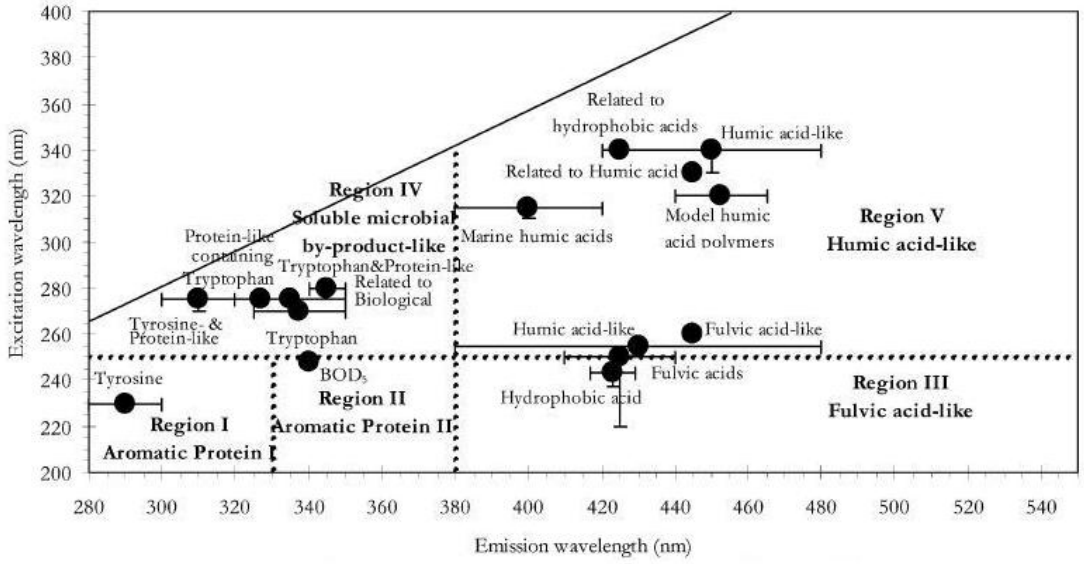

Figure 5.9. Definition of the different EEM peaks and regions adapted from Chen et al. (2003).

For the three other BCR sequential extraction fractions, humic acid-like and fulvic acid-like peaks have been compared with Chen at al. (2003) peaks shown in figure 5.9. In the reducible fraction, the two peaks could be both related to humic acid-like compounds with one (Ex/Em, 260/430) close from the fulvic acids and hydrophobic acid peaks. The third fraction (oxidisable), the peak could be compared with only humic acid-like compounds. Plaza et al. (2006) found that municipal sewage waste compounds had one main humic acid fluorophore compounds that was identified at 340/437 and could be linked with the peak found in the reducible and oxidisable fractions. In the last fraction (residual), the lower excitation wavelength peak could be identified as humic acid-like compounds with a shorter emission wavelength due to the high acidity of the solution (Reynolds, 2002 and Mobed et al., 1996). The second peak (higher excitation wavelength) could not be related to any other compounds from Chen et al. (2003) peaks due to

the high quenching from the pH. The hydrophobic acids peak (Ex/Em, 340/420-430) was the closest peak from it.

Fluorescence spectroscopy analysis on each BCR sequential extraction fraction showed the presence of organics extracted in the exchangeable and oxidisable fractions as expected but also in the reducible and residual fractions. NPOC analysis on the reducible and residual extracted solution has been performed to measure the concentration of organic carbon in the fractions (results not shown). Concentrations of organic carbon were around 10 and 80 mg/kg DS in the reducible fraction and 40 and 150 mg/kg DS in the residual fraction. Those concentrations were too low to indicate that those stages played an important role in the extraction of organics and so most organics were extracted in the oxidisable fraction. However, there was a potential of metal organics to be extracted earlier in the reducible fraction and later in the residual fraction. These results could be related with the copper extraction profile observed in section 5.2. The presence of copper in the reducible fraction might be explained by an early dissolution of copper-organics in the reducible fraction, likely to be from copper bound with fulvic acids.

Fluorescence spectroscopy analysis helped to obtain information on the extraction of the organics in the different BCR sequential extraction fractions. All organics related to the biomass and metals bound with it were extracted during the first sequential extraction fraction (exchangeable). Most of the organics were extracted in the oxidisable fraction but fulvic acid-like organics could be extracted in the

reducible fraction and related hydrophobic acids compounds could be extracted in the residual fraction. Fluorescence spectroscopy analysis confirmed the definition of the different fractions of the BCR sequential extraction from an organic side, but it might also explain the presence of copper in the reducible fraction by the release of copper-organic chelates, likely to be copper-fulvic acid-like chelate, in this fraction. However, the extraction of most organics in the oxidisable confirmed the inability to distinguish the binding forms of copper extracted in this fraction.

5.6. Assessment of the use of pH titration in the study of metals speciation in anaerobically digested sludge

The solubility products of compounds in anaerobically digested sludge are pH dependent. A variation of pH has a direct impact on the different chemical equilibriums present in the sludge such as metal precipitates or complexes (see section 2.5). The titration of anaerobically digested sludge with an acid or base solution changes the pH and consequently alters the metals equilibrium between solid and liquid phases. Theses alteration can be clearly observed by the variation of metals concentration in the liquid phase. A series of measurements in the pH range (0-14) allowed the construction of a pC-pH diagram, which was showing the variation of the metal concentration in the liquid phase in function of the pH. Those variations were used to determine the different metal species and their concentrations in the sludge. This technique can be assimilated as a sequential

extraction procedure where metals are released from the solid phase only using acid or base solutions as extracting agent.

The pH titration procedure has been developed in section 4.3.4. The main interest of using titration in comparison with sequential extraction procedure laid on the observation of the change in the solid-liquid equilibrium for a pH range of 4 to 12. The first extracting solution used for the exchangeable fraction (acetic acid) had a pH around 3 (Dodd et al., 2000) and the other extracting solutions had a pH set at 2 or under with nitric acid. So the study of the variation of metal concentrations in the liquid phase for a pH varying from 4 to 8 gave more information on the compounds released in the first BCR sequential extraction fraction. Metals released between pH 2 and 4 could be associated with metals extracted in the exchangeable/reducible fractions.

The aim of this section was to demonstrate the interest of using pH titration to characterize the different metal species extracted in the BCR exchangeable and reducible fractions.

5.6.1. Results

Concentrations of copper and nickel in the liquid phase of anaerobically digested sludge at different pH are shown in table 5.8. The mass concentration (mg/l) measured by ICP-AES were transformed into pC (log of the molar concentration)

to draw the pC-pH diagram shown in figures 5.10 and 5.11. Copper concentrations were included in the range 0.006 - 0.592 mg/l. The highest concentration of copper in the liquid phase was obtained at pH 12 for each sludge (0.592 mg/l for sludge K, 0.164 mg/l for sludge R and 0.066 mg/l for sludge F). The lowest was obtained at pH 6 for each sludge (0.006 mg/l for sludge K and R and 0.008 mg/l for sludge F).

Nickel concentrations in the liquid phase were included in the range of 0.047 - 0.891 mg/l. The highest concentration of nickel in the liquid phase was obtained at pH 2 (0.891 mg/l, 0.535 mg/l and 0.797 mg/l, respectively for the sludge K, R and F). The lowest concentration was achieved at pH 8 for each sludge (0.047 mg/l, 0.048 mg/l and 0.095 mg/l respectively for the sludge K, R and F).

The figure 5.10 shows that the titration curves of three types of anaerobically digested sludge (K, R and F) exhibited a similar pattern in the variation of copper concentrations in the liquid phase in function of the pH. Copper concentration decreased with pH varying from pH 2 to 6 and the lowest concentration of copper was observed at pH 6. The variation was a decrease of around 1 unit which represent a factor 10 in the concentration. After the pH 6, the concentration of copper increased with the pH with a variation included between 1 and 2 units. The highest increase was observed with the sludge K and the lowest with the sludge F.

Table 5.8. Concentrations of copper and nickel in the liquid phase measured during the pH titration analysis

Metal	pH	Sludge F		Sludge K		Sludge R	
		$[Me]_l$ (mg/l)	p[Me]	$[Me]_l$ (mg/l)	p[Me]	$[Me]_l$ (mg/l)	p[Me]
Cu	2	0.046 ± 0.001	-6.14	0.034 ± 0.001	-6.28	0.039 ± 0.001	-6.21
	4	0.015 ± 0.01	-6.63	0.015 ± 0.001	-6.63	0.012 ± 0.001	-6.74
	6	0.003 ± 0.001	-7.36	0.006 ± 0.002	-7.02	0.006 ± 0.001	-7.05
	7	0.009 ± 0.001	-6.84	0.019 ± 0.001	-6.53	0.011 ± 0.001	-6.75
	8	0.018 ± 0.001	-6.56	0.031 ± 0.001	-6.31	0.025 ± 0.001	-6.40
	9	0.012 ± 0.001	-6.71	0.063 ± 0.001	-6.01	0.012 ± 0.001	-6.72
	10	0.026 ± 0.001	-6.38	0.194 ± 0.001	-5.51	0.043 ± 0.001	-6.17
	12	0.066 ± 0.002	-5.98	0.592 ± 0.006	-5.03	0.164 ± 0.001	-5.59
Ni	2	0.797 ± 0.007	-4.87	0.891 ± 0.005	-4.82	0.535 ± 0.004	-5.04
	4	0.315 ± 0.003	-5.27	0.164 ± 0.002	-5.56	0.191 ± 0.002	-5.49
	6	0.152 ± 0.004	-5.59	0.056 ± 0.002	-6.02	0.059 ± 0.001	-6.00
	7	0.126 ± 0.002	-5.67	0.065 ± 0.001	-5.96	0.050 ± 0.002	-6.07
	8	0.095 ± 0.002	-5.79	0.047 ± 0.002	-6.10	0.048 ± 0.002	-6.09
	9	0.307 ± 0.005	-5.28	0.058 ± 0.002	-6.01	0.371 ± 0.005	-5.20
	10	0.194 ± 0.006	-5.48	0.092 ± 0.002	-5.81	0.071 ± 0.002	-5.92
	12	0.178 ± 0.002	-5.52	0.212 ± 0.002	-5.44	0.126 ± 0.002	-5.67

Values are expressed as mean ± standard deviation (n=3) and as p[Me] = log[Me]

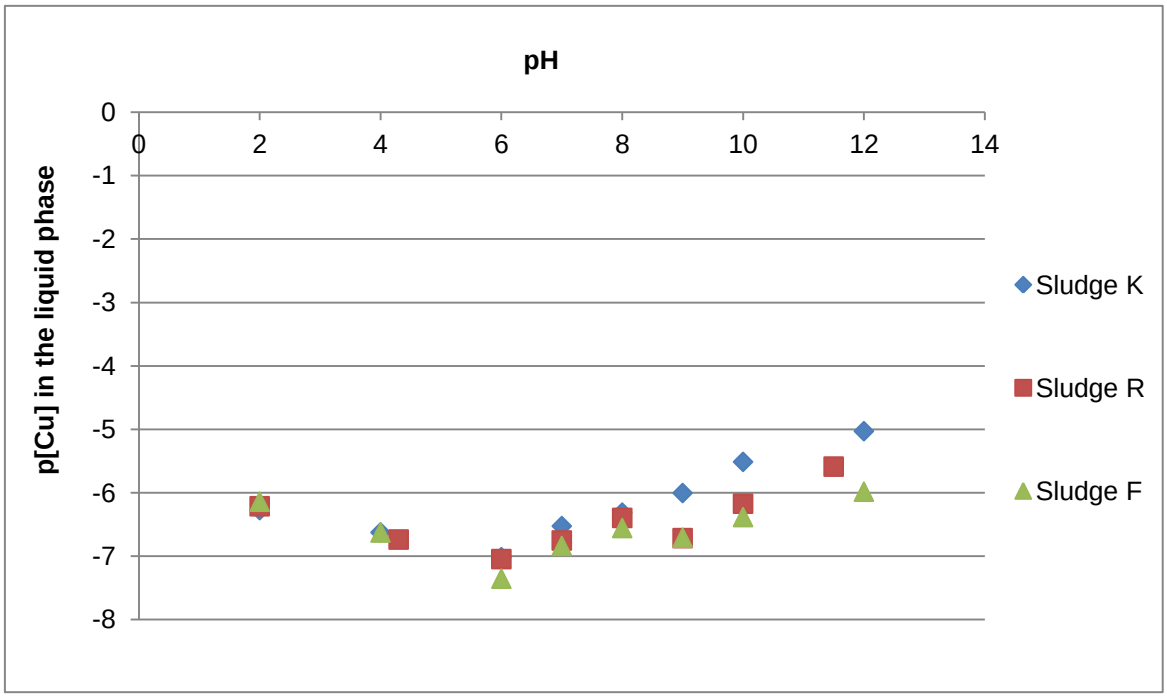

Figure 5.10. p[Cu]-pH diagram for the sludge F, K and R

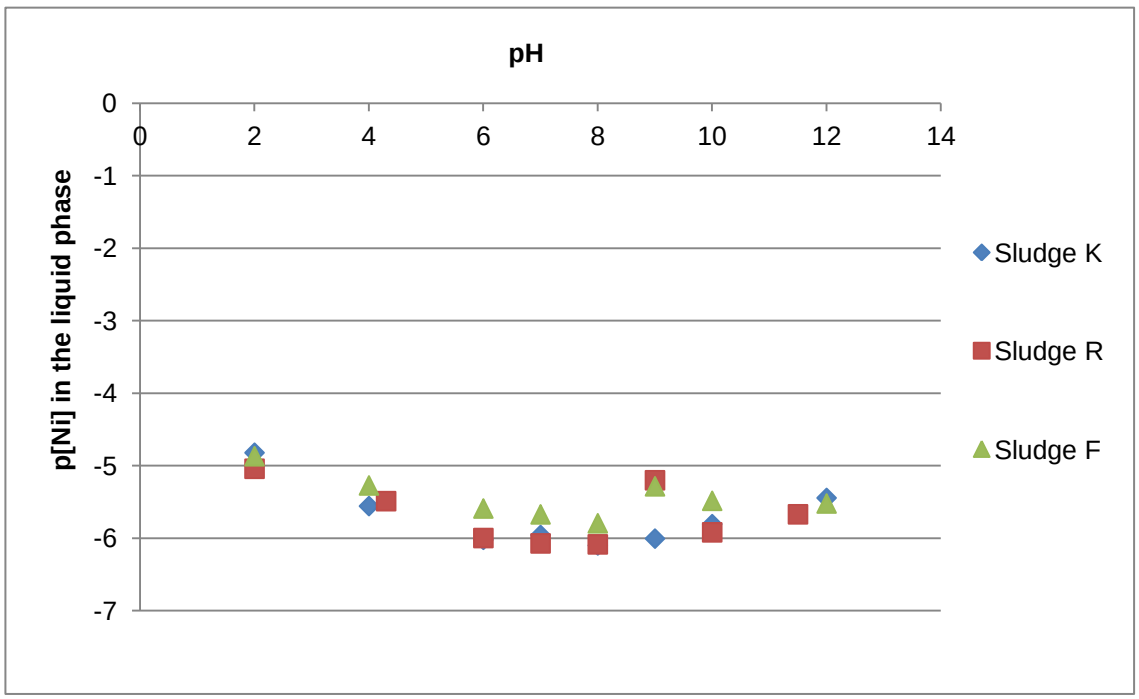

Figure 5.11. p[Ni]-pH diagram for the sludge F, K and R

The figure 5.11 shows that the titration curves of three types of anaerobically digested sludge (K, R and F) exhibited a similar pattern in the variation of the concentration of nickel in the liquid phase in function of the pH. The concentration decreased (1 unit) from the pH 2 to pH 6 and there was a small increase between the pH 9 and 12. At a pH 9, the concentration of nickel showed a disparity with a higher concentration for the sludge F and R.

5.6.2. Discussion

All the titration curves presented a specific pattern in V, where the intensities of the slopes were depending on the strength of the different metal bindings. The tipping point on the curve in a V shape, representing the lowest metals concentration measured in the liquid phase, was obtained at neutral pH, between pH 6 and 8. The pH of anaerobic digester (pH 7-8) was expected to be included in the zone of the tipping point due to the stability of the chemical equilibrium. Under acid and basic pH, the release of metals from precipitates or complexes led to an increase of metal concentrations in the liquid phase. The pH of metals dissolution gave information on the metal binding strength in the sludge and amount of metals dissolved gave information on the quantity of metals present under this chemical form.

Copper concentrations in the supernatant have been measured between 0.018 and 0.085 mg/l during the BCR sequential extraction experiments (results not

shown). During the pH titration, concentrations of copper in the liquid phase at pH 7 and 8 were included in this range. The copper concentrations in the solid phase measured by the total acid digestion or sum of the BCR sequential extraction fractions were included in the range of 0.19-0.62 g/kg DS, which can be converted to 3-10 mg/l (see sections 5.1 and 5.2). The maximum concentration of copper observed at pH 12 was 0.592 mg/l, and so most of the copper was not released during the titration. Results from the BCR sequential extraction procedure showed that the extraction of copper from anaerobically digested sludge required an extracting solution at pH 2 or below and an oxidising agent needed to be present to dissolve copper bindings. This strong binding of copper was caused by its presence as copper sulphide and/or copper-organic chelates.

Alibhai et al. (1985), Gould and Genetelli (1984) and Fletcher and Beckett (1987) showed that the binding of metals with organics (complexation or adsorption) was pH sensitive. A decrease of pH in the sludge increased the competition between protons and metals for the organics binding site and so it reduced the degree of metals complexation (Cheng et al., 1975). The maximum binding for copper with soluble organic matter and soluble fulvic acid was observed at a pH between 6 and 7 (Ryan et al., 1983 and Fletcher and Beckett, 1987). Results from the titration experiment agreed with the maximum uptake of copper by SOM at pH 6-7 with the lowest concentration of copper in the liquid observed at pH 6. The increase of copper in the liquid phase under acidic pH could be related by a release of copper from the fulvic acid complexation and sludge sorption due to the increase of the proton competition. However, copper bound with humic acid was not released

during the titration as its extraction requires a solution at pH of 2 and the presence of an oxidising agent (oxidisable fraction of BCR sequential extraction procedure).

The increase of the copper concentration in the liquid phase under basic pH was more difficult to explain as copper sulphide should not be dissolved and the organic complexation should be stable. So the increase of copper concentration in the liquid phase might be related to an increase of copper inorganic ion or molecule (such as $Cu(OH)_{2,}$ $Cu(OH)^{+}$).

Concentration of nickel in the solid phase of anaerobically digested sludge has been measured using total acid digestion in a range of 1.1 and 1.4 g/kg DS (17.6 - 22.4 mg/l). The maximum concentration of nickel released during the titration was less than 1 mg/l and was obtained at pH 2. So nickel present in the solid phase was also strongly bound and mainly formed as nickel-sulphide or nickel-silicate compounds. During the SEM-EDS analysis, presence of nickel carbonate was observed but the pC-pH diagram demonstrated that the concentration of nickel carbonate was limited as there was no large release of nickel during the titration (between pH 4 and 6, see with manganese chapter 7.3). Callander and Barford (1983b) also calculated that nickel sulphide was the dominant precipitate in the nickel speciation and that the secondary precipitate to forms should be nickel-phosphate. The presence of NiS has been reported in anaerobically digested sludge by Fermoso et al. (2008b), Liu and Fang (1998) and Jong and Parry (2004).

The titration experiment is a useful analytical technique in the study of the metals speciation as it is using the strength of the different metal bindings to identify them. This method can be considered as quantitative and qualitative but some limitations reduce its interest. An additional method needs to be coupled with the titration to obtain the total concentration of metals in anaerobically digested sludge because the range of pH used does not allow the complete solubilisation of the metals. Moreover, some precipitates and complexes are only dissolved at pH under 2, e.g. metal-sulphide.

The use of pH titration in addition of the BCR sequential extraction analysis brought information on the species of metals extracted during the first fraction (exchangeable) and also the second fraction (reducible). The analysis of the pC-pH diagram showed that nickel carbonate detected during the SEM-EDS analysis was not largely present in the sludge. However, no information could be exploited from the titration analysis concerning the oxidisable and residual fractions.

So from the copper analysis, pC-pH diagram confirmed the strong binding of copper, but it could not show if copper was bound with sulphide or organics in the BCR oxidisable fraction. Nevertheless, the presence of the lowest copper concentration at pH 6 confirmed the ability of copper to bind with organics.

5.7. Assessment of the use of geochemical equilibrium model in the study of metals speciation in anaerobically digested sludge

The speciation of metals at the equilibrium in a specific environment could be accurately calculated using the thermodynamic constants of metals reactions potentially occurring in this environment. An example of such calculation has been done by Callander and Barford (1983) with metals in anaerobic digesters. However, due to the large number of potential reactions, their work was limited to the main reactions at a specific concentration.

The use of chemical modelling software is essential in order to take into account the larger number of reactions occurring in the digester. Geochemical equilibrium speciation models were originally developed for use in aqueous systems and they have been successfully used to simulate metals speciation in wastewater treatment systems (Zhang et al., 2008), water streams (Gallios and Vaclavikova, 2008) or sewage sludge (Andres and Francisco, 2008).

The aim of this section was to evaluate the potential of geochemical equilibrium model in the simulation of metals speciation in anaerobically digested sludge and to demonstrate its interest as a complimentary technique alongside other analytical techniques described above.

Phreeqc was the model chosen to develop the simulation of metals speciation in anaerobically digested sludge using experimental concentrations and conditions.

To simplify the modelling, only inorganic precipitations have been taken into account using the total concentration of metals, anions (P, S and inorganic C) and some competitive cations (Ca, Mg, Na and K). The presence of organics or complexing surface, used during the adaptation of the model to simulate metals speciation in anaerobically digested sludge, did not have an effect on the predictions from the model and they were not included in the final simulations. More details on the chemical equilibrium speciation model are described in section 4.5.

5.7.1. Results

The results from the predicted metals speciation are shown in table 5.9 for the seven types of anaerobically digested sludge under study. The input values for iron and other elements (anions, cations and metals) were obtained from their total concentrations measured in each sludge in section 5.2.1. The input values are displayed in appendix E (table E.1) and an example of Phreeqc's simulation for the sludge K is shown in appendix G.

Table 5.9. Prediction of the metals speciation in the seven types of anaerobically digested sludge using Phreeqc

Metals		Sludge						
		K	G	M	H	S	R	F
Liquid phase (concentration in mg/l)	Co	8.3×10^{-8}	1.1×10^{-7}	1.6×10^{-7}	1.7×10^{-7}	1.9×10^{-7}	2.0×10^{-7}	1.5×10^{-7}
	Cu	5.9×10^{-2}	4.9×10^{-2}	2.7×10^{-2}	2.2×10^{-2}	2.2×10^{-2}	1.4×10^{-2}	2.5×10^{-2}
	Fe	0.14	0.15	0.17	0.17	0.18	0.20	0.18
	Mn	7.7×10^{-6}	8.8×10^{-6}	1.2×10^{-5}	1.1×10^{-5}	1.2×10^{-5}	1.3×10^{-5}	2.4×10^{-5}
	Ni	1.4×10^{-9}	2.0×10^{-9}	3.1×10^{-9}	3.1×10^{-9}	3.8×10^{-9}	3.8×10^{-9}	3.1×10^{-9}
	Zn	1.1×10^{-5}	1.1×10^{-5}	9.2×10^{-6}	8.5×10^{-6}	8.5×10^{-6}	7.8×10^{-6}	8.5×10^{-6}
Solid phase (concentration in g/kg DS)	Co as CoS	0.071	0.071	0.068	0.062	0.086	0.074	0.080
	Cu as Covellite	0.50	0.29	0.35	0.61	0.27	0.40	0.19
	Fe as Pyrite	7.2	6.7	6.2	5.0	4.8	5.9	9.8
	Fe as Vivianite	2.7	3.4	12.6	14.9	17.6	18.2	19.3
	Mn as $MnHPO_4$	0.35	0.35	0.71	0.22	0.24	0.3	0.35
	Ni as NiS	1.1	1.1	1.2	1.2	1.1	1.3	1.3
	Zn as Sphalerite	0.73	0.57	1.5	0.66	0.88	0.82	0.86

From the model, metals were predicted to be completely bound in the solid phase with a low concentration remaining in the liquid phase. Iron was predicted to have the highest concentration in the liquid phase with 0.14-0.20 mg/l. The second highest metal concentration predicted in the liquid phase was for copper, with a concentration varying between 0.022 and 0.059 mg/l. The remaining metals had

predicted concentrations below 10 nanograms per liter (manganese: 1.1-8.8 x 10^{-6} mg/l; zinc: 1.1-8.2 x 10^{-6} mg/l; cobalt: 8.3-20 x 10^{-8} mg/l and nickel: 1.4-3.8 x 10^{-9} mg/l).

In the solid phase, metals (except manganese) were predicted to be precipitated with sulphide to form insoluble compounds. Cobalt, copper, nickel and zinc were exclusively present in the solid phase as monosulphide precipitates, respectively CoS, covellite (CuS), NiS and sphalerite (ZnS). Their concentrations as sulphide precipitates in the different types of sludge were corresponding to their total concentrations measured using total acid digestion and used as input values. This confirmed the complete precipitation of those metals with sulphide.

Iron was also predicted to precipitate with sulphide as pyrite (FeS_2). However, its precipitation was only partial and iron was also predicted to be present in the solid phase as vivianite ($Fe_3(PO_4)_2.8H_2O$). The concentrations of the two precipitates varied between the seven types of sludge with 4.8-9.8 g/kg DS for iron precipitated as pyrite and 2.7-19.3 g/kg DS for iron precipitated as vivianite. The total concentrations of iron (sum of the two precipitates) corresponded to the total concentrations measured using total acid digestion and used as input values. The behaviour of iron in anaerobically digested sludge has been fully developed in chapter 6.

Finally, manganese was predicted to be precipitated with phosphate to form $MnHPO_4$ compound. The concentrations of manganese as $MnHPO_4$ varied from

0.22 g/kg DS to 0.71 g/kg DS, corresponding to the total concentrations measured using total acid digestion and used as input values.

5.7.2. Discussion

Phreeqc, a geochemical equilibrium model, was used to simulate the inorganic phase of the metals speciation for the seven types of anaerobically digested sludge using experimental concentrations and conditions (appendix E). The simulation results (table 5.9) demonstrated the strength of sulphide binding from the thermodynamic aspect. In absence of any kinetics limitation, most of the metals were predicted to bind in the solid phase with sulphide to form insoluble precipitates. Only manganese and iron were predicted to precipitate with phosphate. Concerning iron, the formation of vivianite was the result of a sulphide limitation (see chapter 6).

The simulation of metals speciation by the model followed the thermodynamic predictions with sulphide precipitation as the main reaction (Callander and Barford, 1983). Those predictions also agreed with the literature which found that cobalt, copper, iron, nickel and zinc were precipitated with sulphide in anaerobically digested sludge (section 2.4).

Concerning the two metals chosen to assess the different analytical techniques in this chapter, copper was predicted to form covellite (mineral) with sulphide, while

nickel was predicted to form a precipitate (NiS) with sulphide. Their predicted low concentrations in the liquid phase and the presence of one specific compound in the solid phase demonstrated that sulphide precipitation should be the only reaction controlling the copper and nickel behaviour in anaerobically digested sludge.

Results from the different analytical techniques demonstrated that the speciation of copper and nickel was composed of several compounds and so the predictions from the model were not completely in accordance with the experimental values. Sulphide precipitates should be extracted in the BCR oxidisable or residual fraction and the presence of nickel and copper in the two first fractions (exchangeable and reducible) demonstrated that weakly bound compounds were formed in the sludge (tables 5.3 and 5.4, figures 5.4 and 5.5). Those weakly bound compounds were not predicted by the model. Several differences between experimental and model results were also observed for the cobalt, zinc and manganese in chapter 7 (section 7.3-7.5).

The difference was mainly due to the limitation of the model to simulate perfectly anaerobically digested sludge. The model calculated the speciation at the equilibrium for an ideal reactor; however an anaerobic digester could not be considered as such. One of the limitations was the absence of consideration by the model of secondary reactions, such as phosphate precipitation or organic complexation, influencing the metals speciation. These reactions were not predicted because the main reaction was enough to reach the equilibrium for

these metals. The large amount of sulphide in comparison with metals concentration allowed their complete precipitation. Moreover, the order of metals precipitation with sulphide was dependent on their solubility products and copper and nickel were predicted to form sulphide precipitates before iron (section 6.2.3).

The second limitation was the absence of a well-defined organic complexation and biomass adsorption model specifically designed for anaerobically digested sludge simulation. No characterization of the potential biomass or organic bindings was done during this study on the different types of sludge, preventing their integration into the model simulation. The use of organic binding was only limited at the chapter 7 simulation, using pre-defined organic binding model (see section 4.5).

Despite the limitations observed in the simulation of metals speciation in anaerobically digested sludge, there were some benefits in the use of the model as a complementary technique in this research. The compilation of all the potential inorganic reactions gave useful information on the thermodynamic order of the controlling reactions for one specific metal. Moreover, the opportunity of modifying the conditions, the element concentrations or removing some precipitates was used to enhance or confirm some results obtained using experimental analysis and also to simulate the effects of one factor on the metals behaviour.

The use of the model was consequently limited to support several experimental results in the following two chapters. The specificity of iron in anaerobically digested sludge (high concentration and absence of organic interaction) allowed a

comparison between model (Phreeqc and Visual Minteq) predications and experimental results in order to confirm the different reactions controlling the iron behaviour (chapter 6). In chapter 7, model (Visual Minteq) was used in combination with pH titration in order to determine or confirm the different metal species released during the titration.

5.8. General discussion and conclusion

Determination of the metals speciation in anaerobically digested sludge is complicated by the nature of the sludge and the multitude of reactions occurring in the anaerobic digester. Thermodynamic and kinetic play both a controlling role in the different metals reactions. Several analytical techniques have been developed to measure different aspect of the metals speciation but all of them have a shadow zone where no information is given from a qualitative or quantitative point of view.
Sequential extraction procedures have been particularly designed to observe the metals behaviour in soil, sludge and sediment samples. However, its use has mainly been limited to describe the metals mobility in the studied matrix and from the results exposed above there was a lack of clear information on the metals species extracted in each fractions. Banerjee (2002) defined each fraction of the sequential extraction procedure as an isolated phase and Dodd et al. (2000) explained that the extraction is define by the element reactivity rather than a individual characterization of each phase.

Copper analysis using the BCR sequential extraction procedure, which was mainly extracted in the oxidisable fraction, could not dissociate the copper bound with sulphide or organics. Adamo et al. (1996) also observed this impossibility to distinguish the copper speciation released in the oxidisable fraction using only sequential extraction. Moreover, Dodd et al. (2000) pointed also out the presence of uncertainties related to the sequential extraction such as not completely selective reagent, unanticipated dissolution or redistribution between species. Fluorescence spectroscopy analysis showed that a small part of organics were extracted in the reducible fraction.

The improvement on the definition of each sequential extraction fraction and the compounds extracted in it increased the potential and interest of using the BCR sequential extraction procedure in the study of metals speciation. Nevertheless, several studies noticed the impact of some artefacts (such as re-precipitation and early release) on the metal extraction and could locally create a change on the results. Gustavsson (2012) showed that there was a change in sulphur "speciation" during the sequential extraction procedure creating a different behaviour for the metals bound with it. In this study, the presence of copper at difference percentage in the reducible fraction could be linked with an early release of copper-organics. BCR sequential extraction method was proven to be repeatable and liable as the Tessier's method by Davidson et al. (1994); however, some errors could be caused by the complexity of the matrix, the sludge sensibility and the experimental errors. Although there was some indistinguishable data in

the results, sequential extraction analysis brought a first and strengthen base of information that needed to be completed using other analytical techniques.

Zimmerman and Weindorf (2010) concluded their review of different sequential extractions on metals speciation in soil by the interest of combining the data from sequential extraction with other analytical results. In their study, Zimmerman and Weindorf (2010) combined the sequential extraction with XRD to observe any change of the chemical structure after each extraction. Adamo et al. (1996) and Dodd et al. (2000) used SEM-EDS to identify the chemical compounds still present in the samples after each extraction.

In this research, the combination of other analytical techniques with the BCR sequential extraction procedure (such as SEM-EDS, titration, fluorescence spectroscopy and model simulation) increased the information on the speciation of nickel and copper and also on the specificity of the reagents and their potential of extraction. However, the low metals concentrations limited the availability of the information from these techniques. Moreover, several analytical techniques could not be applied due the complexity of the sludge environment. The XRD technique that has been used by Zimmerman and Weindorf (2010) has restricted interest in anaerobically digested sludge as most of the metals were precipitated as amorphous compounds. A summary of the advantages and disadvantages of each assessed analytical techniques is shown on the table 5.10.

Table 5.10. Summary of the assessed analytical techniques: advantages and disadvantages.

Analytical techniques	Advantages	Disavantages
BCR sequential extraction procedure	● ·Quantitative and semi-qualitative analysis	● No differentiation between several compounds extracted in the same fraction
	● Information on organic and inorganic fractions	● Potential early or late release of a compound across several fractions
Scanning electron microscopy coupled with energy dispersive spectroscopy	● Qualitative information on metal precipitates	● No quantitative analysis
	● Determination of metal species present in the sludge	● No information on the organic fraction
pH titration	● Quantitative and qualitative analysis	● Detection limited to weakly bound compounds (reducible + exchangeable BCR SE)
	● Detection of the metal species extracted in a BCR SE fraction	● A total metal concentration analysis is required
Fluorescence spectroscopy	● Determination of the fractions containing metal-organic complexes	● No determination of the specific binding between metals and organics
	● Qualitative detection of fluorophore organics	● No quantitative analysis
Geochemical equilibrium model	● Complete information on the metals speciation at the equilibrium in an ideal reactor	● No kinetic effect included in the calculation
	● Simulation of pH titration experiment	● Organic complexation and adsorption are not developed enough.
	● Determination of the metal species extracted in a BCR SE fraction	● Limitation on the simulation of several reactions for one metal

In conclusion, this study demonstrated that a method combining a suite of analytical techniques needed to be developed in order to obtain complete and detailed results on the speciation on the metals under study. The BCR sequential extraction procedure was used as the reference point and complementary techniques including titration, SEM-EDS analysis and model simulation were systematically used to develop and confirm the results shown by the BCR sequential extraction procedure.

CHAPTER 6. IRON BEHAVIOUR IN ANAEROBICALLY DIGESTED SLUDGE IN THE CASE OF CPR-IRON DOSING

6.1. Introduction

Following chapter 5 and its conclusions, a suite of analytical techniques were applied to investigate the iron speciation in the solid phase of anaerobically digested sludge and to determine the reactions that influence the formation of iron precipitates. Iron was chosen due to its high concentrations in sewage sludge from wastewater treatment works, which occurs primarily as results of upstream iron dosing for chemical phosphorus removal (CPR) during wastewater treatment. The chemical phosphorus removal used in some wastewater treatment offered a wide range of iron concentrations in different anaerobic digesters.

Iron, by its high concentration, plays an important role in the chemistry of anaerobically digested sludge, particularly in the inorganic fraction, and may influence other elements speciation (trace metals) present in this fraction. Metcalf and Eddy (2003) reported that the median concentration of iron in wastewater solid is 17,000 mg/kg Dry Solid (DS) and it is 10 times higher than the median concentration of the second highest heavy metal, zinc with 1,700 mg/kg DS. Moreover, the iron concentration is also increased during the iron dosing for

chemical phosphorus removal and/or hydrogen sulphide control (Carliell-Marquet et al., 2010 and Zhang et al., 2009) and a large addition of iron may create disequilibrium in the inorganic fraction leading to the failure of the digester. The effect of the iron dosing on digesters has already been studied (Yeoman et al., 1990; Johnson et al., 2003; Smith and Carliell-Marquet, 2006; Carliell-Marquet et al., 2010 and Zhang et al., 2009) but most of this research focused on its impact on the methane production.

From the literature and thermodynamic data (see sections 2.4 and 2.5), iron speciation should be controlled by the sulphide concentration and iron would precipitate mostly as ferrous sulphide (FeS) and/or pyrite (FeS_2) (Morse and Luther, 1999; Zhang et al., 2010, Callander and Barford, 1983 and Oleszkiewicz and Sharma, 1989). However, Miot et al. (2009) demonstrated that iron may precipitate as vivianite ($Fe_3(PO_4)_2.8.H_2O$) at high phosphate concentration and under anaerobic condition. Carliell-Marquet et al. (2010) and Ofverstrom et al. (2011) also observed the presence of ferrous phosphate precipitates in iron dosed anaerobically digested sludge.

So even if sulphide is controlling the iron speciation, phosphate may significantly precipitate with iron to influence the overall speciation, especially in iron dosed anaerobically digested sludge. An understanding of the reactions controlling iron speciation in the inorganic fraction is consequently necessary for predicting the fate of iron in the digester and the effects of an increase of its concentration on other metals speciation and a potential metal inhibition.

The aim of this chapter was to investigate the behaviour of iron in the anaerobically digested sludge by characterizing the different iron chemical forms and the reaction controlling its speciation. To achieve this aim, a characterization of the iron speciation has been done first using the suite of analytical techniques developed in the previous chapter. The second objective was to compare the iron fractionation profiles of anaerobically digested sludge with a large range of iron concentration. Finally the impact of phosphate and sulphide on the iron speciation has been investigated using a comparison of their fractionation profiles and prediction from the chemical equilibrium models.

The study of iron speciation in anaerobically digested sludge was conducted using sludge from full scale anaerobic digesters. Seven digesters from UK wastewater treatment works have been selected based on their iron dosing regimes at the treatment works to obtain a range of iron concentrations. The full description of the experiments is detailed in section 4.1. The results obtained in this section have been collected using a combination of different analytical techniques described in chapter 4.

6.2. Results

6.2.1. Total acid digestion and BCR sequential extraction procedure

The BCR sequential extraction procedure was the first analytical technique used in the study of iron speciation in anaerobically digested sludge. This technique gave

indication on the iron fractionation profile and the strength of iron bindings in the seven types of sludge used in this experiment. Phosphorus and sulphur extraction profiles were also analysed to observe their variation in function of the iron concentration.

Table 6.1. Concentrations of iron in the solid and liquid phases of 7 anaerobically digested sludge

Sample		Liquid phase			Solid phase	
Sludge	Iron dosing	Concentration (mg/l)	% of total iron		Acid digestion (g/kg DS)	Σ SE fractions (g/kg DS)
			Acid digestion	Σ SE fractions		
K	No	0.35 ± 0.21	0.1	0.2	12.6 ± 0.3	9.7 ± 1.2
G	No	0.34 ± 0.06	0.1	0.2	13.1 ± 1.0	10.2 ± 0.7
M	Mix	0.47 ± 0.19	0.1	0.1	21.3 ± 2.6	18.9 ± 1.3
H	Mix	0.49 ± 0.25	0.1	0.1	22.6 ± 0.8	19.8 ± 0.8
S	Mix	0.57 ± 0.37	0.1	0.1	26.7 ± 1.1	22.5 ± 1.9
R	Yes	0.64 ± 0.06	0.1	0.1	27.3 ± 2.4	23.9 ± 0.9
F	Yes	0.58 ± 0.02	0.1	0.1	33.0 ± 1.5	28.8 ± 0.9

The concentrations are expressed as mean ± standard deviation (n=6) and percent of total

The tables 6.1 and 6.2 show respectively the concentrations of iron in the liquid and solid phases and in each fraction of the BCR sequential extraction procedure. The liquid phase represents the filtrate solution (<0.45 µm) and the iron measured in this phase was considered to be present as soluble chemical forms (see sections 4.2.1, 2.3 and 2.8).

Iron concentrations in the liquid phase were low in comparison with the concentrations in the solid phase and they were included between 0.3 and 0.7

mg/l. Only 0.1% (on average) of the total iron was present in the liquid phase and so 99.9% of the iron was bound in the solid phase. Most of the iron was immobilized in the sludge and even in high iron concentration sludge (R and F), the reactions governing iron speciation kept it in the solid phase. So the study of iron speciation focused mainly on the solid phase.

Iron concentrations in the solid phase of the different anaerobic digesters were in the range from 9.7 g/kg DS to 28.8 g/kg DS using the sum of the sequential extraction fractions and from 12.6 g/kg DS to 33 g/kg DS using total acid digestion. In both cases a similar factor (around 3) was observed between the lowest and highest iron concentrations. However, the amount of iron extracted during the total acid digestion was always higher than the amount extracted during the BCR sequential extraction procedure. The percentage of recovery from the iron extracted during the BCR sequential extraction in comparison with the total iron concentrations measured using total acid digestion method was similar across the seven types of sludge at around 85%. This difference in the total concentrations between the two methods showed a loss of 15% of iron during the BCR sequential extraction procedure.

Table 6.2. Concentrations of iron in each BCR SE extraction fraction for the 7 anaerobically digested sludge

Sample		Concentrations of iron in each BCR sequential extraction fraction							
Sludge	Iron dosing	Exchangeable		Reducible		Oxidisable		Residual	
		%	g/kg DS	%	g/kg DS	%	g/kg DS	%	g/kg DS
K	No	54	5.2 ± 0.8	21	2.0 ± 0.6	0	< d.l.	25	2.4 ± 0.1
G	No	61	6.2 ± 0.6	15	1.6 ± 0.1	0	< d.l.	24	2.4 ± 0.2
M	Mix	63	11.9 ± 0.7	19	3.5 ± 0.4	0	< d.l.	18	3.4 ± 0.6
H	Mix	67	13.4 ± 0.6	21	4.2 ± 0.5	0	< d.l.	12	2.2 ± 0.2
S	Mix	67	15.0 ± 0.5	23	5.3 ± 1.0	0	< d.l.	10	2.2 ± 0.3
R	Yes	66	15.8 ± 0.5	16	3.8 ± 0.8	0	< d.l.	18	4.3 ± 0.3
F	Yes	82	23.5 ± 0.8	9	2.6 ± 0.3	0	< d.l.	9	2.7 ± 0.1

The concentrations are expressed as mean ± standard deviation (n=6) and percent of total

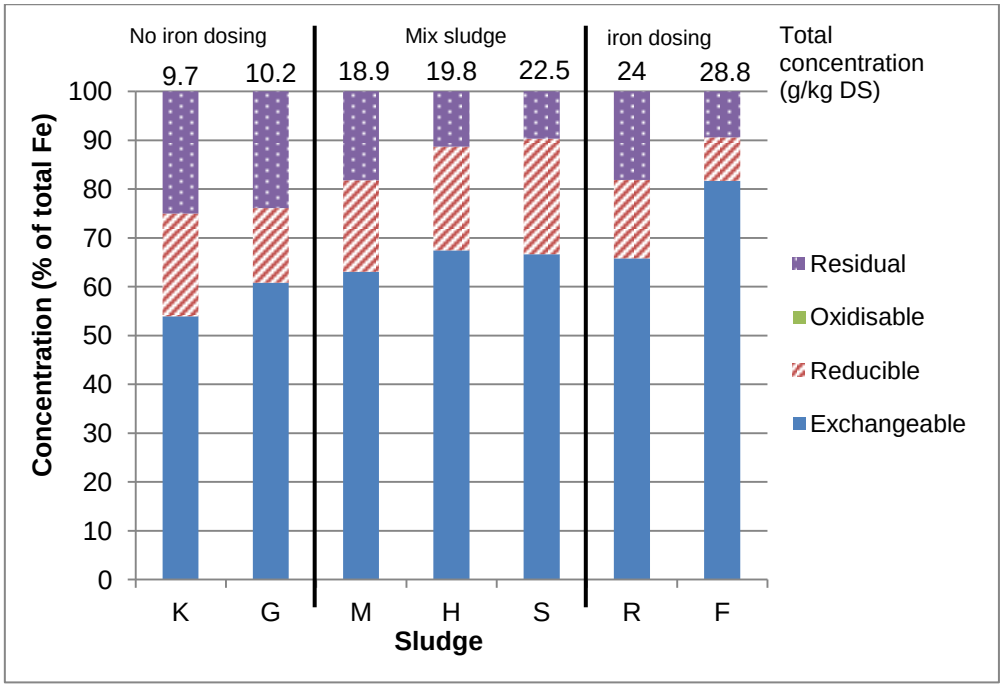

Figure 6.1. Iron fractionation profiles in the 7 anaerobically digested sludge

In figure 6.1, the BCR exchangeable fraction was the main fraction with more than 50% of the total iron extracted in this fraction. The maximum percentage was obtained for the sludge F (highest iron concentration) with 76% of the total iron. Iron was also extracted in two other fractions: reducible and residual. The

reducible and residual fractions represented each between 9% and 25% of the total iron. The concentrations of iron in the oxidisable fraction were below the detection limit and they have been considered to be nil.

Two main systems reacting with metals are phosphorus and sulphur and their concentrations in anaerobically digested sludge and BCR sequential fractions have been measured to assist the study of iron speciation. The third system, carbonate has not been measured due to the alteration of the extracting solution on the carbonate analysis. Tables 6.3 and 6.4 show respectively the total concentrations of phosphorus in the liquid and solid phases and its concentrations in each fraction from the BCR sequential extraction procedure. Similar results are shown for sulphur in tables 6.5 and 6.6.

Concentrations of phosphorus in the liquid phase were the highest in the two undosed sludge (K and G) while they were the lowest in the high iron concentration sludge (R and F). The difference of phosphorus percentages confirmed the significance of iron on the phosphorus speciation with 4-7% of total phosphorus in the liquid phase for undosed sludge and less than 2% for iron dosed sludge. The total concentrations of phosphorus were independent of the total iron concentrations due to the disparity in the amount of phosphorus entering in the different anaerobic digesters. However, the figure 6.2 shows a similar relation between the phosphorus concentrations in the liquid phase in function of the total iron concentrations.

Table 6.3. Concentrations of phosphorus in the solid and liquid phases of 7 anaerobically digested sludge

Sample		Liquid phase			Solid phase	
Sludge	Iron dosing	Concentration (mg/l)	% of total phosphorus		Acid digestion (g/kg DS)	Σ SE fractions (g/kg DS)
			Acid digestion	Σ SE fractions		
K	No	22.5 ± 2.4	4.1	5.0	26.1 ± 0.7	21.6 ± 2.1
G	No	30.5 ± 3.3	5.0	6.9	29.3 ± 0.3	20.5 ± 1.5
M	Mix	8.6 ± 1.6	1.3	1.9	33.0 ± 1.2	21.8 ± 2.3
H	Mix	7.1 ± 1.5	1.0	1.5	35.3 ± 0.8	23.6 ± 0.7
S	Mix	5.5 ± 1.8	0.8	1.1	34.9 ± 1.3	24.5 ± 4.5
R	Yes	2.7 ± 0.7	0.4	0.6	31.9 ± 0.4	23.4 ± 4.1
F	Yes	3.7 ± 0.6	0.5	1.1	34.0 ± 2.6	17.2 ± 1.1

The concentrations are expressed as mean ± standard deviation (n=6) and percent of total

Concentrations of phosphorus in the solid phase were included in the range of 26 g/kg DS and 35 g/kg DS using total acid digestion method and 17 g/kg DS and 25 g/kg DS using the sum of the BCR sequential extraction fractions. The amount of phosphorus extracted during the total acid digestion was always higher than the amount extracted during the sequential extraction as observed with iron. The percentage of recovery from the sum of phosphorus extracted during the sequential extraction in comparison with the total phosphorus concentration measured by total acid digestion varied from 50-85% between the seven types of sludge. This difference in the total concentration between the two methods used showed a proportional loss of phosphorus during the BCR sequential extraction procedure.

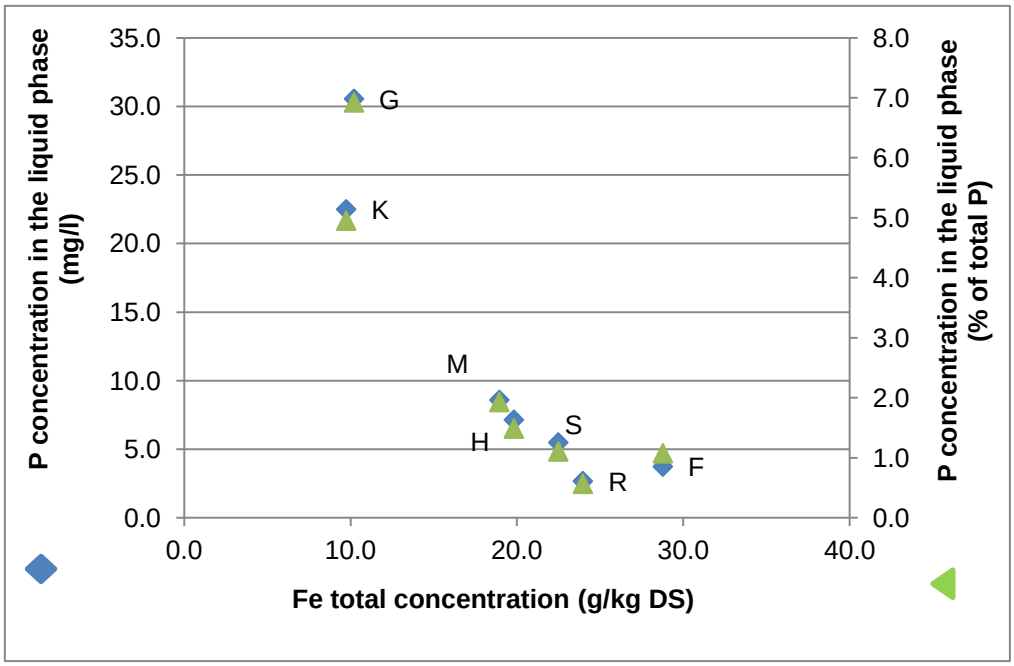

Figure 6.2. Phosphorus concentration in the liquid phase in function of the total iron concentrations

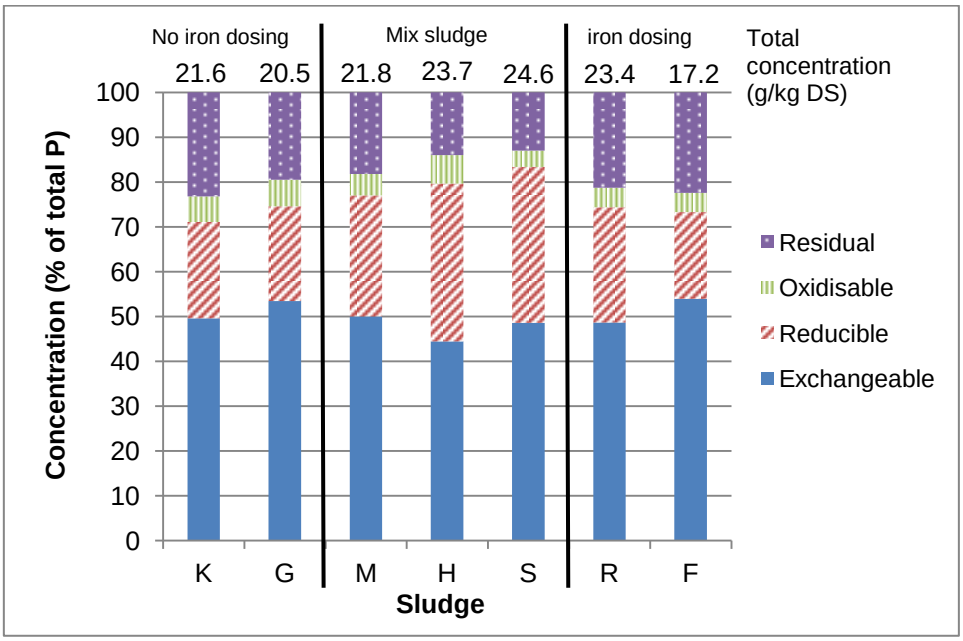

Figure 6.3. Phosphorus fractionation profiles in the 7 anaerobically digested sludge

A similar pattern of phosphorus fractionation was observed in all sludge sampled, regardless of their iron contents (figure 6.3). The exchangeable fraction was a

dominant fraction with around 50% of phosphorus and most of phosphate precipitates should be extracted in this fraction. The second highest fraction in phosphorus content was the BCR reducible fraction that contained between 19% and 35% of the total phosphorus. Remaining phosphate precipitates and phosphate-oxide precipitates should be extracted in this reducible fraction. The residual fraction contained between 14 and 23% and represented the third highest fraction in phosphorus content. Strongly bound compounds containing phosphorus such as silicate compounds were extracted in this fraction. The last fraction with around 5% of the total phosphorus was the oxidisable fraction that could be attributed to the phosphorus present in the organics.

Table 6.4. Concentrations of phosphorus in each BCR SE fraction for the 7 anaerobically digested sludge

Sample		Concentrations of phosphorus in each BCR sequential extraction fraction							
Sludge	Iron dosing	Exchangeable		Reducible		Oxidisable		Residual	
		%	g/kg DS	%	g/kg DS	%	g/kg DS	%	g/kg DS
K	No	50	10.7 ± 0.8	21	4.6 ± 0.4	6	1.2 ± 0.1	23	5.0 ± 1.3
G	No	53	11.0 ± 1.0	21	4.3 ± 0.3	6	1.2 ± 0.3	20	4.0 ± 0.2
M	Mix	50	10.9 ± 0.4	27	5.9 ± 0.8	5	1.0 ± 0.2	18	4.0 ± 0.9
H	Mix	45	10.5 ± 1.2	35	8.3 ± 0.4	6	1.5 ± 0.6	14	3.3 ± 0.5
S	Mix	48	11.9 ± 1.7	35	8.5 ± 2.5	4	0.9 ± 0.2	13	3.2 ± 0.2
R	Yes	49	11.4 ± 1.5	26	6.0 ± 1.5	4	1.0 ± 0.2	21	5.0 ± 1.0
F	Yes	54	9.3 ± 1.0	20	3.3 ± 0.6	4	0.7 ± 0.1	22	3.9 ± 0.2

The concentrations are expressed as mean ± standard deviation (n=6) and percent of total

Concentrations of sulphur in the liquid and solid phase are shown in tables 6.5 and 6.6. Concentrations of sulphur in the liquid phase were comprised between 4.8 and 8.3 mg/l for the sludge except for the sludge F where the concentration was higher, 13.8 mg/l. The percentages of sulphur in the liquid phase were mainly

included between 2.1-3.1% and 3.3-4.2% of the total sulphur concentration (except for the sludge F with 4.3% and 5.2%).

Table 6.5. Concentrations of sulphur in the solid and liquid phases of 7 anaerobically digested sludge

Sample		Liquid phase			Solid phase	
Sludge	Iron dosing	Concentration (mg/l)	% of total sulphur		Acid digestion (g/kg DS)	Σ SE fractions (g/kg DS)
			Acid digestion	Σ SE fractions		
K	No	8.3 ± 3.4	3.1	4.2	13.2 ± 0.7	9.4 ± 1.0
G	No	6.1 ± 0.2	2.4	3.4	12.2 ± 0.4	8.7 ± 1.1
M	Mix	5.9 ± 0.9	2.4	3.3	12.0 ± 1.1	8.8 ± 1.9
H	Mix	4.8 ± 1.2	2.2	3.3	10.5 ± 1.9	7.0 ± 1.0
S	Mix	5.8 ± 0.6	2.5	4.1	11.1 ± 0.5	6.7 ± 0.2
R	Yes	6.0 ± 0.7	2.1	3.3	14.2 ± 0.7	8.8 ± 0.4
F	Yes	13.8 ± 1.2	4.3	5.2	15.5 ± 0.6	12.5 ± 2.1

The concentrations are expressed as mean ± standard deviation (n=6) and percent of total

Concentrations of sulphur in the solid phase varied between 10.5 and 15.6 g/kg DS using total acid digestion and 6.7 and 12.5 g/kg DS using the sum of the sequential extraction fractions. The measure of total sulphur concentration using the total acid digestion method gave higher values than the sum of fractions (similar to iron and phosphorus analysis). No pattern in sulphur concentration in the solid or liquid phase can be observed depending on the sludge.

Table 6.6. Concentrations and percentages of sulphur in each BCR sequential extraction fraction for the 7 anaerobically digested sludge

Sample		Concentrations of sulphur in each BCR sequential extraction fraction							
Sludge	Iron dosing	Exchangeable		Reducible		Oxidisable		Residual	
		%	g/kg DS	%	g/kg DS	%	g/kg DS	%	g/kg DS
K	No	5	0.5 ± 0.1	5	0.4 ± 0.4	18	1.7 ± 0.2	72	6.8 ± 0.5
G	No	7	0.6 ± 0.1	2	0.2 ± 0.0	19	1.6 ± 0.3	72	6.3 ± 0.8
M	Mix	9	0.8 ± 0.1	3	0.2 ± 0.1	24	2.1 ± 0.8	64	5.6 ± 1.0
H	Mix	8	0.6 ± 0.1	4	0.3 ± 0.1	21	1.5 ± 0.3	67	4.7 ± 0.6
S	Mix	6	0.4 ± 0.0	6	0.4 ± 0.3	23	1.6 ± 0.3	65	4.3 ± 0.5
R	Yes	6	0.6 ± 0.1	6	0.5 ± 0.3	19	1.7 ± 0.1	69	6.1 ± 0.3
F	Yes	7	0.9 ± 0.2	5	0.6 ± 0.3	21	2.6 ± 0.6	67	8.4 ± 1.2

The concentrations are expressed as mean ± standard deviation (n=6) and percent of total

From the definition of the BCR sequential extraction procedure, sulphide precipitates should be extracted in the oxidisable fraction but the dominant fraction was the residual fraction, which contained between 64 and 72% of the total sulphur (table 6.6 and figure 6.4). The second highest fraction was the oxidisable fraction with 18 and 24% of the total sulphur. Those results suggested that most of the sulphide compounds are extracted in the residual fraction instead of the oxidisable fraction and so sulphide precipitates form stronger compounds than expected during the development of the sequential extractions procedures. The two other fractions, exchangeable and reducible fractions, contained respectively around 7 and 4 % of the total sulphur. A similar pattern of sulphur fractionation was observed in all sludge sampled, regardless of their iron content.

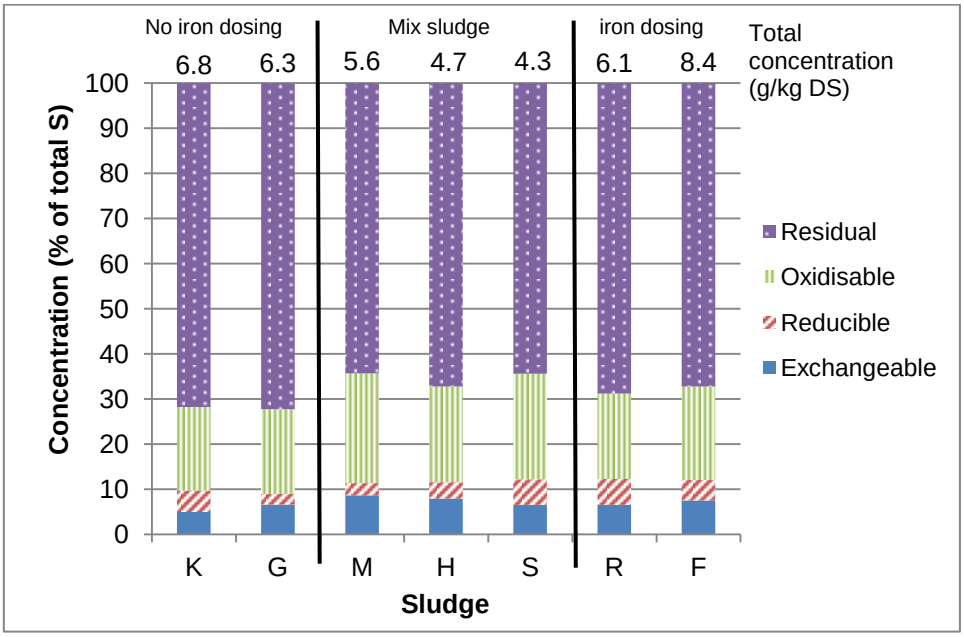

Figure 6.4. Sulphur fractionation profiles in the 7 anaerobically digested sludge

The concentrations of iron, phosphorus and sulphur measured in the solid phase using the total acid digestion were higher than calculated as the sum of the sequential extractions fractions. This difference could be due to a loss of material during the different stages of the procedures, e.g. extractions, centrifugation or washing. The figure 6.5 showed similar patterns for iron and sulphur in the difference of values between the two methods. A linear curve with a coefficient of 0.93 for Fe and 0.98 for S was present when the concentrations as the sum of the sequential extraction fractions was plotted against the total concentration obtained by total acid digestion. However, for phosphorus no pattern seemed to be apparent.

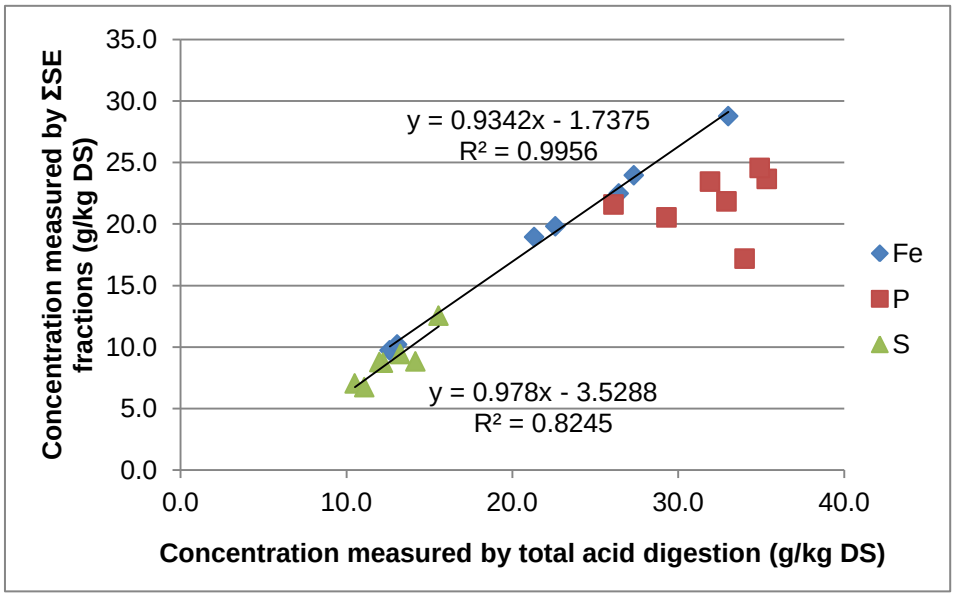

Figure 6.5. Total concentrations of Fe, P and S measured by ΣSE fractions versus their concentrations measured by total acid digestion

Due to similar coefficient, a relation between the loss of iron and sulphur could be linked. However, a mass comparison using the g/kg DS unit could be misleading as the ratio between elements in a compound is molar. A similar variation in the difference of concentrations (in mol/kg DS) was observed between iron and sulphur except for the sludge R and F (figure 6.6). Moreover the gap between the two curves was constant and the mean ratio S/Fe was calculated at 2.2 (± 0.17, excluding R&F and ± 0.47 including all the sludge). This result could be showing that a part of FeS_2 present in the sludge was not extracted (and measured) during the sequential extraction. However, the same amount of FeS_2 should be dissolved in the residual fraction as the last step of the sequential extraction was identical as the total acid digestion (see chapter 4.3.2 and 4.3.3). One explanation could be a change in the speciation during the SE procedure and a modification (protection or re-precipitation) that would protect against its dissolution during the last step.

Concerning the change in the gap for the sludge F, part of the non extracted iron could have bound with phosphorus instead of sulphur and benefited of a similar protection from the last extracting solution of the sequential extraction. This explanation was corroborated with the larger difference in the sludge F between the phosphorus concentrations measured by total acid digestion and the sum of the fractions than the other sludge.

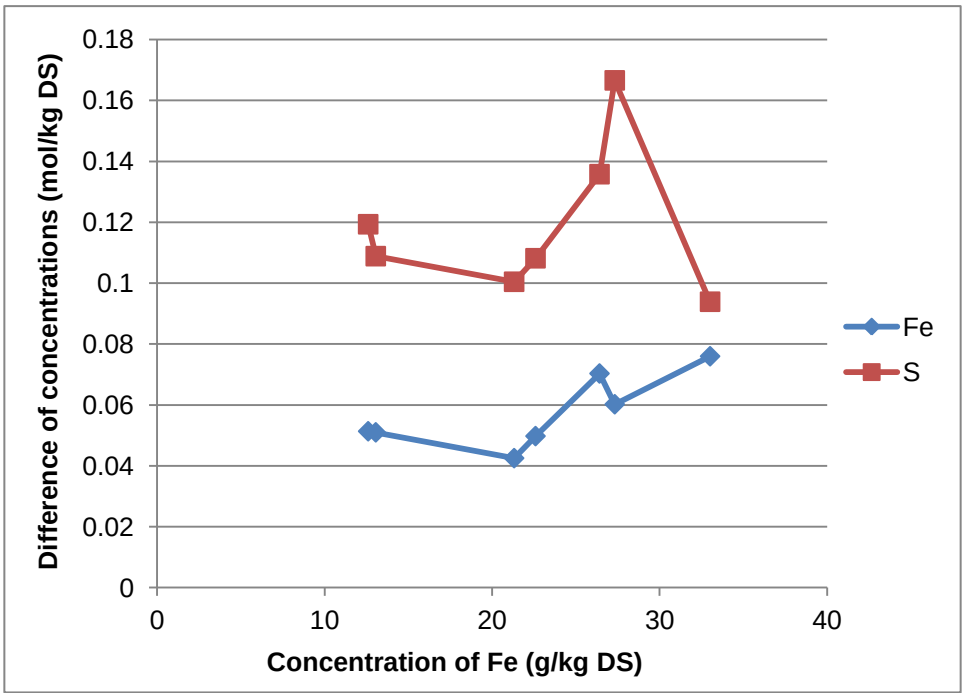

Difference of concentrations was between the two values obtained by total acid digestion and ΣSE fractions. Concentration of Fe was measured by total acid digestion

Figure 6.6. Comparison of iron and sulphur losses during BCR sequential extraction in the anaerobically digested sludge

Iron was mainly extracted in the exchangeable fraction, and so it should be adsorbed and/or precipitated as iron-phosphate or iron-carbonate. The increasing of iron concentrations did not change the pattern of the speciation but there is an amplification of the dominance of the exchangeable fraction with an augmentation

of the total iron concentration. The concentrations of iron in each sequential extraction fraction were plotted as a function of the total iron concentrations and the figure 6.7 shows that the additional iron is mainly extracted into the first fraction (exchangeable). A linear relation was clearly observed between the total concentration and the exchangeable fraction (see equation 6.1). The linear equation was calculated as.

$$[Fe]_{exchangeable} = 0.86 \times [Fe]_{total} - 3.5$$

Equation 6.1. Linear relation between the concentration of Fe in the BCR exchangeable fraction and its total concentration

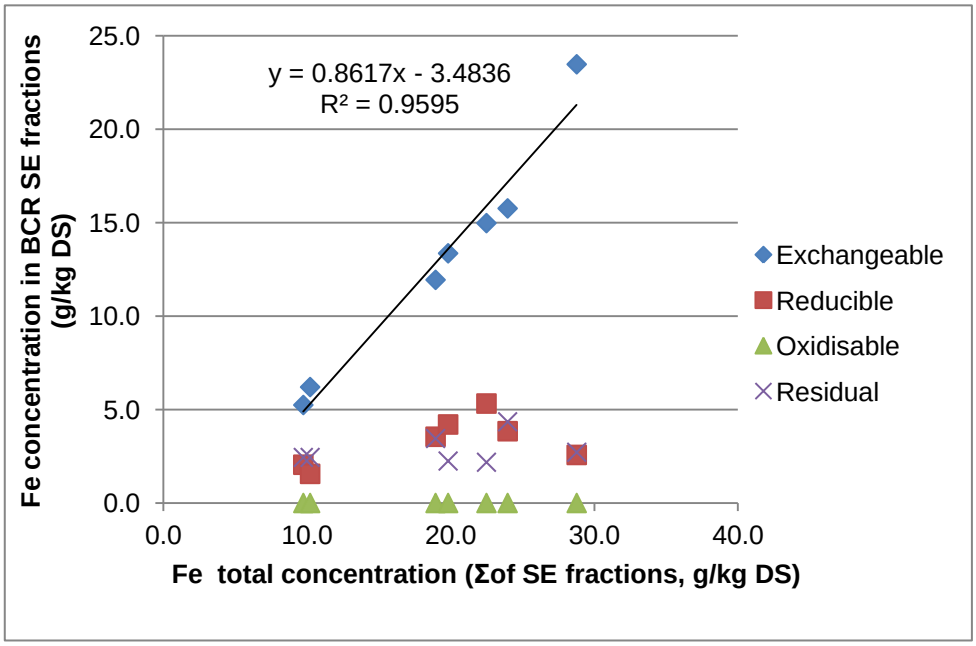

Figure 6.7. Iron concentrations in each BCR SE fractions in function of the total iron concentration

By contrast, the concentrations of iron in the reducible and residual fractions were not related to the total iron concentration. The figure 6.7 shows that the increase of

the total concentration in the sludge lead to an augmentation of iron as adsorbed or easily extractable precipitates, likely iron-phosphate or iron carbonate. The y-intercept of the linear regression showed a negative value, which implied that the iron extracted in the exchangeable fraction were not the primary compounds to be formed at low iron concentrations. So the first iron compound to be precipitated was extracted in the residual or reducible fraction. From a similar analysis on the reducible and residual fractions, results suggested that the first precipitate to be formed was extracted in the residual fraction, which was corresponding to iron-sulphide following the sulphur fractionation profiles. However, more information is required to confirm it due to the absence of clear linear relation between the concentrations of iron extracted in the residual fraction and the total iron concentrations.

The presence of iron in the reducible fraction (10-30%) suggested that iron oxides might be present in the AD or that iron co-precipitates with other metal oxide. However, the presence of phosphorus in this fraction also suggested that iron was more likely to be present as a complex iron phosphate oxide (Smith et al., 2009). In figure 6.8, the augmentation of the total phosphorus increased the concentration of phosphorus in the exchangeable and also the reducible fraction. For the reducible fraction, the augmentation was higher than for the exchangeable fraction and so it can be deduced that phosphorus has the tendency to form stronger precipitates when its total concentration increased.

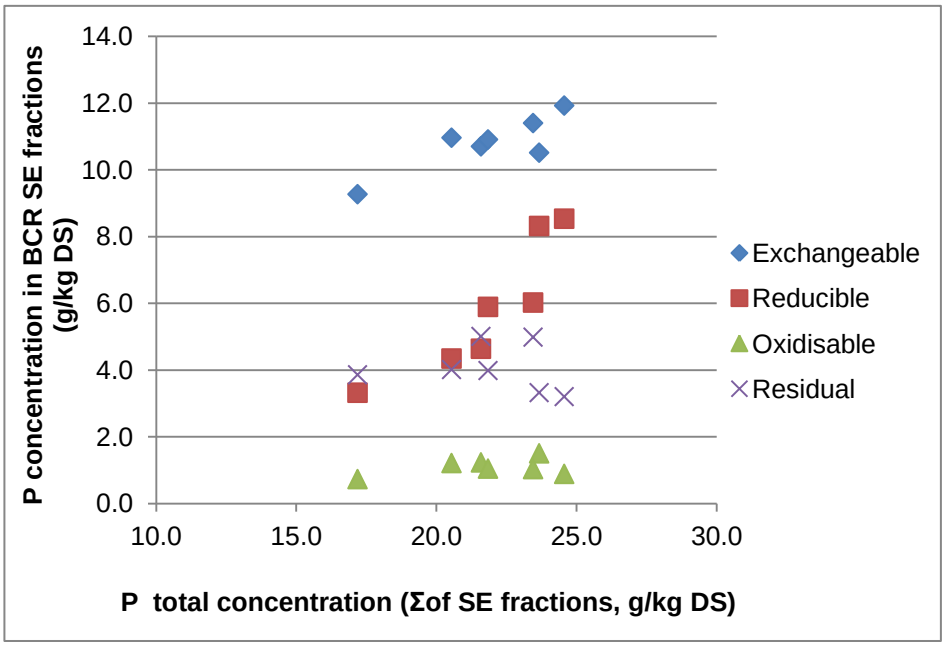

Figure 6.8. Phosphorus concentrations in each BCR SE fractions in function of the total phosphorus concentration

Moreover, the figure 6.9 shows a similar variation of phosphorus and iron concentrations in the reducible fraction in the different sludge. However, no ratio between the two curves has been found and this was due to the higher concentrations of phosphorus (molar and mass) than iron and the presence of other cations reacting with phosphate.

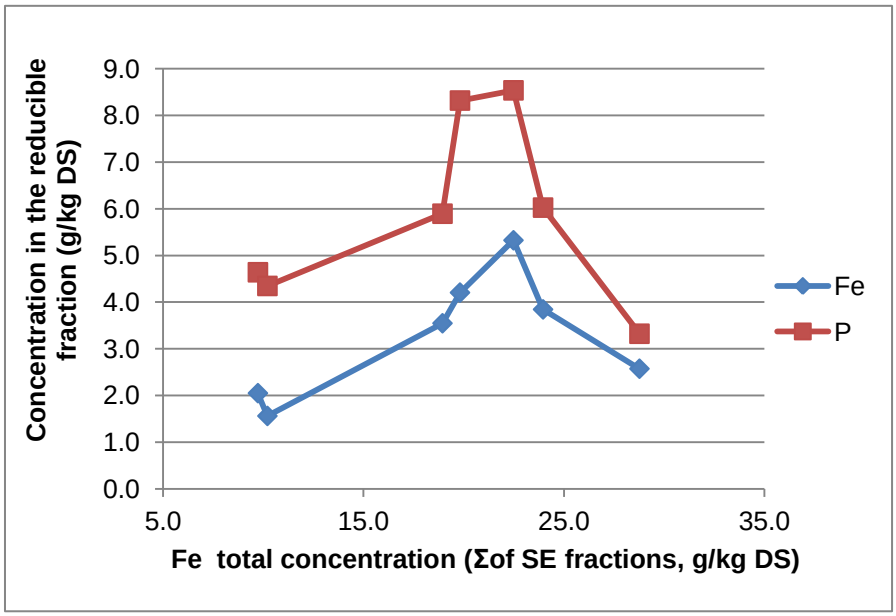

Figure 6.9. Comparison of iron and phosphorus concentration in the BCR reducible fraction in function of the total iron concentration

A percentage of iron comprised between 10 and 30% was extracted in the last fraction. Iron sulphide compounds were expected to be extracted in the oxidisable fraction but the presence of a high concentration of sulphide in the last fraction tended to confirm that iron sulphide precipitates were not systematically extracted in the oxidisable fraction but in the residual fraction (Adamo et al., 1996 and Van der Veen et al., 2007). In figure 6.10, an augmentation of sulphur concentration in anaerobically digested sludge increased mainly the concentration of sulphur in the residual fraction and also secondarily in the oxidisable fractions. This confirmed that sulphide precipitates were not only extracted in the oxidisable fraction but were mainly extracted in the residual fraction.

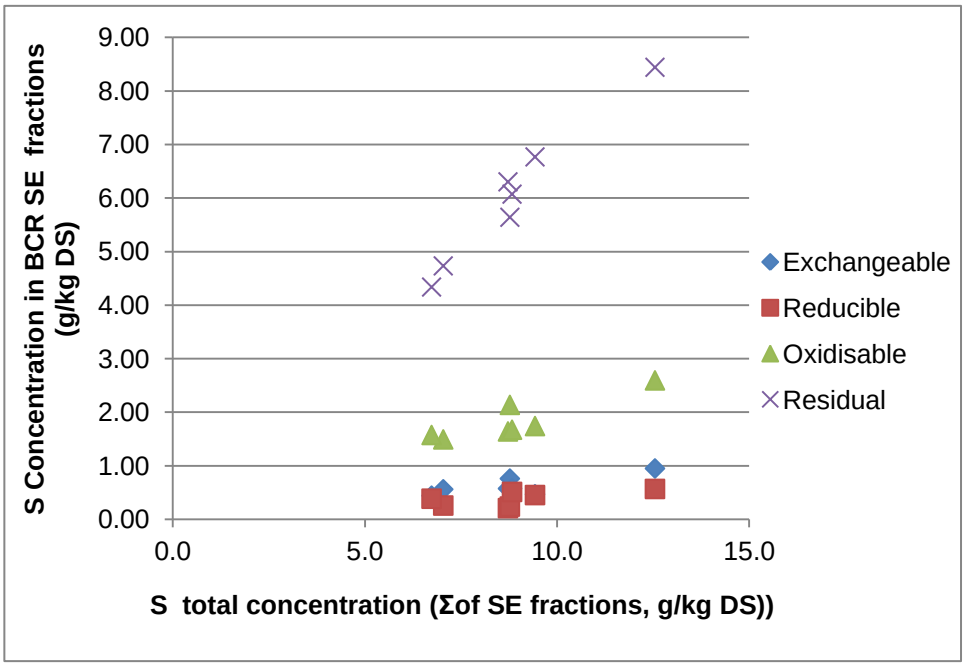

Figure 6.10. Sulphur concentration in each BCR SE fractions in function of the total sulphur concentration

6.2.2. Scanning electron microscope coupled with electron detection spectroscopy

Results from the BCR sequential extraction analysis showed that iron interacts with sulphur and phosphate to form ferrous sulphide and ferrous phosphate compounds. However, there was a lack of information concerning the exact chemical forms of those iron precipitates present in the sludge. So SEM-EDS analysis has been applied on the same sludge used for the sequential extraction procedure to confirm the presence of those compounds and obtain information on their molecular forms and structures.

The possibility of having iron-phosphate compounds extracted in the two first fractions (exchangeable and reducible) showed that iron might form different precipitates with phosphate. Carliell-Marquet et al. (2010) suggested that iron forms ferrous phosphate and ferrous hydroxyl-phosphate compounds and Ofverstrom et al. (2011) and De Sousa et al. (1997) observed the presence of vivianite ($Fe_3(PO_4)_2.8H_2O$) in anaerobically digested sludge supplemented by iron salts. The main objective was to confirm the presence of vivianite in anaerobically digested sludge and determine the presence of other ferrous-phosphate precipitates.

A specific iron phosphate compound (A-D) has been detected using SEM-EDS analysis in anaerobically digested sludge (from undosed and iron-dosed digester) in this research (see section 4.1.1). Pictures and elemental analysis of those compounds are shown in figure 6.11 and table 6.7.

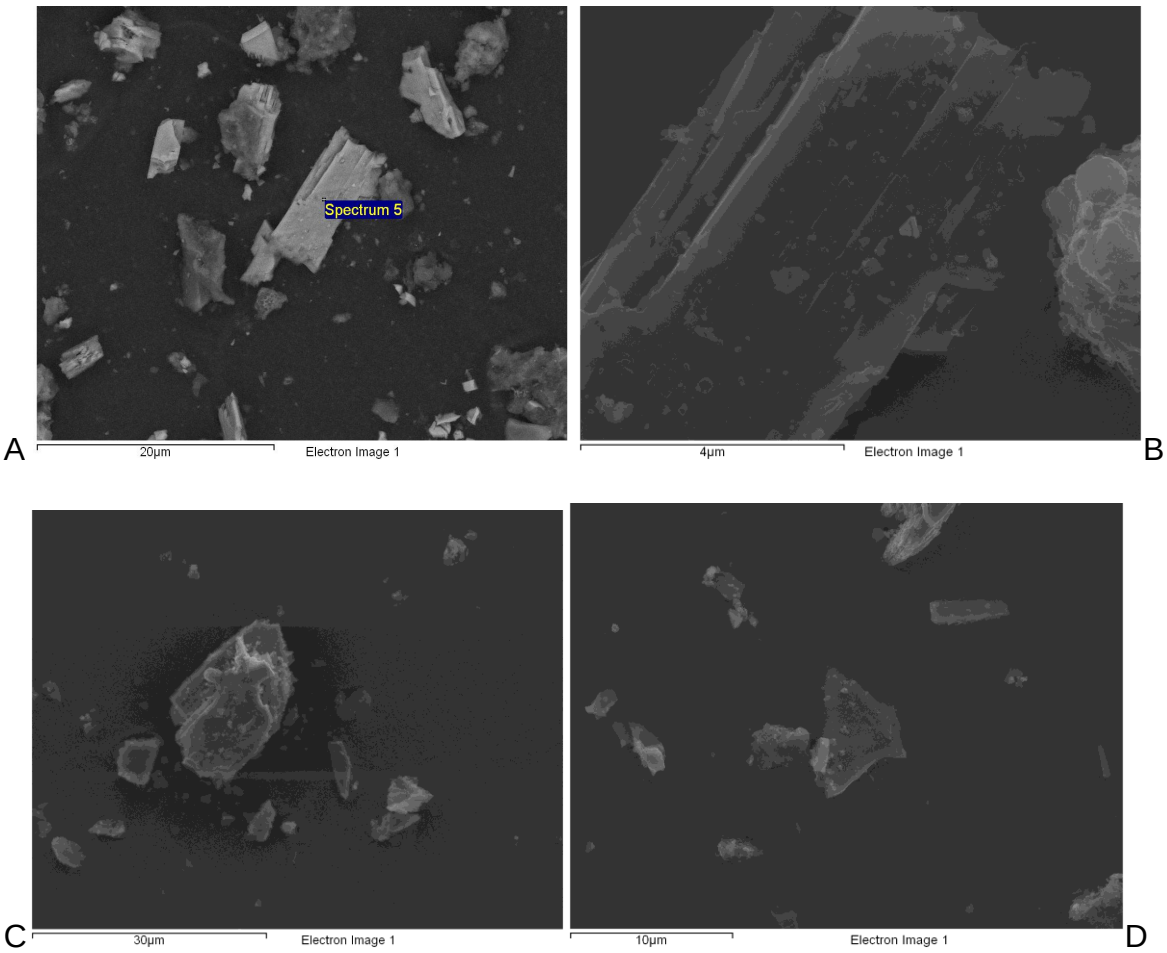

Figure 6.11. Pictures of vivianite detected in anaerobically digested sludge by SEM-EDS

Table 6.7. Elemental analysis of the vivianite precipitates observed in figure 6.11

Sample	Element concentration (as atomic percent)				
	Fe	P	O	Ca	Mg
A	16	12	70	1	1
B	13	11	74	1	1
C	15	12	71	1	1
D	11	10	77	1	1
Average	13.75	11.25	73	1	1

The five same elements were present at a similar atomic percent in the four precipitates (A-D) detected in different sludge (figure 6.11 and table 6.7). Iron, phosphorus and oxygen were the main elements of those precipitates (respectively 14%, 11 % and 73%); calcium and magnesium were present only at low concentrations (1% for each). This low atomic percent of magnesium and calcium suggested the hypothesis that these two elements were present in the solid as inclusion or substitution. From their chemical properties, calcium and magnesium were only suitable to replace iron atoms in the structure.

The ratio Fe/P was around 1.3 but taking into consideration the hypothesis that calcium and magnesium replace iron, the ratio Fe-Ca-Mg/P increased to 1.5. The other ratios with oxygen were 5 for O/Fe-Ca-Mg and 7 for O/P. So one of the structures of the compounds was $Fe_3P_2O_{14.5}$ and could be written as a hydrated ferrous phosphate with the formula $Fe_3(PO_4)_2.6.5H_2O$. Miot et al (2009) and Nriagu (1971) found that vivianite is one of the most stable precipitates formed between phosphorus and iron under anaerobic condition with high phosphate concentration. The vivianite formula is $Fe_3(PO_4)_2.8H_2O$ and close from the structure of the compounds found in sludge. Nriagu (1971) also described that magnesium and calcium (along with copper and zinc) might form similar compound with phosphate ($Ca_3(PO_4)_2$ and $Mg_3(PO_4)_2$) and so this substantiated the potential of iron replacement by calcium and magnesium in the compound.

Frost et al. (2003) showed that natural vivianite was dehydrated in a range of temperature of 105-420°C and the dehydration occurred in five steps. The first

step of dehydration with a loss of one water molecule occurred at the temperature of 105°C, the same temperature used for drying our digested sludge samples (chapter 4.4.4). So the deficit of water molecules in the vivianite formula measured in this research might be explained by a loss of water during the drying operation of the sludge. Anthony et al. (2011) demonstrated that vivianite follows a monoclinic crystal system and so precipitates as prismatic crystals that are flattened and elongated on two axes. The microscopic pictures (figure 6.11) shows that the compounds observed in the sludge fitted with the crystal structure description of vivianite (particularly on the picture B) and confirmed the presence of vivianite in anaerobically digested sludge (see appendix C.4).

Vivianite was not the only iron phosphate compounds detected in anaerobically digested sludge (compounds E-G, figure 6.12 and table 6.8). The ratio Fe/P/O was variable from one compound to another and the presence of other elements (other than Mg and Ca) was also noticed. The compound E showed no specific crystal structure and it was identified as delvauxite, $CaFe_4(PO_4)_2(OH)_8.4H_2O$, following the same process used for the identification of vivianite. Anthony et al. (2011) described delvauxite as amorphous compounds formed in nodules, surficially botryoidal to reniform. However, in the absence of information on the structure due to the amorphous structure, the identification could not be confirmed in opposition with vivianite.

The compounds F and G were also amorphous and had a ratio Fe/P close from 1, suggesting the presence of ferric phosphate. However, the presence of other

elements such as silicon, aluminium or sodium disturbed the ratio between Fe/P/O and complicated the identification of these compounds. Most of the compounds detected in the sludge are co-precipitates, with generally a mixture of 3 or more precipitates with inclusion of different elements (developed below in figure 6.15). Often, the identification was also obscured by the aggregation of biomass or organics around the inorganic precipitates.

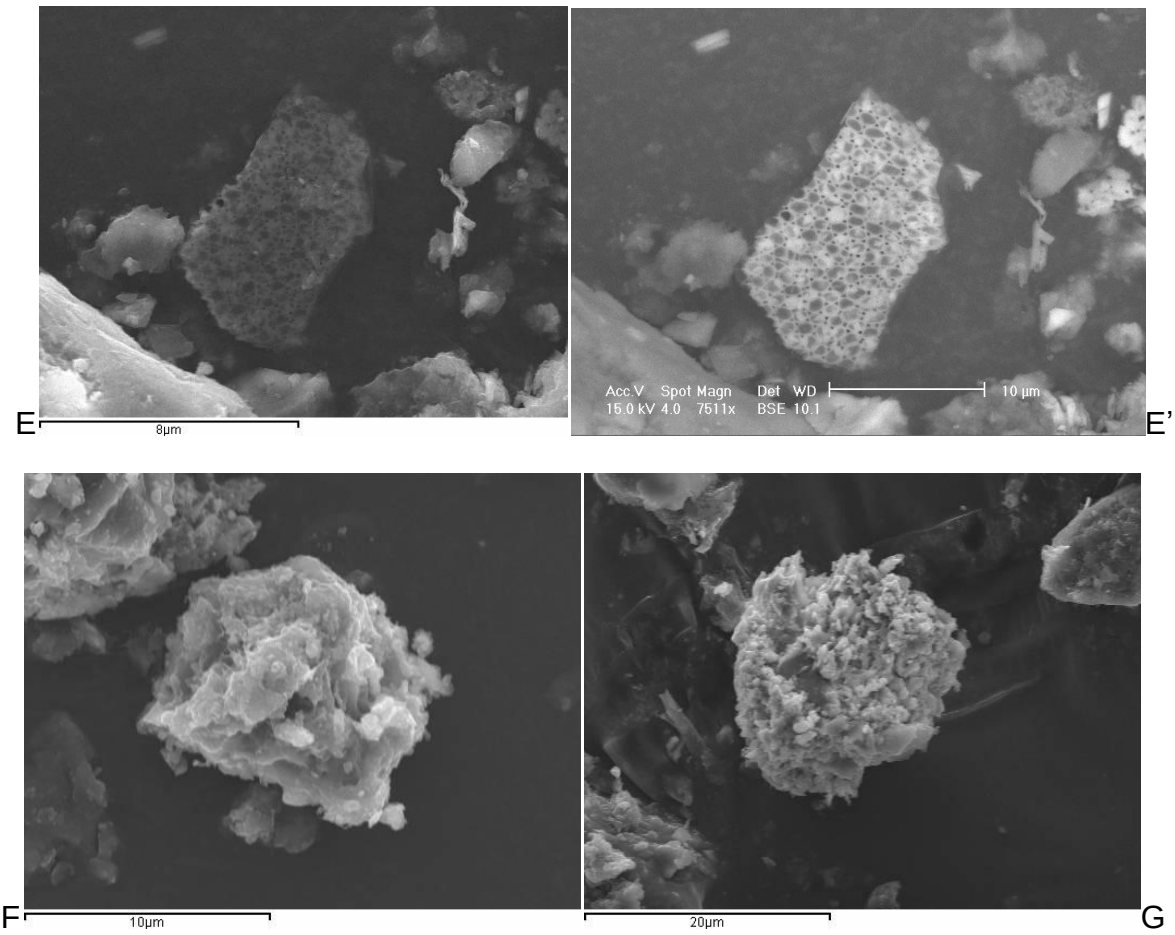

Figure 6.12. Pictures of iron-phosphate precipitates detected in anaerobically digested sludge by SEM-EDS

E' is the BSE picture of the compound E

Table 6.8. Elemental analysis of the iron-phosphate precipitates observed in figure 6.12

Sample	Element concentration (as atomic percent)										
	Al	Ca	Cl	Fe	K	Mg	Na	O	P	S	Si
E	<1	3	-	14	<1	-	-	74	7	2	-
F	2	-	-	11	-	1	1	69	13	1	2
G	1	<1	2	11	-	-	-	72	13	<1	-

Sulphide precipitation is considered to be the main regulator of metals speciation in anaerobic digesters (Zhang et al., 2010; Oleszkiewicz and Sharma, 1989; Kaksonen et al., 2002 and Van der Veen et al., 2007). Callander and Bradford (1983) found that iron and sulphide should thermodynamically react to form iron sulphide precipitates. Pyrite (FeS_2) and ferrous sulphide are two compounds likely to be formed in anaerobic digester (Kaksonen et al., 2003 and Van der Veen et al., 2007). However, even if pyrite is considered as the most stable precipitate, the pyritization is a slow process and so there is question concerning the sludge retention time being enough to observe the presence of in anaerobically digested sludge (Pourbaix, 1963 and Nielsen et al., 2005, see section 2.6). Some iron sulphide precipitates were detected in the sludge and are shown in figure 6.13 and table 6.9.

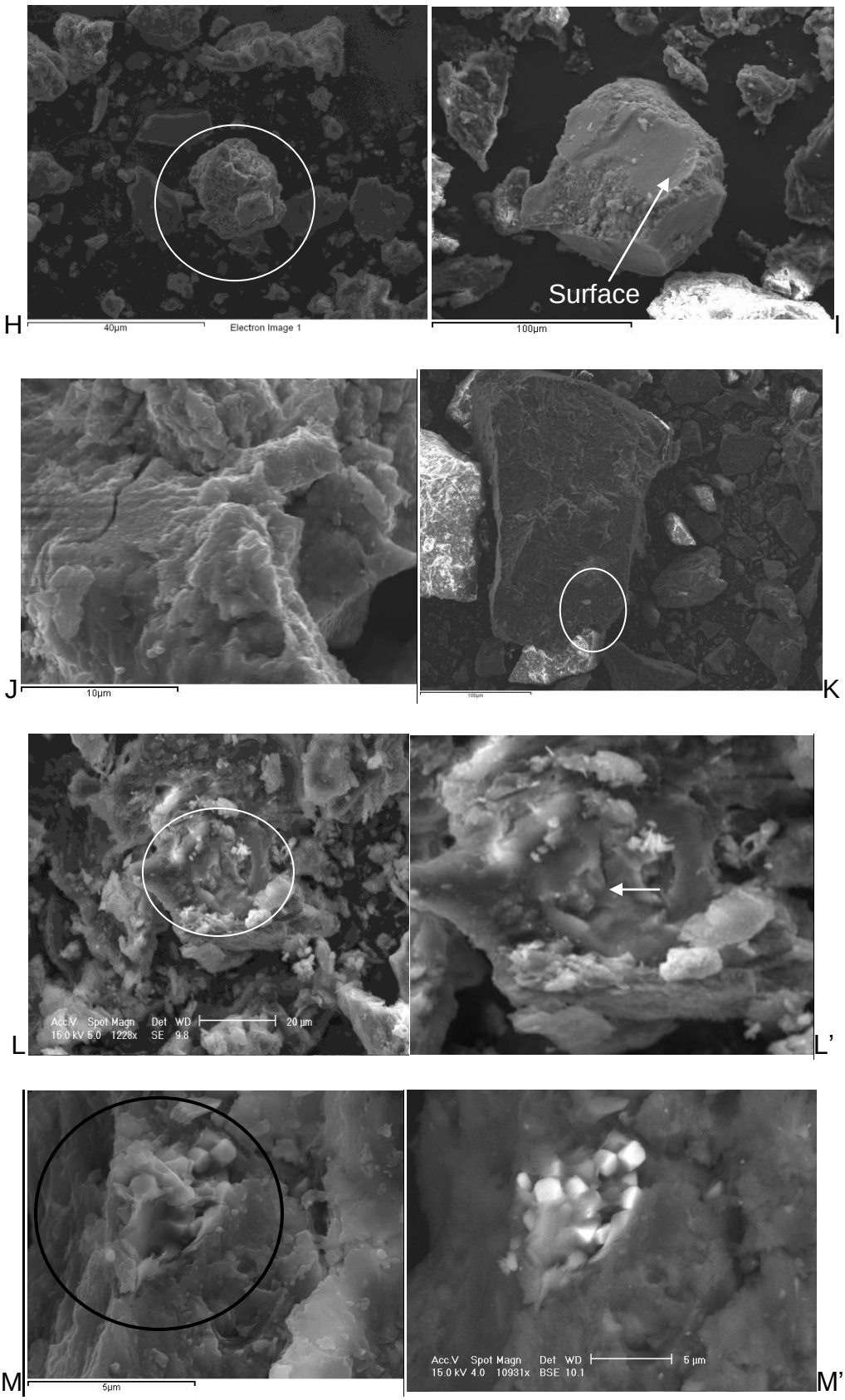

Figure 6.13. Pictures of iron-sulphide precipitates detected in anaerobically digested sludge by SEM-EDS (M' is the BSE picture of M and L' is the zoom of L)

Table 6.9 Elemental analysis of the iron-sulphide precipitates observed in figure 6.13

Sample	Element concentration (as atomic percent)								
	Al	Ca	Fe	Na	O	P	S	Si	Zn
H	-	<1	43	-	14	-	43	-	-
I	-	1	28	4	33	-	33	-	-
J	1	<1	28	-	44	1	26	-	1
K	2	<1	19	-	61	-	18	1	-
L	-	-	23	4	36	-	35	-	-
M	-	-	31	-	-	-	68	1	-

Samples H-K contained a high concentration and a similar amount (molar ratio) of iron and sulphur. A percentage of oxygen (14-61%) and traces of calcium, sodium and other elements were also detected in the precipitates. This ratio 1:1 showed that ferrous sulphide has been precipitated in the different anaerobically digested sludge. The presence of oxygen could be explained by an oxidation during the sample preparation, as the drying was done in open air and the SEM-EDS analysed the molecular composition on the surface of the solid (section 4.4.4).

Ferrous sulphide is a metal-stable amorphous compound (Nielsen et al., 2005) and the samples H-K did not exhibit any specific crystal structure (in opposition with sample M) and was identified as ferrous sulphide. Concerning the samples I and K, ferrous sulphide precipitates were detected on the surface of solid which has been identified as calcium phosphate (results not shown). The compound M contains 31% of iron, 68% of sulphur and traces of silicon. From this ratio (1:2), a formula FeS_2 was deduced. The solid possessed also a crystalline cubic form.

One of the pyrite crystal habits is cubic and confirmed that the compound M was pyrite (see appendix C.3). The compound L contained a ratio S:Fe of 1.5, with 23% of iron and 35% of sulphur. This ratio could suggested the presence of ferric sulphide (Fe_2S_3), which is a powder compound where iron is present as Fe(III). However, the presence of Fe(III) was unlikely under anaerobic condition. Moreover, on the picture L', we can observe some cubic crystal similar to the picture G that could suggest that the compound was a mix of FeS and pyrite (figure 6.13). This agreed with Nielsen et al. (2005) who established that ferrous sulphide was a pyrite precursor.

Anaerobic digesters cannot be considered as simple chemical reactors and there are a wide number of elements and reactions (biological, chemical and physical) taking place. In the study on iron-phosphate and iron-sulphide precipitates, several elements such as sodium, magnesium or aluminium were incorporated or adsorbed on those compounds. The iron co-precipitation might also occur following different pathways such as precipitate aggregation, metal incorporation and metal sorption (Van Hullebusch et al., 2006 and Jong and Parry, 2004). So it was important to take into account the risk of co-precipitation to measure its impact on the iron speciation.

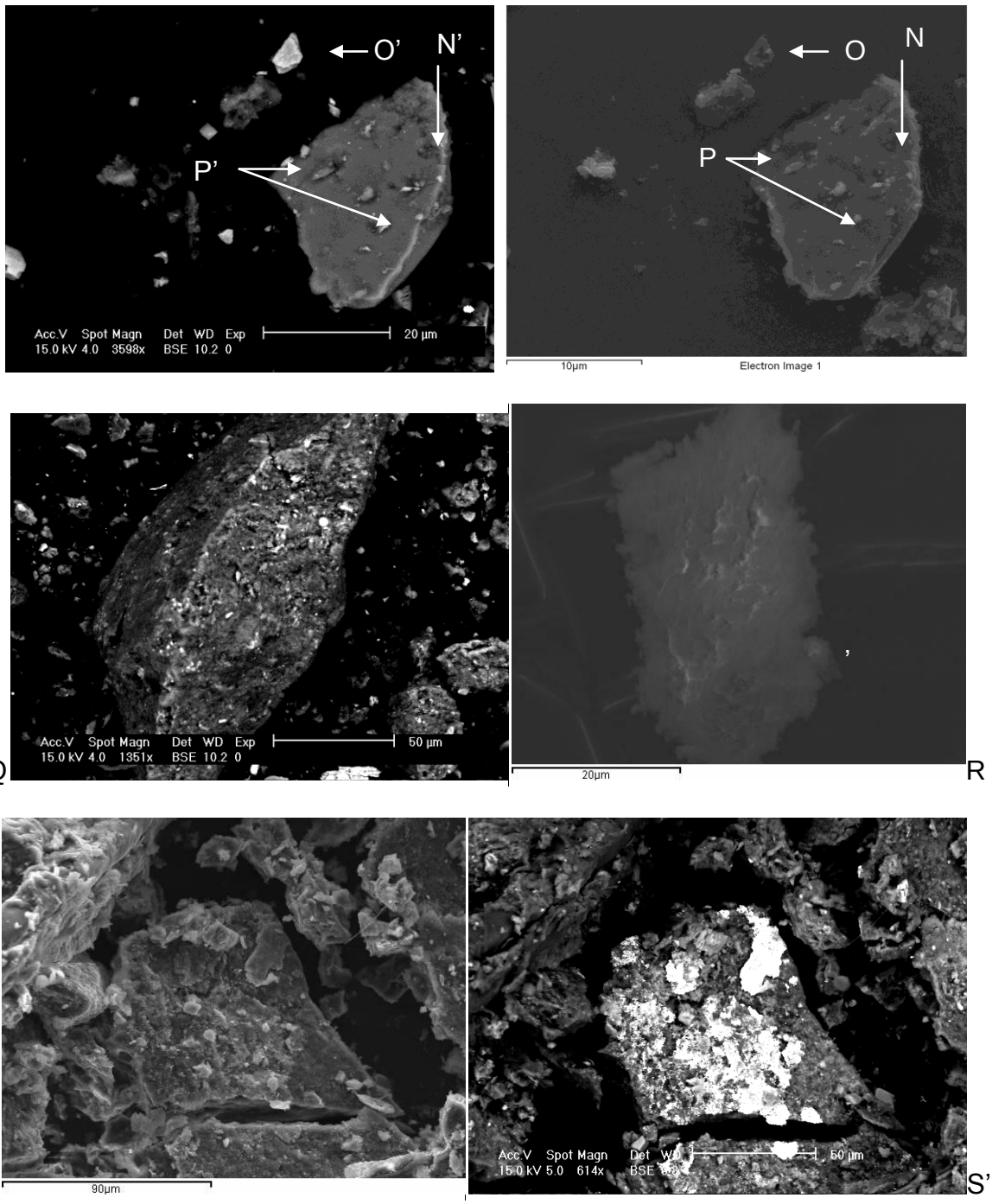

Q R

S S'

Top left and Q and S' are BSE pictures

Figure 6.14. Pictures of co-precipitates detected in anaerobically digested sludge by SEM-EDS

Table 6.10. Elemental analysis of the vivianite/SiO_2 precipitates observed in figure 6.14

Sample	Element concentration (as atomic percent)					
	Fe	P	O	Ca	Mg	Si
N	-	-	65	-	-	35
O	15	12	71	1	1	-
P	5	4	70	<1	<1	21

Table 6.11. Elemental analysis of co-precipitates observed in figure 6.14

Sample	Element concentration (as atomic percent)											
	Al	Ca	Cl	Fe	K	Mg	Na	Ni	O	P	S	Si
Q	3	4	<1	2	1	1	1	-	73	4	2	8
R	4	8	-	3	2	2	3	-	63	9	1	5
S	3	3	1	3	<1	2	8	6	64	4	2	4

Examples of co-precipitation, sorption and inclusion are shown in figure 6.14 and tables 6.9 and 6.10. The image taken using back scattering emission showed the presence of high atomic number element on the side or attached to the main compounds formed with lower atomic number element (O' and P', figure 6.14). The main compound, N, was composed with silicate and oxygen and from the atomic percent, it has been identified as SiO_2. Silicon dioxide is a common compounds and its origin can be multiple: soil contamination, cosmetic, food and others. The compound O has been identified as vivianite ($Fe_3(PO_4)_2.8H_2O$).

The last compound (P) possessed the same elements as vivianite (Fe, P, Ca and Mg) and also silicon; so from the picture and elemental analysis a mix between the compound N and O probably occurred in the digester. The atomic percent of Fe

and P were lower than for the compound O but the ratio Fe/P was kept. Considering that for the vivianite the ratio O/Fe and O/P was respectively 5.3 and 8, the remaining oxygen was available for combining with silicon (around 40%). And so the ratio $O_{remaining}$/Si was 2 and this was corresponding with the formula of the compound N, SiO_2. The elemental analysis showed that the compound P was an aggregation of two compounds vivianite and silicon dioxide. It would be more appropriate to suppose that vivianite precipitated on the surface of the silicon dioxide if we consider the difference of size, concentration and the high probability that silicon dioxide has already been formed prior to entering into the wastewater sludge matrix (see appendix C.4).

The use of BSE images was interesting to detect sorption or surface precipitation of metals on other precipitates and organics. In figure 6.14, the bright zones on the BSE pictures (Q and S') showed the presence of elements with high atomic number element on the surface of larger compounds. The percentage of carbon in the compounds could not be measured as the samples were carbon coated prior analysis (see chapter 4.4.4). So the solid composition could not be identified as no element (expect oxygen) was present at high concentration. Most of the main anions (P and S), cations (Ca, Mg, K and Na) and other elements (Al, Si and Fe) were aggregate on the solid and its surface. None of them had a percentage over 10% and generally their percentage varied from 1% to 6%. Presence of metals, such as Ni (8%) and Fe (3%), has been measured on the surface. The structural difference between compounds Q, R and S demonstrated that different processes

occurred such as chemisorptions, surface precipitation, co-precipitation and metals inclusion.

6.2.3. Modelling simulation

The use of an equilibrium chemical speciation model to predict metal speciation has been rarely done for anaerobically digested sludge (Aquino and Stuckey, 2007); nonetheless several researches have used it for water streams and sewage sludge (Andres and Francisco, 2008; Celen et al., 2007 and Gallios and Vaclavikova, 2008). In this study, chemical modelling has been used to simulate the iron speciation from the total concentration measured in the seven anaerobically digested sludge using only thermodynamic values. The predicted (from chemical speciation model) values have been compared to the experimental results to confirm some analytical finding and observe the impact of kinetic rates on the iron speciation.

To simplify the modelling, only inorganic precipitations have been taken into account using the total concentration of metals, anions (P, S and inorganic C) and some competitive cations (Ca, Mg, Na and K) as the presence of organics or complexing surface did not have any impact of iron speciation. These approximations need to be taken into account when the model results are compared with the experimental results. Finally, the database used by Phreeqc (minteq.v4) contains mostly crystal precipitates and only a few amorphous solids

(only covellite for copper-sulphide precipitate). More details on the chemical equilibrium speciation model are described in section 4.5. The input values are displayed in the appendix E and an example of Phreeqc's simulation for the sludge K is shown appendix G.

Table 6.12. Predicted iron speciation from Phreeqc's simulation

Sample		Initial	Predicted concentration				
Sludge	Iron dosing	Total Fe	Liquid	Fe as Vivianite	Fe as Pyrite	Fe as Vivianite	Fe as Pyrite
		mmol/l	mmol/l			g/kg DS	
K	No	3.5	0.0025	0.96	2.6	2.7	7.2
G	No	3.6	0.0027	1.2	2.4	3.4	6.7
M	Mix	6.8	0.0031	4.5	2.2	12.6	6.2
H	Mix	7.1	0.0031	5.3	1.8	14.9	5
S	Mix	8.0	0.0033	6.3	1.7	17.6	4.8
R	Yes	8.5	0.0036	6.5	2.1	18.2	5.9
F	Yes	10.4	0.0033	6.9	3.5	19.3	9.8

The results from the predicted iron speciation are shown in table 6.12 for the seven types of anaerobically digested sludge under study. The input values for iron and other elements (anions, cations and metals) have been obtained from the total concentration (liquid and solid phases) measured in each sludge in section 6.2.1 (see appendix E). From the simulation, concentrations of iron in the liquid phase were low and constant between the different sludge (0.0025-0.0036 mmol/l or 0.14-0.20 mg/l). The predicted values were lower than the experimental values (0.34-0.64 mg/l) and so the predicted percentage of iron present in the liquid phase was included between 0.03-0.07% instead of 0.1% (experimental values). The difference might be explained by a complexation of iron by organics than predicted by the chemical speciation model.

Phreeqc predicted that iron was precipitated in the solid phase into two compounds under anaerobic condition: pyrite and vivianite. If pyrite was not allowed to precipitate, greigite (Fe_3S_4) and ferrous sulphide were predicted to precipitate instead of pyrite. Those two compounds have been found to be pyrite's precursor (Gustavsson, 2012 and Nielsen et al., 2005) and it could explain thermodynamically the order of sulphide precipitation. The experimental analysis by SEM-EDS showed that ferrous sulphide and pyrite were both present in the sludge and so the sludge retention time was not enough to obtain a complete transformation from ferrous sulphide to pyrite.

The formation of pyrite did not increase with an increase of total iron concentration, the variation was included between 4.8 and 7.2 g/kg DS except for the sludge F where the concentration of iron as pyrite was higher, 9.8 g/kg DS (table 6.12). On the other hand, the formation of vivianite increased with the augmentation of the total iron concentration. A linear relation was observed between the concentration of iron precipitated as vivianite and the total iron concentration (figure 6.15) and it was represented by the linear equation (equation 6.2).

$$\mathbf{[Fe]_{vivianite} = 0.95x\ [Fe]_{total} - 5.6}$$

Equation 6.2. Linear relation between the predicted concentration of Fe as vivianite and its total concentration (using Phreeqc)

Similarities between the predicted concentration of iron as vivianite or pyrite and experimental concentrations of iron in different BCR sequential extraction fractions was observed and plotted in figure 6.15.

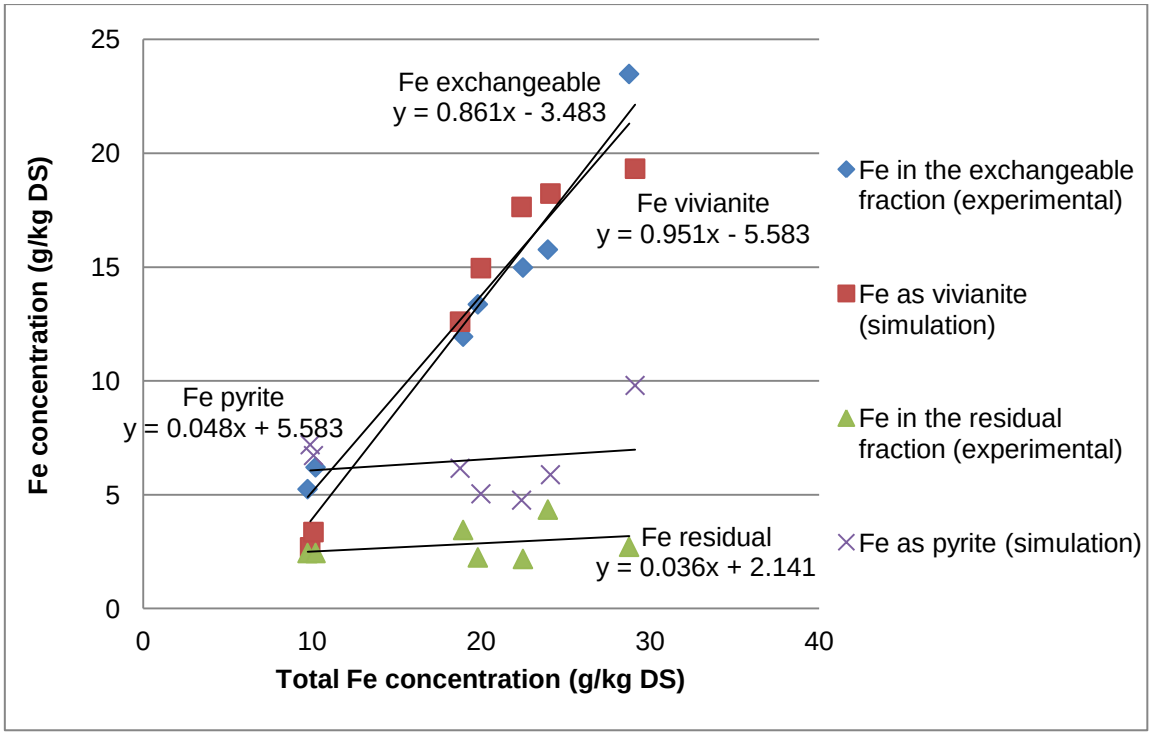

Figure 6.15. Comparison of iron concentrations between experimental and predicted values obtained with Phreeqc

The iron concentrations in the exchangeable fraction and the concentrations of iron as vivianite presented similar concentrations with the different sludge. A similar pattern was also observed between the concentration of pyrite predicted by the model and the concentration of iron in the residual fraction. However, concentrations of iron in the residual fraction were systematically lower than the predicted concentrations of iron as pyrite. The sludge F exhibited the highest difference between the model and the experiments. The prediction of vivianite

concentration was lower than the iron present in the exchangeable fraction and pyrite concentration was higher than the iron extracted in the residual fraction. This difference could be linked with the sulphur concentration in the liquid phase measured in the sludge F (13.8 mg/l, see table 6.5) which was higher than the concentrations observed in the other sludge (5-8 mg/l, see table 6.5). So the thermodynamics suggested that more pyrite were precipitated in the digester, but kinetic and a potential phosphate bulking reduced the pyrite formation to increase the vivianite precipitation (Zhang et al., 2009).

For each sludge, a variation of iron concentration was simulated using Visual Minteq model from 0 to 30 g/kg DS and the average (across the 7 types of sludge) concentrations of iron as vivianite and as pyrite were plotted in figure 6.16. The first compound to be precipitated was pyrite and iron was only converted into pyrite until all sulphide was consumed and became the limiting factor. Then the concentration of pyrite stayed constant and the iron started and kept precipitating as vivianite. Chemical speciation model was also used to simulate the impact of sulphide and phosphate on the iron precipitation and confirming that sulphide controls the iron speciation.

A variation of sulphide concentration (0-40 g/kg DS, figure 6.17), following the same protocol as iron concentration variation, showed that in the absence of sulphide all the iron was precipitated as vivianite. Sulphide precipitates first with copper, nickel, zinc and cobalt prior to the formation of pyrite. Then the increase of sulphide concentration led to change of iron precipitation from vivianite to pyrite

until all the iron was precipitated as pyrite. In opposition, a variation of phosphate (0-40 g/kg DS, results not shown) showed that in absence of phosphate, iron was precipitated as pyrite and siderite ($FeCO_3$). The concentration of pyrite stayed constant with the increase of phosphate but the siderite concentration decreased and iron precipitated as vivianite until no siderite was left. This series of simulation showed, from the thermodynamic, that iron speciation was primarily controlled by sulphide, then phosphate and finally carbonate.

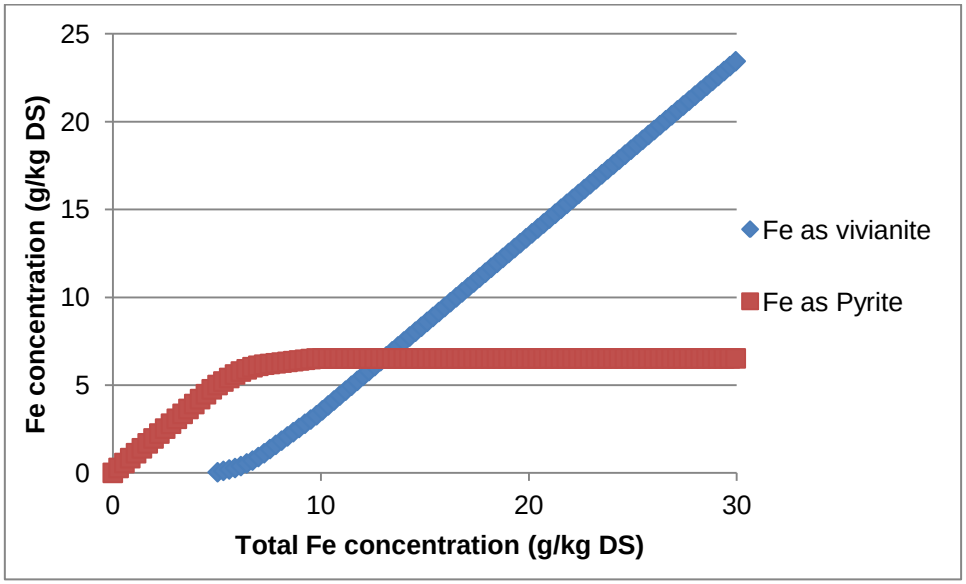

The two curves are the average of the predicted results obtained from all anaerobically digested sludge under study

Figure 6.16. Predicted iron fractionation in function of total iron concentration using Visual Minteq

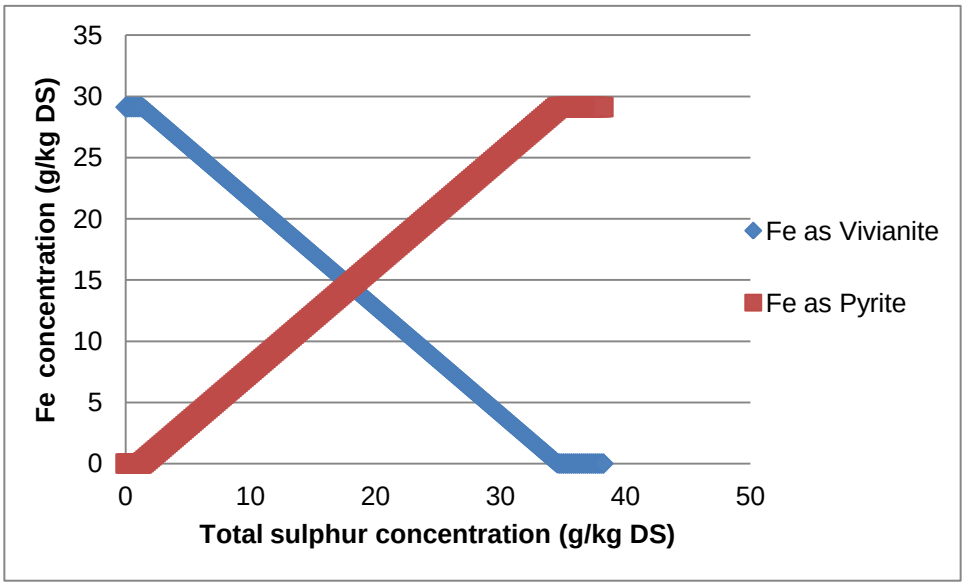

The two curves are the average of the predicted results obtained from all anaerobically digested sludge under study

Figure 6.17 . Predicted iron fractionation in function of total sulphur concentration using Visual Minteq

6.3. Discussion

Fuentes et al. (2008) analysed anaerobically digested sludge using the same BCR sequential extraction procedure and found that most of the iron was extracted in the residual fraction (90%). The concentrations of iron in the sludge under their study (25 g/kg DS) were included in the range of the digester analysed in this research. Other studies (Alvarez et al., 2002 and Van der Veen et al., 2007) showed similar results concerning the partitioning of iron in anaerobically digested sludge. Others (Carliell-Marquet et al., 2010, Dodd et al., 2009 and Smith and Carliell-Marquet, 2009) found comparative results with those obtained during this

research, with high percentage of iron in the first steps of the sequential extraction procedures (exchangeable and reducible fractions). Several hypotheses could be suggested to explain this difference. An alteration of the sample prior the extraction could have modified the iron speciation or a perturbation in the sequential extraction procedure could have produced a none extraction or re-reprecipitation of the iron during its first steps. The lack of information on the phosphorus contents in each fraction or the practical method used to analyse the sample could not confirm any hypotheses.

Fuentes et al. (2008) also observed that the sum of the iron concentration in the fractions was lower than the total concentration measured using the total acid digestion method. The iron recovery from their research was 87%, which is similar to the percentage of recovery found in this research (85%). The iron that was not recovered during the sequential extraction seemed to be independent of the iron partitioning and the experimental manipulations but conditioned by the sequential extraction procedure.

The presence of iron in the exchangeable fraction could be interpreted as iron-carbonate precipitate (such as siderite) or iron-phosphate precipitate. However, SEM-EDS analysis did not exhibit any evidence of the presence of iron-carbonate precipitates in anaerobically digested sludge and model simulation showed that the formation of iron-carbonate occurs only in absence of available phosphate and sulphide. Callander and Barford (1983) and Mosey et al. (1971) found that the carbonate might precipitate with iron but it only forms secondary or tertiary

compounds with iron as the carbonate system is not dominant for iron speciation. In the case of Mosey et al. (1971), the phosphate system (only sulphide and carbonate) was not taken into account to understand the factors controlling the iron speciation. Van Langerak et al. (1999) found that iron precipitated with carbonate only at high iron concentration in a system containing only iron, carbonate, phosphate and calcium. Using the model simulation, siderite appeared oversaturated only when vivianite, pyrite and other ferrous sulphide compounds were not allowed to precipitate and so indicates that iron-phosphate and ferrous sulphides compounds were formed prior to the formation of iron carbonate precipitates.

Analysis of the sludge using SEM-EDS provided evidence of the presence of vivianite in the different sludge (iron dosed and non-iron dosed sludge) and the modelling confirmed the thermodynamic stability of vivianite in each sludge. The high solubility product (35.8; Al-Borno and Tomsen, 1994) showed that vivianite could compete with the formation of pyrite (pK_{sp} around 16, Giblin and Howarth, 1984 and Davidson, 1991) from a thermodynamic approach.

The simulation predicted that the concentration of vivianite should be lower than the one observed during the experimental analysis (assuming that iron present in the BCR exchangeable and reducible fractions was mainly extracted as iron-phosphate precipitate). This was essentially observed for the undosed sludge (K and G); the model predicted a concentration of iron as vivianite of 3 g/kg DS and experimental values found the iron concentration of 6 g/kg DS in the exchangeable

fraction and 2 g/kg DS in the reducible fraction. Iron is mainly entering in the anaerobic digester as ferric phosphate ($FePO_4$) and under anaerobic condition the compound is thought to be dissolved to allow the reduction of iron (III) to iron (II) (Carliell-Marquet et al., 2010). A high amount of phosphate is surrounding the iron following the dissolution of ferric phosphate and it creates a bulk limiting the sulphide availability for iron precipitation (Zhang et al., 2009). Carliell-Marquet et al. (2010) also observed an increase of iron phosphate concentration when there was an augmentation of the total concentration of iron. So the phosphate bulking disturbed the thermodynamic equilibrium and enhanced kinetically the formation of iron phosphate compounds.

The presence of iron in the two first BCR sequential extraction fractions suggested that there were different iron phosphate precipitates in anaerobically digested sludge. The figure 6.15 shows a similar variation between the iron concentrations in the exchangeable fraction and predicted as vivianite (modelling) in function of the total iron concentration. The similarity in the linear equation (0.86 and 0.95, respective coefficient) infers that vivianite was mainly extracted in the exchangeable fraction and so the iron extracted in the reducible fraction precipitated differently with phosphate. This was corroborated by a similar variation of concentration of iron and phosphorus in the reducible fraction without any ratio. If vivianite was mainly extracted in the reducible fraction, a 1.5 molar ratio should be present between the two concentrations in the reducible fraction. Moreover, SEM-EDS analysis detected ferrous phosphate and ferrous-hyrdoxy-phosphate precipitates other than vivianite, such as delvauxite. This agreed with

Smith et al. (2009) who suggested that the iron might re-precipitate in the anaerobic digester as Fe-OH-P compounds.

The controlling reaction in the iron speciation is the precipitation of iron by sulphide. From the literature, sulphide precipitation is supposed to be the most abundant reaction with iron (Morse and Luther, 1999; Fermoso et al., 2008; Mosey et al., 1971; Callander and Barford (1983)). Results showed that iron sulphide might be the first compound to be precipitated and the presence of sulphur in the liquid phase suggested that sulphide availability should not be the limiting factor for the formation of iron sulphide. This limitation was likely to be kinetic as the model found the concentration of iron as pyrite was comprised between 4.8 g/kg DS and 9.8 g/kg DS and the sulphide concentration in the liquid phase was below 1 mg/l. Moreover, models exhibited a higher concentration of pyrite than the concentration of iron in the residual phase, which could be explained by the kinetic limitation developed earlier.

SEM-EDS analysis showed the presence of two iron-sulphide compounds: amorphous ferrous sulphide and pyrite. Nielsen et al. (2005) used the pourbaix diagram to predict the formation of iron precipitate in function of the pH/pE condition and found that with the anaerobic digester condition (ORP< -200mV and alkaline solution) pyrite was expected to be the most stable inorganic precipitate. This was confirmed by the model simulation predictions. However the low formation kinetic and the variation of the redox potential in the digester (by the addition of a new sludge at different redox potential), it was more likely to obtain

ferrous sulphide (samples H-K, figure 6.13). After the introduction of iron into the anaerobic digester, iron was firstly reduced to ferrous ion and then precipitated as ferrous sulphide. With a high SRT the formation of pyrite could be observed by the transformation of ferrous sulphide to pyrite (sample M, figure 6.13). Nielsen et al. (2005) showed that ferrous sulphide was a precursor of pyrite and the presence of both precipitates in the solid E (figure 6.13) confirmed it. The results agreed with Nielsen et al (2005) and Miot et al (2009) that found that iron was incorporated in diverse sulphur minerals including pyrite and ferrous sulphide.

Iron sulphide compounds presented a large degree of resistance during the extraction as most of the sulphur was extracted in the last fraction and no iron was extracted in the oxidisable fraction. Van der Veen et al. (2007) already noticed that iron sulphide was not extracted in the oxidisable fraction and Gustavsson (2012) demonstrated that iron monosulfide was dissolved during the oxidisable fraction but a secondary Fe phase was formed with sulphate. Moreover, a similar loss of iron and sulphur during the sequential extraction procedure (figure 6.6) inferred that pyrite was dissolved and re-precipitated of during one of the three first steps of the sequential extraction (likely to be the oxidisable fraction).

Iron was also present in the inorganic fraction as co-precipitation, metal inclusion or sorption. Several types of those compounds were detected using SEM-EDS analysis but their presence was complicated to quantify with the sequential extraction analysis or with the modelling simulation. Iron included in other compounds was extracted in the same time as the main compound/solid. The low

concentration of iron in those compounds (around 3%) reduced any detection in the specific fraction. The model took into account only crystal precipitates and has not been set with an ion exchange competency.

Finally, the co-precipitation occurred with metals and cations in iron sulphide and phosphate precipitates. Calcium and magnesium were included into the vivianite and represented around 1% each. Other essential metals could be included into ferrous sulphide such as zinc (figure 6.13 and table 6.9). Nickel has also been observed as a multi element precipitate (including iron) on the surface of some compounds (figure 6.14 and table 6.11). Concerning the metal inclusion into ferrous sulphide and pyrite, Morse and Luther (1999) showed that nickel and cobalt were the two metals more likely to co-precipitate with iron-sulphide compounds. None of those co-precipitates have been found in the sludge but Van Hullesbusch et al. (2006) observed it in the UASB reactor sludge.

Experimental values and model predictions exhibited that two main compounds were responsible for the control of iron speciation. Figure 6.7 showed that an increase of iron concentration enhanced the vivianite production and in opposition the iron present as iron sulphide stayed constant. However, vivianite precipitation should not be the dominant reaction as the linear regression (equation 6.1) has a y-intercept negative suggesting that iron was firstly precipitated with another anion. Sulphide precipitation should be the controlling reaction as the y intercept of the linear regression was positive and thermodynamic data predicted iron-sulphide

precipitates to be the most stable compounds under anaerobic condition (see chapter 2.4).

The confirmation of sulphide precipitation controlling the iron speciation was done using model predictions. Figures 6.16 and 6.17 showed that at low iron concentration, ferrous sulphide was the only compound to be formed and vivianite appeared when all the sulphide was precipitated. Model predicted that sulphide availability needed to be limited to observe the precipitation of iron as vivianite but the experimental values showed that sulphur concentration in the liquid phase was still important (4-10 mg/l, table 6.5) and that ferrous sulphide precipitation was lower than the amount predicted. Several reasons could explain this reduction such as the slow kinetic of pyrite precipitation, the formation of a phosphate bulk surrounding the iron (both theory developed above), or the proportion of sulphur part or bond with organics and others cations. For the sludge F, this unavailability of sulphide for iron was clearly shown as the sulphur concentration in the liquid phase was high and iron was more precipitated as vivianite than pyrite in opposition as the model prediction. So the kinetic limitation of the formation of pyrite favoured the formation of iron phosphate.

6.4. Conclusion

The combination of the three techniques (Sequential extraction, SEM-EDS and model simulation) gave us quantitative and qualitative information on the iron

behaviour in anaerobically digested sludge. Sulphide was confirmed to be the first anion controlling the iron speciation and it agreed with previous research investigations and thermodynamic predictions (Callander and Barford, 1983, Oleszkiewicz and Sharma (1989), Morse and Luther (1999)). However, phosphates also had an important impact on the iron speciation as iron-phosphate compounds occurred as secondary precipitates but represented the main fraction in all the anaerobically digested sludge.

Sulphide precipitated strongly with iron to form ferrous sulphide and pyrite. Both precipitates were extracted in the BCR residual fraction. Experimental and modelling results confirmed that sulphide precipitation was the controlling reaction of iron speciation but represented only 10-25% of the total iron. In the range of iron concentration studied, sulphides availability was not enough to immobilize all the iron and so the phosphate system precipitated with iron as a secondary reaction.

Phosphate precipitated mainly with iron to form vivianite but also precipitated as diverse ferrous phosphate and ferrous-hydroxy phosphate. Those precipitates represented 75-90% of the total iron and were extracted in the BCR exchangeable and reducible fractions depending on their binding strengths. An augmentation of the iron concentration in the anaerobically digested sludge, e.g. during the iron dosing, had for results an augmentation of the vivianite in the digester (figure 6.16).

The partitioning of iron into two specific fractions, phosphate and sulphide, revolutionized the perception on the iron behaviour in anaerobically digested sludge. The presence of iron bound with phosphate at high concentration and the quick limitation of sulphide for iron precipitation demonstrated that iron was potentially more bioavailable than predicted by other studies (Callander and Barford, 1983; Zhang et al., 2009 and Oleszkiewicz and Sharma, 1989). The extraction of vivianite in the BCR exchangeable fraction revealed that iron was weakly bound and could easily react with the liquid phase. However, results were not sufficient to quantify this bioavailability and other research needs to be undertaken.

CHAPTER 7. METALS BEHAVIOUR IN ANAEROBICALLY DIGESTED SLUDGE IN THE CASE OF MeEDTA SUPPLEMENTATION

7.1. Introduction

The effect of metals supplementation on the gas production has been studied on UASB reactors by Fermoso et al. (2008a), Bartacek et al. (2008) and Van Hullebusch et al. (2006). Other studies on completely stirred tank reactor (Percheron et al., 1997) and anaerobic film expanded bed reactor (Kelly and Switzenbaum, 1984) have been detailed by Fermoso et al. (2009). The main aim of these researches was to observe the effect of metals supplementation on the stimulation of the different biological conversions occurring in the sludge (particularly methane production). However, the understanding of the metals supplementation effects on metals speciation and chemical equilibriums in the sludge is essential to optimize this process. Bartacek et al. (2010) and Van Hullebusch et al. (2006) started some investigations in this direction by calculating the sorption capacity of cobalt by granular sludge in order to determine the effect of metals dosing on the microorganisms activities.

Metals speciation and their behaviour in anaerobically digested sludge were the only part studied in this research from the metals supplementation and there was

no consideration on its impact on the methane production. The biological aspect and effect of metals supplementation on the acetate conversion by micro-organisms have been detailed by Ishaq (2012) who works in collaboration with this research. Ishaq (2012) demonstrated that metals supplementation as MeEDTA chelates might have beneficial effect on the methane production in case of metals deficiency. However, he noticed that metals reacted differently with the sludge and so he raised several questions concerning the availability of some supplemented metals. Cobalt was found to have a key role in the enhancement of the biogas (Ishaq, 2012 and Bartacek et al., 2008) and similar beneficial effects have been observed when cobalt was added on its own or with other metals (Ishaq, 2012). From the observations made by Ishaq (2012), the behaviour of supplemented metals seemed to be dependent on the metals speciation in the digester and their affinities with EDTA.

The supplementation of metals in anaerobic digesters disturbs the equilibrium established between the solid and the liquid phase by a high increase of metals in the liquid phase. In consequence the system reacts in order to reach a new equilibrium. The bioavailability of supplemented metals is set by their fates in the digesters, which are controlled by those reactions. Metals might either stay bound in the liquid phase or be transferred into the solid phase to be taken up by microorganism or immobilized by precipitation, complexation and adsorption. In the case of supplementation using weakly bound metals, metals are quickly transferred and immobilized into the solid phase. However, by its strong binding capacity, EDTA maintains metals bound in the liquid phase longer than weak

binding (Fermoso et al., 2008a and Bartacek et al., 2007). So an understanding of the metals behaviour in anaerobically digested sludge is necessary to optimize the metals supplementation by identifying their fate and availability in the digesters.

In the previous chapters (5 and 6), different analytical techniques used in the study of metals behaviour in anaerobically digested sludge were assessed and applied on the determination of iron, copper and nickel speciation in the solid phase. During the study of iron speciation, un-dosed and iron dosed anaerobically digested sludge were used to obtain a wide range of iron concentrations and gave information on its behaviour in anaerobic digesters. So the supplementation of MeEDTA was also used to investigate the speciation and behaviour of cobalt, manganese and zinc in the solid phase of anaerobically digested sludge following the same principle used for the iron speciation.

The aim of this chapter was to characterize the mechanisms controlling the fate of each supplemented metals (as MeEDTA) and their relations with an increase of bioavailability. First, an investigation of the fate of the metals bound with EDTA was necessary by an observation of the effect of metals supplementation on the solid/liquid equilibrium. Then the speciation of zinc, manganese and cobalt in anaerobically digested sludge was characterized using the supplementation to identify the reactions controlling the metals behaviour (analogously of the research conducted with the iron dosing). Finally, the kinetic of cobalt transfer reactions from the liquid to the solid phase was investigated to determine the mechanisms controlling those reactions.

Two main solutions have been designed to enhance the biogas production. The first solution (called TMC) was a mix of metals, including mainly iron, cobalt, nickel, manganese and zinc. Traces of copper, tungsten and other essential metals were also present inside this solution. The second solution was only containing cobalt at the same concentration as in the TMC solution and it was called CoA in this research. The concentration of CoA was also doubled (CoAx2). Metals in solution were bound with EDTA to increase their solubility and supposedly increase their bioavailability.

The sludges F and K were used as support for this experiment due to their large difference of iron concentration (see chapter 6). The metals supplementation experiment was based on destructive serum bottles as laboratory scale anaerobic digesters to observe any change in the metals speciation during the digestion. Experiments were mainly conducted during a period over approximately 248-336 hours (12-14 days), at 35°C with partial hand-mixing. Serum bottles were destructed over this period to analyze metals concentrations in the liquid and solid phases and their speciation. The dry solid (DS) content was measured in each serum bottle in order to express accurately the metals concentration in the solid phase. However, the reduction of DS through time and its effect on the metals speciation were not considered in this study. Blank samples and gas production measurement were used as reference and control. The complete experimental procedure is described in section 4.1.2 and biogas production curves are reported in the appendix A.

7.2. Fate of essential metals supplemented as MeEDTA in anaerobically digested sludge

As described above, the supplementation of metals in anaerobic digesters disturbs the liquid-solid equilibrium generating chemical reactions to reach a new equilibrium. MeEDTA chelates are strongly bound compounds (see section 2.6) and their bindings may compete with the reactions controlling the metals speciation in anaerobically digested sludge, e.g. sulphide precipitation. So it is essential to identify the reactions controlling the fate of those metals in order to understand their potential availability for microorganism and optimize it.

So the aim of this chapter was the evaluation of the potential of EDTA to keep metals in the liquid phase by characterizing of the variation in the solid-liquid equilibrium due to metals supplementation.

7.2.1. Results

The concentration of metals added in the TMC samples were iron (6.72 mg/l), cobalt (2.24 mg/l), manganese (2.24 mg/l), nickel (2.24 mg/l), zinc (0.224 mg/l), copper (0.0224 mg/l). Concentrations of metals in the two phases (solid and liquid) were measured at time intervals during a period of 248-336 hours (12-14 days). However, the chemical equilibrium might not be totally obtained after this period and so an extra measurement was done after 1128 hours (47 days) for the sludge

F. Results in table 7.1 show the concentrations of the six metals under study (Co, Cu, Fe, Mn, Ni and Zn) in the liquid (noted as $[Me]_l$) and solid phases (noted as $[Me]_s$) measured in the control and TMC samples of the sludge K. Table 7.2 shows the same concentrations of metals measured in the sludge F.

Table 7.1. Metals concentrations in the solid and liquid phases in the control and TMC samples for the sludge K

Sample		Liquid Phase (mg/l)		Solid Phase (mg/kg DS)	
Metal	Hours	Control	TMC	Control	TMC
Cobalt	1	0.002 ± 0.001	2.0 ± 0.1	2.18 ± 0.48	26.3 ± 1.8
	48	0.004 ± 0.001	1.8 ± 0.1	2.45 ± 0.85	40.4 ± 2.6
	248	0.002 ± 0.001	1.1 ± 0.1	1.51 ± 0.05	114 ± 8
Copper	1	0.029 ± 0.002	0.044 ± 0.001	388 ± 41	435 ± 6
	48	0.014 ± 0.001	0.016 ± 0.001	390 ± 27	424 ± 19
	248	0.042 ± 0.001	0.040 ± 0.001	410 ± 17	416 ± 33
Iron	1	0.27 ± 0.02	4.4 ± 0.1	$(8.55 \pm 1.30).10^3$	$(9.70 \pm 0.86).10^3$
	48	0.16 ± 0.01	3.3 ± 0.1	$(9.41 \pm 0.79).10^3$	$(9.57 \pm 0.72).10^3$
	248	0.52 ± 0.01	4.6 ± 0.1	$(9.73 \pm 0.45).10^3$	$(9.83 \pm 0.86).10^3$
Manganese	1	0.023 ± 0.001	0.80 ± 0.01	153 ± 8	289 ± 3
	48	0.012 ± 0.001	0.39 ± 0.01	144 ±11	288 ± 23
	248	0.020 ± 0.001	0.42 ± 0.01	150 ± 6	302 ± 21
Nickel	1	0.089 ± 0.001	2.0 ± 0.1	664 ± 182	557 ± 36
	48	0.061 ± 0.001	2.0 ± 0.1	911 ± 213	842 ± 169
	248	0.17 ± 0.01	2.5 ± 0.1	849 ± 151	722 ± 124
Zinc	1	0.038 ± 0.002	0.26 ± 0.01	442 ± 25	558 ± 29
	48	0.028 ± 0.001	0.078 ± 0.004	466 ± 9	486 ± 17
	248	0.040 ± 0.006	0.21 ± 0.01	458 ±12	502 ± 33

The concentrations are expressed as mean ± standard deviation (n=9)

Table 7.2. Metals concentrations in the solid and liquid phases in the control and TMC samples for the sludge F

Sample		Liquid Phase (mg/l)		Solid Phase (mg/kg DS)	
Metal	Hours	Control	TMC	Control	TMC
Cobalt	1	0.005 ± 0.001	1.9 ± 0.1	23.8 ± 3.1	54.5 ± 1.2
	48	0.005 ± 0.001	1.3 ± 0.1	25.8 ± 1.0	122 ± 8
	144	0.008 ± 0.001	0.67 ± 0.01	26.4 ± 1.0	212 ± 12
	336	0.015 ± 0.002	0.21 ± 0.01	21.7 ± 1.0	258 ± 32
	1128	0.012 ± 0.001	0.081 ± 0.001	23.1 ± 2.5	292 ± 24
Copper	1	0.017 ± 0.001	0.010 ± 0.002	306 ± 6	318 ± 5
	48	0.012 ± 0.001	0.008 ± 0.001	323 ± 15	305 ± 8
	144	0.011 ± 0.001	0.009 ± 0.001	322 ±12	327 ± 13
	336	0.023 ± 0.001	0.026 ± 0.002	314 ±15	337 ± 11
	1128	0.009 ± 0.001	0.007 ± 0.001	366 ± 6	345 ± 19
Iron	1	1.8 ± 0.1	4.9 ± 0.1	$(54.1 \pm 0.8).10^3$	$(56.1 \pm 2.6).10^3$
	48	1.3 ± 0.1	6.3 ± 0.1	$(57.3 \pm 0.8).10^3$	$(56.7 \pm 1.1).10^3$
	144	1.1 ± 0.1	4.3 ± 0.1	$(59.8 \pm 1.7).10^3$	$(55.2 \pm 3.2).10^3$
	336	1.8 ± 0.1	7.2 ± 0.1	$(52.6 \pm 2.4).10^3$	$(48.2 \pm 2.2).10^3$
	1128	0.94 ± 0.03	7.1 ± 0.1	$(61.7 \pm 1.6).10^3$	$(64.7 \pm 3.5).10^3$
Manganese	1	0.004 ± 0.001	0.30 ± 0.01	304 ± 9	497 ± 6
	48	0.003 ± 0.001	0.19 ± 0.01	319 ±15	515 ± 1
	144	0.012 ± 0.001	0.18 ± 0.01	340 ± 1	540 ± 12
	336	0.018 ± 0.001	0.16 ± 0.01	292 ± 8	538 ± 38
	1128	0.021 ± 0.001	0.17 ± 0.01	359 ± 9	558 ± 56
Nickel	1	1.2 ± 0.1	3.0 ± 0.1	$(1.02 \pm 0.78).10^3$	$(0.66 \pm 0.01).10^3$
	48	0.10 ± 0.01	2.0 ± 0.1	$(0.96 \pm 0.08).10^3$	$(1.07 \pm 0.16).10^3$
	144	0.41 ± 0.01	2.9 ± 0.1	$(1.10 \pm 0.27).10^3$	$(0.99 \pm 0.10).10^3$
	336	0.34 ± 0.01	2.3 ± 0.1	$(2.19 \pm 0.01).10^3$	$(1.51 \pm 0.56).10^3$
	1128	0.083 ± 0.001	2.1 ± 0.1	$(1.02 \pm 0.15).10^3$	$(1.50 \pm 0.11).10^3$
Zinc	1	0.038 ± 0.001	0.21 ± 0.01	721 ± 10	752 ± 10
	48	0.12 ± 0.01	0.077 ± 0.001	790 ± 58	754 ± 12
	144	0.021 ± 0.001	0.069 ± 0.001	937 ± 20	848 ± 6
	336	0.058 ± 0.001	0.070 ± 0.001	698 ± 33	769 ± 31
	1128	0.15 ± 0.01	0.12 ± 0.01	898 ±37	869 ± 36

The concentrations are expressed as mean ± standard deviation (n=9)

No variation was observed between the measurement of $[Cu]_l$ in the control and TMC samples for the sludge F and K . For the sludge F, $[Cu]_l$ was included in the range of 0.009 and 0.02 mg/l in the control samples and 0.007 and 0.03 mg/l in the TMC samples. Concerning the sludge K, the range was similar for the control and TMC samples with 0.015 and 0.04 mg/l. The maximum concentration was obtained after 336 hours (248 for sludge K) for all the solutions. The copper supplementation did not have an impact on its concentration in the solid phase due to the low amount of copper added with the TMC solution. For the sludge F, $[Cu]_s$ was measured between 300 and 370 mg/kg DS. For the sludge K, $[Cu]_s$ was 390-440 mg/kg DS.

Iron was the metal with the highest concentration in the TMC solution (6.7 mg/l) and its addition disturbed the liquid-solid phase equilibrium by increasing the concentration of iron in the liquid phase. The control samples had $[Fe]_l$ included in the range of 0.9-1.8 mg/l and 0.2 and 0.5 mg/l for the sludge F and K, respectively. Those concentrations were increased to 4.3-7.2 mg/l (sludge F) and 3.3-4.6 mg/l (sludge K) with the addition of the TMC solution. $[Fe]_l$ was relatively constant in the time and the minimum was observed during the 48 and 144 hours. So most of the iron stayed bound in the liquid phase. No variation was observed in the concentrations of iron in the solid phase for both sludge and samples. It was explained by the absence of transfer from the liquid to the solid phase in the TMC samples coupled with the high concentration of iron already present in the solid phase. $[Fe]_s$ was measured around 53-62 g/kg DS (control) and 48-65 g/kg DS (TMC) for the sludge F. The sludge K, which was undosed anaerobically digested

sludge (see chapter 6 and section 4.1.1), had a lower total iron concentration for the control and TMC samples with 8.6-9.8 g/kg DS.

Manganese, as cobalt and nickel, was present in the TMC solution at the concentration of 2.2 mg/l. The concentration of manganese in the liquid phase without any metal supplementation was measured in a range of 0.003-0.02 mg/l for the sludge F and 0.01-0.02 mg/l for the sludge K. With the TMC addition, $[Mn]_l$ increased to 0.3 mg/l (sludge F) and 0.8 mg/l (sludge K) after 1 hour, and then $[Mn]_l$ decreased to 0.2 mg/l (sludge F) and 0.4 mg/l (sludge K). In opposition with iron or copper, the addition of manganese had also an impact on its concentration in the solid phase. For the sludge F, $[Mn]_s$ in control samples was included in the range of 290-360 mg/kg DS. In TMC samples, $[Mn]_s$ increased to 500-560 mg/kg DS. For the sludge K, a similar outcome was observed with an increase of $[Mn]_s$ from 150 mg/kg DS in the control samples to 290 mg/kg DS in the TMC samples.

The concentration of nickel in the liquid phase increased with the addition of the TMC solution, where nickel was present at a concentration of 2.2 mg/l. $[Ni]_l$ in the control samples was included in the range from 0.1 mg/l to 1.2 mg/l for the sludge F and from 0.06 to 0.2 mg/l for the sludge K. With the addition of TMC, the concentration of nickel in the liquid phase increased to 2.0-3.0 mg/l for the sludge F and K. After 1 hour, most of the nickel was kept in the liquid phase and no variation of $[Ni]_l$ in time was clearly observed that could induce a possible transfer of nickel into the solid phase in the next hours. So the addition of TMC into the digested sludge should not have any impact on the concentration of nickel in the

solid phase. However this hypothesis could not be confirmed due to some complication in the solid phase concentration analysis. The results were disparate and did not exhibit any patterns or consistency. The high values in the standard deviation showed a difference between replicates and probably the presence of a contamination during the metal analysis.

Zinc was present in the TMC solution at a concentration of 0.22 mg/l. $[Zn]_l$ in the liquid phase without any metal supplementation was measured in a range of 0.02 and 0.15 mg/l for the sludge F and 0.02 and 0.04 mg/l for the sludge K. With the TMC solution addition, $[Zn]_l$ increased to 0.2-0.3 mg/l (sludge F and K) after 1 hour and then decreased to similar values measured in the control samples (0.07-0.2 mg/l). The transfer of the low amount of zinc added with the TMC into the solid phase was not observed directly in the solid phase due to the high concentration of zinc already present in it. $[Zn]_s$ was comprised between 700 and 940 mg/kg DS for the sludge F and 400-560 mg/kg DS for the sludge K.

The concentration of cobalt in the TMC solution was 2.2 mg/l that was really higher than the concentration of cobalt present in the control samples (solid and liquid phases). The concentration of cobalt in the liquid phase of the control samples was comprised in the range 0.004-0.02 mg/l for the sludge F and 0.002-0.004 mg/l for the sludge K. With the addition of TMC, $[Co]_l$ decreased with the time from 2.0 mg/l (after 1 hour) to 0.2 mg/l (after 336 hours) for the sludge F and 1.9 mg/l (after 1 hour) to 1.1 mg/l (248 hours) for the sludge K. The equilibrium concentration was obtained around 0.08 mg/l (measured after 1128 hours in the sludge F). In

comparison with other essential metals, cobalt concentration in the solid phase was low in anaerobically digested sludge (20-30 mg/kg DS for the sludge F and 2-3 mg/kg DS for the sludge K) and so the addition of cobalt with the TMC solution affected its concentration in the solid phase. The concentration of cobalt in the solid phase of the sludge F increased from 55 mg/kg DS to 292 mg/kg DS. For the sludge K, the increase was lower as the transfer from the liquid phase was slower than for the sludge F. $[Co]_s$ varied from 26 mg/kg DS to 114 mg/ kg DS.

Cobalt had also been added without any other metals at different concentrations and Ishaq (2012) found that interesting concentrations for the methane enhancement were comprised between the cobalt concentration in the TMC solution (2.2 mg/l, CoA sample) and the double (4.4 mg/l, CoAx2 sample). Results of cobalt concentration in the solid and liquid phase from the addition of cobalt alone are displayed in table 7.3.

For the sludge F, concentrations of cobalt in the liquid phase in the CoA samples decreased from 1.6 mg/l (after 1 hour) to 0.09 mg/l (after 336 hours). Those variations were similar to the cobalt concentrations observed in the TMC samples. With an initial concentration of cobalt double (CoAx2), $[Co]_l$ was measured at 3.4 mg/l (sludge K) and 3.3 mg/l (sludge F) after 1 hour. $[Co]_l$ decreased with time to 1.6 mg/l after 248 hours for the sludge K and 0.2 mg/l for the sludge F after 336 hours. The equilibrium concentration of cobalt in the liquid phase, measured after 1128 hours, was at 0.07 mg/l and that was similar as the value measured in the control, TMC and CoA samples. Concerning the concentration of the cobalt in the

solid phase, results were comparable with the values observed with the TMC addition. For the sludge F, concentrations increased from 82 mg/kg DS to 311 mg/kg DS in CoA samples and from 138 mg/kg DS to 498 mg/kg DS in CoAx2 samples. The cobalt concentration in the solid phase increased from 35 mg/kg DS to 277 mg/kg DS in CoAx2 sample of the sludge K.

Table 7.3. Cobalt concentrations in the solid and liquid phases in the CoA and CoAx2 samples for the sludge F and K.

Sample		Liquid Phase (mg/l)		Solid Phase (mg/kg DS)	
Sludge	Hours	CoA	CoAx2	CoA	CoAx2
Sludge F	1	1.6 ± 0.1	3.3 ± 0.1	82.2 ± 3.3	139 ± 4
	48	0.81 ± 0.01	1.8 ± 0.1	177 ± 7	304 ± 23
	144	0.29 ± 0.01	0.71 ± 0.01	268 ± 12	472 ± 21
	336	0.090 ± 0.001	0.20 ± 0.01	291 ± 6	504 ± 16
	1128	0.044 ± 0.001	0.066 ± 0.001	311 ± 12	498 ± 6
Sludge K	1	-	3.4 ± 0.1	-	35.4 ± 5.4
	48	-	3.0 ± 0.1	-	98.6 ± 2.7
	248	-	1.6 ± 0.1	-	277 ± 15

The concentrations are expressed as mean ± standard deviation (n=9)

7.2.2. Discussion

Ishaq (2012) showed that a metal deficiency occurred 69 % of the time in the wastewater sludge digester samples. So TMC solution was designed to increase metals bioavailability in order to enhance the methane production from micro-organisms. The concentration of metals in TMC solution was generally lower than the initial concentration of those metals in anaerobically digested sludge (solid +

liquid phase) and corroborated the principle that metals bioavailability is not only related to the total metal concentrations. The main exception was concerning cobalt where its total concentration in the sludge was the lowest (average 25 mg/kg DS for the sludge F and 2 mg/kg DS for the sludge K) in comparison with other essential metals). The total concentration of cobalt was between ten and hundred times higher in the TMC and CoA samples.

The other metal that had its total concentration affected by metal supplementation was manganese. The manganese concentration in the solid phase was close to double with the TMC addition. The manganese concentration increased on average from 323 to 530 mg/kg DS in the sludge F and from 149 to 293 mg/kg DS in the sludge K. A change in the total concentration was not observed for the other metals as their concentration in the sludge was much higher than the amount added with the TMC.

However, it is essential to notice that the concentrations of metals in the TMC solution were always higher than their concentrations in the liquid phase (from 2 times higher for copper to over 100 times higher for cobalt and manganese). Jansen et al. (2007) and Osuna et al. (2004) related metals bioavailability with their concentration as free form present in the liquid phase. So the aim of the TMC solution (also CoA - CoAx2 solution) was to increase the concentration of metals in the liquid phase by adding them bound with a strong chelating ligand (EDTA). EDTA has the ability to form stable soluble chelates with metals and protect them against precipitation and sorption (Bartacek et al., 2008 and Fermoso et al., 2009).

However, several concerns were raised concerning the abilities of microorganisms to uptake metals strongly bound with EDTA (Fermoso et al., 2008a).

The initial equilibrium between the liquid and solid phases, measured using control sample results, was disturbed by the addition of TMC solution. This change was quantified by the measurement of the metals concentration in the liquid phase. However, each metal was reacting differently while added into the sludge. The concentrations of nickel and iron in the liquid phase got an increase of around 2 mg/l for nickel and around 4-6 mg/l for iron in the TMC samples. This increase was corresponding to the amount of nickel and iron added with the TMC solution. Similar results were observed for nickel by Bartacek et al. (2010) with 89-98% of the supplied nickel staying in solution as NiEDTA. The results presented in this study agreed with the potential of EDTA to keep nickel soluble but concerning the iron protection, those results could be more surprising as Fe(EDTA) complexes have low stability constant (Callander and Barford, 1983a; section 2.6) and can easily precipitate with sulphide or phosphate (chapter 6). Moreover, manganese that has a similar stability constant was quickly precipitated during the first hour (between 64% and 86% of the total amount of the added manganese).

The low addition of zinc and copper in the TMC samples did not exhibit a large change in their concentration on the liquid phase in comparison with the control samples. Nevertheless it can be noticed that the concentration of zinc was higher in the TMC samples (0.2 mg/l) than in the control samples after 1 hour.

Finally, CoEDTA exhibited a specific reaction when added to anaerobically digested sludge with a slow transfer into the solid phase. After 248-336 hours, there was 50% of the cobalt remaining in the liquid phase for the sludge K and 10% for the sludge F. Fermoso et al. (2008a) showed that only 8% of the CoEDTA dosed in UASB reactors were retained in the solid phase in comparison with 90% of cobalt while added as $CoCl_2$. In this study a larger part of cobalt was transferred in the solid phase of anaerobically digested sludge than in UASB sludge.

The increase of metal concentrations in the liquid phase by the use of TMC solution was dependent on the metals and their concentrations in the TMC solution. However, the assimilation of an increase of metals in the liquid phase as an increase of metals bioavailability could be misleading as the strength of the MeEDTA chelates might also have some negative effects on metals bioavailability. Hayes and Theis (1978) showed that the EDTA chelation with metals was stronger than the binding from the exocellular polymer of the cell walls. Aquino and Stuckey (2007) also demonstrated that EDTA binding was stronger than the chelating sites on the cell surface for iron. In this study, Ishaq (2012) raised the question of metal bioavailability while added as MeEDTA as he demonstrated different levels of bioavailability for MeEDTA chelates. He demonstrated some positive responses from microorganisms to the TMC and CoA supplementation but suggested that further investigations were required to understand the different mechanisms responsible of those responses.

The supplementation of metals using EDTA as chelating agent reacts on the solid-liquid equilibrium differently for each metal. Metals could stay bound in the liquid phase by EDTA (iron and nickel), or be quickly transferred into the solid phase (manganese and zinc) or finally be slowly transferred into the solid phase. Those reactions were not only dependent on the stability constant of the MeEDTA complex but also the speciation of each metal in the solid phase. Several aspects needed to be investigated to understand the mechanism related to the supplementation of metal. Prior to the examination of the solid-liquid phase equilibrium, the understanding of the solid phase and its controlling reactions had to be acquired. Throughout chapters 5 and 6, the behaviour of nickel, copper and iron in the solid phase were investigated and using the MeEDTA supplementation, similar studies was done on the behaviour of manganese, zinc and cobalt in the following sections 7.3-7.5. Then the research focused on the mechanisms related to the specific transfer of cobalt into the solid phase.

7.3. Solid phase speciation of manganese in anaerobically digested sludge in the case of MeEDTA supplementation

The previous section showed that each metal reacted differently when added into anaerobically digested sludge and those reactions were dependent on the metal capacity to bind with EDTA but also on its speciation in the solid phase. Copper, nickel and iron speciation in the solid phase were already investigated in the previous chapter and the study of the speciation of zinc, manganese and cobalt in

the solid phase was done using the metals supplementation to characterize the reactions controlling their speciation.

In opposition with other metals, Callander and Barford (1983b) calculated that manganese precipitated as manganese carbonate in anaerobic digesters, except in the case of high sulphide concentration. From the literature, manganese did not exhibit any specific affinities to bind with sulphide, phosphate or organic matter and so carbonate was acting as main precipitating and controlling agent.

The aim of this section was to investigate the behaviour of manganese in anaerobically digested sludge by characterizing the different manganese chemical forms and the reaction controlling its speciation. To achieve this aim, a characterization of the manganese speciation was done first using the suite of analytical techniques developed in chapter 5. Results from the previous section (7.2) showed that the supplementation of the TMC solution increased the concentration of manganese in the solid phase and so this augmentation was used to determine the reactions governing the manganese speciation.

7.3.1. Results

The BCR sequential extraction procedure was applied on each samples (sludge F and K; control and TMC) used in the previous chapter (7.2) and the experimental

methodology was developed in section 4.3.3. Results for the sludge F are shown in table 7.4 and figure 7.1 and table 7.5 and figure 7.2 for the sludge K.

Table 7.4. Concentrations of manganese in each BCR SE fraction in the sludge F (control and TMC samples)

Concentrations of mangenese in each BCR sequential extraction fraction										
Sludge F		Σ fractions	Exchangeable		Reducible		Oxidisable		Residual	
Samples	Hrs	mg/kg DS	%	mg/kg DS	%	mg/kg DS	%	mg/kg DS	%	mg/kg DS
Control	1	307 ± 26	85	260 ± 23	6	18 ± 4	3	10 ± 2	6	19 ± 6
	48	313 ± 14	83	261 ± 4	6	18 ± 1	5	14 ± 7	6	20 ± 2
	144	341 ± 17	86	294 ± 15	5	15 ± 2	3	10 ± 1	6	22 ± 2
	336	340 ± 17	86	295 ± 12	4	15 ± 4	3	11 ± 2	7	23 ± 7
	1128	349 ± 26	88	307 ± 24	3	10 ± 1	4	13 ± 4	5	18 ± 2
TMC	1	558 ± 24	91	507 ± 20	4	23 ± 2	2	9 ± 1	3	20 ± 3
	48	543 ± 37	91	493 ± 36	4	20 ± 2	2	10 ± 2	3	20 ± 2
	144	581 ± 30	91	528 ± 30	3	20 ± 1	2	10 ± 1	4	22 ± 1
	336	597 ± 17	90	536 ± 9	4	25 ± 4	2	13 ± 3	4	23 ± 10
	1128	626 ± 24	92	579 ± 31	3	19 ± 1	2	10 ± 1	3	17 ± 1

The concentrations are expressed as mean ± standard deviation (n=9) and percent of total

Table 7.5. Concentrations of manganese in each BCR SE fraction in the sludge K (control and TMC samples)

Concentrations of mangenese in each BCR sequential extraction fraction										
Sludge K		Σ fractions	Exchangeable		Reducible		Oxidisable		Residual	
Samples	Hrs	mg/kg DS	%	mg/kg DS	%	mg/kg DS	%	mg/kg DS	%	mg/kg DS
Control	1	213 ± 8	86	183 ± 6	7	15 ± 4	3	5 ± 1	4	9 ± 2
	48	217 ± 2	87	189 ± 2	6	12 ± 2	3	7 ± 1	4	9 ± 1
	248	223 ± 18	87	193 ± 13	4	9 ± 1	4	9 ± 3	5	11 ± 2
TMC	1	386 ± 3	90	346 ± 5	7	26 ± 2	1	5 ± 1	2	9 ± 1
	48	504 ± 3	91	458 ± 3	5	25 ± 1	1	7 ± 1	3	13 ± 5
	248	453 ± 8	93	419 ± 9	4	17 ± 1	1	7 ± 1	2	10 ± 1

The concentrations are expressed as mean ± standard deviation (n=9) and percent of total

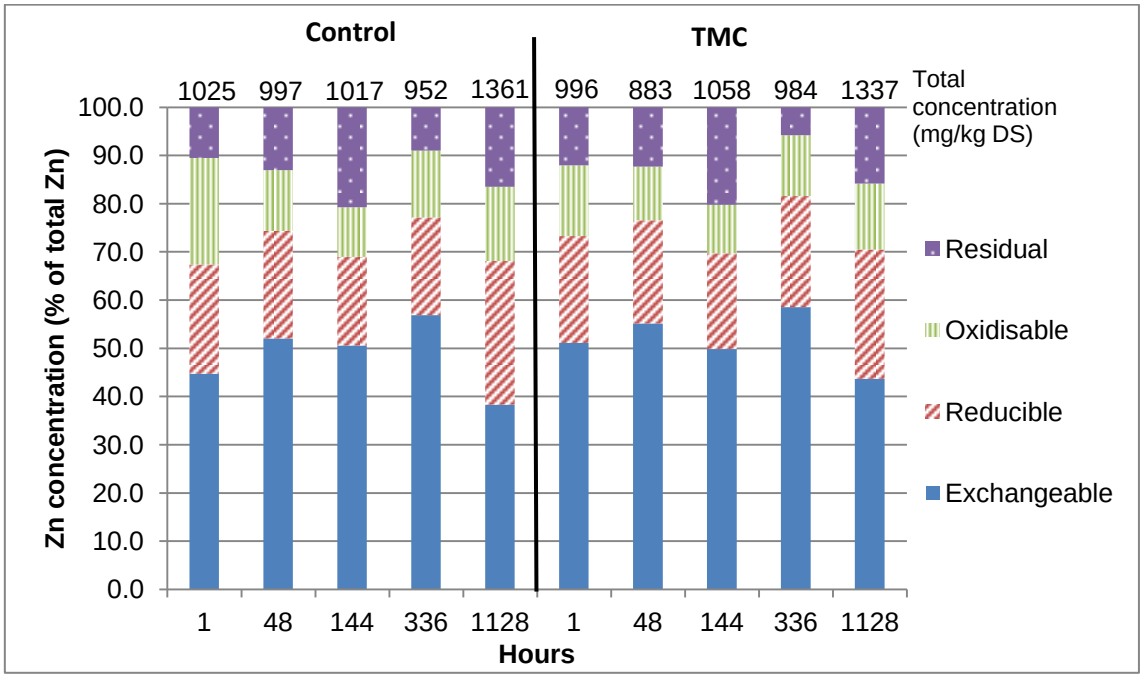

Figure 7.1. Manganese fractionation profiles in control and TMC samples for the sludge F

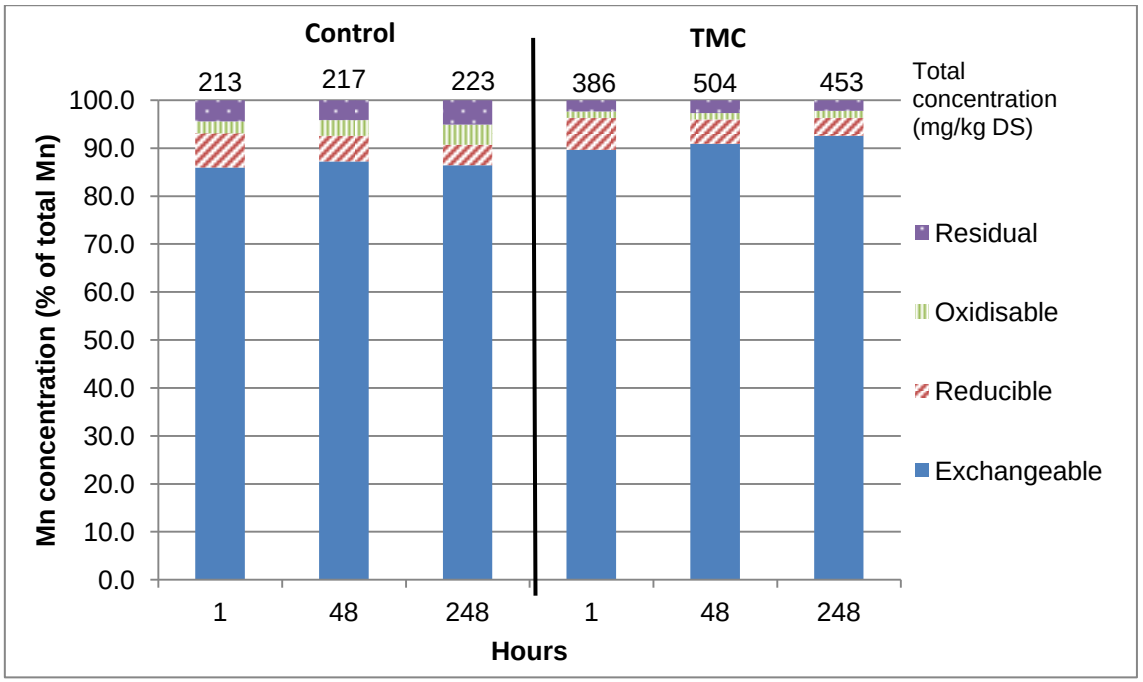

Figure 7.2. Manganese fractionation profiles in control and TMC samples for the sludge K

The BCR sequential extraction profile of manganese did not change in time and was similar across the two types of sludge. The exchangeable fraction represented the main fraction with over 80% of the total manganese. In the control samples, the percentage of manganese extracted in the exchangeable fraction varied between 83% and 88% for the sludge F and 86-87% for the sludge K. In the TMC samples, the percentage increased to 90-93% for both sludges. The remaining manganese was extracted in the three other fractions (reducible, oxidisable and residual) with a percentage below 10% for each fraction.

No variation was observed between the control and TMC samples in the reducible fraction with a percentage comprised between 3% and 7%. However, a decrease in the percentage of manganese extracted was observed for the oxidisable and residual fractions when the TMC solution was supplemented into the anaerobically digested sludge (respectively 3-5% (control) and 1-2% (TMC), sludge F; and 4-7% (control) and 2-4% (TMC), sludge K).

These percentages and their variations showed that an increase of manganese concentration from the TMC supplementation had an effect on the amount of manganese extracted in the exchangeable and reducible fractions. The increase of manganese concentration in the solid phase was around 230-250 mg/kg DS and a similar increase was observed in the exchangeable fraction. An increase of around 10 mg/kg DS was also measured in the reducible fraction. For the oxidisable and reducible fractions, the concentration of manganese stayed constant between the control and TMC samples. So the reaction responsible for

the formation of the chemical manganese species extracted in the two first fractions was also controlling the manganese speciation.

The pH titration analysis has been found useful in the characterization of the chemical species extracted in the exchangeable and reducible fractions (section 5.6). Results from the pH titration of the sludge F and K for manganese are shown in table 7.6 and figure 7.3.

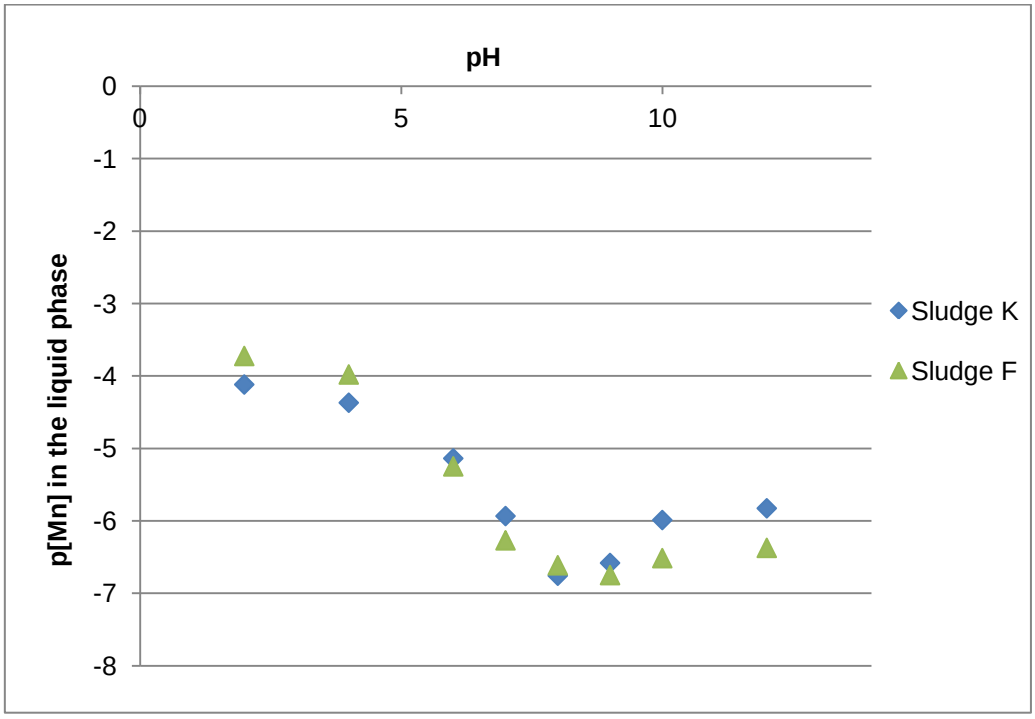

Figure 7.3. p[Mn]-pH diagram for the sludge F and K

The two types of sludge exhibited a similar pattern in the variation of the manganese concentration in the liquid phase in function of the pH. The highest concentration of manganese was obtained at pH 2 and the main decrease was observed between pH 4 and 8 for the sludge K and F. The variation was in an

order of 3 units and represented a decrease of 1000 times the manganese concentration in the liquid phase between the acid and neutral pH. Under basic pH, the manganese concentration increased with the pH but the variation was restricted to a maximum of 1 unit.

Table 7.6. Concentrations of manganese in the liquid phase measured during the pH titration analysis

Metal	pH	Sludge F		Sludge K	
		$[Mn]_l$ (mg/l)	p[Mn]	$[Mn]_l$ (mg/l)	p[Mn]
Mn	2	10.4 ± 0.8	-3.72	4.19 ± 0.46	-4.12
	4	5.77 ± 0.05	-3.98	2.35 ± 0.09	-4.37
	6	0.311 ± 0.003	-5.25	0.400 ± 0.023	-5.14
	7	0.030 ± 0.001	-6.27	0.064 ± 0.004	-5.93
	8	0.013 ± 0.001	-6.61	0.010 ± 0.001	-6.76
	9	0.010 ± 0.001	-6.75	0.014 ± 0.001	-6.58
	10	0.017 ± 0.001	-6.52	0.057 ± 0.001	-5.99
	12	0.023 ± 0.001	-6.37	0.0082 ± 0.001	-5.83

The concentrations are expressed as mean ± standard deviation (n=3) and log $[Mn]_l$

Results from the BCR sequential extraction procedure and pC-pH diagram showed that manganese was mainly bound with a compound easily extractable, likely carbonate. However, Visual Minteq predicted that manganese should be completely precipitated with phosphate to form $MnHPO_4$ (pKs: -25.4, HydroGeologic and Allison Geoscience Consultants, 1999).

A simulation of the pH titration experiment was done to obtain more information on the compound being extracted between pH 4 and 8 using Visual Minteq model. The sludge F was modelled using experimental concentrations measured in section 7.2 (input values are shown in the appendix E). Then a simulation of titration was done using the experimental conditions (titration using HCl or NaOH solution under anaerobic condition). The simulated concentrations of manganese in the liquid phase were plotted against the pH and the two curves (experimental and simulated) were compared to each other to determine the main precipitate (see section 4.5).

The simulation of the titration on the sludge F with manganese precipitated as $MnHPO_4$ showed that the variation of p[Mn] in function of the pH was different from the variation observed with sludge F (figures 7.3 and 7.4). From the literature, carbonate precipitation controls the manganese speciation and the model can be set up to precipitate manganese with carbonate as amorphous compound and crystal compound (rhodochrosite). Both compounds have similar thermodynamic constant (pKs: -10.5 and 11, HydroGeologic and Allison Geoscience Consultants, 1999) and so have comparable behaviour in anaerobically digested sludge. The formation of rhodochrosite was forced during the simulation when $MnHPO_4$ was not allowed to precipitate. The titration curve, using the simulated sludge with manganese precipitated as rhodochrosite, demonstrated a similar pattern between the simulation and the sludge F (figure 7.4). Three methods agreed on the presence of manganese carbonate as main precipitate for the manganese speciation.

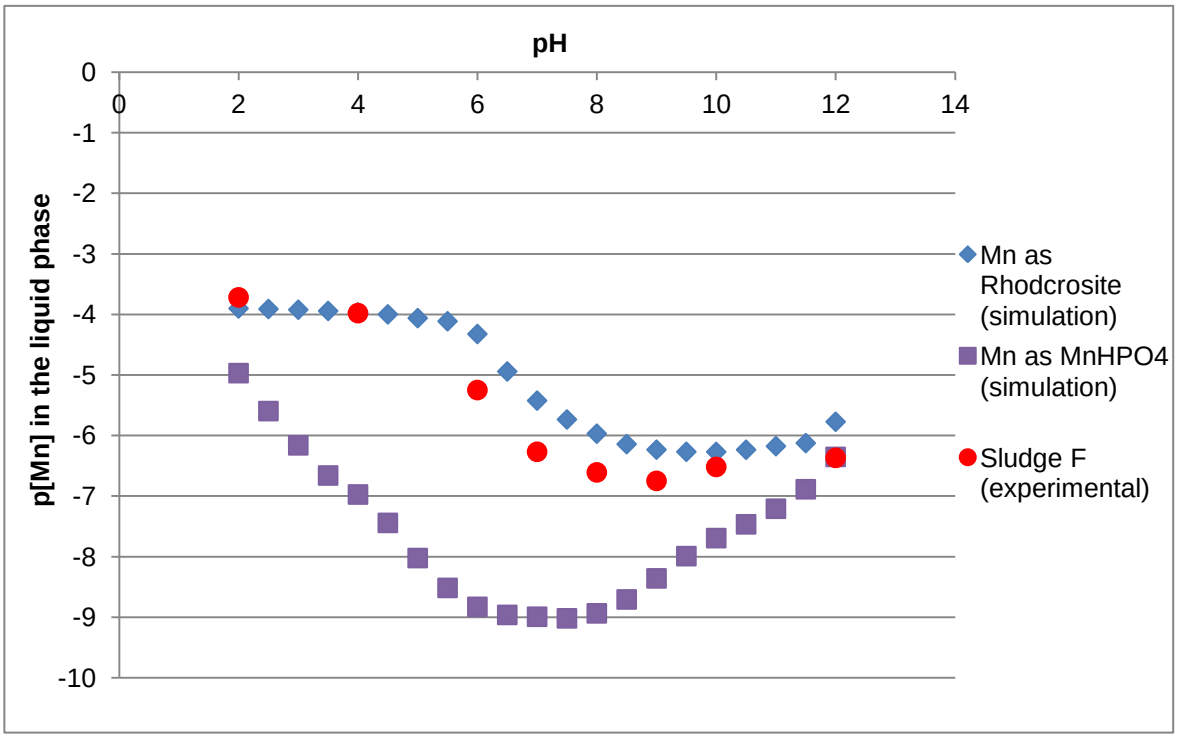

Figure 7.4. p[Mn]-pH diagram of Visual Minteq sludge simulation in comparison with experimental values (sludge F)

7.3.2. Discussion

Manganese partitioning was similar across the sludge and was mainly extracted in the BCR exchangeable fraction with more than 78% of the total manganese. Alvarez et al. (2002) and Solis et al. (2002) found also that manganese was largely extracted in the BCR exchangeable fraction but their percentages were lower than in this study with respectively 55% and 40%. Metals extracted in the exchangeable fraction were supposed to be bound with the biomass, carbonate and potentially phosphate. In the literature review (sections 2.4 and 2.5), thermodynamic data show that manganese does not exhibit any particular affinity with organic and sulphide (in comparison with other metals). Callander and Barford (1983b)

calculated that the formation of manganese sulphide precipitate only occurs under a high sulphide concentration and in any other cases, manganese precipitates with carbonate. However, they did not consider the potential of the formation of manganese phosphate as it has been set up in the modelling software database. Thermodynamic calculation using equilibrium models showsedthe potential of manganese to be present in anaerobically digested sludge as manganese phosphate or manganese carbonate and the BCR sequential extraction results were not sufficient to differentiate them.

In section 5.6, pH titration has been proved to be an interesting and powerful technique to determine the binding of metals extracted in the BCR exchangeable fraction and potentially in the BCR reducible fraction. In the sludge F and K, most of the manganese was released between pH 4 and 7 and the remaining between pH 2 and 4. This result agreed with the BCR sequential extraction results that shown that most of the manganese is released in the first fraction using solution of 0.11M of acetic acid at pH around 3 (Dodd et al., 2000).

Visual Minteq was used to simulate the pC-pH diagram with manganese present as MnHPO4 or $MnCO_3$. The best fitting curve with the sludge curve occurred when manganese was precipitated as $MnCO_3$. The pH zone of the manganese released also agreed with the thermodynamic of the formation/dissolution of manganese carbonate. For an average alkalinity of 3000 mg/l measured in anaerobic digester (Metcalf and Eddy, 2003), the drop of pH from 7 to 6 reduced the reaction quotient in comparison with the equilibrium constant of $MnCO_3$ by the reduction of the

carbonate (CO_3^{2-}) concentration in the sludge (first carbonate pKa at 6.4). Combination of the BCR sequential extraction and pH titration showed that most of the manganese was bound with carbonate in anaerobically digested sludge and agreed with Callander and Barford (1983b) that calculated the formation of $MnCO_3$ in the anaerobic digesters without high sulphide concentration. Moreover, carbonate was a stronger ligand than EDTA to react with the supplemented manganese (TMC solution) and most of the added manganese precipitated as $MnCO_3$ (extraction in the exchangeable fraction).

7.4. Solid phase speciation of zinc in anaerobically digested sludge in the case of MeEDTA supplementation

From the literature, zinc is mainly present in anaerobic digesters as zinc sulphide precipitates (Callander and Barford, 1983b; Hayes and Theis, 1978 and Jong and Parry, 2004). Kaksonen et al. (2003) observed the presence of ZnS in anaerobically digested sludge. However, other studies showed that zinc also reacts with organic matter, mainly with the biomass by adsorption (Lo et al., 2009 and Gould and Genetelli, 1984). So zinc speciation seems to be divided between sulphide precipitation and sludge adsorption.

The aim of this section was to investigate the behaviour of zinc in anaerobically digested sludge by characterizing the effect of sulphide precipitation and biomass adsorption on the zinc speciation. To achieve this aim, a characterization of the

zinc speciation was done first using the suite of analytical techniques developed in chapter 5 and applied on the previous section (7.3) for manganese. However, the absence of effect from the TMC supplementation on the zinc concentration in the solid phase limited the investigation on the zinc behaviour in anaerobically digested sludge.

7.4.1. Results

The BCR sequential extraction procedure was applied on each samples (sludge F and K; control and TMC) used in the previous section (7.2) and the experimental methodology was developed in section 4.2. Results for the sludge F are shown in table 7.7 and figure 7.5 and in table 7.8 and figure 7.6 for the sludge K.

Table 7.7. Concentrations of zinc in each BCR SE fraction in the sludge F (control and TMC samples)

Concentrations of zinc in each BCR sequential extraction fraction										
Sludge F		Σ fractions	Exchangeable		Reducible		Oxidisable		Residual	
Samples	Hrs	mg/kg DS	%	mg/kg DS	%	mg/kg DS	%	mg/kg DS	%	mg/kg DS
Control	1	1025 ± 99	45	459 ± 29	23	232 ± 42	22	227 ± 67	10	108 ± 12
	48	997 ± 3	52	519 ± 14	22	222 ± 1	13	126 ± 5	13	130 ± 16
	144	1017 ± 58	52	514 ± 25	18	187 ± 15	10	105 ± 13	21	211 ± 25
	336	952 ± 28	57	542 ± 49	20	193 ± 7	14	132 ± 13	9	86 ± 15
	1128	1361 ± 82	38	521 ± 45	30	406 ± 56	15	209 ± 9	17	225 ± 18
TMC	1	996 ± 16	51	510 ± 14	22	221 ± 7	15	146 ± 14	12	120 ± 23
	48	883 ± 1	55	487 ± 11	22	189 ± 18	11	99 ± 1	12	109 ± 7
	144	1058 ± 63	50	528 ± 16	20	210 ± 9	10	107 ± 5	20	214 ± 38
	336	984 ± 22	58	576 ± 9	23	227 ± 18	13	124 ± 26	6	57 ± 33
	1128	1337 ± 67	44	584 ± 37	27	359 ± 25	13	183 ± 17	16	212 ± 22

The concentrations are expressed as mean ± standard deviation (n=9) and percent of total

Table 7.8. Concentrations of zinc in each BCR SE fraction in the sludge K (control and TMC samples)

Concentrations of zinc in each BCR sequential extraction fraction										
Sludge K		Σ fractions	Exchangeable		Reducible		Oxidisable		Residual	
Samples	Hrs	mg/kg DS	%	mg/kg DS	%	mg/kg DS	%	mg/kg DS	%	mg/kg DS
Control	1	1049 ± 37	39	408 ± 35	23	247 ± 7	22	231 ± 20	16	163 ± 10
	48	955 ± 17	47	447 ± 49	21	203 ± 35	19	185 ± 9	13	121 ± 2
	248	941 ± 13	41	385 ± 9	19	181 ± 1	20	187 ± 11	20	188 ± 6
TMC	1	770 ± 31	41	312 ± 18	27	207 ± 13	18	140 ± 14	14	111 ± 9
	48	1035 ± 29	44	455 ± 18	21	215 ± 23	23	242 ± 9	12	123 ± 4
	248	884 ± 24	45	401 ± 8	19	165 ± 8	19	168 ± 2	17	150 ± 21

The concentrations are expressed as mean ± standard deviation (n=9) and percent of total

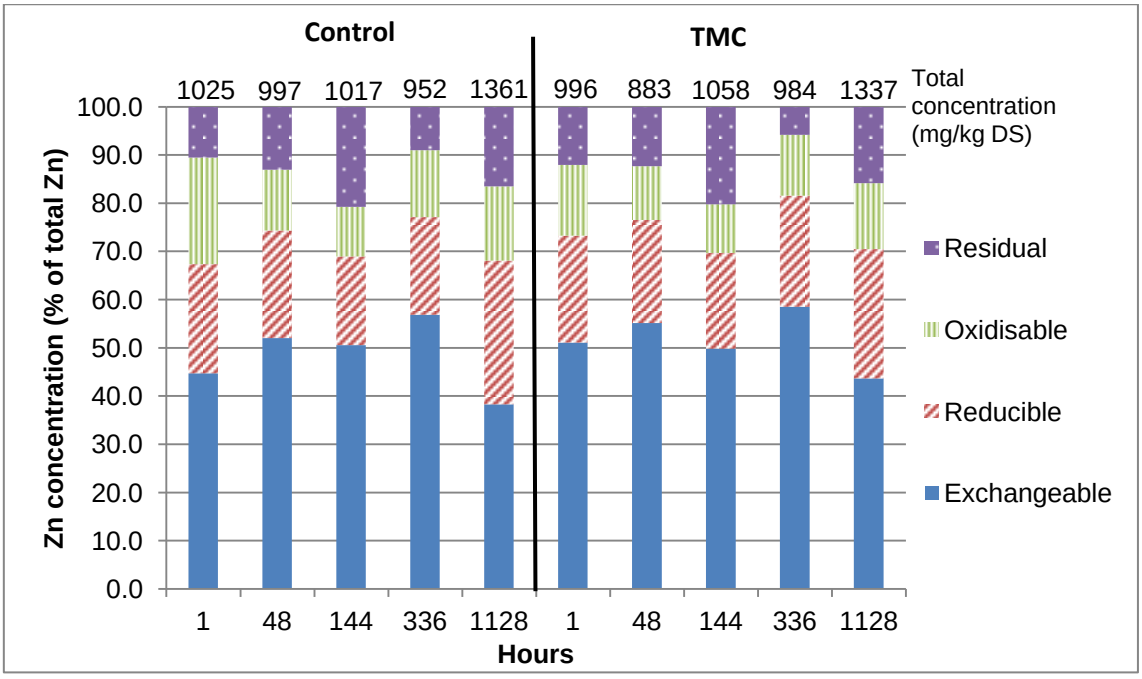

Figure 7.5. Zinc fractionation profiles in control and TMC samples for the sludge F

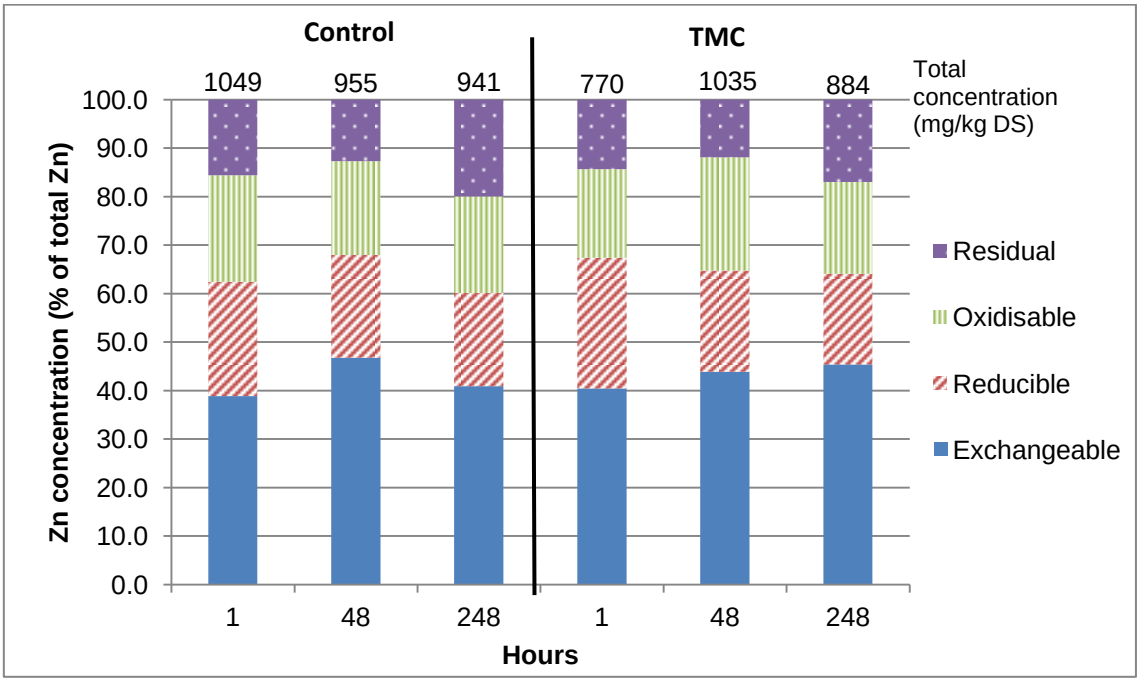

Figure 7.6. Zinc fractionation profiles in control and TMC samples for the sludge K

Zinc BCR sequential extraction profile was similar across the sludge F and K and also between the control and TMC samples. Zinc was largely extracted in the first fraction of the BCR sequential extraction, exchangeable fraction, with a percentage included between 38% and 57% of the total zinc. Adsorbed metals are weakly bound and so they should consequently be extracted in this fraction. However, carbonate and phosphate are also extracted in this fraction.

The second fraction, reducible, contained between 18 and 30% of the total zinc and represented the second highest fraction in zinc contents. Presence of zinc in the reducible fraction suggested that zinc was present in the sludge as hydroxide. However, hydroxide compounds are unlikely to stay precipitate under anaerobic condition and so zinc extracted in the reducible might be the results of a late extraction from the first fraction (exchangeable). The remaining zinc was equally

extracted in the two last fractions of the BCR SE, oxidisable and residual, with respectively a percentage of 10-22% and 6-21% of the total zinc. Zinc present in these fractions was likely to be precipitated with sulphide.

Results from the titration of the sludge F and K are shown in table 7.9 and figure 7.7. The two sludges exhibited a similar pattern in the variation of $[Zn]_l$ in function of the pH. The highest concentration of zinc was obtained at pH 2 and a decrease of the concentration was observed between pH 2 and 6 for both sludge. The variation of an order of 2-3 units represented a decrease of 100-1000 times the concentration between acid and neutral pH. From pH 6, the zinc concentration increased with the pH but the variation was restricted to a maximum of 1 unit. Zinc concentration in the solid phase has been measured in a range of 0.9 and 1.3 g/kg DS and the conversion in mg/l gave a zinc concentration between 18 and 26 mg/l. The maximum of zinc concentration measured in the liquid phase during the titration was lower than this range and so part of the zinc remained strongly bound in the sludge at pH 2. This un-extracted zinc can be related with the zinc extracted in the BCR oxidisable and residual fractions.

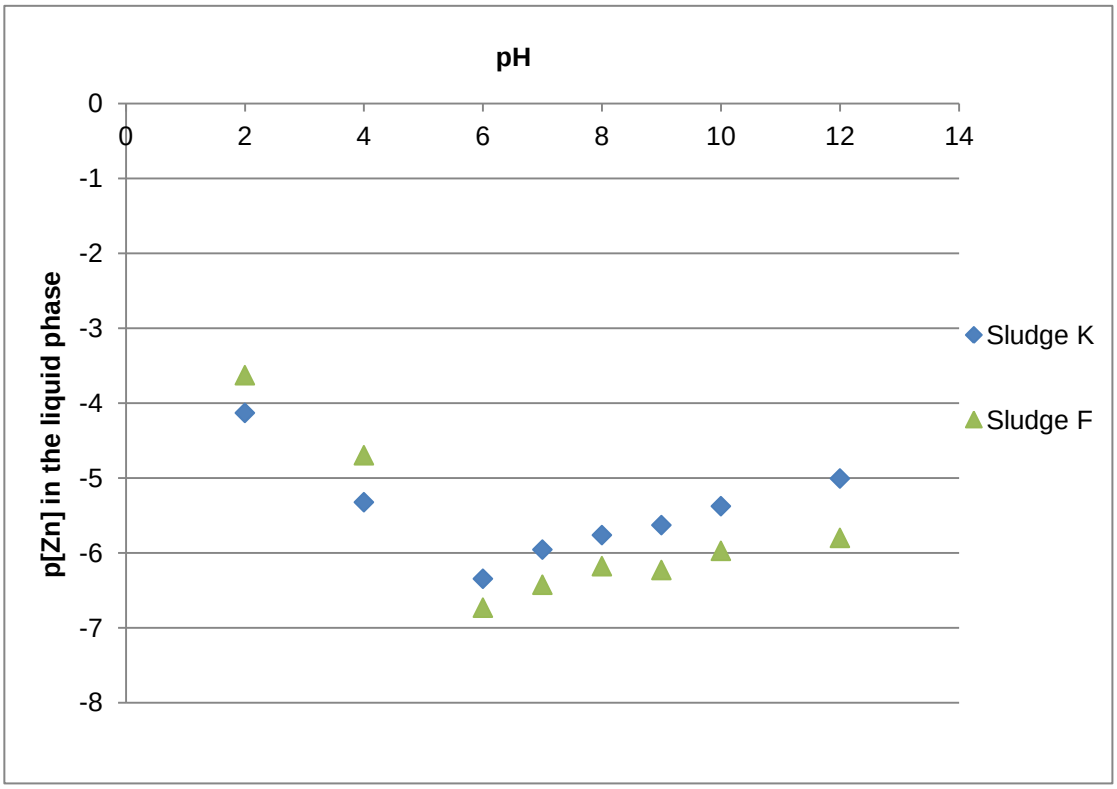

Figure 7.7. p[Zn]-pH diagram for the sludge F and K

Table 7.9. Concentrations of zinc in the liquid phase measured during the pH titration analysis

Metal	pH	Sludge F		Sludge K	
		$[Zn]_l$ (mg/l)	p[Zn]	$[Zn]_l$ (mg/l)	p[Zn]
Zn	2	15.3 ± 0.1	-3.63	4.79 ± 0.03	-4.130
	4	1.30 ± 0.01	-4.70	0.307 ± 0.09	-5.330
	6	0.012 ± 0.001	-6.73	0.029 ± 0.001	-6.350
	7	0.024 ± 0.001	-6.43	0.072 ± 0.001	-5.930
	8	0.043 ± 0.001	-6.18	0.112 ± 0.001	-5.760
	9	0.038 ± 0.001	-6.23	0.152 ± 0.001	-5.630
	10	0.069 ± 0.001	-5.97	0.272 ± 0.001	-5.380
	12	0.103 ± 0.001	-5.80	0.638 ± 0.001	-5.010

The concentrations are expressed as mean ± standard deviation (n=3) and log $[Zn]_l$

As for manganese in section 7.4, Visual Minteq was used to simulate a pC-pH diagram on the sludge F using experimental data (see appendix E and section 4.5). The different pC-pH curves simulated by the model were compared to the experimental to obtain information on the different compounds extracted during the experimental pH titration. Visual Minteq simulation predicted that zinc was completly precipitated as zinc sulphide (sphalerite). However, results from BCR sequential extraction and pH titration show that zinc was also bound with other inorganic and/or organic compounds.

The p[Zn]-pH diagram simulation using Visual Minteq showed that the only presence of sphalerite could not explain the curves observed in the sludge F and K (figures 7.7 and 7.8) as sulphide dissolution requires strong acid and/or odxising reagent. In the equilibrium models, zinc sulphide precipitation could be simulated using two crystal compounds (sphalerite, pK : -10.8 and Wurtzite, pKs : - 8.6). The difference in the solubility constant between wurtzite and sphalerite had an impact on the zinc solubility at different pHs and this was clearly observed in figure 7.8. The curve representing the p[Zn]-pH simulation with wurtzite had the same profile as sphalerite curve but with a p[Zn] higher of 1-2 unit. Those two simulated curves also presented a similar profile as the sludge F curve with a difference in the concentration.

Several other compounds have been used in the simulated sludge but no curve fitted with the curve measured for the sludge F (results not shown). This confirmed

that zinc speciation was composed by several compounds and unfortunately it was impossible to simulate the the presence of several binding in the equilibrium models. Formation of zinc phosphate and/or carbonate has been discarded as the dissolution starts at a pH 7 and the shape of the curves were not matching.

Finally, in absence of zinc sulphide precipitate, concentration of zinc in the liquid phase was influnced by the chelation with soluble organic matters (SOM). In figure 7.9, a fitting curve was calculated by using a ratio 1:1 of the two simulation results obtained with Visual Minteq (only sphalerite or only SOM binding). This calculated curves followed a similar pattern as the experimental curves obtained with the sludge F and K and confirmed that the zinc speciation was mainly divided in two fractions: organics related biomass (SOM) binding and sulphide precipitation (likely to be amorphous precipitates).

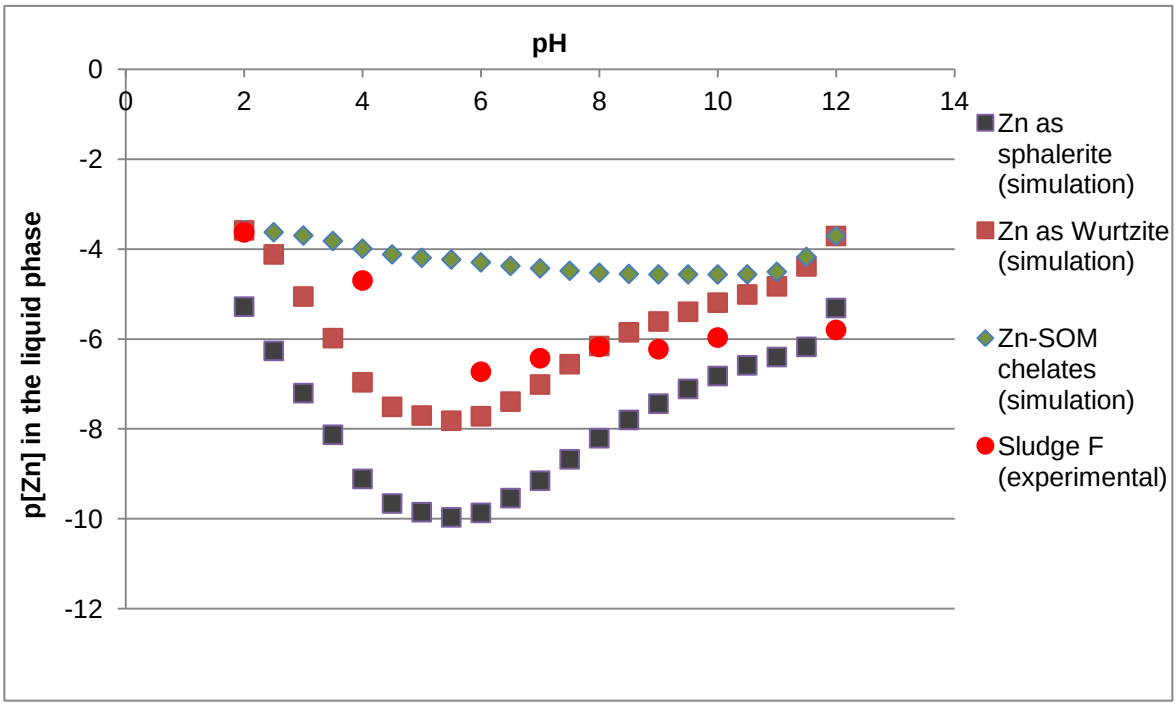

Figure 7.8. p[Zn]-pH diagram of Visual Minteq sludge simulation in comparison with experimental values (sludge F)

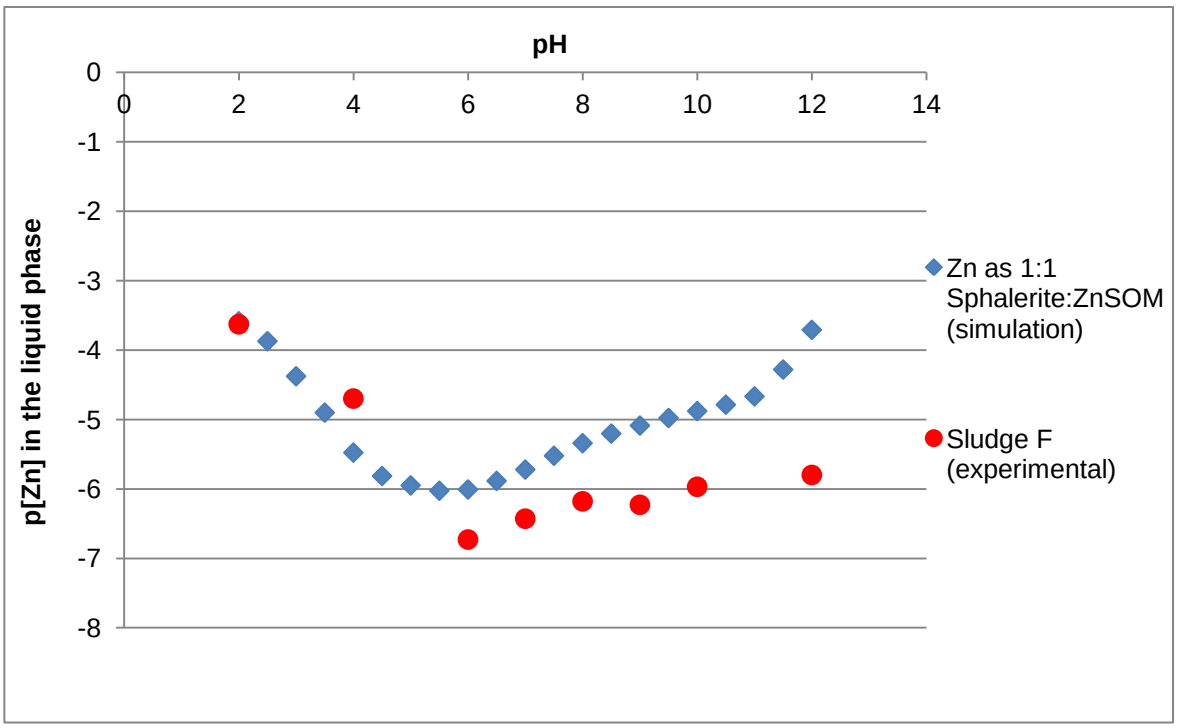

Figure 7.9. p[Zn]-pH diagram of 1:1 sphalerite:Zn-SOM simulation (Visual Minteq) in comparison with experimental values (sludge F)

7.4.2. Discussion

Zinc was extracted in all BCR sequential extraction fractions and no dominant fraction could be clearly identified. Exchangeable and reducible fractions represented more than 60% of the total zinc and the remaining was extracted in the oxidisable and residual fractions. Other studies showed the disparity in the zinc partitioning using the BCR sequential extraction, but they found that the main fraction was oxidisable fraction (Alvarez et al., 2002, Fuentes et al., 2008 and Osuna et al. 2004). Solis et al. (2002) found that zinc was extracted equally in the four BCR sequential extraction fractions with a percentage of 20-30% for each fraction.

From the literature (chapter 2), zinc exhibits high thermodynamic values with the binding of organics, sulphide and phosphate. Gould and Genetelli (1984) found that zinc complexed with solid sludge following the Freundlich isotherm. So the presence of zinc in the BCR exchangeable fraction could be linked as chemisorptions with the biomass and soluble organic matter. Zinc extracted in the oxidisable and residual fractions was likely to be precipitated with sulphide as Jong and Parry (2004) demonstrated that the zinc extracted in the oxidisable fraction was more bound with sulphide than with humic substances. Adamo et al. (1996) and Van der veen et al. (2007) also showed that metal sulphide compounds were not all extracted in the oxidisable but also extracted in the residual fraction.

Moreover, the presence of ZnS in anaerobically digested sludge has been predicted thermodynamically by Callander and Barford (1983b) and has been detected using X-ray spectroscopy by Adamo et al. (1996) and Kaksonen et al. (2003).

The maximum of zinc extracted during the pH titration was lower than the total concentration and so part of the zinc remained strongly bound in the sludge at pH 2. Its extraction required the presence of an oxidising agent or stronger acids. The zinc that was not dissolved during the titration could be assimilated as ZnS, extracted during the two last fractions (oxidisable and residual) of the BCR sequential extraction. Concerning the zinc extracted in the exchangeable and reducible fractions, pC-pH diagram showed that the extraction starts occurring with a pH below 6.

The use of Visual Minteq to simulate the titration curves showed that after sulphide, zinc was preferentially bound with soluble organic matter rather than with carbonate or phosphate. Lo et al. (2009) observed a similar variation on zinc solubility with the pH in municipal solid waste considering only the adsorption process on sludge. The fluorescence spectroscopy analysis on BCR sequential extraction fractions showed that metal bound with SOM and SMP are extracted in the exchangeable fraction and tended to agree that with the presence of zinc in the BCR exchangeable fraction. The presence of organically bound zinc was also described by Carlson and Morrison (1992) and Patidar and Tare (2008) demonstrated that the maximum Metal-SMP complexation was obtained with zinc.

Simulated pC-pH curves obtained using different zinc sulphide compounds (sphalerite and wurtzite) presented a similar pattern that the curves measured in the sludge F and K but the equilibrium model overestimated the precipitation of zinc as zinc sulphide in the sludge. In presence of wurtzite as ZnS precipitate (with a lower solubility product), the proportion of zinc bound with SOM was increased and the curves was getting closer with the experimental curve (sludge F). However, the sorption binding was still higher than predicted and it was likely due to the formation of amorphous zinc sulphide compounds with a lower solubility product than crystals such as wurtzite and sphalerite. A fitting curve was obtained by the calculation of an average curve between the precipitation of zinc as sphalerite and its adsorption by SOM.

The pH titration analysis using Visual Minteq also showed that the dissolution of sphalerite and wurtzite with the pH could have a significant impact on the zinc concentration in the liquid phase at pH below 3. The dissolution of ZnS in acidified reagent was also observed by Dodd et al. (2000) and could be related at the extraction of zinc in the reducible fraction. With a pH stabilized at 2 with nitric acid, the second extracting solution could be responsible for an early released of some zinc sulphide in the reducible fraction. However, equilibrium models also showed that most of zinc sulphide stay precipitated at pH 2 and their dissolution required stronger reacting agent.

From the combination of the analytical results, the percentage of zinc present as sulphide precipitates (extracted in the oxidisable and residual fractions) and

adsorbed onto the sludge (exchangeable fraction) were similar (around 40% each). However, several questions could not be answered concerning the form of zinc extracted in the reducible fraction and the reaction controlling the zinc speciation between sulphide precipitation and adsorption process.

7.5. Solid phase speciation of cobalt in anaerobically digested sludge in the case of MeEDTA supplementation

As for most of the metals, cobalt speciation has been found to be controlled by sulphide precipitation in the literature (Van der veen et al., 2007; Gustavsson, 2012). Fermoso et al. (2008a) also expressed that cobalt precipitate as CoS when supplemented in UASB reactor. However, cobalt exhibited similar thermodynamic constant as zinc (inorganic and organic reactions) and so cobalt could also interact with organics, particularly EPS (Van Hullebusch et al., 2006).

The aim of this section was to investigate the behaviour of cobalt in anaerobically digested sludge by characterizing the effect of sulphide and adsorption on the cobalt speciation. To achieve this aim, a characterization of the cobalt speciation was done first using the suite of analytical techniques developed in chapter 5 and applied on the previous sections (7.3 and 7.4) for manganese and zinc. However, the BCR sequential extraction procedure could not be applied on the control samples of both sludges due to the low concentration of cobalt in the solid phase. So two sets of sample, CoA2 and TMC, were used to observe the cobalt

speciation and behaviour using different concentrations of cobalt in the solid phase.

7.5.1. Results

The BCR sequential extraction procedure has been applied on each sample (sludge F and K; CoA2 and TMC) used in the previous section (7.2) and the experimental methodology is developed in section 4.3.3. Results for the sludge K are shown in table 7.10 and figure 7.10 and table 7.11 and figure 7.11 for the sludge F.

Table 7.10.Concentrations of cobalt in each BCR SE fraction in the sludge K (TMC and CoAx2 samples)

Concentrations of cobalt in each BCR sequential extraction fraction										
Sludge K		Σ fractions	Exchangeable		Reducible		Oxidisable		Residual	
Samples	Hrs	mg/kg DS	%	mg/kg DS	%	mg/kg DS	%	mg/kg DS	%	mg/kg DS
Control	1	28 ± 2	90	25 ± 1	10	3 ± 1	0	< d.l.	0	< d.l.
	48	51 ± 3	87	44 ± 4	11	5 ± 1	2	1 ± 1	1	< 1
	248	143 ± 4	79	113 ± 4	6	9 ± 1	15	21 ± 2	0	< d.l.
TMC	1	45 ± 1	92	41 ± 1	8	4 ± 1	0	< d.l.	0	< d.l.
	48	114 ± 7	83	94 ± 7	9	11 ± 1	7	8 ± 1	1	1 ± 1
	248	322 ± 5	75	243 ± 3	6	21 ± 2	18	57 ± 1	0	1 ± 1

The concentrations are expressed as mean ± standard deviation (n=9) and percent of total

Table 7.11. Concentrations of cobalt in each BCR sequential extraction fraction in the sludge F (TMC and CoAx2 samples)

Concentrations of cobalt in each BCR sequential extraction fraction										
Sludge F		Σ fractions	Exchangeable		Reducible		Oxidisable		Residual	
Samples	Hrs	mg/kg DS	%	mg/kg DS	%	mg/kg DS	%	mg/kg DS	%	mg/kg DS
Control	1	44 ± 1	94	41 ± 1	6	3 ± 1	0	< d.l.	0	< d.l.
	48	106 ± 16	92	97 ± 12	6	6 ± 3	3	3 ± 2	0	< d.l.
	144	208 ± 12	78	162 ± 6	9	18 ± 3	12	25 ± 2	1	2 ± 2
	336	271 ± 18	70	191 ± 10	10	27 ± 3	17	47 ± 4	2	7 ± 4
	1128	307 ± 17	78	240 ± 11	7	21 ± 3	14	44 ± 4	1	2 ± 1
TMC	1	118 ± 4	94	111 ± 3	6	8 ± 2	0	< d.l.	0	< d.l.
	48	279 ± 12	75	211 ± 8	11	31 ± 7	13	36 ± 9	1	2 ± 2
	144	478 ± 8	68	326 ± 20	10	46 ± 4	19	93 ± 10	3	13 ± 8
	336	571 ± 31	73	414 ± 23	9	54 ± 2	17	95 ± 8	1	8 ± 2
	1128	622 ± 23	75	469 ± 36	8	50 ± 3	16	98 ± 9	1	5 ± 2

The concentrations are expressed as mean ± standard deviation (n=9) and percent of total

The concentration of cobalt in the solid phase increased with time and it was related with the slow transfer of cobalt into the solid phase during the metals supplementation experiments (section 7.2). The difference of $[Co]_s$ between TMC and CoAx2 samples was around 2 for the sludge K and varies between 2 and 2.7 for the sludge F. The two sludges displayed similar extraction profiles from the BCR sequential extraction for TMC and CoAx2 samples; inducing that the cobalt speciation in the solid phase was not dependent on the cobalt concentration.

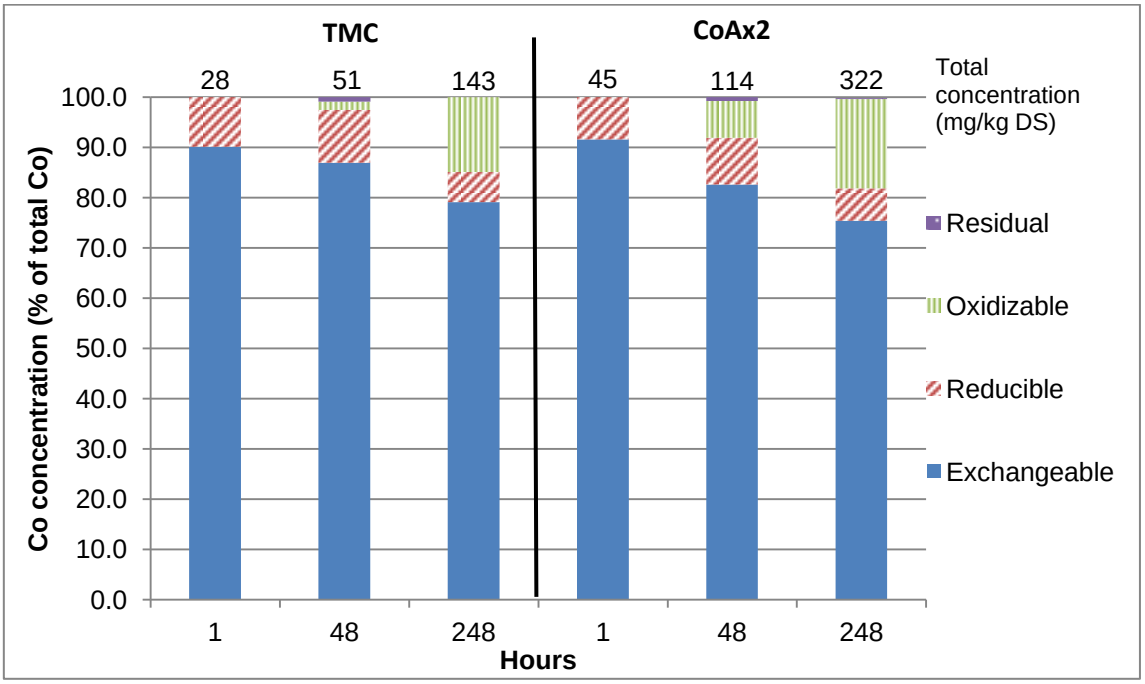

Figure 7.10. Cobalt fractionation profiles in control and TMC samples for the sludge K

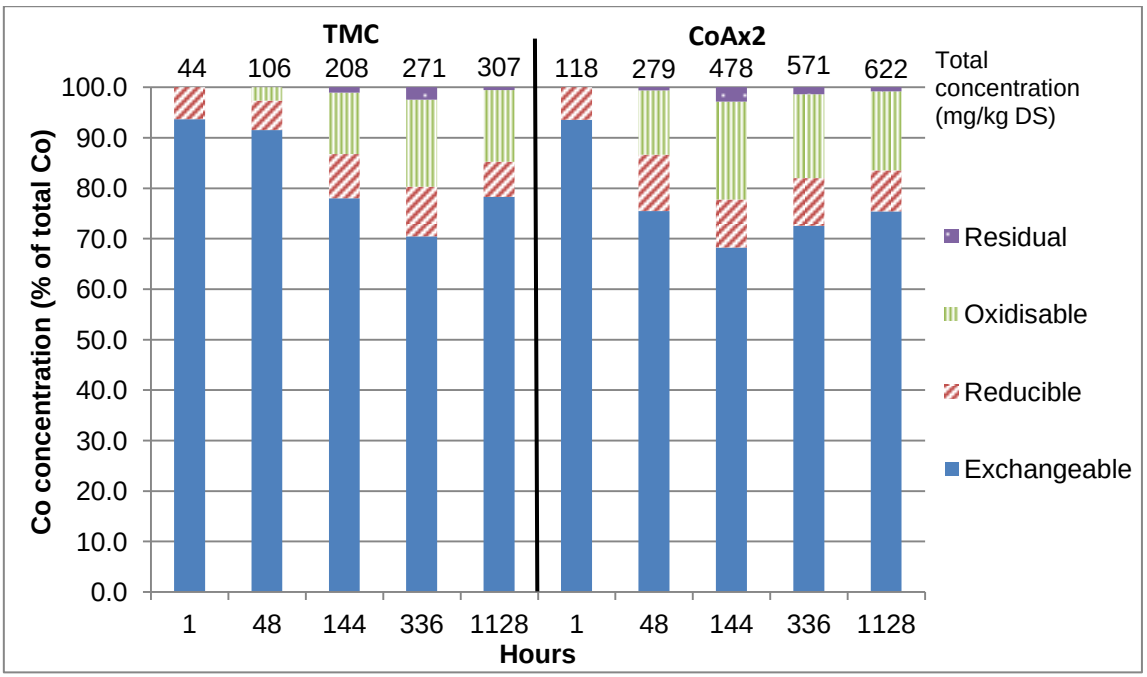

Figure 7.11. Cobalt fractionation profiles in control and TMC samples for the sludge F

After 1 hour, most of the cobalt (over 90%) present in the solid phase was extracted in the exchangeable fraction and the remaining was extracted in the reducible fraction. The percentage of cobalt extracted in the exchangeable fraction decreased with time and after 248 (and 336) hours, the percentage of cobalt in this fraction was included between 70 and 79%. During the same period, the percentage of cobalt in the reducible fraction varied between 6 and 11% of the total cobalt. After 48 hours, cobalt started to be extracted in the oxidisable fraction and the percentage was comprised between 2 and 13%. Then it increased to 15-18% after 248-336 hours. After 1128 hours (close from equilibrium), no evolution of the partitioning profile was observed in comparison with the hour 248-336, with a cobalt percentage of 75-78% in the exchangeable fraction, 7-8% in the reducible fraction, 14-16% in the oxidisable fraction and 1% in the residual fraction.

An increase of the cobalt concentration in the solid had repercussions on the profile of cobalt in the three first BCR sequential fractions. However, the variation of cobalt percentage in the BCR sequential extraction fractions did not reflect the increase of cobalt concentration in each fraction. In the period 1-336 hours, the concentration of cobalt in the exchangeable fraction increased from 41 mg/kg DS to 191 mg/kg DS (TMC) and 111 mg/kg DS to 414 mg/kg DS (CoAx2) for the sludge F and from 25 mg/kg DS to 113 mg/kg DS (TMC) and 41 mg/kg DS to 243 mg/kg DS (CoAx2) for the sludge K.

During the same period, the concentration of cobalt extracted in the reducible fraction also increase from 3 mg/kg DS to 27 mg/kg DS (TMC) and from 8 mg/kg

DS to 54 mg/kg DS (CoAx2) for the sludge F and from 3 mg/kg DS to 9 mg/kg DS (TMC) and from 4 mg/kg DS to 21 mg/kg DS (CoAx2) for the sludge K. The cobalt concentration in the oxidisable fraction reached the values of 47 mg/kg DS (TMC) and 95 mg/kg DS (CoAx2) for the sludge F and 21 mg/kg DS (TMC) and 57 mg/kg DS (CoAx2) for the sludge K. These results showed that the main transfer of cobalt from the liquid phase was related with a weak binding compound that can be extracted in the exchangeable fraction. The formation of strongly bound compound (likely to be CoS) occurred only after 48 hours, potentially due to a slow kinetic of reaction.

Results from the titration of the sludge F and K for cobalt are shown in table 7.12 and figure 7.12. The two types of sludge exhibited a similar pattern in the variation of cobalt concentrations in the liquid phase in function of the pH. The highest concentration of cobalt was obtained at pH 2 and the main decrease was observed between pH 2 and 6, but the concentration kept decreasing until pH 9 for the sludge F. The variation of p[Co] between the minimum and maximum was an order of 2 units and represented a decrease of 100 times between the acid and neutral pH. Under basic pH, cobalt concentration increased slowly with the pH and the p[Co] value was limited around -6.2.

Table 7.12. Concentrations of manganese in the liquid phase measured during the pH titration analysis

Metal	pH	Sludge F		Sludge K	
		$[Co]_l$ (mg/l)	p[Co]	$[Co]_l$ (mg/l)	p[Co]
Co	2	0.483 ± 0.003	-5.09	0.044 ± 0.001	-6.13
	4	0.187 ± 0.003	-5.50	0.016 ± 0.001	-6.56
	6	0.034 ± 0.001	-6.24	0.006 ± 0.001	-7.02
	7	0.027 ± 0.001	-6.35	0.006 ± 0.001	-7.02
	8	0.021 ± 0.001	-6.46	0.008 ± 0.001	-6.88
	9	0.020 ± 0.001	-6.48	0.011 ± 0.001	-6.75
	10	0.028 ± 0.001	-6.32	0.025 ± 0.001	-6.37
	12	0.044 ± 0.002	-6.12	0.033 ± 0.001	-6.25

The concentrations are expressed as mean ± standard deviation (n=3) and log $[Co]_l$

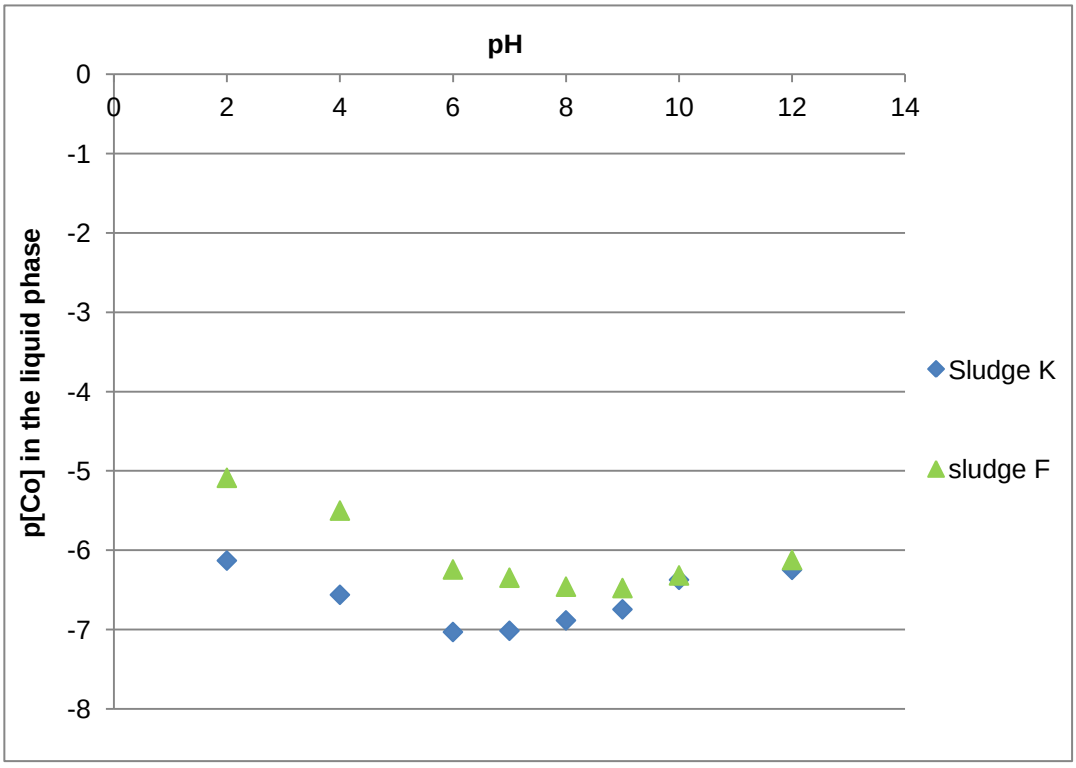

Figure 7.12. p[Co]-pH diagram for the sludge F and K

As for manganese and zinc in sections 7.4 and 7.5, Visual Minteq was used to simulate a pC-pH diagram on the sludge F using experimental data (see appendix E and section 4.5). The different pC-pH curves simulated by the model were compared to the experimental curve to obtain information on the different compounds extracted during the experimental pH titration

Visual Minteq predicted that cobalt should be precipiated as cobalt sulphide in anaerobically digested sludge. However, results from the BCR sequential extarction and pH titration showed evidence of other bindings that cobalt sulphide precipitates. The model was used to simulate the titration on the sludge F with allowing or not CoS to precipitate. The cobalt complexation with soluble organic matter was the most stable binding in the case of no CoS precipitation Results from the simulations (figure 7.13) showed that the simulated pH titration curve with cobalt bound with soluble organic matter fitted with the experimental curve (sludge F). The presence of CoS in the sludge was likely to keep more cobalt in the solid phase for pH included between 4 and 11.

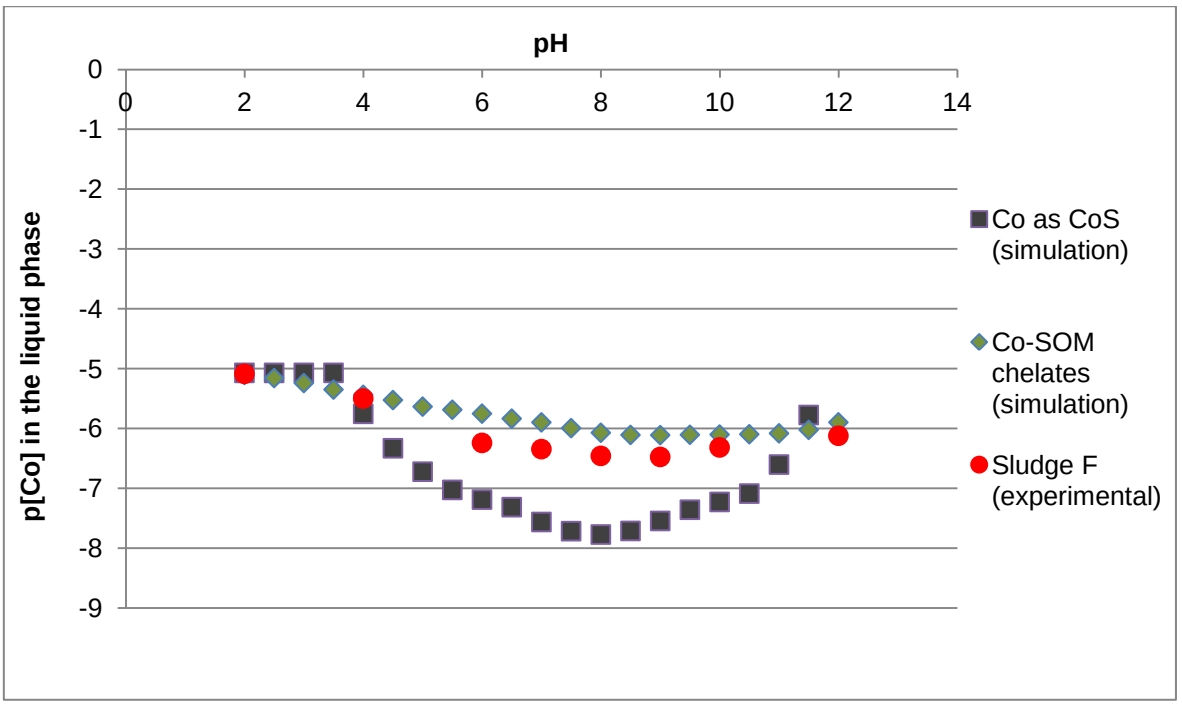

Figure 7.13. p[Co]-pH diagram of Visual Minteq sludge simulation in comparison with experimental values (sludge F)

7.5.2. Discussion

The BCR sequential extraction showed that the cobalt supplemented in anaerobically digested sludge was mainly extracted in the exchangeable fraction. The presence of cobalt in the oxidisable fraction was only significant after 48 hours. The percentage of cobalt in this fraction increased with time while it was decreasing in the exchangeable fraction. However, these variations in the percentage were not related to change on the cobalt speciation but it was the result from a higher increase in the oxidisable fraction than in the exchangeable fraction.

After 248 hours a pseudo-equilibrium seemed to be obtained in the solid phase and around 75% of the cobalt was extracted in the exchangeable fraction while only 15% was extracted in the oxidisable fraction. Andres et al. (2008) observed that cobalt was mostly extracted in the oxidisable and residual fractions of digested sludge (around 90%) and only 10% in the first fractions. The difference between this two sequential extraction results might be explain by the fact that in this experiments the cobalt was added to the digested sludge and was not already present in the entering sludge. Several studies observed that cobalt was bound with sulphide under anaerobic condition (Patidar and Tare, 2008; Van der veen et al., 2007; Smith, 2006) but can also interact with EPS and other iron mineral compounds (Van hullebsuch et al., 2008; Gustavsson, 2012 and Fermoso et al., 2008a).

Equilibrium models predicted that cobalt was mainly precipitated as CoS in the anaerobically digested sludge. However, the comparison between titration curves from the sludge F and simulation curves using Visual Minteq confirmed that the binding between cobalt and soluble organic matter was the most dominant in the exchangeable fraction and anaerobically digested sludge. The presence of cobalt sulphide in the sludge was more limited than predicted by the equilibrium model. In the case of cobalt supplementation into anaerobically digested sludge, cobalt seemed to react primarily with the biomass. The formation of cobalt sulphide did not occur before a few days and seemed limited in comparison with cobalt sorption. The speciation of cobalt was independent of the cobalt concentration and it was not limited by SOM binding site or sulphide as there was no change in the

percentage of cobalt in the BCR sequential extraction fraction when the cobalt was added as TMC concentration or its double.

7.6. Mechanisms controlling the solid-liquid equilibrium of cobalt when supplemented as CoEDTA in anaerobically digested sludge

Several studies showed that metals availability for microorganism was closely related to their presence in the liquid phase under their free forms (Jansen et al. (2007) and Osuna et al. (2004). Fermoso et al. (2009) and Oleszkiewicz and Sharma (1990) also demonstrated that some metals bound with organics produced by the biomass could also be uptake and used by microorganisms. However, there is the potential of having metals present in the solid phase that could be transfer into available forms in case of metals deficiency in the anaerobic digester. This potential “pool” of secondary-available metals needs to be measured and analysed in order to obtain a complete evaluation of the metal bioavailability (Gustavsson, 2012). To understand those mechanisms, it is essential to have good knowledge on the metals solid phase speciation and the different solid-liquid phase interactions.

During the study of the liquid-solid equilibrium of metals, results shown above (section 7.2) confirmed the partial or total solidification of supplemented metals and also showed that metals reacted differently with the sludge. Copper and zinc were mostly transferred into the solid phase after 48 hours, while most the

manganese was quickly precipitated as $MnCO_3$. The nickel and iron added into the sludge did not seem reacting with the solid phase and stayed in the liquid phase. Cobalt represented the most interesting metal in the study of the interaction between solid and liquid phases as its transfer to the solid phase occurred through a slow kinetic reaction during the 336 hours of the experiments. Moreover, the speed of reactions differed between the sludge F and K, inducing that the kinetic was dependent on the sludge composition. The difference in the iron concentration (due to iron dosing for the sludge F) might have been responsible for these variations of kinetics.

The aim of this section was to characterize the mechanisms related to the transfer of cobalt from the liquid phase to the solid phase when supplemented as CoEDTA. First, the kinetic order of the reactions controlling the transfer was experimentally measured to obtain information on the limiting factors. Then the behaviour of other metals, especially iron, was also studied in order to determine their potential role in the transfer of cobalt.

7.6.1. Results

This experiment followed the same method used in section 7.2 and used serum bottle as anaerobic digester. The complete method is described in section 4.1.2. The concentrations of metals are given as mol/l to calculate the different kinetics of the reactions. The two types of sludge were experimented twice and F1-K1 values

were corresponding to the results obtained during the analysis of the section 7.2 (called F and K, sludge condition described in table 4.3).

In the sludge F, cobalt has been dosed using three different solutions, TMC, CoA and CoAx2. The cobalt concentrations in the liquid phase have been measured in time to study the fate of the supplemented cobalt (table 7.13 and figure 7.14). After 1 hour, $[Co]_l$ was reduced from 38 to 33.1 µmol/l in the TMC sample, from 38 to 26.6 µmol/l in the CoA sample and from 75.9 to 55 µmol/l in the CoAx2 sample. $[Co]_l$ kept decreasing with time to a concentration of 3.6, 1.5 and 3.4 µmol/l for respectively TMC, CoA and CoAx2 samples after 336 hours.

Starting at the same initial concentration (38.0 µmol/l) the transfer into the solid phase was quicker for the CoA sample in comparison with TMC sample. The slower kinetics of cobalt transfer in TMC samples was also noticed when compared with the kinetic of CoAx2 samples. TMC and CoAx2 samples had similar cobalt concentration in the liquid phase after 144 hours confirming the difference of kinetic between the two samples. The measurement obtained with the sludge F2, with CoA solution, showed a similar curve pattern with an accentuation of the shape. The equilibrium, 0.5-1 µmol/l, was also reached quicker (between 96 and 120 hours) with sludge F2 than with the sludge F1. The concentration $[Co]_l$ obtained after 1 hour, 22.8 µmol/l, was lower than the value obtained with the sludge F1-CoA sample.

Table 7.13. Concentrations of cobalt ($[Co]_l$) in TMC, CoA and CoAx2 samples for sludge F1 and F2

Sludge	Hours	$[Co]_l$ (µmol/l)		
		TMC	CoA	CoAx2
Initial Concentration		38.0	38.0	75.9
Sludge F1	1	33.1 ± 0.3	26.6 ± 0.1	55.5 ± 0.1
	48	22.4 ± 0.1	13.7 ± 0.1	30.4 ± 0.2
	144	11.3 ± 0.1	5.0 ± 0.1	11.9 ± 0.1
	336	3.6 ± 0.1	1.5 ± 0.1	3.4 ± 0.1
Sludge F2	1	-	22.8 ± 0.3	-
	12	-	11.9 ± 0.7	-
	24	-	7.9 ± 0.2	-
	36	-	3.9 ± 0.1	-
	48	-	2.3 ± 0.2	-
	72	-	1.1 ± 0.1	-
	96	-	0.9 ± 0.1	-
	120	-	0.8 ± 0.1	-
	168	-	0.7 ± 0.1	-
	240	-	0.6 ± 0.1	-
	312	-	0.5 ± 0.1	-

The concentrations are expressed as mean ± standard deviation (n=3).

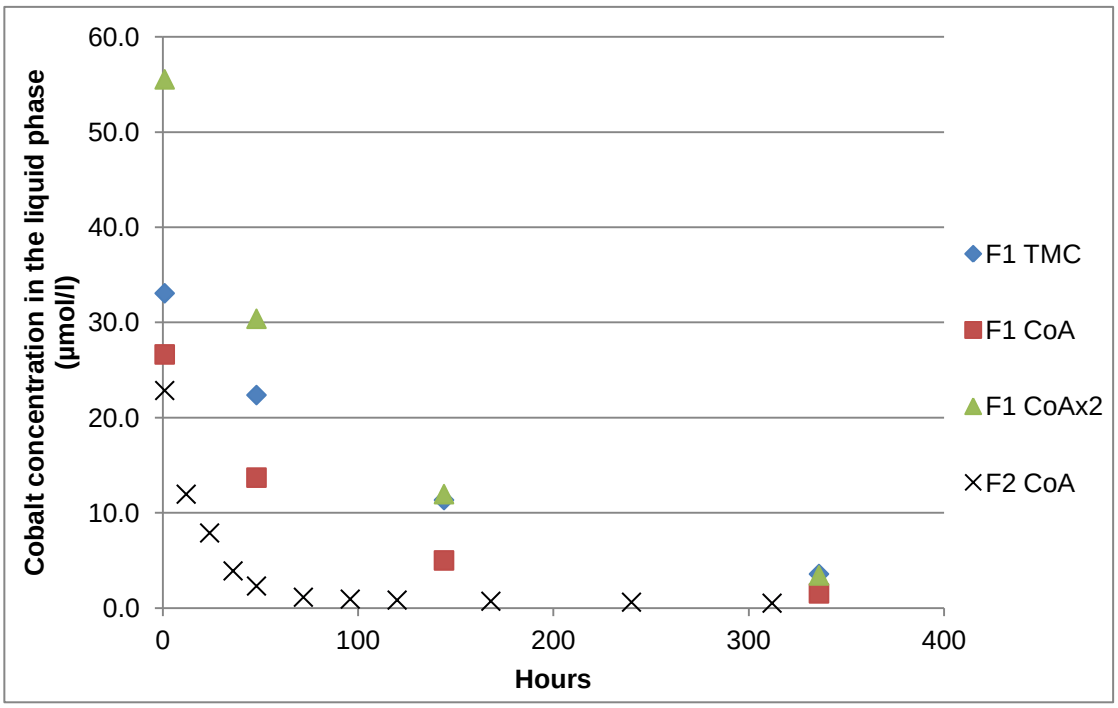

Figure 7.14. $[Co]_l$ in TMC, CoA and CoAx2 samples for sludge F1 and F2

A similar experiment has been repeated with the sludge K and results are shown in table 7.14 and figure 7.15. The transfer of added cobalt from the liquid to solid phase had a slower kinetic than for the sludge F and presented a linear curve pattern. After 1h, $[Co]_l$ in the sludge K1 was respecitvely 33.7 µmol/l for TMC sample and 57.5 µmol/l for CoAx2 sample. Those values were close from the values measured in the sludge F (33.1 µmol/l and 55.5 µmol/l). However, after 48 hours the gap between the two sludge increased as $[Co]_l$ for the sludge K1 was measured at 31.1 µmol/l (TMC sample) and 50.5 µmol/l (CoAx2 sample).

The equilibrium was still not obtained after 288 hours with values of 18.7 µmol/l and 26.6 µmol/l. The kinetic was also slower when dosing with the TMC solution than with CoAx2 solution. Similar observations have been done with the sludge F. The measurement obtained with the sludge K2, with CoA sample, showed a similar linear curve pattern with an increase of kinetic and the equilibrium was still not reached after 312 hours. The concentration obtained after 1 hour was 22.8 µmol/l and 5.3 µmol/l after 312 hours, and those values were lower than for the sludge K1.

Table 7.14. Concentrations of cobalt ($[Co]_l$) in TMC, CoA and CoAx2 samples for sludge K1 and K2

Sludge	Hours	$[Co]_l$ (µmol/l)		
		TMC	CoA	CoAx2
Initial Concentration		38.0	38.0	75.9
Sludge K1	1	33.7 ± 0.1	-	57.5 ± 0.1
	48	31;1 ± 0.1	-	50.5 ± 0.2
	248	18.7 ± 0.1	-	26.6 ± 0.1
Sludge K2	1	-	22.7 ± 0.1	-
	12	-	19.5 ± 0.3	-
	24	-	18.0 ± 0.4	-
	36	-	16;1 ± 0.1	-
	48	-	15.1 ± 0.1	-
	72	-	13.2 ± 0.3	-
	96	-	12.4 ± 0.5	-
	120	-	10.5 ± 0.3	-
	168	-	9.2 ± 0.2	-
	240	-	6.8 ± 0.1	-
	312	-	5.3 ± 0.1	-

The concentrations are expressed as mean ± standard deviation (n=3)

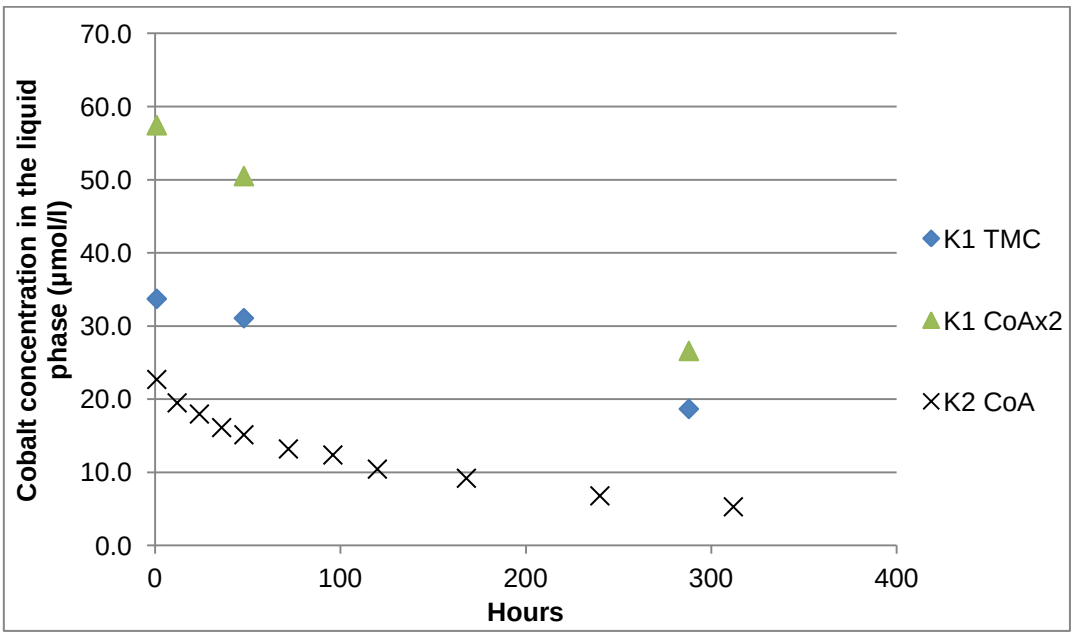

Figure 7.15. $[Co]_l$ in TMC, CoA and CoAx2 samples for sludge K1 and K2

Results from cobalt dosing in the sludge F and K showed that cobalt was transferred into the solid phase following two paths. There was a fast reaction where 10-40% of the cobalt was precipitated or sorbed during the 1 first hour. Then the remaining cobalt was reacting more slowly and the equilibrium might not be reached after 300 hours.

The amount of cobalt reacting as fast or slow reaction did not depend on the sludge condition or cobalt concentration as the largest amount of cobalt reacting fastly occurred for F2-CoA and K2-CoA samples. However, the slow kinetic reaction was likely to be depend on the sludge composition as there was an observable difference in the order of reaction between the sludge F and K. The transfer of cobalt in the solid phase was slower for the sludge K than for the sludge F. The kinetic order of the slow reaction could be determined and measured using the linear relation between $Ln[Co]_l$ and time for a first order reaction and $1/[Co]_l$ and t for a second order reaction (see appendix D).

From the figure 7.14, the relation between $[Co]_l$ and time exhibited an exponential pattern for the sludge F that could write as $[Co]_l = [Co]_0 \times e^{-kt}$ and could be directly related as a 1^{st} order kinetic reaction. The first order kinetic was confirmed by the presence of a linear curve between $Ln[Co]_l$ and t (figure 7.16 and table 7.15) and no relation between $1/[Co]_l$ and t (figure 7.17 and table 7.15). For the sludge F2-CoA, two linear curves could be observed, the first with the higher slope from 1 hour to 72 hours and the second between 72 hours and 312 hours. The change of slope at the hour 72 was related with the solution reaching a solid-phase

equilibrium for cobalt and so a reduction of the reaction's speed due to the cobalt limitation. The highest value of the kinetic constant was measured in F2-CoA sample (0.043 h^{-1}), then F1-CoA and F1-CoA2 samples had the same kinetic constant, 0.008 h^{-1} and finally F1-TMC sample had slightly lower value (0.007 h^{-1}).

Table 7.15. Ln$[Co]_l$ and 1/$[Co]_l$ calculated in TMC, CoA and CoAx2 samples for sludge F1 and F2

Sludge	Hours	TMC		CoA		CoAx2	
		ln $[Co]_l$	1/$[Co]_l$	ln $[Co]_l$	1/$[Co]_l$	ln $[Co]_l$	1/$[Co]_l$
Sludge F1	1	3.5	0.03	3.3	0.04	4.0	0.02
	48	3.1	0.04	2.6	0.07	3.4	0.03
	144	2.4	0.09	1.6	0.20	2.5	0.08
	336	1.3	0.28	0.42	0.65	1.2	0.29
Sludge F2	1	-	-	3.1	0.04	-	-
	12	-	-	2.5	0.08	-	-
	24	-	-	2.1	0.13	-	-
	36	-	-	1.4	0.26	-	-
	48	-	-	0.83	0.44	-	-
	72	-	-	0.11	0.89	-	-
	96	-	-	-0.08	1.1	-	-
	120	-	-	-0.20	1.2	-	-
	168	-	-	-0.36	1.4	-	-
	240	-	-	-0.51	1.7	-	-
	312	-	-	-0.70	2.0	-	-

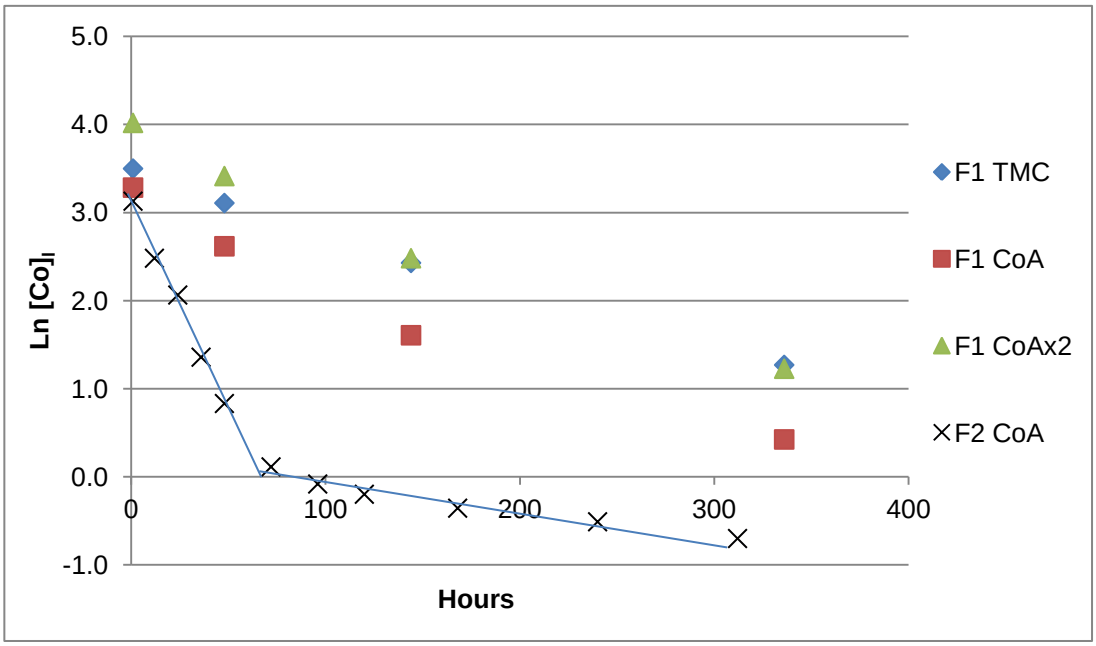

Figure 7.16. Ln$[Co]_l$ in TMC, CoA and CoAx2 samples of sludge F1 and F2

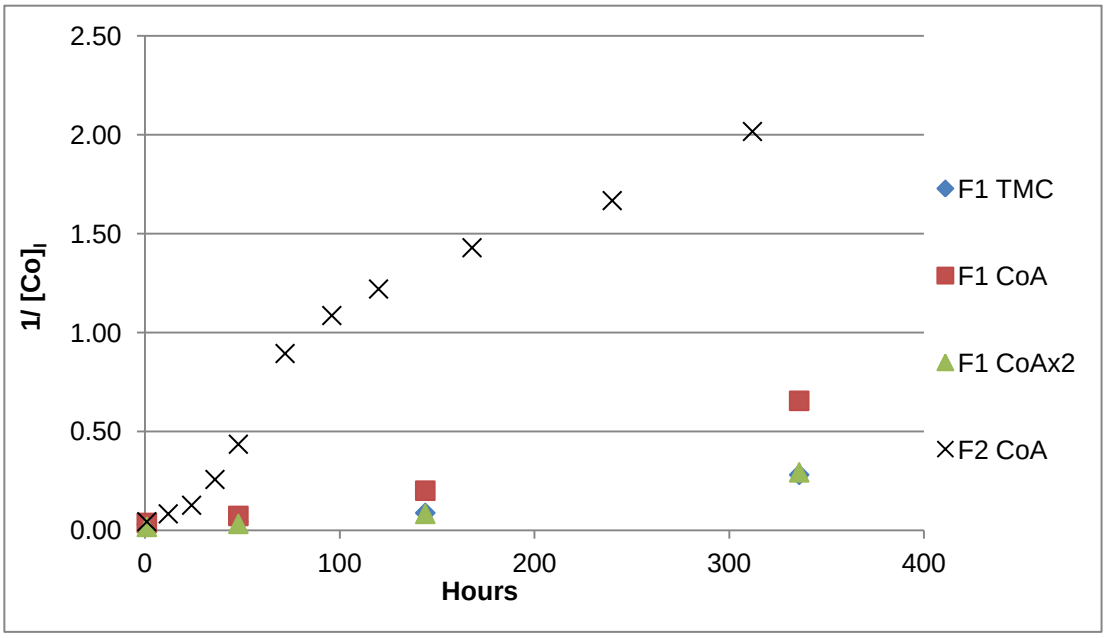

Figure 7.17.1/$[Co]_l$ in TMC, CoA and CoAx2 samples of sludge F1 and F2

In comparison with the sludge F, cobalt in the sludge K was transferred into the solid phase following a linear curve suggesting that the reaction was following a second order kinetic reaction (figure 7.15). A linear curve was observed between

the $1/[Co]_l$ and t for any of sludge K samples (figure 7.19 and table 7.16) and no relation was observed between $Ln[Co]_l$ and t (figure 7.18 and table 7.16). This indicated that cobalt reacted following a 2^{nd} order kinetic reaction. The kinetic constant of the 2^{nd} order was measured using the linear regression for the three curves and the highest values has been obtained for the K2-CoA sample with 0.0004 h^{-1}. In oposition with the kinetic constant of sludge F samples, K1-CoAx2 had the lowest values with 0.00007 h^{-1} and K1-TMC was slighty higher with 0.00009 h^{-1}.

Table 7.16. $Ln[Co]_l$ and $1/[Co]_l$ calculated in TMC, CoA and CoAx2 samples for sludge K1 and K2

Sludge	Hours	TMC		CoA		CoAx2	
		ln $[Co]_l$	$1/[Co]_l$	ln $[Co]_l$	$1/[Co]_l$	ln $[Co]_l$	$1/[Co]_l$
Sludge K1	1	3.5	0.03	-	-	4.1	0.02
	48	3.4	0.03	-	-	3.9	0.02
	288	2.9	0.05	-	-	3.3	0.04
Sludge K2	1	-	-	3.1	0.04	-	-
	12	-	-	3.0	0.05	-	-
	24	-	-	2.9	0.06	-	-
	36	-	-	2.8	0.06	-	-
	48	-	-	2.7	0.07	-	-
	72	-	-	2.6	0.08	-	-
	96	-	-	2.5	0.08	-	-
	120	-	-	2.3	0.10	-	-
	168	-	-	2.2	0.11	-	-
	240	-	-	1.9	0.15	-	-
	312	-	-	1.7	0.19	-	-

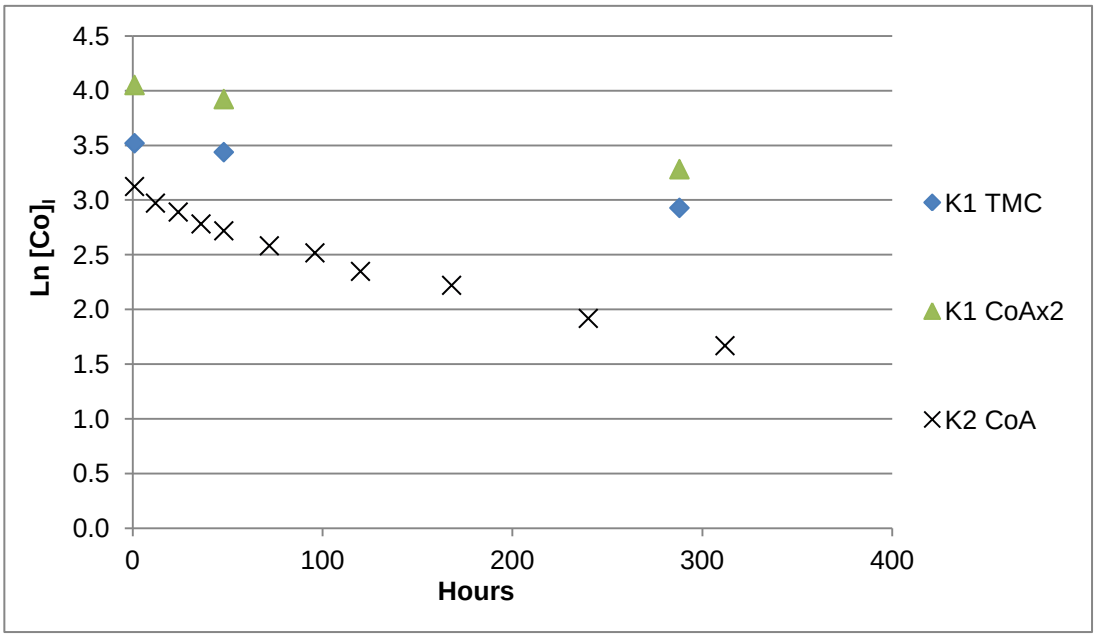

Figure 7.18. Ln[Co]$_l$ in TMC, CoA and CoAx2 samples of sludge K1 and K2

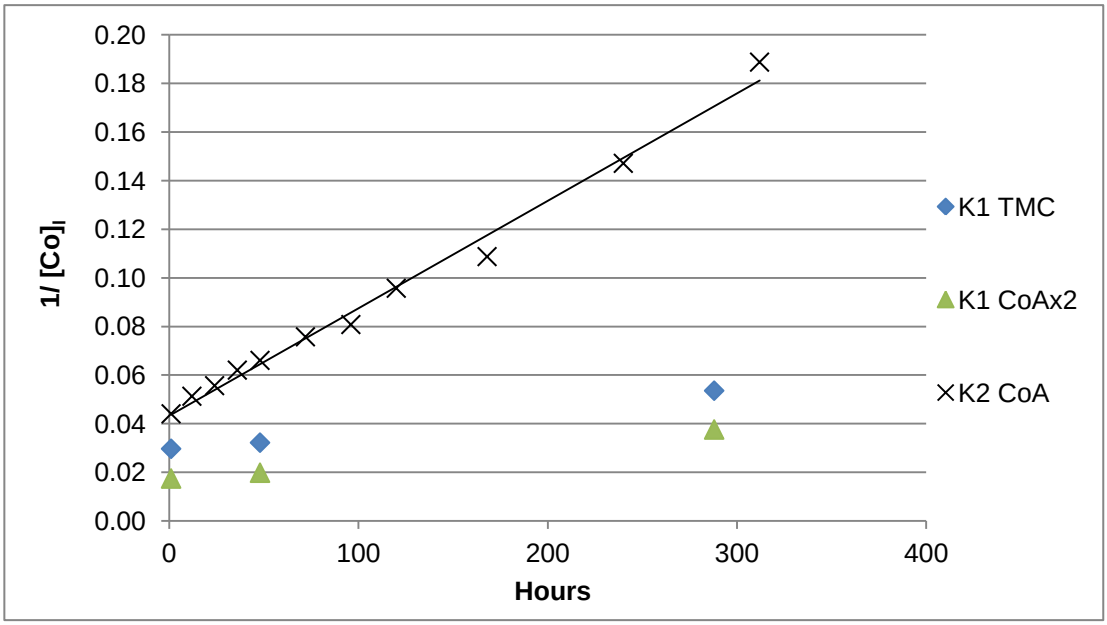

Figure 7.19. 1/[Co]$_l$ in TMC, CoA and CoAx2 samples of sludge K1 and K2

The difference of kinetic order between the sludge F and K indicated that the reaction of dissociation between cobalt and EDTA might be influenced by the sludge composition and was dependent of the concentration of another counter

ion. The 1st order kinetic reaction observed in sludge F samples showed that the reaction speed is only dependent on the CoEDTA concentration, which was assimilated as $[Co]_l$ (see appendix D). However, the 2nd order reaction observed in sludge K samples showed that the reaction was dependent on the CoEDTA (assimilated as $[Co]_l$) and the counter-ion that was binding with EDTA when cobalt was released.

The interpretation of this disparity between the two types of sludge might be explained by the presence of two different reactions of CoEDTA with the sludge or by the presence of a pseudo 1st order reaction in the sludge F. An excess of the counter-ion in the sludge F reduced the limiting effect of this ion on the reaction and so its kinetic would be dependent only on the concentration of CoEDTA in the solution. A second order kinetic reaction was consequently written as a pseudo first order reaction (see appendix D). The observation of other metals behaviour in relation with the sorption/precipitation of cobalt was needed to validate one of the two interpretations.

The concentration of the five other metals under study in the liquid phase was measured in the sample F2-CoA and K2-CoA and compared with the control samples of both sludge (tables 7.17 and 7.18). Copper and nickel concentrations in the liquid phase were not affected by the addition of CoEDTA in the sludge and $[Cu]_l$ was included in the range of 0.13-0.37 µmol/l for F2 and 0.24-1 µmol/l for sludge K2. For nickel, the range was 0.54-1.02 µmol/l for F2 and 0.39-1.12 µmol/l for K2 (table 7.17).

Manganese reacted differently to the addition of CoEDTA in the sludge F or K (table 7.18). Manganese concentration in the liquid phase increased with time in the F2-CoA sample from 0.31 µmol/l to a maximum of 0.89 µmol/l after 48 hours and then it varied in the range of 0.49-0.70 µmol/l while in the control sample (F2-control) $[Mn]_l$ was included between 0.07 and 0.32 µmol/l. In the sludge K, $[Mn]_l$ had similar range for the samples K2-CoA (0.17-0.55 µmol/l) and K2-control (0.10-0.50 µmol/l).

Zinc appeared to react in opposite manner to manganese, and $[Zn]_l$ was affected by the cobalt addition in the sludge K while only a small increase was observed for the sludge F (range of 0.13-0.46 µmol/l for F2-control and 0.26-0.68 µmol/l for F2-CoA) (table 7.18). In the K-control samples, zinc concentration in the liquid phase was higher than F-blank with a range of 0.61-1.01 µmol/l. With the cobalt addition, $[Zn]_l$ was slightly higher (+ 0.15 µmol/l on average) than in the control sample from 1 to 72 hours and then $[Zn]_l$ increased from 0.92 to the maximum of 1.42 µmol/l (hour 312) while the concentrations in the control sample stay stable between 0.61-0.84 µmol/l during the same period.

Finally iron concentration in the liquid phase was disturbed by cobalt addition in both sludges (table 7.18). Several variations on $[Fe]_l$ prevent any determination on a specific pattern from the effect of CoEDTA addition on the iron speciation but an increase of $[Fe]_l$ was observed in the sample F2-CoA and K2-CoA. $[Fe]_l$ was included in a the range of 20.2-99.2 µmol/l in F2-CoA samples while the

concentration was decreasing from 57.6 µmol/l to 17.1 µmol/l (hour 312) with a minimum of 9.0µmol/l (hour 120) in F2-control sample. In the sludge K, $[Fe]_l$ was constant between 4.3 and 9.1 µmol/l in F2-control and an increase of $[Fe]_l$ was observed from 6.5 µmol/l to 18.4 µmol/l in F2-CoA samples.

Iron is the only metal of the five studied having a large difference of concentration between the two sludge (F2-control and K2-control). The difference of concentration was related to the high concentration of iron in the solid phase in the sludge F (see chapter 6.2) due to iron dosing for chemical phosphorus removal purpose in the wastewater treatment plant. On average, $[Fe]_l$ was four times higher in F2-control (21.4 µmol/l) than in K2-control (5.6 µmol/l). The dissolution of iron in the presence of CoEDTA and its high concentration in the liquid phase of the sludge F inferred that the transfer of cobalt into the solid phase followed a second order kinetic reaction, which was reduced as a pseudo first order for the sludge F.

Table 7.17. $[Cu]_l$ and $[Ni]_l$ measured in control and CoA samples for sludge F2 and K2.

Concentration of metals in the liquid phase (µmol/l)					
Metal	Hours	Samples			
		F2-control	F2-CoA	K2-control	K2 CoA
Cu	1	0.21 ± 0.01	0.24 ± 0.02	0.35 ± 0.05	0.27 ± 0.01
	12	0.13 ± 0.02	0.22 ± 0.02	0.27 ± 0.02	0.30 ± 0.05
	24	0.30 ± 0.04	0.20 ± 0.01	0.33 ± 0.02	0.31 ± 0.09
	36	0.26 ± 0.01	0.28 ± 0.01	0.31 ± 0.04	0.24 ± 0.03
	48	0.26 ± 0.03	0.31 ± 0.01	0.65 ± 0.01	0.47 ± 0.11
	72	0.30 ± 0.04	0.25 ± 0.03	0.70 ± 0.10	0.61 ± 0.02
	96	0.29 ± 0.04	0.29 ± 0.02	1.00 ± 0.06	0.73 ± 0.02
	120	0.30 ± 0.03	0.24 ± 0.02	0.83 ± 0.06	0.80 ± 0.01
	168	0.30 ± 0.04	0.30 ± 0.03	0.88 ± 0.02	0.75 ± 0.03
	240	0.30 ± 0.03	0.37 ± 0.04	0.74 ± 0.01	0.79 ± 0.02
	312	0.22 ± 0.01	0.13 ± 0.01	0.70 ± 0.03	0.80 ± 0.03
Ni	1	0.55 ± 0.04	0.65 ± 0.05	0.70 ± 0.41	0.84 ± 0.20
	12	0.64 ± 0.08	0.65 ± 0.07	0.39 ± 0.01	0.49 ± 0.01
	24	1.0 ± 0.1	0.65 ± 0.05	0.48 ± 0.01	0.64 ± 0.16
	36	0.9 ± 0.03	0.95 ± 0.14	0.59 ± 0.14	0.64 ± 0.16
	48	0.68 ± 0.08	0.92 ± 0.18	0.49 ± 0.10	0.77 ± 0.08
	72	0.60 ± 0.08	0.68 ± 0.08	0.79 ± 0.22	0.81 ± 0.17
	96	0.64 ± 0.06	0.56 ± 0.01	0.86 ± 0.22	0.91 ± 0.19
	120	0.54 ± 0.03	0.55 ± 0.08	1.01 ± 0.23	0.89 ± 0.13
	168	0.67 ± 0.11	0.97 ± 0.29	0.79 ± 0.02	0.90 ± 0.09
	240	0.62 ± 0.12	0.72 ± 0.02	0.93 ± 0.15	1.1 ± 0.3
	312	0.59 ± 0.15	0.64 ± 0.05	1.1 ± 0.1	0.99 ± 0.01

Table 7.18. $[Fe]_l$, $[Mn]_l$, and $[Zn]_l$ measured in control and CoA samples for sludge F2 and K2.

Concentration of metals in the liquid phase (µmol/l)					
Metal	Hours	Samples			
		F2-control	F2-CoA	K2-control	K2 CoA
Fe	1	58 ± 2	44 ± 5	6.9 ± 0.8	6.5 ± 0.8
	12	32 ± 19	32 ± 10	5.6 ± 0.7	7.8 ± 2.2
	24	37 ± 19	72 ± 5	6.1 ± 0.6	7.8 ± 0.3
	36	14 ± 6	22 ± 3	5.5 ± 0.2	10.5 ± 0.4
	48	25 ± 12	99 ± 8	9.1 ± 0.6	13.9 ± 0.3
	72	9.8 ± 0.7	34 ± 4	7.1 ± 0.8	10.1 ± 0.5
	96	9.5 ± 0.8	37 ± 8	6.9 ± 0.2	10.6 ± 0.3
	120	9.0 ± 0.4	87 ± 5	6.4 ± 0.5	9.4 ± 1.1
	168	13 ± 4	41 ± 1	6.4 ± 0.7	7.7 ± 0.2
	240	11 ± 3	57 ± 5	4.3 ± 0.2	18.1 ± 1.5
	312	17 ± 2	90 ± 11	4.6 ± 0.1	18.4 ± 1.1
Mn	1	0.32 ± 0.06	0.31 ± 0.04	0.43 ± 0.06	0.44 ± 0.06
	12	0.07 ± 0.02	0.62 ± 0.05	0.42 ± 0.03	0.51 ± 0.09
	24	0.09 ± 0.06	0.88 ± 0.03	0.47 ± 0.07	0.51 ± 0.05
	36	0.07 ± 0.01	0.69 ± 0.01	0.37 ± 0.07	0.51 ± 0.01
	48	0.08 ± 0.01	0.89 ± 0.06	0.50 ± 0.02	0.55 ± 0.04
	72	0.19 ± 0.01	0.70 ± 0.04	0.30 ± 0.01	0.39 ± 0.03
	96	0.26 ± 0.05	0.62 ± 0.02	0.31 ± 0.01	0.38 ± 0.01
	120	0.31 ± 0.02	0.66 ± 0.04	0.28 ± 0.01	0.43 ± 0.06
	168	0.12 ± 0.02	0.63 ± 0.07	0.27 ± 0.03	0.26 ± 0.01
	240	0.13 ± 0.02	0.46 ± 0.03	0.12 ± 0.01	0.18 ± 0.01
	312	0.13 ± 0.02	0.68 ± 0.01	0.10 ± 0.01	0.17 ± 0.02
Zn	1	0.33 ± 0.06	0.32 ± 0.03	0.83 ± 0.05	1.0 ± 0.1
	12	0.16 ± 0.06	0.32 ± 0.05	0.80 ± 0.03	0.95 ± 0.05
	24	0.42 ± 0.04	0.47 ± 0.08	0.77 ± 0.03	0.95 ± 0.07
	36	0.13 ± 0.03	0.38 ± 0.04	0.68 ± 0.04	0.78 ± 00.4
	48	0.40 ± 0.14	0.62 ± 0.05	1.0 ± 0.1	1.2 ± 0.1
	72	0.38 ± 0.06	0.41 ± 0.04	0.75 ± 0.01	0.92 ± 0.01
	96	0.40 ± 0.08	0.63 ± 0.03	0.83 ± 0.15	1.1 ± 0.1
	120	0.46 ± 0.06	0.68 ± 0.05	0.84 ± 0.02	0.94± 0.04
	168	0.27 ± 0.01	0.37 ± 0.02	0.71 ± 0.10	1.1 ± 0.1
	240	0.25 ± 0.04	0.26 ± 0.02	0.61 ± 0.07	1.1 ± 0.1
	312	0.40 ± 0.09	0.35 ± 0.07	0.75 ± 0.01	1.4 ± 0.1

Visual Minteq simulation has been used to simulate the effect of CoEDTA addition on both sludge using only thermodynamic data. The sludge F and K were

modelled using experimental concentrations measured in section 7.2 and the input values are shown in the appendix E. Then an addition of a CoEDTA solution was simulated as a single stage titration using experimental concentrations (see section 4.5).

Results (table 7.19) show that all the cobalt was precipitated into the solid phase and predicted to be bound with sulphide (see section 7.5). At the same time, an increase of iron and manganese concentration in the dissolved phase was predicted. Nickel and zinc also had their concentrations in the liquid phase increased with the addition of CoEDTA but it was limited in comparison with iron and manganese. At equilibrium, Visual Minteq predicted that EDTA was mainly bound with iron (48% sludge K and 69% sludge F). Manganese was the second metal bound with EDTA with a percentage of 45% in the sludge K and 22% in the sludge F. Zinc and nickel ware also bound with EDTA and represent only around 1% of the total EDTA binding. Finally calcium and magnesium also formed EDTA complexes and they represented between 5 and 7 % of the binding.

In the previous section (section 7.4), it had been demonstrated that the simulation of zinc speciation in anaerobically digested sludge could not be clearly expressed due to the impossibility to form amorphous zinc sulphide or a mix of several bindings. In the case where sphalerite was not allowed to precipitate (zinc precipitated as wurtzite), the percentage of ZnEDTA complexes increased to 35% in the sludge K and 42% in the sludge F while the iron and manganese bound with EDTA was reduced to 31-40% (Fe) and 13-30% (Mn) (table 7.19).

Table 7.19. Predicted percentage of each element bound with EDTA from the simulation of CoA samples in the sludge F and K (Visual Minteq).

Element bound with EDTA	Sludge F		Sludge K	
	ZnS as Sphalerite	ZnS as Wurtzite	ZnS as Sphalerite	ZnS as Wurtzite
Zn^{2+}	0.5	42.5	0.4	34.5
Ni^{2+}	1.3	0.7	0.9	0.6
Co^{2+}	0.1	0.1	0.1	0.1
Mn^{2+}	21.7	12.6	45.4	30.0
Fe^{2+}	69.4	40.1	47.9	31.4
Ca^{2+}	5.1	2.9	3.0	1.9
Mg^{2+}	1.8	1.0	2.2	1.4
H^{2+}	0.1	0.1	0.1	0.1

Values are expressed in percent (%)

Simulation and experimental values agreed to demonstrate that dissolution of CoEDTA and the transfer of cobalt into the solid phase were dependent on the speciation of other metals. Iron was the main reacting metal but manganese and zinc could also be dissolved to react with EDTA. The reaction kinetic followed a second order and so it was dependent on the concentration of CoEDTA and the reacting metals. However, in the case of an excess of metals (mainly iron) in the liquid phase, the reaction kinetic followed a pseudo-first order.

7.6.2. Discussion

The supplementation of cobalt bound with EDTA created a disequilibrium between the liquid and solid phases due to the strong chelating capacity of EDTA. Bartacek et al. (2008) and Fermoso et al. (2009) already demonstrated the potential of EDTA to retain metals in solution and avoid a quick precipitation by sulphide. Results obtained using TMC and CoA samples also demonstrated that there was an exchange of metals bound with EDTA and the solid phase.

Copper, having the highest stability constant with EDTA (see chapter 2.6), was not affected by the presence of CoEDTA in the liquid phase. On the other hand, iron (low stability constant) was highly reactive with EDTA by staying in solution as FeEDTA in the TMC samples or by its solubilisation in the CoA samples. Manganese and zinc were also affected by the addition of CoEDTA and may be extracted from the solid phase to bind with EDTA. Finally, nickel stayed bound with EDTA in the TMC samples but it was not reactive when EDTA was only supplemented as CoEDTA.

The disparity between the metals reactions with EDTA and their stability constant revealed that the behaviour of MeEDTA was not only related to their complex stability but also by the speciation of metals present in the solid phase. Alibhai et al. (1985) and Hayes and Theis (1978) showed that the binding of metals with EPS and cell wall's site were weaker than the binding of those metals with EDTA. A large amount of iron, manganese and zinc had been extracted in the

exchangeable fraction confirming their presence as weakly bound compounds that could easily be dissolved by EDTA. In the case of nickel, the high stability constant of NiEDTA retained it from any precipitation or sorption into the solid phase and on the other hand the nickel present in the solid phase was also too strongly bound to avoid any dissolution in presence of CoEDTA.

Cobalt supplemented as CoEDTA exhibited a specific interaction between the two phases (liquid and solid) that could be related by the medium binding strength of CoEDTA (in comparison with other metals under study) and by the low cobalt concentration in the solid phase. Fermoso et al. (2010) observed that cobalt had two retention stages when supplemented in UASB reactors, a slow and fast retention. Even if any straight correlation can be established due to the difference in the process, this research also showed that cobalt was transferred into the solid phase using two pathways, a fast and slow transfer. The fast reaction can be related to precipitation and/or chemisorptions (Fermoso et al., 2010) and results from the solid phase analysis in the previous chapter showed that most of the cobalt was adsorbed with the biomass (see section 7.5).

Ong et al. (2010) observed that metals have a quick surface binding with activated sludge biomass followed by a slow intracellular diffusion. Similar reaction stages could be happening in anaerobically digested sludge with the cobalt supplementation. The amount of cobalt quickly adsorbed was limited by the binding site availability and in a second stage cobalt binding was potentially dependent on the kinetic of metal intracellular diffusion to free binding site. Similar

observations have been made by Bartacek et al. (2010) on the nickel sorption onto UASB sludge. However, the concentration cobalt following the fast reaction was about double in the CoAx2 samples in comparison CoA and TMC samples suggesting that other factors could have driving this reaction.

Several sorption models have been used by Bartacek et al. (2010) to measure the potential of UASB sludge to adsorb supplemented metals, and they found that Weber-Morris model was the best fit due to the slow kinetic of the intra-particle diffusion. Langmuir and Freundlich isotherms were also used by Ong et al. (2010) for the metals adsorption on activated sludge. However, in this research, the lack of information on the sludge sorption capacity precluded the use of these models and so only reaction kinetic models were used to define the cobalt transfer into the solid phase. The slow reaction for the cobalt transfer followed a second order kinetic and so the dissolution rate of CoEDTA was also depending on other metals concentration in the liquid phase that was reacting with EDTA. The kinetics of reaction could be reduced to a pseudo-first order if the reacting metals were in excess in the liquid phase. Iron has been determined to be the main metal reacting with EDTA to allow the cobalt sorption and precipitation.

Those reactions were against the solubility products of the different MeEDTA chelates and the predictions made from it. Irving and Williams (1948) demonstrated that cobalt had higher affinity with organics than iron and so the release of cobalt should occur only with metals having a stronger binding capacity with EDTA. However, in anaerobically digested sludge, the presence of other

reactions and equilibriums modified the affinities of metals with EDTA and they need to be taken into account in the different simulations. For example, Patidar and Tare (2008) showed that cobalt had better affinity with SMP complexation than iron. Equilibrium models integrated most of those reactions and predicted that cobalt was completely precipitated while iron, manganese and zinc were bound with EDTA.

The reactions driving the transfer of cobalt into the solid phase could be divided into two different stages. A first reaction occurred during the first hour where cobalt was dissociated from EDTA to react with organics related to the biomass such as EPS. This reaction might be limited by the number of available binding site. The second reaction was slower and could take more than 336 hours where cobalt was released from the EDTA binding to precipitate with sulphide or to react with the biomass. The kinetic of those reactions was likely to be dependent on the concentration of CoEDTA but also on the concentrations of iron, manganese and/or zinc in the liquid phase to bind with EDTA. However, the entire mechanism controlling the cobalt transfer was not fully understood and further research investigations are required to complete it.

7.7. General discussion and conclusion

The deficiency of available metals can be one of the causes responsible for the low performance of anaerobic digesters and can lead to its failure (Ishaq, 2012).

Metals supplementation is an interesting option to increase the metals availability and enhance the biogas production. The use of a cocktail of metals bound with EDTA offered the advantage to increase the concentrations of metals in the liquid phase and potentially their availability. The addition of MeEDTA disturbed the equilibrium between the solid and liquid phases and the reactions to reach the new equilibrium were different for each metal. Some metals were quickly transferred in the solid phase (copper, zinc and manganese) while others stayed in the liquid phase (iron and nickel). Moreover, each metal plays a specific biological role and cannot be replaced by the use of other metals. The metals supplementation interest needs a study of the liquid-solid equilibrium of each metal including its interaction with other metals.

Cobalt, by its low concentration, is often responsible of the metals deficiency in anaerobically digested sludge (Ishaq, 2012). In comparison with the other metals present in the TMC solution, most of the cobalt was slowly transferred into the solid phase. This slow transfer could be assimilated at continuous dosing system and the concentration of CoEDTA in the liquid phase could act as a pool of available cobalt for micro-organisms and so limiting the deficiency effects. The kinetics of this transfer were dependent on the availability of the cobalt binding site and also on the availability of counter metals to bind with EDTA. In the case of metals excess (sludge F) the maximum speed was obtained during the first 48 hours where the mirco-organism activity was at its maximum (see appendix A and Ishaq, 2012). The importance of other metals availability in the cobalt transfer was

also demonstrated by the difference of speed between the TMC and CoA samples.

The presence of metals bound with EDTA in the TMC solution reduced the availability of those metals to react with CoEDTA and so it limited its speed of transfer to solid phase. The reaction of iron with CoEDTA was demonstrated by an increase of the concentration of iron in the liquid phase for the CoA sample. However, no increase was observed in the TMC samples where FeEDTA was already present in the liquid phase. The speciation of metals in the solid phase and their liquid-solid phase equilibriums had also an important role in the cobalt transfer. Manganese and zinc, which formed weakly bound compounds in anaerobically digested sludge, were also reacting with CoEDTA. The addition of MnEDTA with the TMC solution led to the manganese precipitation as $MnCO_3$, its principal form in the solid phase. In the CoA samples, some manganese could be released from the solid phase to bind with EDTA.

Metals supplementation using EDTA as chelating agent had a specific impact on the liquid-solid equilibrium of each metal present in anaerobically digested sludge. The change on the equilibrium was dependent on the chemical speciation of the metal in the sludge, its affinity with the ligand and finally the other metals speciation. Metals supplementation therefore requires more information on the metals requirement of the sludge and the chemical behaviour of those metals in order to predict an improvement on the digester performance.

CHAPTER 8. GENERAL DISCUSSION

This research was included in a large project on the interest to enhance the biogas production by metals supplementation in anaerobic digestion process. Several results (Ishaq, 2012; Gustavsson, 2012 and Fermoso et al., 2008b&c) demonstrated that some digesters suffered from a deficiency of available metals and this limitation could be eliminated by the supplementation of essential metals. However, this process was not fully controlled nor optimized as the mechanisms related to the metals bioavailability were not entirely understood. This absence of knowledge was directly related to the lack of understanding of the metals behaviour in anaerobically digested sludge.

The main aims of this research were the investigation of the chemical speciation of the six main essential metals and their controlling reactions in anaerobically digested sludge. This investigation was one of the first steps in the optimization of the metals supplementation process in anaerobic digesters. Several objectives were completed to fulfil those aims. The first objective was the application of a suite of techniques to study metals speciation in anaerobically digested sludge. Then, this suite of techniques was applied to two case studies to determine the metals speciation in the solid phase and to characterize the behaviour of these metals when supplemented as MeEDTA.

8.1. Development of a suite of techniques to study metals speciation in anaerobically digested sludge

Availability of metals was determined by their total concentrations and the environmental condition affecting their speciation (pH, redox potential, precipitation, chelation and kinetic (Oleszkiewicz and Sharma, 1990)). So a study of the metals speciation was also mandatory with the measure of the total concentration of metals in anaerobically digested sludge in order to evaluate the metals bioavailability and/or behaviour (Hassler et al., 2004 and Adamo et al., 1996). The term speciation refers to its distributions amongst its chemical forms or species (Bourg 1995) and so a suite of analytical techniques was applied to sludge samples to obtain qualitative and quantitative information on the metals species.

Sequential extraction procedures were one of the main techniques used in the analysis of metals availability and mobility in environmental samples (Van Hullebusch et al., 2005 ; Perez-Cid et al., 1996 and Pueyo et al., 2008). However, Dodd et al. (2000) expressed that sequential extraction defines an element's reactivity rather than individual characterization of each phase and so complementary techniques were needed to obtain information on the metals species extracted at each stage of the procedure (Adamo et al., 1996). The assessment of the BCR sequential extraction, in section 5.2, confirmed the inability to distinguish the different species extracted in a same fraction. So several analytical techniques (see chapter 5) were assessed to determine their interests in

the study of metals speciation in anaerobically digested sludge and a suite of techniques was successfully applied in two case studies (chapters 6 and 7).

The development of this suite of techniques demonstrated that the combination of several analytical techniques increased the information on the characterization of the metals speciation. However, the choice of the analytical techniques used was highly dependent on the type binding detection that was investigated. In this study, pH titration was perfectly adapted to detect the weakly bound compounds (manganese or cobalt) but did not give any information on the strongly bound compounds such as sulphide precipitate. So others analytical procedures, such as X-ray absorption spectroscopy, should be assessed in order to cover all the bindings that can potential to be formed under anaerobic condition. X-Ray spectroscopy has been successfully used to determine the different species of selenium in biofilm (Van Hullenbusch et al., 2007) and should be a useful analytical technique in the determination of strongly bound compounds.

Nevertheless, the assessment of the different techniques and the application of a suite of techniques were essential to have a constructive approach (interest and limitation of each technique) on the study of metals speciation in anaerobically digested sludge. The suite of techniques allowed this research to go further on the understanding of metals speciation and behaviour than previous study that only used sequential extraction procedures to measure the metals mobility (Fuentes et al., 2008; Alvarez et al., 2002 and Chao et al., 2006). Moreover, this study

combined also the experimental values with equilibrium model prediction in particular to validate the different findings.

The use of chemical equilibrium speciation models (Phreeqc and Visual Minteq) in parallel to experimental analysis was determinant in the study of metals behaviour in anaerobically digested sludge. In section 6.2.3, models simulated the iron speciation in the seven types of anaerobically digested sludge and its predictions fitted with the experimental results. Moreover, models were used to simulate the effect of a variation of the sulphide or phosphate concentrations (figures 6.16-6.17) on the iron speciation and those results were useful in the determination of the reactions governing iron behaviour. Models were also mainly used to validate results from the pH titration.

From those promising results, more work should be undertaken to improve the model and obtain a similar level of accuracy as for the biological and physical models developed by Batstone et al. (2002) in the ADM1 model. The interest of the use of chemical equilibrium models has already been demonstrated by Unsworth et al. (2006) on the metals speciation in freshwater, by Ali (2005) on the crystallization of struvite from nutrient rich wastewater and by Gallios and Vaclavikova (2008) on the removal of chromium from water streams. So the development of an equilibrium speciation model integrating all the reactions occurring in the anaerobic digesters is essential in order to predict easily the behaviour of each metal in the sludge. Moreover, the number of experimental analyses would be considerably reduced to obtain similar information on the

speciation of metals. This model could also be used to achieve several simulations to optimize the metals supplementation in function of each anaerobic digester and its specific parameters.

8.2. Metals speciation in anaerobically digested sludge (cobalt, copper, iron, manganese, nickel and zinc)

Throughout the three previous chapters (5-7), the speciation of metals in the solid phase of anaerobically digested sludge was investigated using model simulation and the suite of techniques developed in chapter 5.

Literature (Morse and Luther, 1999; Fermoso et al., 2009; Mosey et al., 1971; Callander and Barford 1983) demonstrated that most of metals should be present in anaerobically digested sludge as sulphide precipitates, using thermodynamic data. However, results presented in this study established that metals speciation is more diversified and complicated in anaerobic digesters. Although metals (except manganese) were identified as sulphide precipitates in the anaerobically digested sludge, the speciation of metals was also dependent on several other chemical reactions occurring in the digester. Carbonate and phosphate precipitation, organic chelation and adsorption contributed to controlling the behaviour of metals in the solid phase.

The presence of those weakly bound metals changed the perspective on the view of metals mobility in anaerobically digested sludge. An increase of metals mobility changed the relations between metals and micro-organisms as the availability is directly related with the speciation (Zandvoort et al., 2006). So the previous system, considering sulphide concentration controlling the metals concentration in the liquid phase (Mosey et al. (1971) and Mosey and Hughes (1975) could not be applied due to a potential and easier release of weakly bound metals from the solid phase.

Moreover, the fate of supplemented metals was influenced by the metals speciation and the reactions governing it. Copper that have been measured strongly bound in the solid phase showed no interaction with EDTA during the different experiments. In the opposite, iron (precipitated with phosphate), manganese (precipitated with carbonate), cobalt and zinc (bound with the biomass) were partially weakly bound in the sludge and exhibit several exchanges between the solid and liquid phases during the process of metals supplementation.

Results from the study of metals speciation demonstrated that metals were principally present in the solid phase and so, the liquid–solid equilibrium determining the concentration of metals in the liquid phase was controlled by the reactions establishing the metals speciation in the solid phase. The supplementation of metals in anaerobically digested sludge disturbed this equilibrium and the system reacted in order to obtain a new equilibrium in those new conditions. The optimization of metals supplementation needs a full

understanding of the digester reactions to reach the new equilibrium and so a study of the effect of the supplementation on metal speciation in the solid phase is necessary to establish the reactions controlling each metal behaviour.

8.3. Effect of metals supplementation on the solid phase speciation of iron, cobalt and manganese in anaerobically digested sludge

The study of metals speciation in chapters 6 and 7 was completed using metals supplemented anaerobically digested sludge. Those two case studies were also used to investigate the chemical reactions controlling the metals speciation in the solid phase and consequently the reactions controlling the solid-liquid phase equilibrium.

The partitioning of iron into two phases (phosphate and sulphide precipitates) alters the understanding of the iron mobility in anaerobic digesters by demonstrating that iron was present in the sludge under weakly bound precipitates. Moreover, phosphate precipitation were found to be the controlling reaction of the iron speciation due to a limitation of sulphide availability and so, in the case of an increase of iron concentrations, the formation of vivianite and other ferrous-phosphate precipitates was observed in anaerobically digested sludge. The formation of weaker bound iron precipitates was higher than predicted by other studies (Callander and Barford, 1983ab; Zhang et al., 2009 and Oleszkiewicz and Sharma, 1990) and so it affected the impact of iron dosing on

the iron bioavailability or toxicity on micro-organisms (Carliell-Marquet et al., 2010 and Smith and Carliell-Marquet, 2009). The effect have been demonstrated in the case of CoEDTA supplementation as the difference of iron concentration in the solid phase alters the concentration of iron in the liquid phase that increased the kinetic of dissociation of CoEDTA (see next section, 8.4).

Cobalt had the lowest total concentration of the six metals under study and no speciation could have been defined without any cobalt supplementation (section 7.2 and 7.5). The second order kinetic reaction of transfer from the liquid to the solid phase of cobalt exhibited that cobalt was firstly bound with biomass related organics; the precipitation of cobalt by sulphide appeared only 2 days after the supplementation (figures 7.10-7.11 and tables 7.10-7.11). Then both reactions kept binding cobalt until reaching the cobalt liquid-solid equilibrium. The speciation of cobalt was independent of the cobalt concentration and it was not limited by organics binding site or sulphide as there was no change in the percentage of cobalt in the different BCR SE when the cobalt was added as TMC concentration or its double. Precipitation and chelation reactions were fast and so the transfer limitation was only related to the reaction between metals and CoEDTA.

Those results demonstrated that the supplementation of cobalt in anaerobically digested sludge offered an interest in the increase of its bioavailability for micro-organisms. The low sulphide precipitation and a large binding of cobalt with biomass suggested that cobalt was uptake during its transfer from the liquid phase to the solid phase and so the supplementation fulfilled its role. However, its

transfer did not seem to be limited by the availability of the binding site but by the kinetic of dissociation of CoEDTA. So it was essential to understand the factor influencing the kinetic of reaction to optimize the supplementation process.

Similar experiments should also be undertaken with zinc, copper and nickel in order to investigate their controlling reactions and would help in the understanding of their behaviour in anaerobically digested sludge.

8.4. Effect of MeEDTA supplementation on metals solid-liquid phase equilibrium

EDTA was a strong chelating agent that have been used during metals supplementation to keep metals longer into the liquid phase and avoid a quick precipitation or adsorption (Fermoso et al., 2008a; Oleszkiewicz and Sharma, 1989 and Aquino and Stuckey, 2007). So the presence of EDTA or MeEDTA disturbed the metals liquid-solid equilibrium and the chemical system reacted in order to reach the new equilibrium. The reactions governing these exchanges determined the potential bioavailability of the supplemented metals.

The affinity between metals and EDTA in anaerobically digested sludge was not only dependent on their stability constant (table 2.4) but also on the metals speciation in the solid phase (sections 7.2 and 7.6). Copper and nickel had similar stability constants with EDTA (pK_{sm}18-19, Hogfeldt (1982)) but behaved differently

when supplemented as MeEDTA. Copper precipitated quickly in the solid phase while nickel stayed in solution. Zinc and manganese were also quickly transferred into the solid phase while iron, that have similar stability constant as manganese (pK_{sm}13.5-14.5, Hogfeldt (1982)), stayed in solution. The difference of MeEDTA behaviour was explained by the specific speciation of metals. Copper was strongly bound by sulphide or humic substance in the solid phase and those bindings had “priority” on CuEDTA binding. In opposite, the balance between NiEDTA and Ni-solid binding favoured, thermodynamically, the presence of NiEDTA in solution. This balance between solid binding and EDTA could also have explained the behaviour of iron, zinc and manganese.

Cobalt, by its low concentration in the solid phase and its speciation, presented a specific kinetic of transfer. The second order kinetic reaction demonstrated that the release of cobalt from the EDTA binding was dependent on the concentration of CoEDTA and on the concentration of the metals (mainly iron) reacting with EDTA. In the case of high concentration of iron in the liquid phase, due to iron dosing, the kinetic order became a pseudo first order kinetic only dependent on the concentration of CoEDTA. With iron, manganese and zinc might react with CoEDTA but nickel and copper stayed in the solid phase.

Those results demonstrated that prior any supplementation, it was important to distinguish the metals speciation and their controlling reactions in order to predict their fate in the sludge. An understanding of the mechanism controlling the fate of supplemented metals helps in the determination of the best counter ion to bind

with the metals, the type of dosing or metals that need to be dosed. In the example under study, the supplementation of MeEDTA as pulse dosing, appeared to be an interesting choice for cobalt as it was slowly transfer into the solid phase with a main part being extracted in the BCR exchangeable fraction and so potentially bioavailable. For iron, EDTA binding was too strong to allow any transfer to solid phase and so a low availability for microorganism. However, more research investigations have to be undertaken concerning the bioavailability of metals in order to have clear definition on the bioavailability fractions and its different chemical species.

8.5. Factors potentially influencing the metals speciation

This research was undertaken to understand, determine and quantify the main reactions controlling the behaviour of metals in anaerobically digested sludge. However, some simplifications were made due to the complexity of the sludge matrix. A difference between the results from the equilibrium model simulations and the various experiments demonstrated that an anaerobic digester was not an ideal system and it did not reach a complete equilibrium. Several factors, such as mixing, which were not taken into account in this study, might influence the particular speciation of the metals in one specific anaerobic digester.

The primary aim of the mixing process in anaerobic digesters is to ensure a physical, chemical and biological uniformity (Bridgeman, 2012). However, mixing

plays an important role in the biogas production by increasing the biological conversion and the release of the biogas from the sludge (Karim et al., 2005). The optimization of the mixing process, through the reduction of particle size and heat loss, the minimization of grit deposition and the increase of substrate transfer, has contributed to enhance the biogas production by creating a favourable environment to microorganisms and facilitate the biological conversion of substrates (Wu, 2010; Karim et al., 2005; Bridgeman, 2012 and Bello-Meddoza, 1998). The mixing process has been improved by research using computational fluid dynamics on the shape of the digester, e.g. rectangular, cylindrical or egg shaped, and on the type of mixing, e;g; mechanical, pumped or gas recirculation (Wu, 2010).

The influence of mixing on the sludge uniformity might have an impact on the behaviour of metals in anaerobically digested sludge. In chapter 6, a higher formation of vivianite in comparison with the model prediction has been justified by the presence of phosphate bulk around the iron released from ferric phosphate precipitates entering in the digester. No information has been collected on the different mixing process used in the seven digesters and so no study could have been undertaken to determine the effect of mixing on the strength of this bulk and so the potential limitation of sulphide to form ferrous sulphide due to the bulking effect (Carliell-Marquet et al., 2010 and Zhang et al., 2009). A well mixed digester might reduce this bulking effect and favour the formation of sulphide precipitates as it has been predicted by the model. However, the speed of the different reactions occurring in the sludge (ferric-phosphate dissolution, iron reduction and

ferrous phosphate precipitation, Carliell-Marquet et al., 2010) should also limit the impact of mixing on the metals speciation.

In chapter 7, the absence of the mixing system in the serum bottle should also influence the kinetics of metal transfer from the liquid phase to the solid phase. The attenuation of the contact time between the two phases might reduce the availability of potential reactions (adsorption or precipitation, Bartacek et al., 2008; Fermoso et al., 2009) allowing the transfer of metals bound with EDTA to the solid phase. In the case of cobalt, results showed that the concentration of the counter-ion (mainly iron) reacting with EDTA played an important role in the speed of cobalt transfer. A better mixing system should increase this ion availability to react with CoEDTA and also its potential extraction from the solid phase to bind with EDTA. Consequently, this should increase the kinetics of the release of cobalt from EDTA binding and so its transfer to the solid phase. Fermoso et al. (2010) also observed two retention stages (one slow and one fast) of cobalt in the liquid phase, while supplemented as CoEDTA in a mixed UASB reactor; suggesting that the mixing might only affect the speed of the reactions.

As it has been discussed with mixing, other factors might influence the speciation or behaviour of metals depending on the anaerobic digester conditions. Biological reactions occurring in anaerobic digesters influence the organic composition of the sludge and consequently have an effect on the behaviour of metals reacting with organics (Gould and Genetelli, 1978 and Fermoso et al., 2009). During the anaerobic digestion process, the composition of organic matter is largely modified

by the biological degradation from the microbial community (Gerardi, 2003) and so the complexation of metals by organics can be affected by it. In order to simplify the study, this factor was not taken into account and, in chapter 7, only acetate was added in the feed to avoid the effect of the different biodegradation stages on the metals behaviour.

The breaking down of larger organics (e.g. humic substances) to smaller organics (e.g. propionate, butyrate) during the disintegration, hydrolytic and acid phases modify the number and configuration of the metals binding sites (Fletcher and Beckett, 1987). Hawari and Mulligan (2006) also demonstrated the effect of living biomass on the metals biosorption in comparison with nonviable biomass. Results showed that zinc, cobalt or copper speciation was influenced by organics complexation; with zinc and cobalt, the complexation occurred only with biomass related organics. Thus the speciation of these metals might be influenced by a change in the organic fraction of the sludge.

In the case of a closed system, such as serum bottle (chapter 7), the evolution of the organic phase throughout the 14 days of experiment should be significant with the biological degradation of substrates. The impact of this evolution on the metals speciation was limited in this research by using only acetate feed. The low methane production in the control sample (appendix A), demonstrated a low biological activity due to the use of digested sludge as a source of volatile solid. However, the use of more complex substrates as feed should change the behaviour of those metals due to a modification of the organics phase.

The results shown in sections 7.2 and 7.6 demonstrated that the fate of MeEDTA was depending on the difference of binding strengths of the metal with EDTA and the compound controlling the solid phase. In the case of cobalt or zinc, the complexation/adsorption of organics played an important role in their speciation and any change in the organic fraction should affect the behaviour of these metals. The concentration of organics with a large potential of bindings sites, such as carbohydrates, proteins, amino-acids, should be increased during the hydrolysis stage, favouring the complexation of metals with organics. The biological degradation of these organics during the acidogenesis stage should release the bound metals, which should react with sulphide or other organics to stay in the solid phase or be released into the liquid phase.

Concerning the kinetics of transfer of cobalt in the solid phase, an increase in the number of available binding sites, due to the presence of more complex substrates, should facilitate the complexation of cobalt with the biomass and so it should increase the speed of transfer. However, several findings demonstrated that the speed of transfer were mainly dependent on the dissociation of CoEDTA by its reaction with a counter-ion (mainly iron), limiting the effect of the binding sites availability on the kinetics of transfer. Consequently, more investigations are needed in order to determine the effect of a change in the organic fraction on the kinetics of cobalt transfer into the solid phase.

These two examples of factors influencing the metals speciation demonstrated that the findings obtained during this study were only a first step in the

determination of the metals behaviour in anaerobically digested sludge. The importance of other factors not yet mentioned, such as pH, redox potential, temperature or sludge origin (urban/rural/industrial, ratio primary:secondary sludge, wastewater treatment process), should also be taken into consideration as they might influence the metals behaviour. Future studies on this subject should try to integrate these factors in order to improve the results developed in this research.

CHAPTER 9. CONCLUSIONS AND RECOMMENDATIONS

Within this chapter, conclusions which relate to the aims of this research are presented. These are followed by recommendations for application and further work in this area.

9.1. Conclusions

This study demonstrated that through an assessment of each analytical technique, the suite of techniques employed during this research was able to characterize the speciation of metals qualitatively and quantitatively. Moreover, the predictions from the two chemical equilibrium models fitted with the experimental results demonstrating the interest of integrating chemical models into the existing ADM1 model.

The characterization of the metals speciation in anaerobically digested sludge in this study demonstrated that the behaviour of metals was not only controlled by sulphide precipitation but they were also present as weakly bound compounds (phosphate/carbonate precipitates and biomass chelation). The quantification of those weakly bound metals offers a new perspective on the potential metals bioavailability related with their mobility, particularly in the case of metals supplementation.

This study demonstrated that the addition of metals in the solid phase of anaerobically digested sludge was mainly controlled by secondary reactions due to sulphide limitation. Consequently metals formed weaker bound compounds that were easier to react and more mobile in the sludge. An increase of weakly bound metal compounds might favour their bioavailability to micro-organisms and affect the welfare of the anaerobic digester.

This study demonstrated that the fate of metal bound EDTA was dependent on the stability constant of MeEDTA and on the metal speciation in the solid phase of anaerobically digested sludge. The transfer of metal from the liquid phase to the solid phase was the result of favourable balance between the binding strength of MeEDTA and the reactions controlling the metal behaviour. So an evaluation of the speciation of the metal in the solid phase and the binding strength of the supplemented metal species is essential prior in metal addition in order to predict its bioavailability and potential beneficial effect on the anaerobic digester.

This study demonstrated that cobalt was transferred to the solid phase following a second order kinetic when supplemented as CoEDTA. The speed of reaction was limited by the concentration of CoEDTA and the counter metals (mainly iron) reacting with EDTA. In the case of a high concentration of metals in the liquid phase, the order of the reaction could be assimilated as a first order kinetic reaction and the speed was only dependent on the concentration of CoEDTA. The slow kinetic of dissociation of CoEDTA appeared to be suitable for the purpose of metals supplementation as the transfer from the two phases occurred over a

similar period as the sludge retention time (around 14 days) with a maximum during the two first days in the case of a pseudo first order reaction.

9.2. Recommendations and further work

There are three recommendations that are applicable to the study of the behaviour of metals in anaerobically digested sludge:

- New analytical techniques, such as X-ray absorption spectroscopy, need to be assessed for integration into the suite of techniques already developed in this study. A particular focus should be given to the understanding of the metal species extracted in the oxidisable BCR sequential extraction fractions and other stronger bonds.

- This study has a large focus on the inorganic precipitation process in the study of metals speciation and more investigation has to be undertaken on the adsorption and organic chelation processes.

- Some improvements could be done on the prediction of metals speciation in anaerobically digested sludge by chemical equilibrium speciation models. Those improvements should prioritize on the integration of well defined adsorption process.

There are two recommendations for further work that are applicable in the study of the enhancement of the biogas production by the supplementation of metals:

- This study focused on the fate of metals supplemented as MeEDTA and new research should focus on the fate of metals supplemented with others anions, such as weaker organics (NTA, citrate) or inorganic (chloride).

- In parallel to the investigation of the mechanisms controlling the fate of metal supplementation, a study on the definition of metals bioavailability and their chemical forms should be undertaken in order to optimize the metals supplementation.

There is a recommendation for further work that is applicable in the study of nutrient recovery:

- In this study several phosphate compounds have been identified and further investigation on the metals speciation, its controlling reactions and the phosphate speciation should be undertaken in order to evaluate the potential of nutrient recovery from anaerobically digested sludge.

REFERENCES

Adamo, P., Dudka, S., Wilson, M.J., et al. (1996) Chemical and mineralogical forms of Cu and Ni in contaminated soils from the Sudbury mining and smelting region, Canada. **Environmental Pollution**, 91(1): 11-19.

Al-Borno, A. and Tomson, M.B. (1994) The temperature dependence of the solubility product constant of vivianite. **Geochimica et Cosmochimica Acta**, 58(24): 5373-5378.

Ali, I. (2005) **Struvite Crystallization from Nutrient Rich Wastewater**. PhD thesis, James Cook University.

Alibhai, K. R. K., Mehrotra, I. and Forster C.F. (1985) Heavy-Metal Binding to Digested-Sludge. **Water Research**, 19(12): 1483-1488.

Alvarez, E. A., Mochon, M. C., Sanchez, J.C.J., et al. (2002) Heavy metal extractable forms in sludge from wastewater treatment plants. **Chemosphere**, 47(7): 765-775.

Andres, N. F. and Francisco, M. S. (2008) Effects of sewage sludge application on heavy metal leaching from mine tailings impoundments. **Bioresource Technology**, 99(16): 7521-7530.

Anthony, J. W., Bideaux, R. A., Bladh, K. W., et al. (Eds.). **Handbook of Mineralogy** [online]. Chantilly : Mineralogical Society of America. http://www.handbookofmineralogy.org/

APPA-AWWA-WEF (1985) **Standard methods for the examination of water and wastewater.** 16th Ed. Washington D.C: APHA.

Aquino, S. F. and Stuckey, D. C. (2007) Bioavailability and toxicity of metal nutrients during anaerobic digestion. **Journal of Environmental Engineering**, 133(1): 28-35.

Artola, A., Balaguer, M. D. and Rigola, M. (1997) Heavy metal binding to anaerobic sludge. **Water Research** 31(5): 997-1004.

Banerjee, A. D. K. (2002) Heavy metal levels and solid phase speciation in street dusts of Delhi, India. **Environmental Pollution** 123: 95-105.

Bartacek, J., Fermoso, F. G., Baldo-Urrutia, A.M., et al. (2008) Cobalt toxicity in anaerobic granular sludge: influence of chemical speciation. **Journal of Industrial Microbiology & Biotechnology**, 35(11): 1465-1474.

Bartacek, J., Fermoso, F. G., Catena, A.B., et al. (2010) Effect of sorption kinetics on nickel toxicity in methanogenic granular sludge. **Journal of Hazardous Materials**, 180(1-3): 289-296.

Basolo, F. and Johnson, R.C. (1964) **Coordination chemistry: the chemistry of metal complexes**. New York: Benjamin W.A.

Batstone, D.J., Keller, J., Angelidaki, I., et al. (2002) **Anaerobic Digestion Model No. 1 (ADM1)**. London: IWA Publishing.

Bello-Mendoza, R. and Sharratt, P.N. (1998) Modelling the effects of imperfect mixing on the performance of anaerobic reactors for sewage sludge treatment. **J. Chem. Technol. Biotechnol.**, 71: 121-130.

Bertrand, M., Weber, G. and Schoefs, B. (2003) Metal determination and quantification in biological material using particle-induced X-ray emission. **Trends in Analytical Chemistry**, 22(4): 254-262.

Bridgeman, J. (2012) Computational fluid dynamics modelling of sewage sludge mixing in anaerobic digester. **Advances in Engineering Software**, 44:54-62.

Bourg, A.C.M. (1995) “Speciation of heavy metals in soils and groundwater and implications for their natural and provoked mobility.” In Salomons, W., Forstner, U. and Mader, P. **Heavy Metals Problems and Solutions**. Springer. pp. 19-31.

Buzier, R., Tusseau-Vuillemin, M. H. and Mouchel, J.M. (2006) Evaluation of DGT as a metal speciation tool in wastewater. **Science of the Total Environment**, 358(1-3): 277-285.

Callander, I. J. and Barford, J. P. (1983a) Precipitation, Chelation, and the Availability of Metals as Nutrients in Anaerobic-Digestion.1. Methodology**. Biotechnology and Bioengineering**, 25(8): 1947-1957.

Callander, I. J. and Barford, J. P. (1983b) Precipitation, Chelation, and the Availability of Metals as Nutrients in Anaerobic-Digestion.2. Applications. **Biotechnology and Bioengineering**, 25(8): 1959-1972.

Carliell-Marquet, C.M., Smith, J., Oikonomidis, I., et al. (2010) Inorganic profiles of chemical phosphorus removal sludge. **Water Management**, 163: 65-77.

Carlson, C. E. A. and Morrison, G. M. (1992) Fractionation and Toxicity of Metals in Sewage-Sludge. **Environmental Technology**, 13(8): 751-759.

Celen, I., Buchanan, J. R., Burns, R.T., et al. (2007) Using a chemical equilibrium model to predict amendments required to precipitate phosphorus as struvite in liquid swine manure. **Water Research**, 41(8): 1689-1696.

Chao, W., Li, X. C., Wang, P.F., et al. (2006) Extractable fractions of metals in sewage sludges from five typical urban wastewater treatment plants of China. **Pedosphere**, 16(6): 756-761.

Chemical Rubber Company (1972) **Handbook of chemical and physics**. 53rd Ed. Cleveland: Chemical Rubber Co.

Chen, W., Westerhoff, P., Leenheer, J.A., et al. (2003) Fluorescence excitation - Emission matrix regional integration to quantify spectra for dissolved organic matter. **Environmental Science & Technology**, 37(24): 5701-5710.

Cheng, M.H., Patterson J.W. and Minear, R.A. (1975) Heavy metals uptake by activated sludge. **J. Water Pollution Control Fed.**, 47: 362-376.

Christensen, J.B., Botma, J.J. and Christensen, T.H. (1999) Complexation of Cu and Pb by DOC in polluted groundwater: A comparison of experimental data and predictions by computer speciation models (WHAM and MINTEQA2). **Water Research**, 33(15): 3231-3238.

da Silva, J.C.G.E., Machado, A. A. S. C., Oliveira, C.J.S., et al. (1998) Fluorescence quenching of anthropogenic fulvic acids by Cu(II), Fe(III) and UO22+. **Talanta** 45(6): 1155-1165.

Davidson W. (1991) The solubility of iron sulphides in synthetic and natural waters at ambient temperature. **Aquatic Sciences**, 53 (4): 309-329.

Davidson, C. M., Thomas, R. P., McVey, S.E., et al. (1994) Evaluation of a Sequential Extraction Procedure for the Speciation of Heavy-Metals in Sediments. **Analytica Chimica Acta**, 291(3): 277-286.

de Sousa, J.T., Vazoller, R.F. and Foresti, E. (1997) Phosphate removal in an UASB reactor treating synthetic substrate simulating domestic sewage. **Braz. J. Chem. Eng.** [online], 14(4); Available from: http://dx.doi.org/10.1590/S0104-66321997000400002.

Dewil, R., Baeyens, J., Roels, J., et al. (2009) Evolution of the Total Sulphur Content in Full-Scale Wastewater Sludge Treatment. **Environmental Engineering Science**, 26(4): 867-872.

Dodd, J., Large, D.J., Fortey, N.J., et al. (2000) A petrographic investigation of two sequential extraction techniques applied to anaerobic canal bed mud. **Environmental Geochemistry and Health**, 22(4): 281-296.

Fermoso, F.G., Bartacek, J., Chung L.C., et al. (2008a) Supplementation of cobalt to UASB reactors by pulse dosing: CoCl2 versus CoEDTA(2-) pulses. **Biochemical Engineering Journal**, 42(2): 111-119.

Fermoso, F.G., Collins, G., Bartacek, J., et al. (2008b) Role of nickel in high rate methanol degradation in anaerobic granular sludge bioreactors. **Biodegradation**, 19(5): 725-737.

Fermoso, F.G., Collins, G., Bartacek, J., et al. (2008c), Zinc deprivation of methanol fed anaerobic granular sludge bioreactors. **Journal of Industrial Microbiology & Biotechnology**, 35(6): 543-557.

Fermoso, F.G., Bartacek, J., Jansen, S., et al. (2009) Metal supplementation to UASB bioreactors: from cell-metal interactions to full-scale application. **Science of the Total Environment**, 407(12): 3652-3667.

Fermoso, F.G., Bartacek J., Manzano R., et al. (2010) Dosing of anaerobic granular sludge bioreactors with cobalt: Impact of cobalt retention on methanogenic activity. **Bioresource Technology**, 101(24): 9429-9437.

Fernandes, M.C.M.M., Paniago, E.B. and Carvalho, S. (1997) Copper(II) mixed ligands complexes of hydroxamic acids with glycine, histamine and histidine. **Journal of the Brazilian Chemical Society***,* 8(5): 537-548.

Fitch, A. and Helmke, P.A. (1989) Donnan Equilibrium Graphite-Furnace Atomic-Absorption Estimates of Soil Extract Complexation Capacities. **Analytical Chemistry**, 61(11): 1295-1298.

Fletcher, P. and Beckett, P.H.T. (1987) The Chemistry of Heavy-Metals in Digested Sewage-Sludge .2. Heavy-Metal Complexation with Soluble Organic-Matter. **Water Research**, 21(10): 1163-1172.

Francis, A.J. and Dodge, C.J. (1990) Anaerobic Microbial Remobilization of Toxic Metals Coprecipitated with Iron-Oxide. **Environmental Science & Technology**, 24(3): 373-378.

Fristoe, B.R. and Nelson P.O. (1983) Equilibrium Chemical Modeling of Heavy-Metals in Activated-Sludge. **Water Research**, 17(7): 771-778.

Frost, R.L., Weier, M.L., Martens, W., et al. (2003) Dehydration of synthetic and natural vivianite. **Thermochimica Acta**, 401(2): 121-130.

Fuentes, A., Llorens, M., Saez, J., et al. (2008) Comparative study of six different sludges by sequential speciation of heavy metals. **Bioresource Technology**, 99(3): 517-525.

Gali, A., Benabdallah, S., Astals, S., et al. (2009) Modified version of ADM1 model for agro-waste application. **Bioresource Technology**, 100(11): 2783-2790

Gallios, G.P. and Vaclavikova, M. (2008) Removal of chromium (VI) from water streams: a thermodynamic study. **Envirn. Chem. Lett.**, 6: 235:240.

Gamble, D. S., Schnitze, M. and Hoffman, I. (1970) Cu2+-Fulvic Acid Chelation Equilibrium in 0.1 M Kcl at 25.0 Degrees C. **Canadian Journal of Chemistry**, 48(20): 3197-3204.

Gerardi, M.H. (2003) **The Microbiology of Anaerobic Digesters**. Hoboken, New Jersey: John Wiley & Sons, Inc..

Giblin, A.E. and Howarth, R.W. (1984) Porewater evidence for a dynamic sedimentary iron cycle in salt marshes. **Limnol Oceanogr.**, 29(1): 47-63.

Gonzalez-Gil, G., Lens, P. N. L., Van Aelst, A., et al. (2001) Cluster structure of anaerobic aggregates of an expanded granular sludge bed reactor. **Applied and Environmental Microbiology**, 67(8): 3683-3692.

Gonzalez-Gil, G., Jansen, S., Zandvoort, M.H., et al. (2003) Effect of yeast extract on speciation and bioavailability of nickel and cobalt in anaerobic bioreactors, **Biotechnology and Bioengineering**, 82(2): 134-142.

Gould, M.S. and Genetelli, E.J. (1978) Heavy-Metal Complexation Behavior in Anaerobically Digested Sludges. **Water Research**, 12(8): 505-512.

Gould, M.S. and Genetelli, E.J. (1984) Effects of Competition on Heavy-Metal Binding by Anaerobically Digested Sludges. **Water Research**, 18(1): 123-126.

Gustavsson, J. (2012) **Cobalt and nickel bioavailability for biogas formation**. PhD thesis, Linköping University, Linköping Studies in Arts and Science No 549.

Hassler, C.S., Slaveykova, V.I. and Wilkinson, K.J. (2004) Some fundamental (and often overlooked) considerations underlying the free ion activity and biotic ligand models. **Environmental Toxicology and Chemistry**, 23(2): 283-291.

Hayes, T.D. and Theis, T.L. (1978) Distribution of Heavy-Metals in Anaerobic Digestion. **Journal Water Pollution Control Federation**, 50(1): 61-72.

Hering, J.G. and Morel, F.M.M. (1990) Kinetics of Trace-Metal Complexation - Ligand-Exchange Reactions. **Environmental Science & Technology** 24(2): 242-252.

Hoban, D.J. and Van Den Berg, L. (1979) Effect of Iron on Conversion of Acetic Acid to Methane During Methanogenic Fermentations. **Journal of Applied Microbiology** 47(1): 153-159.

Hogfeldt, E., International Union of Pure and Applied Chemistry (1982) **Stability constants of metal-ion complexes, Part A**. **Inorganic ligands**. Oxford: Pergamon.

HydroGeoLogic, Inc. and Allison Geoscience Consultants, Inc. (1999) **MINTEQA2/PRODEFA2, A Geochemical Assessment Model for Environmental Systems: User Manual Supplement for Version 4.0**. Athens : U.S.E.P.A

Irving, H. and Williams, R.J.P. (1948) Order of Stability of Metal Complexes. **Nature**, 162: 746-747.

Ishaq, F. (2012) **Trace metal supplementation in wastewater sludge digesters**. PhD thesis, University of Birmingham.

Jansen S., Gonzalez-Gil, G. and van Leeuwen, H.P. (2007) The impact of Co and Ni speciation on methanogenesis in sulfidic media - Biouptake versus metal dissolution. **Enzyme and Microbial Technology**, 40(4): 823-830.

Jensen, D. L., Ledin, A. and Christensen, T.H. (1999) Speciation of heavy metals in landfill-leachate polluted groundwater. **Water Research**, 33(11): 2642-2650.

Johnson, D.K., Carliell-Marquet, C.M. and Forster, C.F. (2003) An examination of the treatment of iron-dosed waste activated sludge by anaerobic digestion. **Environmental Technology**, 24(8): 937-945.

Jong, T. and Parry, D.L. (2004) Adsorption of Pb(II), Cu(II), Cd(II), Zn(II), Ni(II), Fe(II), and As(V) on bacterially produced metal sulfides. **Journal of Colloid and Interface Science**, 275(1): 61-71.

Kaksonen, A.H., Riekkola-Vanhanen, M. L. and Puhakka, J.A. (2003) Optimization of metal sulphide precipitation in fluidized-bed treatment of acidic wastewater. **Water Research***,* 37(2): 255-266.

Kalis, E.J.J., Weng, L.P., Dousma, F., et al. (2006) Measuring free metal ion concentrations in situ in natural waters using the Donnan Membrane Technique. **Environmental Science & Technology***,* 40(3): 955-961.

Karim, K., Klasson, K.T., Hoffmann, R., et al. (2005) Anaerobic digestion of animal waste: Effect of mixing. **Bioresource Technology**, 96: 1607-1612.

Kelly, C.R. and Switzenbaum, M.S. (1984) Anaerobic treatment: temperature and nutrient effects. **Agric. Wastes**, 10:135–54.

Kojima, I., Kato, A. and Iida, C. (1992) Microwave Digestion of Biological Samples with Acid Mixture in a Closed Double Ptfe Vessel for Metal Determination by One-Drop Flame Atomic-Absorption Spectrometry. **Analytica Chimica Acta**, 264(1): 101-106.

Lake, D.L., Kirk, P.W.W. and Lester, J.N. (1985) The Effects of Anaerobic-Digestion on Heavy-Metal Distribution in Sewage-Sludge. **Water Pollution Control**, 84(4): 549-558.

Lake, D.L., Kirk, P.W.W. and Lester, J.N. (1989) Heavy-Metal Solids Association in Sewage Sludges. **Water Research**, 23(3): 285-291.

Lin, C. Y., Chou, J. and Lee, Y.S. (1998) Heavy metal-affected degradation of butyric acid in anaerobic digestion, **Bioresource Technology**, 65(1-2): 159-161.

Liu, Y. and Fang, H.H.P. (1998) Precipitates in anaerobic granules treating sulphate-bearing wastewater, **Water Research**, 32(9): 2627-2632.

Lo, H.M., Lin, K.C., Liu, M.H., et al. (2009) Solubility of heavy metals added to MSW. **Journal of Hazardous Materials**, 161(1): 294-299.

Lobinski, R., Moulin, C. and Ortega, R. (2006) Imaging and speciation of trace elements in biological environment. **Biochimie**, 88(11): 1591-1604.

Metcalf & Eddy, Inc. (2003) **Wastewater engineering: treatment and reuse**. 4th ed. Boston: McGraw-Hill.

Mingot, J.I., Obrador, A., Alvarez, J.M. et al. (1995) Acid-Extraction and Sequential Fractionation of Heavy-Metals in Water-Treatment Sludges. **Environmental Technology**, 16(9): 869-876.

Miot J., Benzerara, K., Morin, G., et al. (2009) Transformation of vivianite by anaerobic nitrate-reducing iron-oxidizing bacteria. **Geobiology** 7(3): 373-384.

Mobed, J.J., Hemmingsen, S. L., Autry, J.L., et al. (1996) Fluorescence characterization of IHSS humic substances: Total luminescence spectra with absorbance correction. **Environmental Science & Technology**, 30(10): 3061-3065.

Morse, J.W. and Luther, G.W. (1999) Chemical influences on trace metal-sulfide interactions in anoxic sediments. **Geochimica Et Cosmochimica Acta**, 63(19-20): 3373-3378.

Mosey, F.E., Swanwick, J.D. and Hughes, D.A. (1971) Factors affecting the availability of heavy metals to inhibit anaerobic digestion. **Water Pollution Control,** 70: 668-679.

Mosey, F.E. and Hughes, D.A. (1975) The toxicity of heavy metal ions to anaerobic digestion. **Water Pollution Control**, 74: 18–39.

Nielsen, A.H., Lens, P.N.L., Vollersten J., et al. (2005) Sulfide-iron interactions in domestic wastewater from a gravity sewer. **Water Research**, 39(12): 2747-2755.

Nielsen, P.H. and Keiding, K. (1998) Disintegration of activated sludge flocs in presence of sulfide. **Water Research** 32(2): 313-320.

Nriagu, J.O. (1972) Stability of vivianite and ion-pair formation in the system $Fe_3(PO_4)_2$-H_3PO_4-H_2O. **Geochimica et Cosmochimica Acta**, 36: 459-470.

Ofverstrom, S., la Cour Jansen, J. and Dauknys, R. (2011) Impact of iron salts dosing on anaerobic digestion process and stuvite/vivianite formation: a review. ***Proceedings of the 12th International Conference on Environmental Science and Technology***. Rhodes, 8-10 September 2011. pp. 1341-1346.

Oleszkiewicz, J.A. and Sharma, V.K. (1990) Stimulation and Inhibition of Anaerobic Processes by Heavy-Metals - a Review. **Biological Wastes** 31(1): 45-67.

Ong, S.A., Toorisaka, E., Hirata, M., et al. (2010) Adsorption and toxicity of heavy metals on activated sludge. **ScienceAsia** 36: 204-209.

Osuna, M.B., van Hullebusch, E.D., Zandvoort, M.H., et al. (2004) Effect of cobalt sorption on metal fractionation in anaerobic granular sludge. **Journal of Environmental Quality**, 33(4): 1256-1270.

Patidar, S. K. and Tare, V. (2008) Soluble microbial products formation and their effect on trace metal availability during anaerobic degradation of sulfate laden organics. **Water Science and Technology**, 58(4): 749-755.

Penumathsa, B.K.V., Premier, G.C., Kyazze, G., et al. (2008) ADM1 can be applied to continuous bio-hydrogen production using a variable stoichiometry approach. **Water Research**, 42(16): 4379-4385.

Percheron, G., Bernet, N. and Moletta, R. (1997) Start-up of anaerobic digestion of sulfate wastewater. **Bioresource Technology**, 61(1): 21-27.

Perez-Cid, B., Lavilla, I. and Bendicho, C. (1996) Analytical assessment of two sequential extraction schemes for metal partitioning in sewage sludges. **Analyst**, 121(10): 1479-1484.

Perez-Cid, B., Lavilla, I. and Bendicho, C. (1999) Application of microwave extraction for partitioning of heavy metals in sewage sludge, **Analytica Chimica Acta**, 378(1), 201-210.

Pourbaix, M. (1963) **Atlas D'equilibres Electrochimiques**. Paris: Gauthier-Villars & Cie.

Plaza, C., Brunetti, G. and Senesi N. (2006) Fluorescence characterization of metal ion-humic acid interactions in soils amended with composted municipal solid wastes. **Analytical and Bioanalytical Chemistry**, 386(7-8): 2133-2140.

Pueyo, M., Mateu, J., Rigol, A., et al. (2008) Use of the modified BCR three-step sequential extraction procedure for the study of trace element dynamics in contaminated soils. **Environmental Pollution**, 152(2): 330-341.

Ramirez, I., Volcke, E.I.P., Rajinikanth, R., et al. (2009) Modeling microbial diversity in anaerobic digestion through an extended ADM1 model. **Water Research**, 43(11): 2787-2800.

Rauret, G., Lopez-Sanchez, J.F., Sahuquillo, A., et al. (2000) Application of a modified BCR sequential extraction (three-step) procedure for the determination of extractable trace metal contents in a sewage sludge amended soil reference material (CRM 483), complemented by a three-year stability study of acetic acid and EDTA extractable metal content. **Journal of Environmental Monitoring**, 2(3): 228-233.

Reynolds, D. M. (2002) The differentiation of biodegradable and non-biodegradable dissolved organic matter in wastewaters using fluorescence spectroscopy. **Journal of Chemical Technology and Biotechnology**, 77(8): 965-972.

Robards, K. and Starr, P. (1991) Metal Determination and Metal Speciation by Liquid-Chromatography - a Review. **Analyst** 116(12): 1247-1273.

Ryan, D.K. and Weber, J.H. (1982) Fluorescence Quenching Titration for Determination of Complexing Capacities and Stability-Constants of Fulvic-Acid. **Analytical Chemistry**, 54(6): 986-990.

Ryan, D.K., Thompson, C.P. and Weber, J.H. (1983) Comparison of Mn2+, Co2+, and Cu2+ Binding to Fulvic-Acid as Measured by Fluorescence Quenching. - **Canadian Journal of Chemistry**, 61(7): 1505-1509.

Saar, R.A. and Weber, J.H. (1982) Fulvic-Acid - Modifier of Metal-Ion Chemistry. **Environmental Science & Technology**, 16(9): A510-A517.

Scancar, J., Milacic, R., Strazar, M., et al. (2000) Total metal concentrations and partitioning of Cd, Cr, Cu, Fe, Ni and Zn in sewage sludge. **Science of the Total Environment**, 250(1-3): 9-19.

Schink, B. (1992) **The Prokaryotes** 2nd.Springer Verlag, New York

Serkiz, S.M., Allison, J.D., Perdue, E.M., et al. (1996) Correcting errors in the thermodynamic database for the equilibrium speciation model MINTEQA2. **Water Research**, 30(8): 1930-1933.

Sheng, G.P. and Yu, H.Q. (2006) Characterization of extracellular polymeric substances of aerobic and anaerobic sludge using three-dimensional excitation and emission matrix fluorescence spectroscopy. **Water Research**, 40(6): 1233-1239.

Sigel, H. (1984) **Metal ions in biological systems, vol 18**. New York: Marcel Dekker, Inc.

Smith, J.A. (2006) **An Investigation into the Anaerobic Digestibility of Iron-dosed Activated Sludge**. PhD thesis, Univeristy of Birmingham.

Smith, J.A. and Carliell-Marquet, C. M. (2009) A novel laboratory method to determine the biogas potential of iron-dosed activated sludge. **Bioresource Technology** 100(5): 1767-1774.

Solis, G.J., Alonso, E. and Riesco, P. (2002) Distribution of metal extractable fractions during anaerobic sludge treatment in southern spain WWTPs. **Water Air and Soil Pollution**, 140(1-4): 139-156.

Stiff, M.J. (1971) Chemical States of Copper in Polluted Fresh Water and a Scheme of Analysis to Differentiate Them. **Water Research**, 5(8): 585-599.

Stover, R.C., Sommers, L.E. and Silveira, D. (1976) Evaluation of Metals in Wastewater-Sludge. **Journal Water Pollution Control Federation**, 48(9): 2165-2175.

Takeno N. (2005) **Atlas of Eh-pH diagrams**. Geological survey of Japan open file report No.419. pp 101-102.

Temminghoff, E.J.M., Plette, A.C.C., Van Eck, R., et al. (2000) Determination of the chemical speciation of trace metals in aqueous systems by the Wageningen Donnan Membrane Technique, **Analytica Chimica Acta**, 417(2): 149-157.

Tessier, A., Campbell, P.G.C. and Bisson, M. (1979) Sequential Extraction Procedure for the Speciation of Particulate Trace-Metals. **Analytical Chemistry**, 51(7): 844-851.

Unsworth, E.R., Warnken, K.W., Zhang, H., et al. (2006), Model predictions of metal speciation in freshwaters compared to measurements by in situ techniques. **Environmental Science & Technology**, 40(6): 1942-1949.

Van der Veen, A., Fermoso F.G. and Lens P.N.L. (2007) Bonding form analysis of metals and sulfur fractionation in methanol-grown anaerobic granular sludge. **Engineering in Life Sciences**, 7(5): 480-489.

Van Hullenbusch, E., Farges, F., Lenz, M. et al. (2007) Selenium speciation in biofilms from granular sludge bed reactors used for wastewater treatment. **X-Ray Absorption Fine Structure-XAFS**, 13: 229-231.

Van Hullebusch, E.D., Gieteling, J., Zhang, M., et al. (2006) Cobalt sorption onto anaerobic granular sludge: Isotherm and spatial localization analysis. **Journal of Biotechnology**, 121(2): 227-240.

Van Hullebusch, E.D., Utomo, S., Zandvoort, M.H., et al. (2005) Comparison of three sequential extraction procedures to describe metal fractionation in anaerobic granular sludges. **Talanta**, 65(2): 549-558.

Van Langerak, E.P.A., Beekmans, M.M.H., Beun, J.J., et al. (1999) Influence of phosphate and iron on the extent of calcium carbonate precipitation during anaerobic digestion. **Journal of Chem. Tech. and Biotech.**, 74(11): 1030-1036.

Watson, J.H.P., Ellwood, D.C., Deng, Q., et al. (1995) Heavy metal adsorption on bacterially produced FeS. **Minerals Engineering**, 8: 1097-1108.

Wu, B. (2010) CFD simulation of mixing in egg-shaped anaerobic digesters. **Water Research**, 44: 1507-1519.

Yeoman, S., Lester, J. N. and Perry, R. (1990) The Effects of Chemical Phosphorus Precipitation on Anaerobic-Digestion. **Environmental Technology**, 11(8): 709-720.

Zandvoort, M. H., van Hullebusch, E. D., Fermoso, F.G. et al. (2006) Trace metals in anaerobic granular sludge reactors: Bioavailability and dosing strategies. **Engineering in Life Sciences,** 6(3): 293-301.

Zeikus, J.G. (1977) The Biology of Methanogenic Bacteria. **Bacteriological Reviews***,* 41(2): 514-541.

Zhang, L. S., Keller, J. and Yuang, Z. (2009) Inhibition of sulfate-reducing and methanogenic activities of anaerobic sewer biofilms by ferric iron dosing. **Water Research,** 43(17): 4123-4132.

Zhang, L. S., Keller, J. and Yuang, Z. (2010) Ferrous Salt Demand for Sulfide Control in Rising Main Sewers: Tests on a Laboratory-Scale Sewer System. **Journal of Environmental Engineering**, 136(10): 1180-1187.

Zhang, Y., Jiang, J. G. and Chen, M. (2008) MINTEQ modeling for evaluating the leaching behavior of heavy metals in MSWI fly ash. **Journal of Environmental Sciences-China**, 20(11): 1398-1402.

Zhang, Y., Zhang Z., Suzuki, K. et al. (2003) Uptake and mass balance of trace metals for methane producing bacteria. **Biomass & Bioenergy**, 25(4): 427-433.

Zimmerman, A.J. and Weindorf, D.C. (2010) HeavyMetal and TraceMetal Analysis in Soil by Sequential Extraction: A Review of Procedures. **International Journal of Analytical Chemistry** [online], ID 387803. Available from: http://www.hindawi.com/journals/ijac/2010/387803/

Appendix A. Biogas measurement in the metal supplementation experiments

The biogas produced in anaerobic digesters is composed by several gases such as methane (CH_4), carbon dioxide (CO_2) and hydrogen sulphide (H_2S). Methane is the main gas and the most important from a calorific interest. So the measurement of the percentage of methane is the biogas is essential in the study of the enhancement of biogas production by metal supplementation. However, in this research the biogas production is only used as control of the behaviour of each serum bottle and so only the biogas production have been measured.

The volume of biogas produced has been measured regularly to avoid a high pressure in the serum bottle that might disturb the chemical speciation of the different species present in anaerobically digested sludge. The analytical method has been used by Ishaq (2012) and described below.

Biogas accumulated in the headspace of the bottles and was measured. The pressure in the headspace was measured using a manometer and then converted into volume using the ideal gas equation ($PV = nRT$).

.

Where:

P Pressure (N/m^2)

V Volume (m^3)

n Moles

R Universal gas constant

T Temperaure (K)

A.1 Biogas production with the sludge F1 and K1

The metal supplementation experiment using the sludge K1 and F1 has been developed in sections 7.2 and 7.6. The volumes of biogas produced during the experiment are shown in table A.1 and figure A.1.

For the sludge F1, the volumes of biogas produced presented a similar in time between the four solutions (control, TMC, CoA and CoAx2). After 302 hours, the means of the volume produced by the serum bottle were respectively 175.7 ml (control), 178.6 ml (TMC), 177.3 (CoA) and 175.7 ml (CoAx2). The maximum increase was observed between 14 and 64 hours, where the microorganism activity was at its higher potential (Ishaq, 2012).

Table A.1. Volume (ml) of biogas produced by the sludge F1 and K1

Times (hours)	Sludge F1				Sludge K1		
	Control	TMC	CoA	CoAx2	Control	TMC	CoA
0	0	0	0	0	0	0	0
14	16.7 ± 0.9	17.4 ± 1.6	16.1 ± 0.5	15.8 ± 0.5	8.0 ± 0.3	7.9 ± 0.6	8.3 ± 1.1
19	27.6 ± 1.0	28.7 ± 2.0	26.2 ± 0.6	26.2 ± 1.0	14.3 ± 0.4	14.3 ± 0.9	14.5 ± 1.7
24	37.4 ± 1.0	38.2 ± 2.1	35.6 ± 0.4	35.4 ± 1.2	17.7 ± 0.3	17.5 ± 0.8	17.8 ± 1.8
37	55.6 ± 1.0	56.5 ± 2.2	53.1 ± 0.4	52.9 ± 1.0	42.5 ± 0.6	43.4 ± 0.9	44.0 ± 2.4
42	64.4 ± 1.0	65.8 ± 2.5	61.9 ± 0.4	61.9 ± 1.2	54.8 ± 0.5	56.2 ± 0.9	56.7 ± 2.5
45	69.5 ± 0.9	71.2 ± 2.5	67.2 ± 0.4	67.2 ± 1.1	61.8 ± 0.1	63.8 ± 1.1	63.9 ± 2.5
64	95.4 ± 1.3	98.0 ± 2.5	93.1 ± 0.3	92.7 ± 1.1	83.8 ± 0.3	84.7 ± 0.7	86.5 ± 1.8
111	134.1 ± 1.6	134.5 ± 1.9	130.1 ± 1.7	129.1 ± 0.6	93.3 ± 0.5	94.5 ± 0.9	95.6 ± 1.8
136	147.4 ± 1.9	148.2 ± 1.5	144.3 ± 2.3	143.3 ± 0.9	113.5 ± 0.3	114.7 ± 1.1	115.2 ± 1.5
184	160.4± 2.6	162.2 ± 1.9	160.3 ± 3.1	159.2 ± 0.7	139.5 ± 0.6	140.5 ± 1.4	139.4 ± 1.6
208	165.8 ± 3.0	168.1 ± 2.4	166.6 ± 3.2	165.5 ± 0.8	149.7 ± 1.1	151.1 ± 1.6	149.3 ± 1.2
279	172.5 ± 3.3	175.3 ± 2.8	174.1 ± 3.2	172.7 ±0.9	157.8 ± 1.1	159.2 ± 1.8	157.1 ± 1.9
302	175.7 ± 3.4	178.6 ± 2.9	177.3 ± 3.3	175.7 ± 0.9	163.9 ± 1.1	165.6 ± 2.3	162.9 ± 2.2

The volumes (ml) are expressed as mean ± standard deviation

For the sludge K1, the volumes of biogas produced were similar in time between the three solutions used in this experiment (control, TMC and CoA). After 302 hours, the means of the volume produced by the serum bottle were respectively 163.9 ml (control), 165.6 ml (TMC) and 162.9 ml (CoA). The maximum increase was observed between 24 and 45 hours, where the microorganism activity was at its higher potential (Ishaq, 2012).

At any time, the volume of biogas between the three solutions was similar and confirming a parallel in the biological activities in each solution. Moreover, the low standard deviation values validated that each serum bottle had been working similarly.

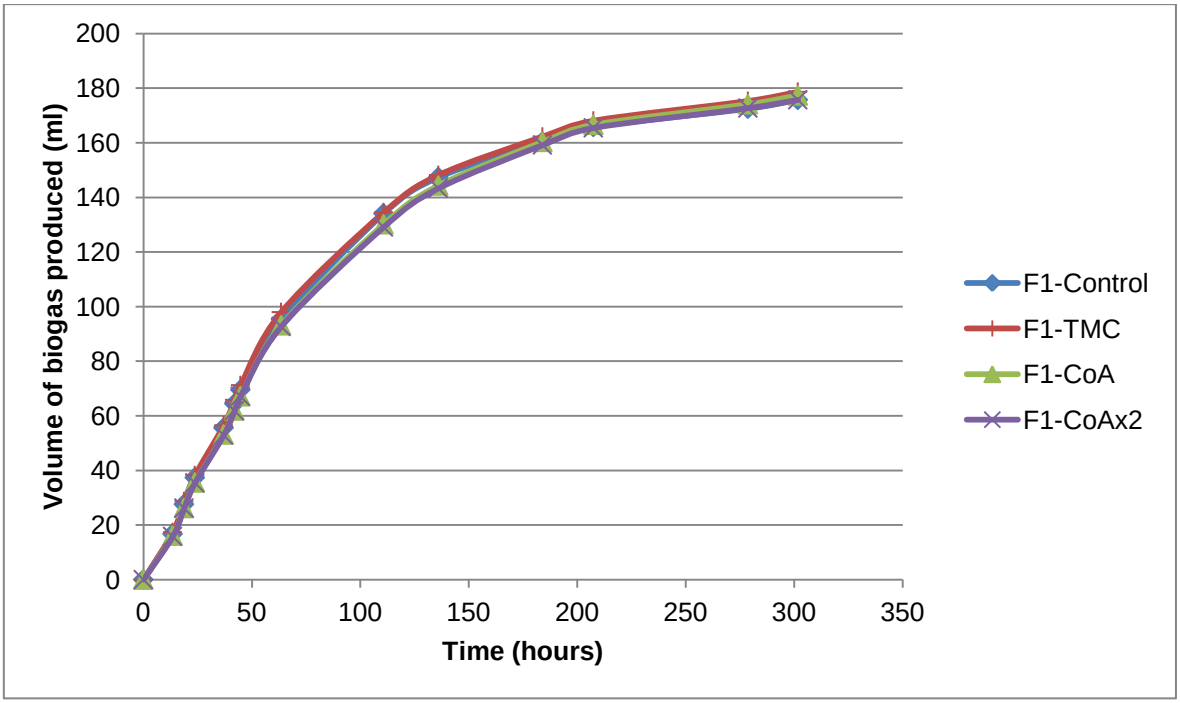

Figure A.1. Biogas production for the sludge F1

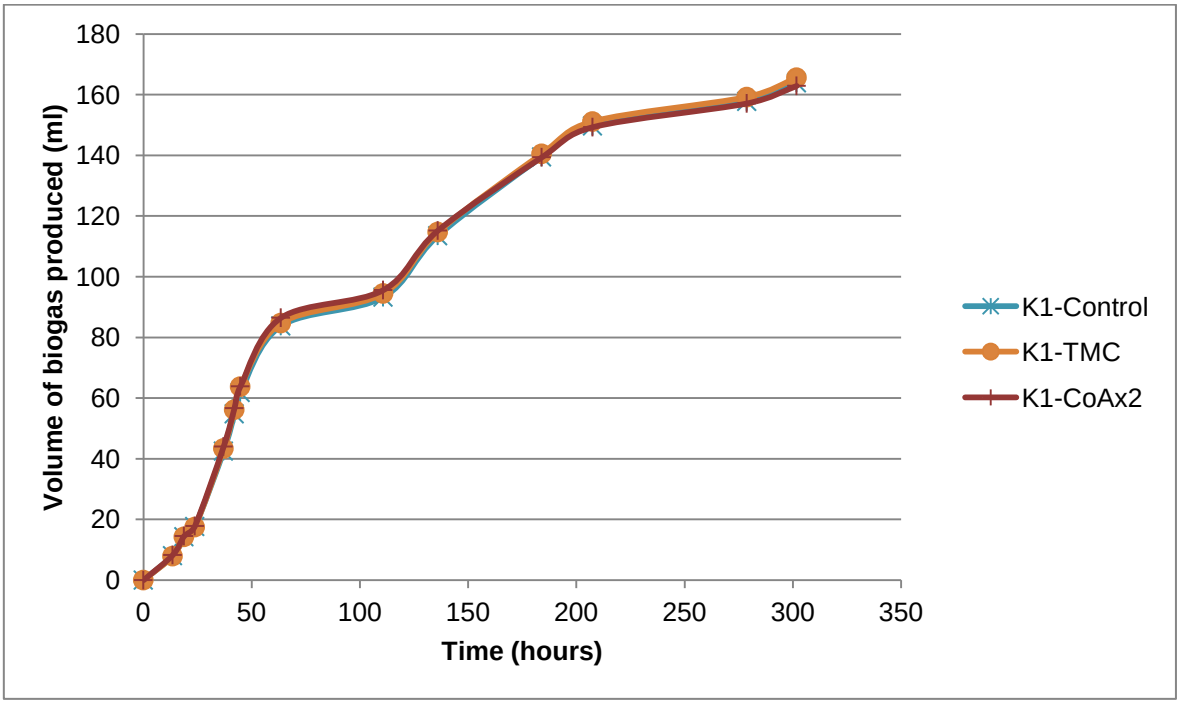

Figure A.2. Biogas production for the sludge K1

A.2 Biogas production with the sludge F2 and K2

The metal supplementation experiment using the sludge K2 has been described in section 7.6. The volumes of biogas produced during the experiment are shown in table A.2 and figure A.2.

For the sludge F2, the volumes of biogas produced presented a similar pattern in time between the control and the CoA solutions. After 311 hours, the means of the volume produced by the serum bottle were respectively 191.5 ml (control) and 204.5 ml (CoA). The maximum increase was observed between 16 and 67 hours, where the microorganism was at its higher potential (Ishaq, 2012). At any time, the volumes of biogas produced by the CoA and control solution were similar except for the two last measurements where the volumes from controls were lower than for CoA solution. This difference might be explained by a higher standard deviation values in those two measurements, suggesting the presence of difference between the serum bottles.

Table A.2. Volume (ml) of biogas produced by the sludge F2 and K2

Time (hours)	Sludge F2		Sludge K2	
	Control	CoA	Control	CoA
0	0	0	0	0
15	22.4 ± 1.1	20.5 ± 1.4	22.2 ± 2.4	13.7 ± 1.1
23	38.9 ± 1.3	36.6 ± 2.2	43.7 ± 4.0	27.9 ± 1.4
39	70.1± 1.9	67.4 ± 3.6	82.2 ± 5.7	55.9 ± 3.0
47	94.5 ± 3.3	93.8 ± 4.9	104.0 ± 6.8	73.6 ± 2.3
62	123.3 ± 3.7	120.2 ± 5.4	134.9 ± 8.3	99.6 ± 3.3
71	137.3 ± 3.5	135.8 ± 5.8	150.6 ± 8.7	116.2 ± 3.9
88	155.9 ± 4.3	154.7 ± 5.9	166.9 ± 8.2	140.1 ± 4.0
95	173.6 ± 3.9	173.1 ± 4.4	173.8 ± 7.3	150.9 ± 3.9
120	180.2 ± 1.1	183.5 ± 3.8	180.0 ± 7.6	166.5 ± 2.8
144	185.0 ± 0.9	189.1 ± 3.7	185.7 ± 6.5	175.6 ± 2.3
165	190.5 ± 1.4	193.9 ± 3.0	188.1 ± 6.4	178.9 ± 2.1
238	189.5 ± 7.3	197.5 ± 3.0	198.1 ± 7.0	188.8 ± 2.8
311	191.5 ± 8.3	204.5 ± 3.7	204.2 ± 8.6	195.4 ± 3.2

The volumes (ml) are expressed as mean ± standard deviation

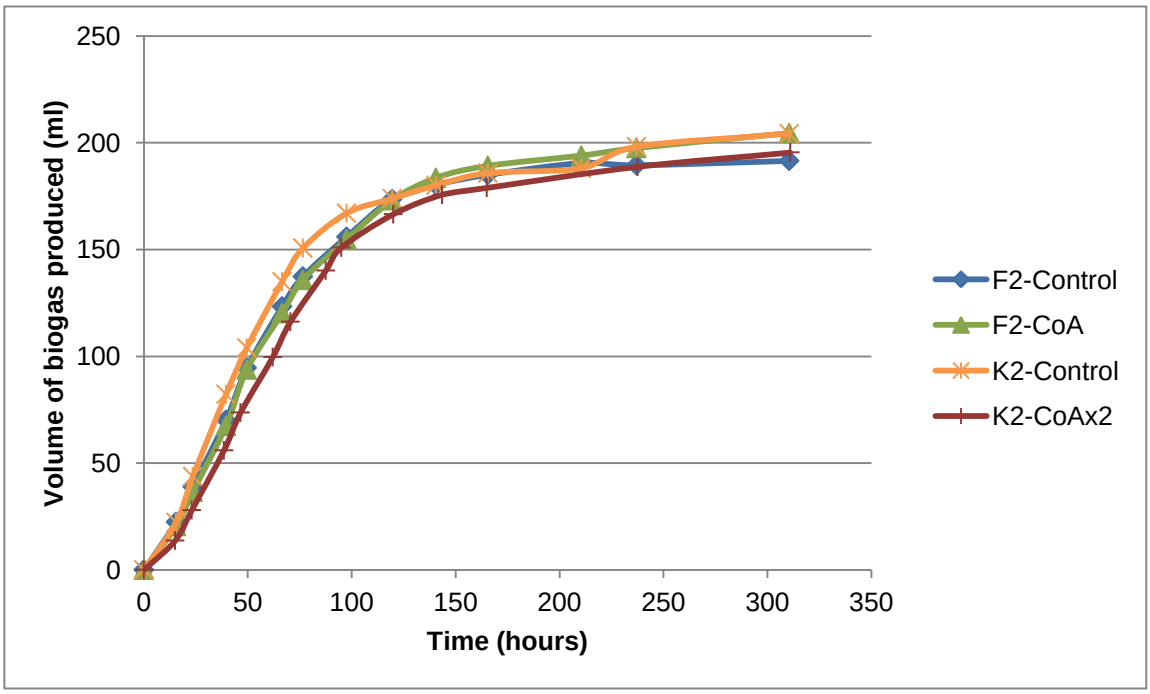

Figure A.3. Biogas production for the sludge F1 and K1

For the sludge K2, the volumes of biogas produced presented a similar pattern in time between the control and the CoA solutions. After 311 hours, the means of the volume produced by the serum bottle were respectively 204.2 ml (control) and 195.4 ml (CoA). The maximum increase was observed between 15 and 88 hours, where the microorganism activity was at its higher potential (Ishaq, 2012). At any time, the volume of biogas produced by the CoA solution was lower than the volume produced in the control solution. However, the pattern of the curves was similar and it was confirming a parallel in the biological activities in both solutions.

Concerning the standard deviation, values were all below a limit of 10% RSD, validating that each serum bottle has been working in the same way as the others.

Appendix B. X-Ray diffraction spectroscopy analysis

The two peaks at 2θ: 20 and 27° on the XRD demonstrated that crystals precipitates are present in anaerobically digested sludge. However, organics and other amorphous precipitates disturb the curve baseline and the accuracy of analysis. Moreover the concentration of crystal compound in the sludge is too low for any detection. Several other peaks related to the detected crystal compounds are missing to obtain a complete identification.

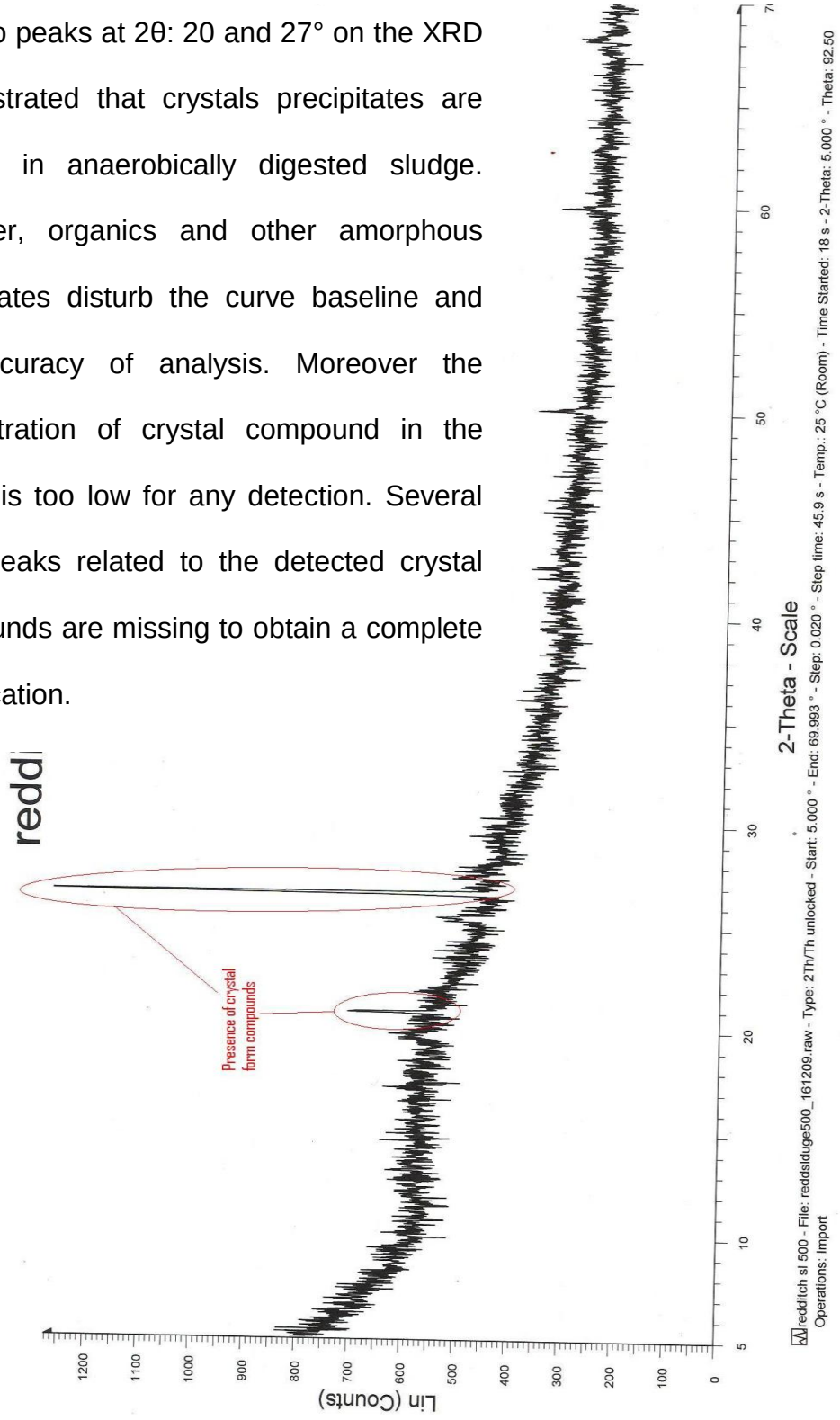

Appendix C: Crystallography

C.1 Aragonite

Aragonite ($CaCO_3$) was observed in anaerobically digested sludge using SEM-EDS analysis (section 5.4). Aragonite precipitates following an orthorhombic crystal system with a dipyramidal class (Anthony et al., 2012). Orthorhombic crystal system can be described as a rectangular prism, with all three bases intersect at an angles of 90° and with different lengths. The morphology of aragonite is described as columnar crystal aggregate and this structure is clearly observed (figure C.1), confirming the classification of the calcium carbonate as aragonite.

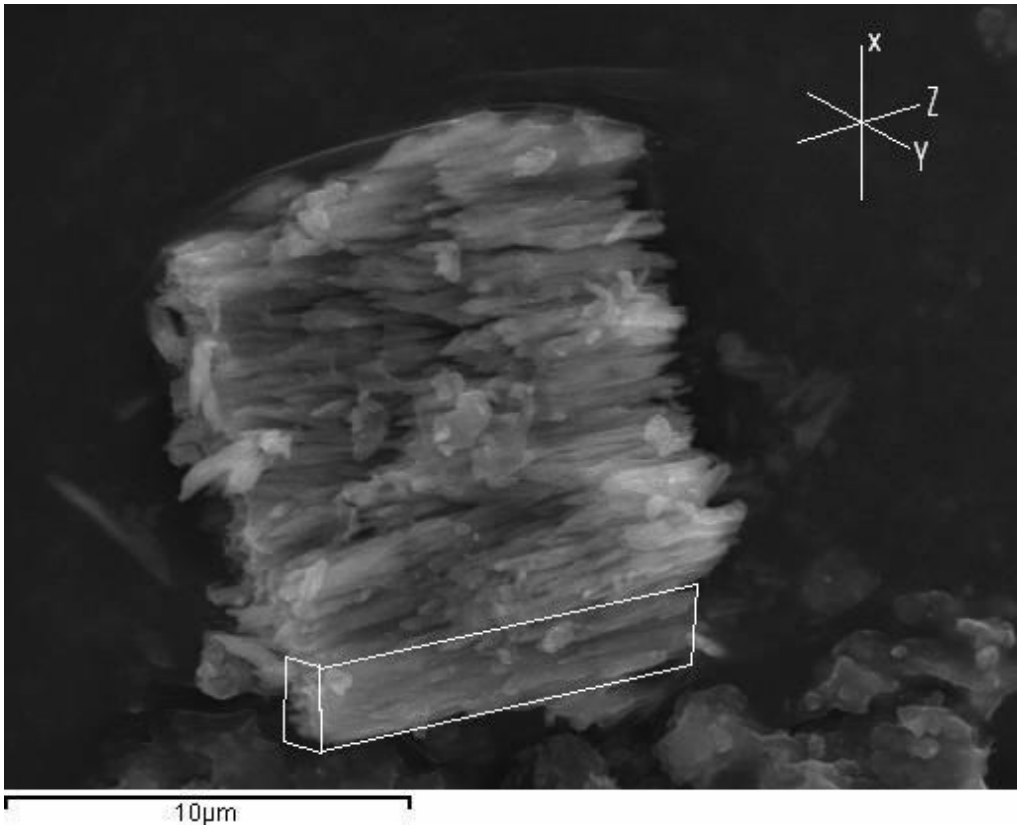

Figure C.1. Presence of othorhombic-dipyramidal crystal structure on the aragonite precipitate detected in anaerobically digested sludge using SEM-EDS analysis.

C.2 Dolomite

Dolomite ($CaMg(CO_3)_2$) was observed in anaerobically digested sludge using SEM-EDS analysis (section 5.4). Dolomite precipitates following a trigonal crystal system with a rhombohedral class (Anthony et al., 2012). Trigonal-rhombohedral crystal system can be described as a cubic system stretched along a diagonal, with three vectors of equal length and no two of which are orthogonal. The stretched cubic form might be observed in figure C.2, confirming the classification of the calcium magnesium carbonate as dolomite.

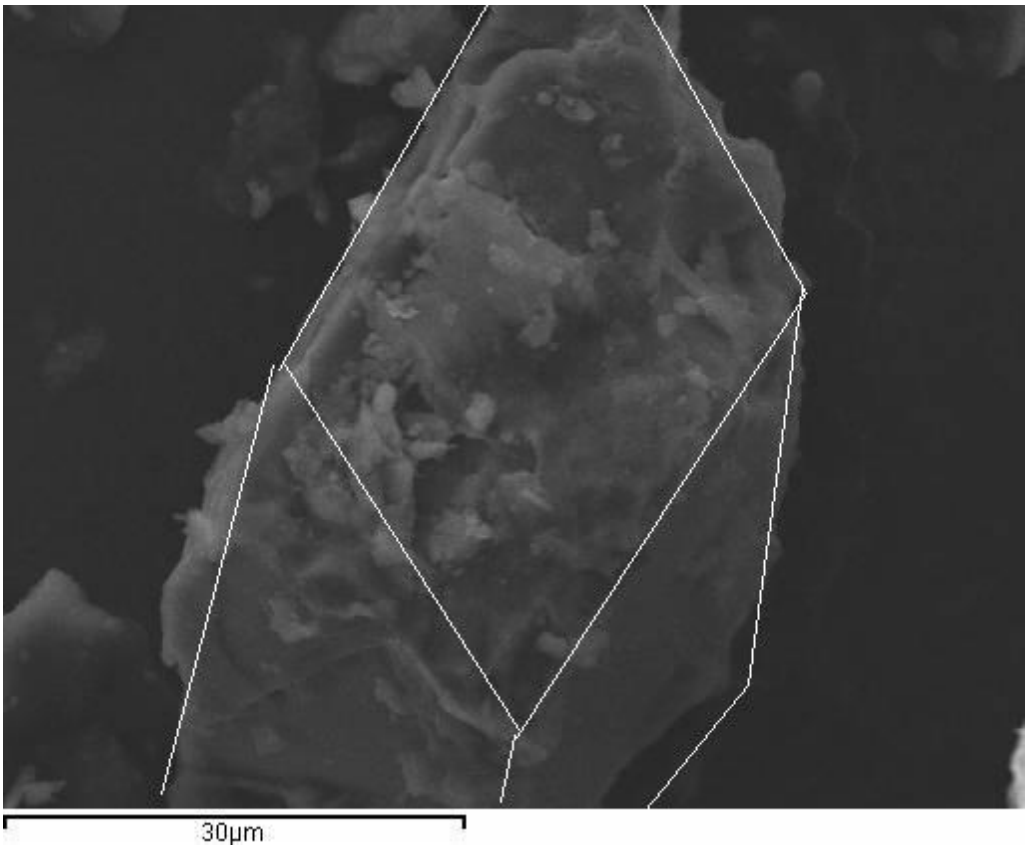

Figure C.2. Presence of trigonal-rhombohedral crystal structure on the dolomite precipitate detected in anaerobically digested sludge using SEM-EDS analysis.

C.3 Pyrite

Pyrite (FeS_2) was observed in anaerobically digested sludge using SEM-EDS analysis (Section 6.2.2). Pyrite precipitates following a cubic crystal system and the presence of cube is clearly observed using backscattering detection in the picture C.3. The EDS analysis confirmed the presence of only iron and sulphide in the compounds with a ratio of Fe/S of ½.

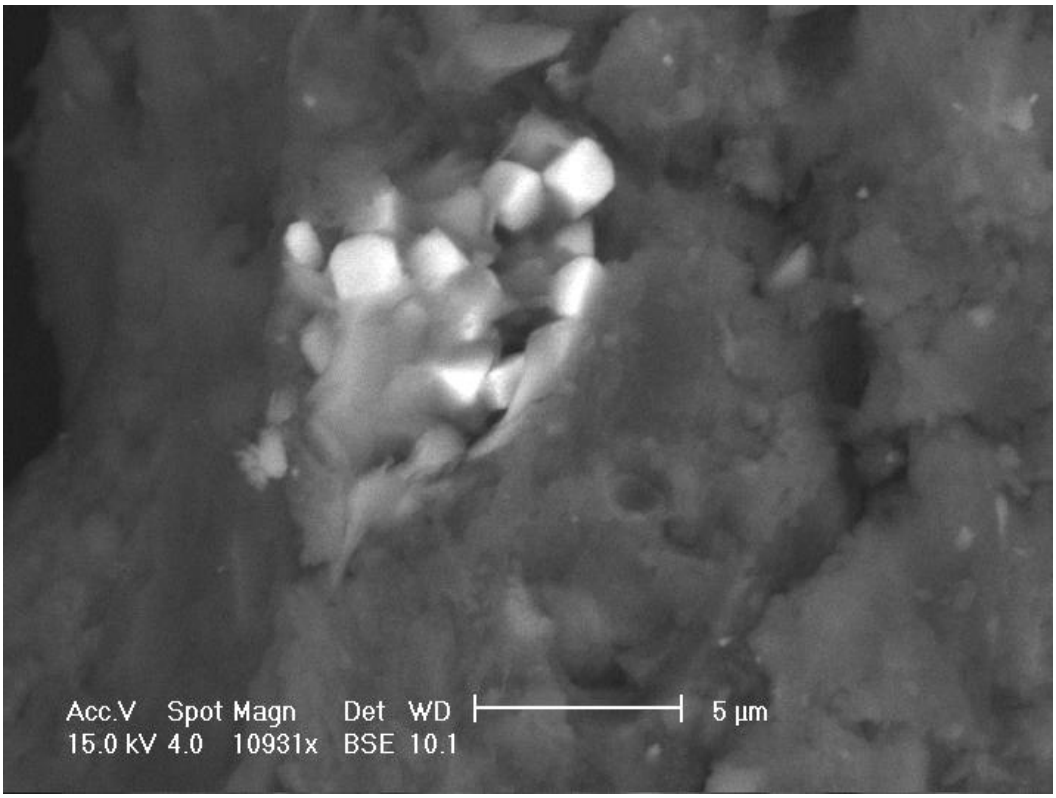

Figure C.3. Presence of cubic crystal structure on the pyrite precipitate detected in anaerobically digested sludge using SEM-EDS analysis.

C.4 Vivianite

Vivianite ($Fe_3(PO_4)_2.8H_2O$) was observed in anaerobically digested sludge using SEM-EDS analysis (section 6.2.2). Vivianite precipitates following a monoclinic

crystal system with a prismatic class (Anthony et al., 2012). Monoclinic-prismatic crystal system can be described as a rectangular prism with a parallelogram base, with three vectors of unequal length and only two of them are perpendicular. The morphology of vivanite is described as flattened following one axis. In figure C.4, the parallelogram base cannot be distinguished due to the angle of the picture. However, the compound is composed of a series of flattened parallelepiped piled on the top of each other. A similar structure is also observed on macroscopic vivianite presented in figure C.5. Finally SEM-EDS analysis showed that vivianite might growth on silicon dioxide under anaerobic condition and the figure C.6, showed a similar interaction at a macroscopic aspect between silicon dioxide and vivianite in the Chicote Grande Mine in Bolivia.

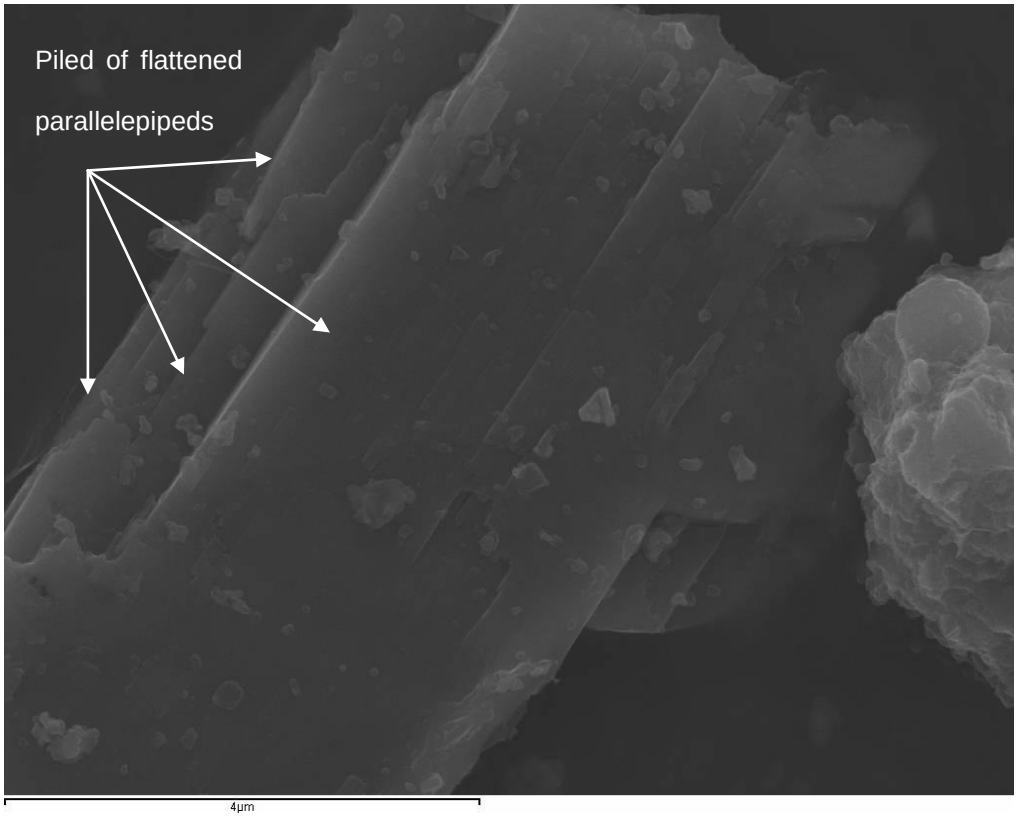

Figure C.4. Presence of piled of flattened parallelepipeds crystal structure on the vivianite precipitate detected in anaerobically digested sludge using SEM-EDS analysis.

Figure C.5. Pictures of macroscopic vivianite extracted in Huanuni mine, Bolivia (www.mindat.org, photos 36945 (left) and 16421 (right))

Figure C.6. Picture of macroscopic vivianite with silicon dioxide extracted in the Chicote Grande mine, Bolivia (www.mindat.org, photos 329869)

Appendix D. Kinetic order of reaction

In chapter 7, cobalt was supplemented in anaerobically digested sludge as $CoEDTA^{2-}$. The reaction of cobalt transfer from the liquid phase to the solid phase can be summarized following a reaction of substitution or dissociation (reaction 1 and 2). Then the free cobalt ion was quickly transferred into the solid phase by precipitation, complexation or adsorption. In this suite of chemical reaction, the speed was limited by the reaction forming the free cobalt ion as adsorption, complexation and precipitation reactions have been described as very fast by Aquino and Stuckey (2007).

The speed of the reaction (r) can be defined as $r = -\frac{\partial[\mathrm{CoEDTA2-}]}{\partial \mathrm{t}}$

$$CoEDTA^{2-} + Me^{2+} \longrightarrow MeEDTA^{2-} +, Co^{2+} \quad [1]$$

$$CoEDTA^{2-} \longrightarrow EDTA^{4-} +, Co^{2+} \quad [2]$$

The speed of reaction can also be defined using the rate law and orders of reactions. For the reaction 2, only one reactant was present with a stoichiometric coefficient of one. So the reaction rate was proportional to the concentration of $CoEDTA^{2-}$ and the order of reaction was 1. It can be written as $r = k\,[CoEDTA^{2-}]$, with k a constant defined in the Arrhenius equation.

Using the two definition of the reaction rate, the concentration of the reactant in function of the time can be defined as:

$$r = -\frac{\partial[\mathrm{CoEDTA2-}]}{\partial \mathrm{t}} = k\,[CoEDTA^{2-}]$$

By integration, the concentration of $CoEDTA^{2-}$ can be expressed in function of time and the initial concentration as:

$$k \times t = \mathrm{Ln}\,[CoEDTA^{2-}]_0 - \mathrm{ln}\,[CoEDTA^{2-}]$$

A linear equation between time and the logarithm of the concentration characterizes a reaction of the first order.

For the reaction 1, two reactants were present with a stoichiometric coefficient of one. So the reaction rate was proportional to the concentration of $CoEDTA^{2-}$ and the concentration of the other metal. So the order of reaction was 2 and the rate equation can be written as:

$$r = k\,[CoEDTA^{2-}] \times [Me^{2+}].$$

However, several approximations have been made to simplify the equation due to the presence of different metals reacting with the $CoEDTA^{2-}$. The main approximation was to consider that the initial concentration of metals reacting was equal to the initial concentration of $CoEDTA^{2-}$. Although the concentration of free metal ion is lower than $[CoEDTA^{2-}]_0$, a dissolution of metals occurred from the solid phase to keep the concentration of free metal ion constant (defined by the equilibrium). Those transfer reactions were considered to be as quick as the precipitation, complexation and adsorption reactions and so it did not affect the speed of the reaction 1. Therefore the amount of metal transferred was equivalent to the amount of $CoEDTA^{2-}$ that has been reacted. Considering $[CoEDTA^{2-}]_0 = [Me^{2+}]_0$, the rate equation can be simplified as:

$$r = -\frac{\partial[\mathrm{CoEDTA2-}]}{\partial \mathrm{t}} = k\,[CoEDTA^{2-}]^2,$$

By integration, the concentration of $CoEDTA^{2-}$ can be expressed in function of time and the initial concentration as:

$$k \times t = 1/[CoEDTA^{2-}] - 1/\,[CoEDTA^{2-}]_0$$

A linear equation between time and the inverse of the concentration characterizes a reaction of the second order.

Appendix E: Input values for the model simulations

The initial input values used for the Phreeqc and Visual Minteq simulation in the three results chapters 5-7. These values were obtained from experimental measurements.

Table E.1. Input values for the model simulations

		Chapters 5 and 6 simulations							Chapter 7 simulations	
Sludge		K	G	M	H	S	R	F	K	F
Iron dosing		No	No	Mix	Mix	Mix	Yes	Yes	No	Yes
Conditions	pH	8	8	8	8.1	8.1	8.1	8.2	8	8.2
	pE	-6.7	-6.7	-6.7	-6.7	-6.7	-6.7	-6.7	-6.7	-6.7
	T (°C)	35	35	35	35	35	35	35	35	35
Metals (mmol/l)	Co	0.024	0.024	0.023	0.021	0.029	0.025	0.027	0.024	0.027
	Cu	0.16	0.090	0.11	0.17	0.085	0.13	0.064	0.13	0.090
	Fe	3.5	3.6	6.8	7.1	8	8.5	10.4	3.2	19.2
	Mn	0.13	0.13	0.26	0.079	0.087	0.11	0.13	0.071	0.11
	Ni	0.38	0.40	0.43	0.44	0.36	0.45	0.47	0.32	0.38
	Zn	0.22	0.18	0.50	0.19	0.27	0.25	0.26	0.15	0.25
Cations (mmol/l)	Ca	8.8	9.6	10.5	10.5	11.9	9.7	11	8.8	11.3
	K	2.6	2.3	2.3	2.7	2.5	2.8	3.0	2.4	2.8
	Mg	4.2	4.4	4.8	5.1	5.3	4.7	5.1	4.4	5.1
	Na	9.7	9.9	9.1	9.3	9.4	9.5	9.9	9.9	9.8
Anions (mmol/l)	C*	34.9	46.8	50.8	43.8	58.3	40.4	51.6	35.3	52.5
	P	13.9	13.2	14.1	15.6	15.8	15.1	11.1	12.3	13.2
	S	5.9	5.5	5.5	4.4	4.2	5.5	7.8	5.7	8.2

Appendix F: Predictions of the metals speciation in the seven anaerobically digested sludge using Phreeqc

Table F.1. Prediction of the metals speciation in the seven types of anaerobically digested sludge using Phreeqc (concentration in mol/l)

Model concentration (mol/l)								
Sludge		K	G	M	H	S	R	F
Iron dosing		No	No	Mix	Mix	Mix	Yes	Yes
Metals in the liquid phase	Co	1.4×10^{-12}	1.9×10^{-12}	2.7×10^{-12}	2.8×10^{-12}	3.3×10^{-12}	3.4×10^{-12}	2.5×10^{-12}
	Cu	9.3×10^{-7}	7.7×10^{-7}	4.3×10^{-7}	3.5×10^{-7}	3.4×10^{-7}	2.2×10^{-7}	4.0×10^{-7}
	Fe	2.5×10^{-6}	2.7×10^{-6}	3.1×10^{-6}	3.1×10^{-6}	3.3×10^{-6}	3.6×10^{-6}	3.3×10^{-6}
	Mn	1.4×10^{-10}	1.6×10^{-10}	2.2×10^{-10}	1.9×10^{-10}	2.1×10^{-10}	2.4×10^{-10}	4.3×10^{-10}
	Ni	2.4×10^{-14}	3.4×10^{-14}	5.3×10^{-14}	5.3×10^{-14}	6.4×10^{-14}	6.5×10^{-14}	5.3×10^{-14}
	Zn	1.7×10^{-10}	1.7×10^{-10}	1.4×10^{-10}	1.3×10^{-10}	1.3×10^{-10}	1.2×10^{-10}	1.3×10^{-10}
Metals in the solid phase	CoS	2.4×10^{-5}	2.4×10^{-5}	2.3×10^{-5}	2.1×10^{-5}	2.9×10^{-5}	2.5×10^{-5}	2.7×10^{-5}
	Covellite (CuS)	1.6×10^{-4}	9.0×10^{-5}	1.1×10^{-4}	1.7×10^{-4}	8.5×10^{-5}	1.3×10^{-4}	6.4×10^{-5}
	Pyrite (FeS_2)	2.6×10^{-3}	2.4×10^{-3}	2.2×10^{-3}	1.8×10^{-3}	1.7×10^{-3}	2.1×10^{-3}	3.5×10^{-3}
	Vivianite ($Fe_3(PO)_4{:}8H_2O$)	3.2×10^{-4}	4.0×10^{-4}	1.5×10^{-3}	1.8×10^{-3}	2.1×10^{-3}	2.2×10^{-3}	2.3×10^{-3}
	$MnHPO_4$	1.3×10^{-4}	1.3×10^{-4}	2.6×10^{-4}	7.9×10^{-5}	8.7×10^{-5}	1.1×10^{-4}	1.3×10^{-4}
	NiS	3.8×10^{-4}	4.0×10^{-4}	4.3×10^{-4}	4.4×10^{-4}	3.6×10^{-4}	4.5×10^{-4}	4.7×10^{-4}
	Sphalerite (ZnS)	2.2×10^{-4}	1.8×10^{-4}	5.0×10^{-4}	1.9×10^{-4}	2.7×10^{-4}	2.5×10^{-4}	2.6×10^{-4}

Table F.2. Prediction of the metals speciation in the seven types of anaerobically digested sludge using Phreeqc (concentration in mg/l and g/kg DS)

Converted concentration									
Sludge			K	G	M	H	S	R	F
Iron dosing			No	No	Mix	Mix	Mix	Yes	Yes
Metals in the liquid phase	Co	mg/l	8.3×10^{-8}	1.1×10^{-7}	1.6×10^{-7}	1.7×10^{-7}	1.9×10^{-7}	2.0×10^{-7}	1.5×10^{-7}
	Cu		5.9×10^{-2}	4.9×10^{-2}	2.7×10^{-2}	2.2×10^{-2}	2.2×10^{-2}	1.4×10^{-2}	2.5×10^{-2}
	Fe		0.14	0.15	0.17	0.17	0.18	0.20	0.18
	Mn		7.7×10^{-6}	8.8×10^{-6}	1.2×10^{-5}	1.1×10^{-5}	1.2×10^{-5}	1.3×10^{-5}	2.4×10^{-5}
	Ni		1.4×10^{-9}	2.0×10^{-9}	3.1×10^{-9}	3.1×10^{-9}	3.8×10^{-9}	3.8×10^{-9}	3.1×10^{-9}
	Zn		1.1×10^{-5}	1.1×10^{-5}	9.2×10^{-6}	8.5×10^{-6}	8.5×10^{-6}	7.8×10^{-6}	8.5×10^{-6}
Metals in the solid phase	Co	g/kg DS	0.071	0.071	0.068	0.062	0.086	0.074	0.080
	Cu		0.50	0.29	0.35	0.61	0.27	0.40	0.19
	Fe^1		7.2	6.7	6.2	5.0	4.8	5.9	9.8
	Fe^2		2.7	3.4	12.6	14.9	17.6	18.2	19.3
	Mn		0.35	0.35	0.71	0.22	0.24	0.3	0.35
	Ni		1.1	1.1	1.2	1.2	1.1	1.3	1.3
	Zn		0.73	0.57	1.5	0.66	0.88	0.82	0.86

Fe^1: Fe precipitated as pyrite Fe^2: Fe precipitated as vivianite

Appendix G: Example of Phreeqc simulation using the sludge K

```
Input file: E:\PhD\Correction\Files\Phreeqc\K3 pe_6.7_tc_woha.pqi
  Output file: E:\PhD\Correction\Files\Phreeqc\K3 pe_6.7_tc_woha.pqo
Database file: C:\Program Files (x86)\USGS\Phreeqc Interactive
2.17.4137\database\minteq.v4.dat

------------------
Reading data base.
------------------

      SOLUTION_MASTER_SPECIES
      SOLUTION_SPECIES
      SOLUTION_SPECIES
      PHASES
      PHASES
      SURFACE_MASTER_SPECIES
      SURFACE_SPECIES
      END
-----------------------------------
Reading input data for simulation 1.
-----------------------------------

      DATABASE C:\Program Files (x86)\USGS\Phreeqc Interactive
2.17.4137\database\minteq.v4.dat
      SOLUTION 1
          temp      35
          pH        8
          pe        -6.7
          redox     pe
          units     mmol/l
          density   1
          C         34.9
          Co        0.024
          Cu        0.16
          Fe        3.5
          Mn        0.13
          N(-3)     28 charge
          Ni        0.38
          P         13.9
          S         5.9
          Zn        0.22
          Ca        8.8
          Na        9.7
          Mg        4.2
          K         2.6
          water    1 # kg
      EQUILIBRIUM_PHASES 1
          Aragonite 0 0
          Bunsenite 0 0
          Ca3(PO4)2(beta) 0 0
          Ca4H(PO4)3:3H2O 0 0
```

```
          Calcite   0 0
          Co3(PO4)2 0 0
          CoCO3     0 0
          CoS(beta) 0 0
          Covellite 0 0
          Cuprite   0 0
          Dolomite(disordered) 0 0
          Ferrihydrite 0 0
          FeS(ppt)  0 0
          Goethite  0 0
          Greigite  0 0
          Hematite  0 0
          Huntite   0 0
          Mackinawite 0 0
          Magnesite 0 0
          Magnetite 0 0
          MnHPO4    0 0
          Ni3(PO4)2 0 0
          NiS(gamma) 0 0
          Pyrite    0 0
          Rhodochrosite 0 0
          Siderite  0 0
          Sphalerite 0 0
          Strengite 0 0
          Vivianite 0 0
          Wurtzite  0 0
          Zn3(PO4)2:4H2O 0 0
          ZnS(am)   0 0
-----------------------------------------
Beginning of initial solution calculations.
-----------------------------------------

Initial solution 1.

-----------------------------Solution composition------------------------
------

      Elements           Molality       Moles

      C                3.506e-002  3.506e-002
      Ca               8.840e-003  8.840e-003
      Co               2.411e-005  2.411e-005
      Cu               1.607e-004  1.607e-004
      Fe               3.516e-003  3.516e-003
      K                2.612e-003  2.612e-003
      Mg               4.219e-003  4.219e-003
      Mn               1.306e-004  1.306e-004
      N(-3)            2.385e-002  2.385e-002  Charge balance
      Na               9.744e-003  9.744e-003
      Ni               3.817e-004  3.817e-004
      P                1.396e-002  1.396e-002
      S                5.927e-003  5.927e-003
      Zn               2.210e-004  2.210e-004

----------------------------Description of solution----------------------
------

                                    pH  =   8.000
```

```
                                    pe  =  -6.700
                       Activity of water  =   0.998
                          Ionic strength  =  6.298e-002
                       Mass of water (kg)  =  1.000e+000
                 Total alkalinity (eq/kg)  =  5.707e-002
                       Total CO2 (mol/kg)  =  3.506e-002
                      Temperature (deg C)  =  35.000
                   Electrical balance (eq)  = -2.666e-015
 Percent error, 100*(Cat-|An|)/(Cat+|An|)  =  -0.00
                                Iterations  =  11
                                   Total H  = 1.111619e+002
                                   Total O  = 5.566787e+001
--------
Partially cut
-----------------------------------------
Beginning of batch-reaction calculations.
-----------------------------------------

Reaction step 1.

Using solution 1.
Using pure phase assemblage 1.

-------------------------------Phase assemblage--------------------------
------
```

Phase	SI	log IAP	log KT	Moles in assemblage: Initial	Final	Delta
Aragonite	-0.63	-9.00	-8.37	0.000e+000	0	0.000e+000
Bunsenite	-12.11	-0.23	11.88	0.000e+000	0	0.000e+000
Ca3(PO4)2(beta)	0.00	-28.61	-28.61	0.000e+000	2.593e-003	2.593e-003
Ca4H(PO4)3:3H2O	-0.84	-47.92	-47.08	0.000e+000	0	0.000e+000
Calcite	-0.48	-9.00	-8.53	0.000e+000	0	0.000e+000
Co3(PO4)2	-19.40	-54.09	-34.69	0.000e+000	0	0.000e+000
CoCO3	-7.44	-17.50	-10.05	0.000e+000	0	0.000e+000
CoS(beta)	0.00	-11.07	-11.07	0.000e+000	2.411e-005	2.411e-005
Covellite	0.00	-21.75	-21.75	0.000e+000	1.598e-004	1.598e-004
Cuprite	-10.17	-12.28	-2.11	0.000e+000	0	0.000e+000
Dolomite	0.00	-16.80	-16.80	0.000e+000	8.485e-004	8.485e-004
Ferrihydrite	-8.34	-5.57	2.77	0.000e+000	0	0.000e+000
FeS(ppt)	-2.03	-5.04	-3.01	0.000e+000	0	0.000e+000
Goethite	-5.72	-5.57	0.15	0.000e+000	0	0.000e+000
Greigite	-8.84	-53.88	-45.03	0.000e+000	0	0.000e+000
Hematite	-8.99	-11.14	-2.15	0.000e+000	0	0.000e+000
Huntite	-1.83	-32.41	-30.58	0.000e+000	0	0.000e+000
Mackinawite	-1.44	-5.04	-3.60	0.000e+000	0	0.000e+000
Magnesite	-0.45	-7.80	-7.35	0.000e+000	0	0.000e+000
Magnetite	-5.83	-3.61	2.22	0.000e+000	0	0.000e+000
MnHPO4	0.00	-25.40	-25.40	0.000e+000	1.306e-004	1.306e-004
Ni3(PO4)2	-27.98	-59.28	-31.30	0.000e+000	0	0.000e+000
NiS(gamma)	0.00	-12.80	-12.80	0.000e+000	3.817e-004	3.817e-004
Pyrite	0.00	-18.22	-18.22	0.000e+000	2.566e-003	2.566e-003
Rhodochrosite	-4.51	-15.10	-10.59	0.000e+000	0	0.000e+000
Siderite	-1.13	-11.46	-10.33	0.000e+000	0	0.000e+000
Sphalerite	0.00	-11.28	-11.28	0.000e+000	2.210e-004	2.210e-004
Strengite	-8.41	-34.86	-26.45	0.000e+000	0	0.000e+000
Vivianite	0.00	-36.00	-36.00	0.000e+000	3.159e-004	3.159e-004

```
Wurtzite       -2.45  -11.28   -8.83   0.000e+000           0  0.000e+000
Zn3(PO4)2:4H2O-19.30  -54.72  -35.42   0.000e+000           0  0.000e+000
ZnS(am)        -2.31  -11.28   -8.96   0.000e+000           0  0.000e+000

----------------------------Solution composition------------------------

      Elements           Molality       Moles

      C                3.336e-002  3.336e-002
      Ca               2.120e-004  2.120e-004
      Co               1.447e-012  1.447e-012
      Cu               9.288e-007  9.287e-007
      Fe               2.511e-006  2.510e-006
      K                2.612e-003  2.612e-003
      Mg               3.371e-003  3.371e-003
      Mn               1.431e-010  1.431e-010
      N                2.385e-002  2.385e-002
      Na               9.744e-003  9.744e-003
      Ni               2.421e-014  2.421e-014
      P                8.015e-003  8.014e-003
      S                8.896e-006  8.896e-006
      Zn               1.715e-010  1.715e-010

----------------------------Description of solution----------------------
------

                                    pH  =   7.314      Charge balance
                                    pe  =  -7.444      Adjusted to
redox equilibrium
                        Activity of water  =   0.999
                           Ionic strength  =  4.597e-002
                       Mass of water (kg)  =  1.000e+000
                Total alkalinity (eq/kg)  =  3.536e-002
                       Total CO2 (mol/kg)  =  3.336e-002
                     Temperature (deg C)  =  35.000
                  Electrical balance (eq)  = -3.364e-015
 Percent error, 100*(Cat-|An|)/(Cat+|An|)  =  -0.00
                                Iterations  =  29
                                   Total H  = 1.111567e+002
                                   Total O  = 5.563646e+001

----------------------------Distribution of species----------------------


                                                    Log       Log
Log
   Species           Molality    Activity  Molality  Activity     Gamma

   OH-              3.479e-007  2.833e-007    -6.459    -6.548    -0.089
   H+               8.950e-008  7.369e-008    -7.048    -7.133    -0.084
   H2O              5.551e+001  9.986e-001     1.744    -0.001     0.000
C(4)         3.340e-002
   HCO3-            2.935e-002  2.439e-002    -1.532    -1.613    -0.080
   H2CO3            3.585e-003  3.585e-003    -2.445    -2.445     0.000
   MgHCO3+          2.705e-004  2.215e-004    -3.568    -3.655    -0.087
   NaHCO3           8.875e-005  8.875e-005    -4.052    -4.052     0.000
   CO3-2            4.087e-005  1.878e-005    -4.389    -4.726    -0.338
   CaHCO3+          3.733e-005  3.119e-005    -4.428    -4.506    -0.078
```

MgCO3	1.540e-005	1.540e-005	-4.812	-4.812	0.000
NaCO3-	2.498e-006	2.076e-006	-5.602	-5.683	-0.080
CaCO3	1.940e-006	1.940e-006	-5.712	-5.712	0.000
FeHCO3+	8.140e-008	6.801e-008	-7.089	-7.167	-0.078
MnHCO3+	2.605e-011	2.156e-011	-10.584	-10.666	-0.082
CoHCO3+	5.093e-013	3.942e-013	-12.293	-12.404	-0.111
ZnHCO3+	1.278e-013	9.894e-014	-12.893	-13.005	-0.111
ZnCO3	1.145e-013	1.145e-013	-12.941	-12.941	0.000
CoCO3	5.450e-014	5.450e-014	-13.264	-13.264	0.000
NiHCO3+	1.503e-014	1.163e-014	-13.823	-13.934	-0.111
NiCO3	2.240e-015	2.240e-015	-14.650	-14.650	0.000
Ca	2.127e-004				
Ca+2	1.150e-004	5.286e-005	-3.939	-4.277	-0.338
CaHPO4	5.216e-005	5.216e-005	-4.283	-4.283	0.000
CaHCO3+	3.733e-005	3.119e-005	-4.428	-4.506	-0.078
CaH2PO4+	3.436e-006	2.855e-006	-5.464	-5.544	-0.080
CaPO4-	2.794e-006	2.321e-006	-5.554	-5.634	-0.080
CaCO3	1.940e-006	1.940e-006	-5.712	-5.712	0.000
CaNH3+2	2.743e-008	9.848e-009	-7.562	-8.007	-0.445
CaOH+	3.987e-010	3.331e-010	-9.399	-9.477	-0.078
Co(2)	1.467e-012				
CoHCO3+	5.093e-013	3.942e-013	-12.293	-12.404	-0.111
Co+2	4.780e-013	1.716e-013	-12.321	-12.765	-0.445
CoHPO4	4.204e-013	4.204e-013	-12.376	-12.376	0.000
CoCO3	5.450e-014	5.450e-014	-13.264	-13.264	0.000
Cu(1)	9.288e-007				
Cu(S4)2-3	7.884e-007	3.280e-007	-6.103	-6.484	-0.381
CuS4S5-3	1.404e-007	6.108e-008	-6.853	-7.214	-0.361
Cu(2)	1.822e-014				
Cu(HS)3-	1.822e-014	1.410e-014	-13.740	-13.851	-0.111
Fe(2)	2.519e-006				
FeHPO4	1.635e-006	1.635e-006	-5.786	-5.786	0.000
Fe+2	5.096e-007	1.830e-007	-6.293	-6.738	-0.445
FeH2PO4+	2.881e-007	2.394e-007	-6.540	-6.621	-0.080
FeHCO3+	8.140e-008	6.801e-008	-7.089	-7.167	-0.078
FeOH+	2.493e-009	2.064e-009	-8.603	-8.685	-0.082
Fe(HS)2	2.177e-009	2.177e-009	-8.662	-8.662	0.000
Fe(HS)3-	1.119e-012	8.663e-013	-11.951	-12.062	-0.111
Fe(OH)2	5.157e-013	5.157e-013	-12.288	-12.288	0.000
Fe(3)	9.003e-018				
Fe(OH)2+	6.090e-018	5.060e-018	-17.215	-17.296	-0.080
Fe(OH)3	2.886e-018	2.886e-018	-17.540	-17.540	0.000
FeHPO4+	1.619e-020	1.345e-020	-19.791	-19.871	-0.080
H(0)	5.216e-003				
H2	2.608e-003	2.636e-003	-2.584	-2.579	0.005
K	2.612e-003				
K+	2.569e-003	2.115e-003	-2.590	-2.675	-0.084
KHPO4-	4.335e-005	3.602e-005	-4.363	-4.443	-0.080
Mg	3.387e-003				
Mg+2	1.833e-003	8.424e-004	-2.737	-3.074	-0.338
MgHPO4	1.147e-003	1.147e-003	-2.940	-2.940	0.000
MgHCO3+	2.705e-004	2.215e-004	-3.568	-3.655	-0.087
MgH2PO4+	1.200e-004	9.969e-005	-3.921	-4.001	-0.080
MgCO3	1.540e-005	1.540e-005	-4.812	-4.812	0.000
MgPO4-	6.960e-007	5.783e-007	-6.157	-6.238	-0.080
MgOH+	1.325e-007	1.112e-007	-6.878	-6.954	-0.076
Mn(2)	1.432e-010				
Mn+2	1.171e-010	4.205e-011	-9.931	-10.376	-0.445

```
   MnHCO3+           2.605e-011  2.156e-011   -10.584   -10.666    -0.082
   MnOH+             3.615e-014  2.992e-014   -13.442   -13.524    -0.082
N(-3)          2.385e-002
   NH4+              2.378e-002  1.913e-002    -1.624    -1.718    -0.094
   NH3               7.492e-005  7.492e-005    -4.125    -4.125     0.000
   CaNH3+2           2.743e-008  9.848e-009    -7.562    -8.007    -0.445
   Ca(NH3)2+2        1.616e-012  5.802e-013   -11.792   -12.236    -0.445
Na             9.744e-003
   Na+               9.407e-003  7.746e-003    -2.027    -2.111    -0.084
   NaHPO4-           2.459e-004  2.043e-004    -3.609    -3.690    -0.080
   NaHCO3            8.875e-005  8.875e-005    -4.052    -4.052     0.000
   NaCO3-            2.498e-006  2.076e-006    -5.602    -5.683    -0.080
Ni             2.454e-014
   NiHCO3+           1.503e-014  1.163e-014   -13.823   -13.934    -0.111
   Ni+2              6.955e-015  3.196e-015   -14.158   -14.495    -0.338
   NiCO3             2.240e-015  2.240e-015   -14.650   -14.650     0.000
P              8.031e-003
   HPO4-2            3.931e-003  1.845e-003    -2.405    -2.734    -0.329
   H2PO4-            2.482e-003  2.062e-003    -2.605    -2.686    -0.080
   MgHPO4            1.147e-003  1.147e-003    -2.940    -2.940     0.000
   NaHPO4-           2.459e-004  2.043e-004    -3.609    -3.690    -0.080
   MgH2PO4+          1.200e-004  9.969e-005    -3.921    -4.001    -0.080
   CaHPO4            5.216e-005  5.216e-005    -4.283    -4.283     0.000
   KHPO4-            4.335e-005  3.602e-005    -4.363    -4.443    -0.080
   CaH2PO4+          3.436e-006  2.855e-006    -5.464    -5.544    -0.080
   CaPO4-            2.794e-006  2.321e-006    -5.554    -5.634    -0.080
   FeHPO4            1.635e-006  1.635e-006    -5.786    -5.786     0.000
   MgPO4-            6.960e-007  5.783e-007    -6.157    -6.238    -0.080
   FeH2PO4+          2.881e-007  2.394e-007    -6.540    -6.621    -0.080
   PO4-3             7.389e-008  1.285e-008    -7.131    -7.891    -0.760
   H3PO4             2.369e-008  2.369e-008    -7.625    -7.625     0.000
S(-2)          6.985e-006
   HS-               4.720e-006  3.654e-006    -5.326    -5.437    -0.111
   H2S               2.114e-006  2.114e-006    -5.675    -5.675     0.000
   S5-2              9.747e-008  3.500e-008    -7.011    -7.456    -0.445
   S4-2              2.528e-008  9.078e-009    -7.597    -8.042    -0.445
   S6-2              1.816e-008  6.522e-009    -7.741    -8.186    -0.445
   S3-2              4.106e-009  1.474e-009    -8.387    -8.831    -0.445
   Fe(HS)2           2.177e-009  2.177e-009    -8.662    -8.662     0.000
   S2-2              4.180e-010  1.501e-010    -9.379    -9.824    -0.445
   ZnS(HS)-          1.602e-010  1.240e-010    -9.795    -9.907    -0.111
   Cu(S4)2-3         2.145e-011  8.925e-012   -10.669   -11.049    -0.381
   Zn(HS)2           9.348e-012  9.348e-012   -11.029   -11.029     0.000
   CuS4S5-3          3.820e-012  1.662e-012   -11.418   -11.779    -0.361
   Fe(HS)3-          1.119e-012  8.663e-013   -11.951   -12.062    -0.111
   Zn(HS)3-          8.408e-014  6.509e-014   -13.075   -13.186    -0.111
   S-2               1.011e-015  4.745e-016   -14.995   -15.324    -0.329
Zn             1.701e-010
   ZnS(HS)-          1.602e-010  1.240e-010    -9.795    -9.907    -0.111
   Zn(HS)2           9.348e-012  9.348e-012   -11.029   -11.029     0.000
   Zn+2              2.306e-013  1.060e-013   -12.637   -12.975    -0.338
   ZnHCO3+           1.278e-013  9.894e-014   -12.893   -13.005    -0.111
   ZnCO3             1.145e-013  1.145e-013   -12.941   -12.941     0.000
   Zn(HS)3-          8.408e-014  6.509e-014   -13.075   -13.186    -0.111
   ZnOH+             3.879e-015  3.002e-015   -14.411   -14.523    -0.111

-------------------------------Saturation indices-------------------------
------
```

Phase	SI	log IAP	log KT	
(Co(NH3)6)(NO3)3	-351.66	-333.72	17.94	(Co(NH3)6)(NO3)3
Anhydrite	-33.95	-38.35	-4.40	CaSO4
Anilite	-1.21	-32.05	-30.84	Cu0.25Cu1.5S
Aragonite	-0.63	-9.00	-8.37	CaCO3
Artinite	-5.53	3.39	8.92	MgCO3:Mg(OH)2:3H2O
BlaubleiI	-2.91	-27.07	-24.16	Cu0.9Cu0.2S
BlaubleiII	-2.09	-29.37	-27.28	Cu0.6Cu0.8S
Brucite	-5.01	11.19	16.20	Mg(OH)2
Bunsenite	-12.11	-0.23	11.88	NiO
Ca3(PO4)2(beta)	0.00	-28.61	-28.61	Ca3(PO4)2
Ca4H(PO4)3:3H2O	-0.84	-47.92	-47.08	Ca4H(PO4)3:3H2O
CaHPO4	-0.20	-19.30	-19.10	CaHPO4
CaHPO4:2H2O	-0.44	-19.30	-18.86	CaHPO4:2H2O
Calcite	-0.48	-9.00	-8.53	CaCO3
Co(OH)2	-11.60	1.50	13.09	Co(OH)2
Co(OH)3	-28.37	-31.21	-2.83	Co(OH)3
CO2(g)	-0.87	-18.99	-18.12	CO2
Co3(PO4)2	-19.39	-54.08	-34.69	Co3(PO4)2
CoCO3	-7.44	-17.49	-10.05	CoCO3
CoFe2O4	-5.21	-9.64	-4.43	CoFe2O4
CoHPO4	-8.73	-27.79	-19.06	CoHPO4
CoO	-11.48	1.50	12.98	CoO
CoS(alpha)	-3.63	-11.07	-7.44	CoS
CoS(beta)	0.00	-11.07	-11.07	CoS
Covellite	0.00	-21.75	-21.75	CuS
Cu(OH)2	-22.09	-13.73	8.35	Cu(OH)2
CuCO3	-21.22	-32.72	-11.50	CuCO3
Cumetal	-2.04	-10.39	-8.35	Cu
Cupricferrite	-29.66	-24.87	4.79	CuFe2O4
Cuprite	-19.28	-21.40	-2.11	Cu2O
Cuprousferrite	-7.26	-16.27	-9.01	CuFeO2
Djurleite	-0.68	-33.46	-32.78	Cu0.066Cu1.868S
Dolomite(disordered)	0.00	-16.80	-16.80	CaMg(CO3)2
Dolomite(ordered)	0.51	-16.80	-17.31	CaMg(CO3)2
Fe(OH)2	-6.04	7.53	13.56	Fe(OH)2
Fe3(OH)8	-23.84	-3.61	20.22	Fe3(OH)8
Ferrihydrite	-8.34	-5.57	2.77	Fe(OH)3
FeS(ppt)	-2.03	-5.04	-3.01	FeS
Goethite	-5.72	-5.57	0.15	FeOOH
Greigite	-8.85	-53.89	-45.03	Fe3S4
H2S(g)	-4.56	-12.57	-8.01	H2S
Hematite	-8.99	-11.14	-2.15	Fe2O3
Huntite	-1.82	-32.41	-30.58	CaMg3(CO3)4
Hydromagnesite	-10.01	-20.02	-10.01	Mg5(CO3)4(OH)2:4H2O
Hydroxylapatite	6.41	-37.93	-44.33	Ca5(PO4)3OH
Lepidocrocite	-6.94	-5.57	1.37	FeOOH
Lime	-21.61	9.99	31.60	CaO
Mackinawite	-1.44	-5.04	-3.60	FeS
Maghemite	-17.52	-11.14	6.39	Fe2O3
Magnesioferrite	-15.22	0.05	15.27	Fe2MgO4
Magnesite	-0.45	-7.80	-7.35	MgCO3
Magnetite	-5.83	-3.61	2.22	Fe3O4
Manganite	-21.76	3.58	25.34	MnOOH
Mg(OH)2(active)	-7.60	11.19	18.79	Mg(OH)2
Mg3(PO4)2	-1.73	-25.01	-23.28	Mg3(PO4)2

```
      MgHPO4:3H2O       0.07  -18.10  -18.18  MgHPO4:3H2O
      Mn3(PO4)2       -23.13  -46.91  -23.78  Mn3(PO4)2
      MnHPO4            0.00  -25.40  -25.40  MnHPO4
      MnS(grn)         -8.67   -8.68   -0.01  MnS
      MnS(pnk)        -12.02   -8.68    3.34  MnS
      Natron           -8.02   -8.95   -0.94  Na2CO3:10H2O
      Nesquehonite     -2.99   -7.80   -4.81  MgCO3:3H2O
      Ni(OH)2         -12.48   -0.23   12.25  Ni(OH)2
      Ni3(PO4)2       -27.97  -59.27  -31.30  Ni3(PO4)2
      NiCO3           -12.12  -19.22   -7.11  NiCO3
      NiS(alpha)       -7.20  -12.80   -5.60  NiS
      NiS(beta)        -1.70  -12.80  -11.10  NiS
      NiS(gamma)        0.00  -12.80  -12.80  NiS
      Periclase        -9.53   11.19   20.72  MgO
      Portlandite     -12.09    9.99   22.07  Ca(OH)2
      Pyrite            0.00  -18.22  -18.22  FeS2
      Pyrochroite     -10.75    3.89   14.64  Mn(OH)2
      Rhodochrosite    -4.51  -15.10  -10.59  MnCO3
      Siderite         -1.13  -11.46  -10.33  FeCO3
      Smithsonite      -7.61  -17.70  -10.09  ZnCO3
      Sphalerite        0.00  -11.28  -11.28  ZnS
      Strengite        -8.40  -34.86  -26.45  FePO4:2H2O
      Sulfur          -10.95  -13.18   -2.24  S
      Tenorite        -21.01  -13.73    7.28  CuO
      Thermonatrite    -9.53   -8.95    0.58  Na2CO3:H2O
      Vivianite         0.00  -36.00  -36.00  Fe3(PO4)2:8H2O
      Wurtzite         -2.45  -11.28   -8.83  ZnS
      Zincite          -9.53    1.29   10.82  ZnO
      Zn(OH)2         -10.91    1.29   12.20  Zn(OH)2
      Zn(OH)2(am)     -10.73    1.29   12.02  Zn(OH)2
      Zn(OH)2(beta)    -9.99    1.29   11.28  Zn(OH)2
      Zn(OH)2(epsilon)  -9.78    1.29   11.07  Zn(OH)2
      Zn(OH)2(gamma)  -10.44    1.29   11.73  Zn(OH)2
      Zn3(PO4)2:4H2O  -19.29  -54.71  -35.42  Zn3(PO4)2:4H2O
      ZnCO3:1H2O       -7.44  -17.70  -10.26  ZnCO3:1H2O
      Znmetal         -23.01    1.90   24.92  Zn
      ZnO(active)      -9.39    1.29   10.68  ZnO
      ZnS(am)          -2.31  -11.28   -8.96  ZnS
      ------------------
End of simulation.
------------------

-----------------------------------
Reading input data for simulation 2.
-----------------------------------

-----------
End of run.
-----------
```

Appendix H: Illustration of the Visual Minteq software

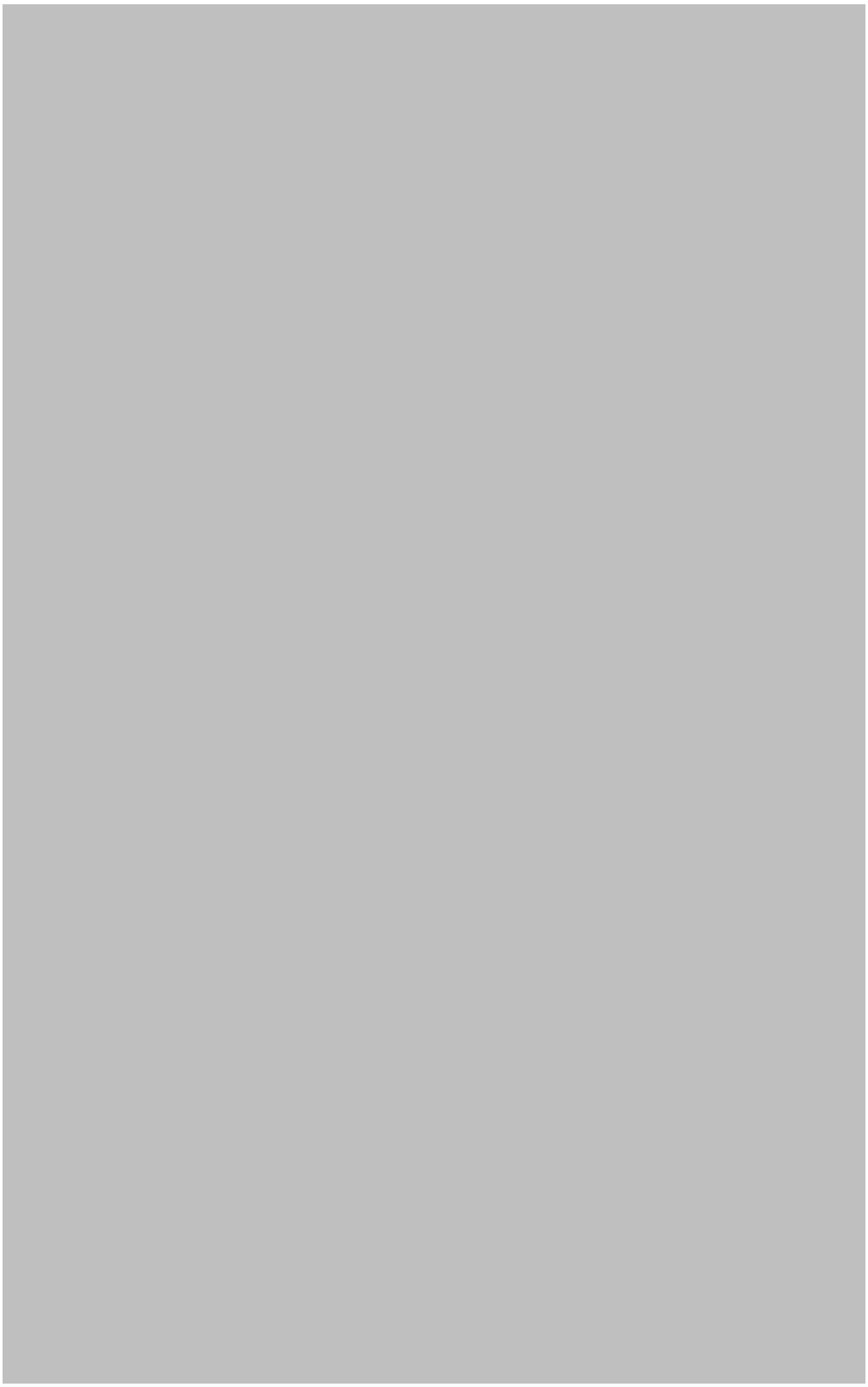

Figure H.1. Screenshot of Visual Minteq's main menu

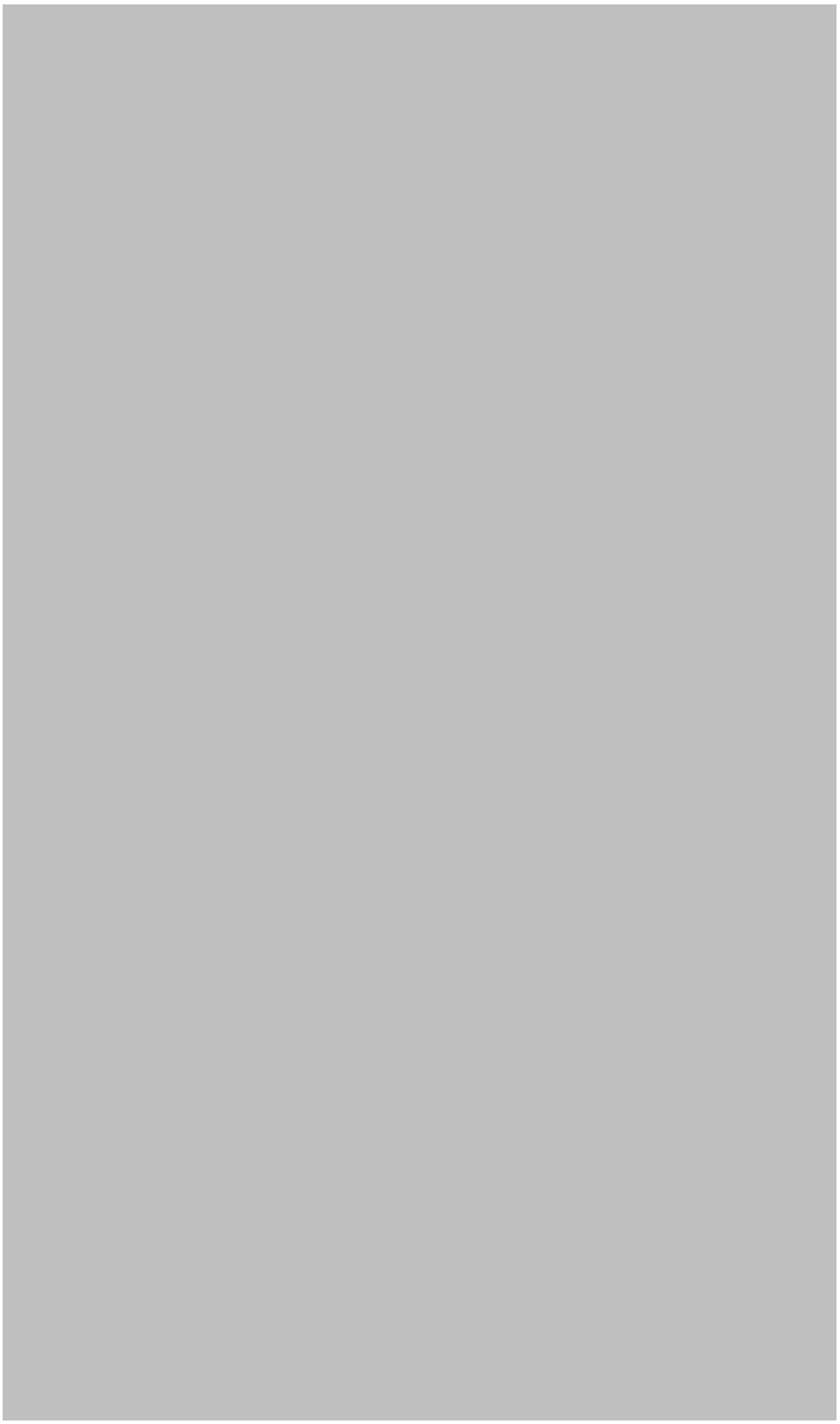

Figure H.2. Screenshot of Visual Minteq's multi-problem menu

Appendix I: Dissemination

I.1 Publications

Roussel J., Ishaq F. Renshaw J.C., Buckley C.A. and Carliell-Marquet C.M. (2010) Metal analysis in anaerobic digester sludge – a preliminary investigation. **Proceeding of the IWA AD 12th conference,** Guadalajara , 31st October-4th November 2010.

Ishaq F., Roussel J, Carliell-Marquet C.M. and Bridgeman J. (2010) Increasing economic performance from sludge digesters using trace element supplements. **Proceeding of the IWA AD 12th conference,** Guadalajara, 31st October-4th November 2010.

Roussel J., Renshaw, J.C., Buckley C.A. and Carliell-Marquet C.M. (2013) Significance of vivianite precipitation on the iron behaviour in the anaerobically digested sludge. **Biochemical Engineering Journal** (Preparation for submission, 01/02/13).

Roussel J., Renshaw, J.C., Buckley C.A. and Carliell-Marquet C.M. (2013) Development of a suite of techniques in the study of metals speciation in anaerobically digested sludge. **Environmental Science and Technology** (Preparation for submission, 01/03/13).

Roussel J., Renshaw, J.C., Buckley C.A. and Carliell-Marquet C.M. (2013) Fate of cobalt in anaerobically digested sludge when supplemented as CoEDTA. **Bioresource Technology** (Preparation for submission, 15/02/13).

I.2 Conferences and workshop attended

May 2011	Platform presentation to the IWA 12th UK Young water professional conference, Edinburgh (UK). “Use of Fluorescence Spectroscopy in the Study of Metal Speciation in Anaerobic Digester”.
Nov 2010	Platform presentation to the IWA 12th Anaerobic Digestion conference, Guadalajara (Mexico). “Metal analysis in anaerobic digester sludge – a preliminary investigation**”.**
Dec 2009	Attendance to the International workshop on anaerobic digestion: an old story for today and tomorrow, Narbonne (France)
May 2009	Poster presentation to the annual University of Birmingham poster conference, Birmingham (UK)
Avril 2009	Attendance to the IWA 10th UK Young water professional conference, London (UK)